



University of HUDDERSFIELD

University of Huddersfield Repository

Sooda, Kartheek K. Y.

Evaluation of the effects of cannabinoids CBD and CBG on human ovarian cancer cells in vitro

Original Citation

Sooda, Kartheek K. Y. (2019) Evaluation of the effects of cannabinoids CBD and CBG on human ovarian cancer cells in vitro. Doctoral thesis, University of Huddersfield.

This version is available at <http://eprints.hud.ac.uk/id/eprint/34866/>

The University Repository is a digital collection of the research output of the University, available on Open Access. Copyright and Moral Rights for the items on this site are retained by the individual author and/or other copyright owners. Users may access full items free of charge; copies of full text items generally can be reproduced, displayed or performed and given to third parties in any format or medium for personal research or study, educational or not-for-profit purposes without prior permission or charge, provided:

- The authors, title and full bibliographic details is credited in any copy;
- A hyperlink and/or URL is included for the original metadata page; and
- The content is not changed in any way.

For more information, including our policy and submission procedure, please contact the Repository Team at: E.mailbox@hud.ac.uk.

<http://eprints.hud.ac.uk/>

Evaluation of the effects of
cannabinoids CBD and CBG on human
ovarian cancer cells *in vitro*

Kartheek Kumar Yadav Sooda

A thesis submitted to the University of Huddersfield in partial fulfilment of the
requirements for the degree of Doctor of Philosophy

September 2018

Copyright Statement

- i. The author of this thesis (including any appendices and/or schedules to this thesis) owns any copyright in it (the "Copyright") and he has given The University of Huddersfield the right to use such Copyright for any administrative, promotional, educational and/or teaching purposes.
- ii. Copies of this thesis, either in full or in extracts, may be made only in accordance with the regulations of the University Library. Details of these regulations may be obtained from the Librarian. This page must form part of any such copies made.
- iii. The ownership of any patents, designs, trademarks and any and all other intellectual property rights except for the Copyright (the "Intellectual Property Rights") and any reproductions of copyright works, for example graphs and tables ("Reproductions"), which may be described in this thesis, may not be owned by the author and may be owned by third parties. Such Intellectual Property Rights and Reproductions cannot and must not be made available for use without the prior written permission of the owner(s) of the relevant Intellectual Property Rights and/or Reproductions.

I) Acknowledgements

I would like to thank my supervisor Dr Farideh Javid for giving me an opportunity to undertake this project and guiding me with her valuable suggestions. I am much indebted to my co-supervisor Dr Simon Allison for his support and guidance throughout the project. I would like to thank my dearest friends Dr Glenn Robinson and Dr Nick Pearman (soon to be) for being there for me and support me through tough times. I have received great support from my extended research family Hollie Griffiths, Sam Shepherd, Alessandro Senopoli, Sam Moxon, Izabela Lepiarz and the entire of my PGR office colleagues. It would not have been possible without the help of my amazing friends Raghava Gundi, Tarun Mabbu, Praneeth Vangapelli, Sunil Muppala and Anil Sajjala. Finally, I would like to thank my parents and family for their love and support.

II) Abstract

Introduction: Ovarian cancer, with over a 90% reoccurrence within 18 months of treatment, and approximately a 30% mortality rate after 5 years, is the leading cause of death in cases of gynaecological malignancies. Acquired resistance, and toxic side effects by clinically used agents are major challenges associated with current treatments, indicating the need for new approaches in ovarian cancer treatment. Increased tumour cell proliferation associated with upregulation of cannabinoid (CB) receptors has been observed in ovarian cancer. As cannabinoids reported to bind to CB receptors, and can potentially modulate their downstream signalling, this raises the possibility of cannabinoids as potential anticancer drugs for ovarian cancer treatment. Amongst the cannabinoids, non-psychoactive CBD and CBG have been shown to have anticancer activities towards prostate and colon cancer cells through multiple mechanisms of action. However, CBD and CBG have yet to be investigated in relation to ovarian cancer therapy either *in vitro* or *in vivo*.

Aim: The aims of this study were to evaluate the potential cytotoxic effects of CBD and CBG in human ovarian cancer cells, their ability to potentiate existing clinically used agents for ovarian cancer, and to perform initial mode of action studies *in vitro*.

Methods: In this study, the cytotoxic effects of CBD and CBG were evaluated in several ovarian cancer cell lines, and in non-cancer cells. Chemosensitivity assays were performed to determine the relative potency, selectivity and combination effects of the cannabinoids CBD and CBG. Effects on the cell cycle, cell death by apoptosis and ROS levels in ovarian cancer cells when treated with CBD or CBG were evaluated. The expression of the cannabinoid receptors CB1, CB2 and GPR55 in ovarian cancer cells, and their possible contribution to CBD and CBG cytotoxicity was also assessed.

Results: CBD and CBG induced dose- dependent and time-dependent cytotoxic effects on the ovarian cancer cells tested with activity at micromolar concentrations towards the A2780 and A2780/CP70 cancer cells whilst displaying less activity against the non-cancer cells. CBD was the more potent of the two cannabinoids. However, the difference observed was not significant compared to CBG. CBD and CBG in combination with the established chemotherapeutic drug carboplatin showed synergistic effects in the cancer cells but importantly, CBD and CBG did not synergise with carboplatin in the non-cancer ARPE19 cells. Preliminary data suggested that the cytotoxicity of CBD and CBG is dependent, in part at least, on the cannabinoid receptor GPR55 whilst CB2 cannabinoid receptor status did not affect the cytotoxicity of the cannabinoids in ovarian cancer cells. GPR55 expression analysis in ovarian cancer tissues showed that the target is expressed at the mRNA level in ovarian cancer patient samples.

Conclusions: Both CBD and CBG showed preferential cytotoxicity against the ovarian cancer cells analysed compared to the non-cancer cells; however, this was less than for carboplatin. Importantly, in contrast to carboplatin, CBD and CBG showed similar activity towards cisplatin sensitive and cisplatin resistant cells indicating distinctive mechanisms of action to platinum drugs. Preferential cytotoxicity towards cancer cells *in vitro* and ability to potentiate carboplatin and overcome cisplatin resistance identify CBD and CBG as promising candidates that warrant further investigation, both in terms of detailed mechanism of action studies and also *in vivo* studies to assess whether this promising activity translates into an *in vivo* setting and their potential for further progression towards the clinic.

III) Abbreviations

Δ^8 -THC	-	Δ^8 -Tetrahydrocannabinol
2-AG	-	2-Arachidonylglycerol
AEA	-	Anandamide
Apaf-1	-	Apoptotic protease-mediated factor
ATCC	-	American type culture collection
ATP	-	Adenosine triphosphate
Bad	-	Bcl2 associated death promoter
BAK	-	Bcl2 homologous antagonist killer
BAX	-	Bcl-2-like protein 4
BRCA1	-	Breast Cancer 1
BRCA2	-	Breast Cancer 2
CA125	-	Cancer antigen 125
CB	-	Cannabinoid
CB1	-	Cannabinoid receptor 1
CB2	-	Cannabidiol
CBC	-	Cannabichromene
CCC	-	Clear cell cancer
CBD	-	Cannabidiol

CBDA	-	Cannabidiolic acid
CBDV	-	Cannabidivarin
CBG	-	Cannabigerol
CBN	-	Cannabichromene
Cdk	-	Cyclin dependant kinases
CI	-	Combination index
DCFDA	-	2', 7'-dichlorodihydrofluorescein diacetate
EC	-	Endometriosis cancer
ECS	-	Endocannabinoid systems
EOC	-	Epithelial Ovarian Cancer
GS	-	Mitogenic growth signals
HER2	-	Human epidermal growth factor 2
HGSC	-	High-grade serous cancer
HSP27	-	Heat shock protein 27
IAP	-	Inhibitory Apoptosis Protein
IC ₅₀	-	Inhibitory concentration at 50 %
IL	-	Interleukins
LGSC	-	Low-grade serous cancer
LPI	-	Lysophosphatidylinositol

MC	-	Mucinous cancer
MTT	-	3-(4,5-dimethylthiazol-2-yl)-2,5-diphenyltetrazolium bromide
PARP	-	Poly (ADP- robose) polymerase
PBS	-	Phosphate buffered saline
PI	-	Propidium Iodide
pRB	-	Retinoblastoma protein
OC	-	Ovarian Cancer
OSE	-	Ovarian surface Epithelium
PSA	-	Prostate-specific antigen
ROS	-	Reactive Oxygen species
Smac	-	Second mitochondrial activator of caspases
SI	-	Selectivity index
TAK1	-	Transforming growth factor beta-activated kinase 1
TP53	-	Tumour protein p53
TRPM8	-	Transient receptor potential cation channel subfamily M 8
TRPV1	-	Transient receptor potential vanilloid receptor 1
UV	-	Ultra violet
VEGF-A	-	Vascular endothelial growth factor A

IV) Contents

I) Acknowledgements	3
II) Abstract.....	4
III) Abbreviations	5
IV) Contents	8
V) List of Tables	13
VI) List of Figures.....	15
VII) Publication.....	19
VIII) Conference Posters	19
CHAPTER 1 : Introduction	20
1.1 Cancer.....	20
1.2 Hallmarks of cancer.....	20
1.2.1 Self- sufficiency of growth signals.....	20
1.2.2 Insensitivity to growth inhibitors	21
1.2.3 Resisting cell death	21
1.2.4 Inducing angiogenesis.....	22
1.2.5 Enabling replicative immortality.....	22
1.2.6 Activating tissue invasion and metastasis	23
1.2.7 Reprogramming of cellular energy metabolism	23
1.2.8 Evading Immune Destruction	24
1.2.9 Tumour- promoting inflammation.....	24
1.2.10 Genome instability and mutation	25
1.3 Ovarian cancer	26
1.3.1 Risk factors and pathogenesis	27
1.3.2 Screening techniques.....	29
1.3.3 Ovarian cancer histology	31
1.3.4 Hallmarks of Ovarian cancer	33
1.3.5 Surgical stages of ovarian cancer.....	38
1.3.6 Treatment	39
1.3.7 Chemotherapy challenges	40
1.3.8 Current research in ovarian cancer treatment.....	40

1.4 Cannabinoids.....	42
1.4.1 Endocannabinoids.....	43
1.4.2 Cannabinoid Receptors:.....	45
1.4.3 Phytocannabinoids:	48
1.4.4 Synthetic cannabinoids	49
1.4.5 Cannabinoids and their anti- cancer activity:	50
1.4.6 Non-psychotropic cannabinoids as potential anticancer drugs:	51
1.4.7 Cannabidiol (CBD)	52
1.4.8 Cannabigerol (CBG).....	54
1.5 Mechanisms associated with anticancer activity of cannabinoids	58
1.5.1 Apoptosis	58
1.5.2 Cell cycle.....	62
1.5.3 Reactive oxygen species (ROS) inducing apoptosis	63
1.6 Rationale and aims of the project	64
1.7 Hypothesis.....	65
CHAPTER 2 : Materials and Methods.....	66
2.1 Materials	66
2.1.1 General materials.....	66
2.1.2 Primary antibodies for western blot.....	67
2.1.3 SiRNA for RNAi mediated transfection	67
2.1.4 Taqman probes for qPCR	67
2.2 Cell culture methods:	68
2.3 Sub- culturing of cells by trypsinisation	68
2.3.1 Cell counting by haemocytometer:	69
2.4 Cryo-preservation of cells:	70
2.5 Chemo sensitivity assay	71
2.5.1 Preparation of MTT solution:.....	71
2.5.2 Drug addition	71
2.5.3 MTT assay:	71
2.5.4 Chemo sensitivity assay with drug washout.....	71
2.5.5 IC ₅₀ determination:.....	72
2.5.6 Selectivity Index:	72
2.5.7 Combination Index:.....	73

2.6 Viability Assay:.....	74
2.7 Mitochondrial membrane potential assay:.....	75
2.8 Annexin- V assay.....	75
2.9 Cell cycle analysis	76
2.10 Caspase 3/7 assay	77
2.10.1 Sensolyte homogenous caspase 3/7 assay:.....	77
2.10.2 ApoTox-Glo™ Triplex Assay (caspase 3/7 activity)	77
2.11 H2DCFDA- ROS assay.....	78
2.12 Western Blot analysis.....	79
2.13 ELISA Pathscan® Apoptosis and Stress assay	80
2.14 siRNA mediated RNAi transfection	81
2.15 mRNA extraction	82
2.16 Reverse transcription (cDNA synthesis):.....	83
2.17 Real-Time qPCR	83
2.18 Statistical Analysis	84
CHAPTER 3 : Evaluation of CBD and CBG cytotoxicity towards ovarian cancer cells <i>in vitro</i> ..	85
3.1 Introduction.....	85
3.2 Results	85
3.2.1 Solvent/ Vehicle effect on A2780 viability:.....	85
3.2.2 <i>In vitro</i> anticancer activity of CBD:	87
3.2.3 <i>In vitro</i> anticancer activity of CBG:	92
3.2.4 Cytotoxicity of CBD and CBG with drug washout experiments:.....	97
3.2.5 Cytotoxicity of Carboplatin:	100
3.2.6 Comparison of carboplatin selectivity towards ovarian cancer cells compared to CBD and CBG:.....	104
3.2.7 Comparison of carboplatin resistance factor with CBD and CBG in ovarian cancer cells	105
3.3 Discussion.....	106
CHAPTER 4 : Evaluation of the combination effects of CBD/ CBG with the chemotherapeutic drugs, <i>In Vitro</i>	110
4.1 Introduction.....	110
4.2 Results	110
4.2.1 Combination effects of CBD with CBG	110
4.2.2 Carboplatin in Combination with CBD or CBG:.....	114

4.2.3	Paclitaxel (Taxol) in combination with CBD or CBG	123
4.3	Discussion	129
CHAPTER 5 Mechanistic studies of CBD and CBG on ovarian cancer cells		132
5.1	Introduction.....	132
5.2	Results	132
5.2.1	Cycle analysis of A2780 and A2780/CP70 cells following CBD or CBG treatment 132	
5.2.2	Mechanistic investigation of CBD/ CBG cytotoxicity on ovarian cancer cells by mitochondrial membrane potential assay	137
5.2.3	Mechanistic investigation of CBD/ CBG induced apoptosis by Annexin V assay 140	
5.2.4	Investigation of Caspase 3/7 Activity in CBD and CBG induced apoptosis.....	144
5.2.5	Investigation of reactive oxygen species (ROS) contribution towards CBD and CBG cytotoxicity.....	145
5.2.6	Rescue of CBD cytotoxicity on ovarian cancer cells by anti- oxidant:.....	148
5.2.7	Effects of CBD or CBG on expression of key proteins involved in apoptosis and stress signalling.....	150
5.3	Discussion.....	158
CHAPTER 6 Investigation of cannabinoids receptors in CBD and CBG induced cytotoxicity on ovarian cancer cells.....		161
6.1	Introduction.....	161
6.2	Results	161
6.2.1	Investigation of expression levels of CB1, CB2 and GPR55 in hypoxia and normoxia conditions.....	161
6.2.2	Investigation of the involvement of GPR55 receptor in CBD and CBG induced cytotoxicity.	165
6.2.3	Investigation CBD and CBG cytotoxicity in the presence of GPR55 antagonist CID16020046.	167
6.2.4	GpR55 RNAi-mediated silencing in A2780 and A2780/ CP70 cells.....	172
6.2.5	Analysis of GPR55 RNA silencing by western blot	174
6.2.6	Analysis of GpR55 RNAi-mediated silencing in A2780 cells by qPCR	175
6.2.7	Evaluation of CBD and CBG cytotoxicity in GPR55 silenced A2780 cells.	177
6.2.8	GPR55 messenger RNA expression levels in ovarian cancer patients.....	178
6.2.9	Investigation of the involvement of CB1 receptor in CBD/CBG induced cytotoxicity.	182

6.2.10 Investigation of the involvement of CB2 receptor in CBD or CBG induced cytotoxicity.	185
6.3 Discussion.....	190
CHAPTER 7 General Discussion& Future Work.....	193
7.1 Potency and selectivity of CBD versus CBG towards human ovarian cancer cells	193
7.2 The combination of CBD or CBG with chemotherapeutic drugs	195
7.3 CBD and CBG mechanisms of action in ovarian cancer cells	197
7.3.1 Cannabinoid receptors in relation to CBD or CBG cytotoxicity in human ovarian cancer cells	200
7.4 Future work- Development of CBD and CBG towards clinic.....	202
CHAPTER 8 Conclusion.....	204
IX) References.....	205
CHAPTER 9 Appendix	220

V) List of Tables

Table 1-2. Different types of drug- receptor interactions.	51
Table 1-3. Pharmacological effects of CBD and CBG discovered so far.....	56
Table 2-1. Indication of combination effects relative to combination index values. Adopted from (Bijnsdorp et al., 2011).....	74
Table 3-1. The mean IC ₅₀ values of CBD on A2780 cells with 0.1% and 1% ethanol respectively	87
Table 3-2 IC ₅₀ values for CBD induced cytotoxicity on ovarian cancer A2780, A2780/CP70, OVACAR-3 cells and non-cancer ARPE19 and PNT2 cells	89
Table 3-3 IC ₅₀ values for CBG induced cytotoxicity.....	94
Table 3-4. The comparison between the IC ₅₀ values of CBD on A2780 cells, when cells were allowed to recover after each time point, and instant MTT viability assay after 24 h, 48 h and 72 h drug exposure.	98
Table 3-5. The comparison between the IC ₅₀ values of CBD on A2780/CP70 cells, when cells were allowed to recover after each time point, and instant MTT viability assay after 24 h, 48 h and 72 h drug exposure	98
Table 3-6 The comparison between the IC ₅₀ values of CBG on A2780 cells, when cells were allowed to recover after each time point, and instant MTT viability assay after 24 h, 48 h and 72 h drug exposure.	100
Table 3-7. The comparison between the IC ₅₀ values of CBG on A2780/CP70 cells, when cells were allowed to recover after each time point, and instant MTT viability assay after 24 h, 48 h and 72 h drug exposure.	100
Table 3-8 The comparison between the IC ₅₀ values of carboplatin on A2780 cells, when cells were allowed to recover after each time point, and instant MTT viability assay after 24 h, 48 h and 72 h drug exposure.	103
Table 3-9. The comparison between the IC ₅₀ values of carboplatin on A2780 CP70 cells, when cells were allowed to recover after each time point, and instant MTT viability assay after 24 h, 48 h and 72 h drug exposure.	103
Table 4-1 The IC ₅₀ (μM) values of CBD alone, CBG alone and, CBD:CBG (1:1, 1:5, 5:1) on both A2780 and A2780/CP70 cells after 24 after 24 h, 48 h and 72 h contact time	113

Table 6-1 $\Delta\Delta$ CT values of CB1, CB2 and GPR55 receptors in A2780, A2780/CP70, and ARPE19 cells.	164
Table 9-1 selective index values of CBD on ovarian cancer cells compared to non- cancer cells ARPE19 and PNT2	220
Table 9-2 selective index values of CBG on ovarian cancer cells compared to non- cancer cells ARPE19 and PNT2	220
Table 9-3 IC ₅₀ values of carboplatin alone, and in combination with CBD or CBG on A2780 cells	220
Table 9-4 IC ₅₀ values of carboplatin alone, and in combination with CBD or CBG on A2780/CP70 cells	221
Table 9-5 IC ₅₀ values of Taxol alone, and in combination with CBD or CBG on A2780 cells	221
Table 9-6 IC ₅₀ values of Taxol alone, and in combination with CBD or CBG on A2780/CP70 cells	221
Table 9-7 Fold change in apoptosis and stress related proteins in A2780 and A2780/CP70 cells treated with CBD for 24 H.....	222
Table 9-8 Fold change in apoptosis and stress related proteins in A2780 and A2780/CP70 cells treated with CBG for 24 H.....	223

VI) List of Figures

Figure 1-1 Hallmarks of cancer and their therapeutic targeting	25
Figure 1-2. Oestrogen induced growth factors results tumour progression in ovarian cancer	28
Figure 1-3 Symptoms and diagnosis of ovarian cancer	30
Figure 1-4. The classification of subtypes of ovarian carcinoma based on histologic subtypes.	31
Figure 1-5. The role of inflammation in the development of ovarian cancer	36
Figure 1-6 Relevance of cancer hallmarks in biology to epithelial ovarian cancer histotypes	38
Figure 1-7. Current molecular target drugs (approved or under clinical investigation) based on hallmarks of ovarian cancer	42
Figure 1-8. The known physiological role of GPR55 in cancer.....	48
Figure 1-9. Chemical structure of Cannabidiol (CBD)	54
Figure 1-10. Chemical structure of Cannabigerol (CBG).....	55
Figure 1-12 pharmacological effects of CBD& CBG, and their proposed mechanism of action..	57
Figure 1-13 schematic representation of Apoptosis. Adopted from.....	61
Figure 2-1. General representation of haemocytometer grid with a square highlighted.....	70
Figure 2-2 Schematic representation of the concept of H2DCFDA- ROS assay.....	78
Figure 2-3 The plan of Pathscan® stress and apoptosis signalling antibody array kit.....	81
Figure 3-1 Solvent or vehicle effect on A2780 cell viability.....	86
Figure 3-2. In vitro cytotoxicity of CBD	89
Figure 3-3 The IC ₅₀ values of CBD.	90
Figure 3-4. The selective index of CBD against ARPE19 and PNT2.....	91
Figure 3-5. In vitro cytotoxicity of CBG	94
Figure 3-6 The IC ₅₀ values of CBG.	95
Figure 3-7. The selective index of CBG against ARPE19 and PNT2.....	96
Figure 3-8 Comparison of cytotoxic effects of CBD in normal vs drug washout MTT assays..	98
Figure 3-9 Comparison of cytotoxic effects of CBG in normal vs drug washout MTT assays.	99

Figure 3-10 . Chemosensitive dose-response curves of A2780 and A2780/CP70 to carboplatin.	102
Figure 3-11. The comparison of chemosensitivity of carboplatin against CBD and CBG on ARPE19 cells.....	104
Figure 3-12.The selectivity index of carboplatin on A2780 (left) and A2780/CP70 (right) cells against ARPE19 cells	105
Figure 3-13. The difference between the resistance factor values of carboplatin, CBD and CBG.	106
Figure 4-1. The Representative comparison of dose-response curves of CBD, and CBG supplied by GW pharmaceuticals and Tocris on A2780 and A2780/CP70.....	111
Figure 4-2 CBD in combination with CBG	113
Figure 4-3 Carboplatin in combination with 100 nM CBD or 100 nM CBG on A2780 cells...116	
Figure 4-4. IC ₅₀ values of carboplatin alone, and in combination with CBD or CBG in A2780 cells.	116
Figure 4-5. Carboplatin in combination with 100 nM CBD or 100 nM CBG on A2780/CP70 cells.	120
Figure 4-6. IC ₅₀ values of carboplatin alone, and in combination with CBD or CBG A2780/CP70 cells.	120
Figure 4-7. Carboplatin in combination with 100 nM CBD or 100 nM CBG on ARPE19 cells	123
Figure 4-8. Taxol in combination with 100 nM CBD/ 100 nM CBG on A2780 cells.....	125
Figure 4-9. IC ₅₀ values of Taxol alone, and in combination with CBD or CBG in A2780 cells	125
Figure 4-10. Taxol in combination with 100 nM CBD or 100 nM CBG on A2780/CP70 cells	128
Figure 4-11. IC ₅₀ values of Taxol alone, and in combination with CBD or CBG in A2780/CP70 cells	128
Figure 5-1 Cell cycle analysis of A2780 cells treated with CBD	133
Figure 5-2. Cell cycle analysis of A2780 cells treated with CBD	134
Figure 5-3 Cell cycle analysis of A2780 cells treated with CBG	134
Figure 5-4 Cell cycle analysis of A278/ CP70 cells treated with CBD.....	135
Figure 5-5 Cell cycle analysis of A278/ CP70 cells treated with CBG.....	136
Figure 5-6 Mitochondrial membrane potential assay on A2780 cells treated with CBD	138
Figure 5-7 Mitochondrial membrane potential assay on A2780 and A2780/CP70 cells treated with CBG.....	139

Figure 5-8. Representation of Annexin V assay analysis.	141
Figure 5-9. CBD Annexin V assay at 24 h	142
Figure 5-10. CBG Annexin V assay at 24 h	143
Figure 5-11. ApoTox-Glo™ Triplex assay of CBD treatment at 24 h	144
Figure 5-12. Sensolyte caspase 3/7 assay of CBG treatment 24 h.	145
Figure 5-13. DCF-DA reactive oxygen species (ROS) assay for CBD cytotoxicity	146
Figure 5-14. DCF-DA reactive oxygen species (ROS) assay for CBG cytotoxicity	147
Figure 5-15 Toxicity of α -tocopherol on A2780 cells and A2780/CP70 cells.....	148
Figure 5-16. The effect of 5 μ M α -tocopherol on CBD cytotoxicity.	149
Figure 5-17. The dose-dependent effect of α -tocopherol on CBD cytotoxicity	150
Figure 5-18. Fold change of Chk 1& 2 protein in A2780, and A2780/ CP70 cells.....	151
Figure 5-19 Fold change of caspase 3& caspase7 in A2780, and A2780/ CP70 cells	153
Figure 5-20. Fold change of phosphorylated p53 in A2780, and A2780/ CP70 cells.....	154
Figure 5-21 . Fold change of phosphorylated Bad and total survivin in A2780, and A2780/ CP70 cells	155
Figure 5-22. Fold change of PARP in A2780, and A2780/ CP70 cells.....	156
Figure 5-23 Fold change of phosphorylated HSP27 and TAK 1 in A2780, and A2780/ CP70 cells.	157
Figure 6-1. The expression of CB1, CB2 and GPR55 receptors	163
Figure 6-2. Fold change in the expression of CB1, CB2 and GPR55 receptors.	164
Figure 6-3. GpR55 protein levels in A2780 and A2780/CP70 cells treated with CBD.	165
Figure 6-4. GpR55 protein levels in A2780 and A2780/CP70 cells treated with CBG.	166
Figure 6-5. Cytotoxicity of CBD in the presence of GpR55 antagonist CID16020046..	168
Figure 6-6. Cytotoxicity of CBG in the presence of GPR55 antagonist.	169
Figure 6-7. Annexin V analysis of CBD in combination with CID16020046 on A2780 cells...171	
Figure 6-8. GPR55 RNA silencing in A2780 and A2780/CP70 cells.	174
Figure 6-9. Western blot analysis of GPR55 transfection.....	174
Figure 6-10. Relative quantification of siRNA knockdown by qPCR.	176
Figure 6-11. CBD/ CBG cytotoxicity on GPR55 KD A2780 cells.....	178
Figure 6-12. Expression of GPR55 in stage 1 ovarian carcinoma histotypes.....	179
Figure 6-13. Expression of GPR55 in stage 3 ovarian carcinoma histotypes.....	180
Figure 6-14. Cytotoxicity of AM251 on A2780 and A2780/CP70 cells.	183

Figure 6-15. Cytotoxicity of CBD or CBG in the presence of CB1 antagonist..	185
Figure 6-16. Cytotoxicity of AM630 on A2780 and A2780/CP70 cells.	187
Figure 6-17. Cytotoxicity of CBD or CBG in the presence of CB2 antagonist.	189
Figure 9-1. Validation of GPR55 antibody for western blot analysis.	224

VII) Publication

1. Sooda, K., Robinson, G., Phillips, R., Allison, S and Javid, F. *The effects of cannabidiol (CBD) and cannabigerol (CBG) on human ovarian cancer cells-* Targeted for British Journal of Pharmacology (submission pending)

VIII) Conference Posters

1. Sooda, K., Allison, S and Javid, F. Investigation of the selective cytotoxicity-induced by cannabidiol (CBD) in human ovarian carcinoma cells, at; 8th European Workshop on Cannabinoid Research, Aug 31- Sep 02, 2017, London, UK.

Available at: <http://www.pa2online.org/abstract/abstract.jsp?abid=33350&period=66>

2. Sooda, K., Robinson, G., Allison, S and Javid, F. Investigation of anticancer activity of pure cannabidiol (CBD) and pure cannabigerol (CBG) both individually and in combination on chemo resistant ovarian carcinoma cells, at; British Pharmacological Society Annual Meeting, Dec 13- 15, 2016, London, UK

Available at: <http://www.pa2online.org/abstract/abstract.jsp?abid=33261>

3. Sooda, K., Hill, T and Javid, F. The effect of cannabidiol (CBD) and cannabigerol (CBG) alone and combination on A2780, human ovarian carcinoma cell line at; British Pharmacological Society Annual Meeting, Dec 15- 17, 2015, London, UK

Available at: <http://www.pa2online.org/abstract/abstract.jsp?abid=32784>

CHAPTER 1 : Introduction

1.1 Cancer

Cancer is a leading cause of death across the world, characterised by uncontrolled division of previously normal cells. The uncontrolled division leads to the accumulation of mutations in the cellular genome. These mutations further leads to the alterations in physiological mechanisms of the cells. The alterations in physiological mechanisms of the cells are responsible for avoiding the programmed cell death, which dictates the accumulation of cellular masses leads to the tumour growth. The ability to invade into surrounding tissue spaces is the characteristic feature of malignant cancer cells which distinguish cancer from normal benign tumours (Weinberg, 2013).

1.2 Hallmarks of cancer

Hanahan and Weinberg, in 2000, described the alterations acquired in the mechanisms of the cancer cells as 'hallmarks' (**Figure 1-1**). The six major hallmarks are i) sustaining growth signalling ii) insensitivity to growth inhibitors, iii) Resisting cell death (evasion of apoptosis), iv) inducing angiogenesis, v) enabling immortality by limitless replicative potential, and vi) activating tissue invasion and metastasis. These hallmarks are essential for cancer cell survival and division (Hanahan and Weinberg, 2000). In 2011, Hanahan and Weinberg extended the hallmarks by adding four further characteristics. The authors classified the deregulation of cellular energetics, and the avoidance of immune destruction as 'emerging hallmarks' whereas the tumour promoting inflammation, and genome instability and mutation as the enabling traits of cancer (Hanahan and Weinberg, 2011).

1.2.1 Self- sufficiency of growth signals

Mitogenic growth signals (GS) are essential for the proliferation of normal cells. In normal cells, the stimulatory growth factors bind to the growth receptors- containing intracellular

tyrosine kinase domains. The GS thus initiates cellular signalling pathways, which regulates the progression of cell cycle, and cellular growth. The GS are regulated by the neighbouring cells (paracrine signalling) or by the actions of complex network of enzymes (proteases, sulfatases etc.) in the extracellular matrix (systemic signalling). Cancer cells however, able to acquire self- sufficiency of growth signals by multiple alternative ways: Autocrine cell proliferative stimulation is involves in the production of growth ligands by cancer cells. Cancer cells may also stimulate surrounding normal cells to produce growth factors. Cancer cells also elevates expression of the receptor proteins, which makes them hyper responsive to growth-factor ligands. Structural alterations of the receptor molecules (deregulating the tyrosine kinase and associated receptor proteins at the cancer cell surface) also makes cancer cells more responsive to growth-factor ligands which facilitates cell division (Hanahan and Weinberg, 2011).

1.2.2 Insensitivity to growth inhibitors

There are number of tumour supressing genes that operate in various ways to control cell proliferation. Among them, retinoblastoma associated (RB) proteins and tumour p53 protein (TP53), are commonly known tumour suppressor gene family proteins which regulates cell proliferation by activating senescence and apoptotic programs. Cancer cells promote cell cycle progression by acquired resistance to the growth inhibitors. This is achieved by promoting the mutations in tumour suppressor genes which leads to the blocking of anti-proliferative signalling pathways (Hanahan and Weinberg, 2011).

1.2.3 Resisting cell death

The rapid proliferation of cancer cells causes physiological stresses including DNA damage. In a normal cell, physiological stress can induce apoptosis, a programmed cell death. However,

cancer cells evade apoptosis by altering the signalling circuitry responsible for apoptosis. Cancer cells approach multiple strategies to avoid cell death; the most notable is the loss of p53 tumour suppressor function. In case of DNA damage, TP53 induces apoptosis by upregulating pro-apoptotic factors such as Noxa and Puma BH3- only proteins. Cancer cells avoid this by losing the TP53 function. Alternatively, cancer cells achieve similar ends by increasing the expression of anti-apoptotic regulators (Hanahan and Weinberg, 2000, Hanahan and Weinberg, 2011).

1.2.4 Inducing angiogenesis

Angiogenesis is the process of post-natal neovasculature, which is required for tumour sustenance. In rapidly proliferating tumour cells, angiogenesis is vital to maintain the supply of nutrients and oxygen. In normal cells, angiogenesis is largely quiescent. In adults, angiogenesis is transiently turned on to facilitate the demands of the physiological processes such as wound healing and female reproductive cycles. In contrast, in the tumour, 'angiogenic switch' is usually on to facilitate the formation new vessels that helps progression of tumour. The tumour microenvironment (hypoxia) and oncogenes upregulates the expression of Vascular endothelial growth factor A (VEGF-A) which contributes to angiogenesis (Hanahan and Weinberg, 2011).

1.2.5 Enabling replicative immortality

Normal cells are able to pass only a limited number of cell divisions. After a finite number of divisions, cells enter into either senescence (an irreversible non-proliferative viable state) or crisis (cell death). This phenomenon is called the Hayflick limit (Luft, 2015). This is due to the loss of telomeres DNA (function to protect chromosomal ends) after each cell cycle (Donate and Blasco, 2011). Cancer cells, however, are able to overcome the Hayflick limit by

upregulating a telomerase reverse transcript enzyme that allow cancer cells to maintain telomerase DNA at a length sufficient to avoid the triggering senescence or apoptosis. This enables cancer cells to attain immortality (Hanahan and Weinberg, 2011).

1.2.6 Activating tissue invasion and metastasis

Cancer cells activate tissue invasion by promoting the degradation of the extracellular matrix, altering the genes encoding cell to cell and cell to ECM adhesion molecules. The best example is, E-cadherin, a prominent cell adhesion molecule involves in the formation of adherens junctions with adjacent epithelial cells. Cancer cells activate invasions by down regulating E-cadherin. Cancer cells, however, upregulate the adhesion molecules involved in cell migration during embryogenesis and cell inflammation. N-cadherin is an adhesion molecule expressed for migration of neurons and mesenchymal cells during organogenesis. Cancer cells upregulate N-cadherin, which helps in tumour metastasis (Hanahan and Weinberg, 2011). Pro-inflammatory substances enhances the activity of survival factors and growth factors, which further induces in tumour invasion and metastasis. (Hanahan & Weinberg 2011).

1.2.7 Reprogramming of cellular energy metabolism

Non-cancer cells metabolise glucose to pyruvate via glycolysis in the cytosol, and pyruvate undergo oxidative phosphorylation in mitochondria in aerobic conditions. Anaerobic or hypoxic conditions favour glycolysis where relatively a little pyruvate is produced. Cancer cells are able to reprogram their glucose metabolism, and thus their energy production in tumour microenvironment. The cancer cells are able to alter the glycolysis even in the presence of oxygen. This phenomenon is called 'aerobic glycolysis' or 'Warburg effect' (Liberti and Locasale, 2016). Cancer cells compensate for the ATPs produced in oxidative phosphorylation by upregulating glucose transporters, GLUT1, which can increases glucose uptake into

cytoplasm. The increased glucose in cytoplasm of cancer cells was efficiently metabolised by the upregulation of multiple enzymes in glycolytic pathway (Jones and Thompson, 2009, Hanahan and Weinberg, 2011).

1.2.8 Evading Immune Destruction

The immune system is responsible for identifying and eradicating potentially mutant cells from the tissues. Cancer cells, however, are able to bypass this immune surveillance to form tumour. Tumour cells are able to achieve this by disabling active immune components. Yang et al, and Shields et al reported that cancer cells release immune suppressive factors like TGF- β to disable CTLs and NK cells (Shields et al., 2010, Yang et al., 2010, Hanahan and Weinberg, 2011).

1.2.9 Tumour- promoting inflammation

Cancer cells have been shown to evade immune responses by promoting inflammation. Tumour cells have shown to suppress the cytotoxic lymphocytes by upregulating the inflammatory cells like regulatory T cells and myeloid – derived suppresser cells (Mougiakakos et al., 2010, Hanahan and Weinberg, 2011). The relation between inflammation and tumour progression has been widely studied since 2000. The upregulation of inflammation by tumour cells shown to contribute multiple hallmark capabilities by supplying bioactive molecules like growth factors, anti- apoptotic factors, extracellular modifying enzymes, and proangiogenic factors which promotes tumour invasion and metastasis (DeNardo et al., 2010, Hanahan and Weinberg, 2011).

1.2.10 Genome instability and mutation

The alterations in the genome by inactivation of tumour suppressor genes enable tumour cells to acquire most of the hallmarks mentioned earlier. The acquisition of mutant genotypes is achieved with series successive clonal expansions.

The above characteristics individually or collectively contribute to the survival and unlimited division of cancer cells.

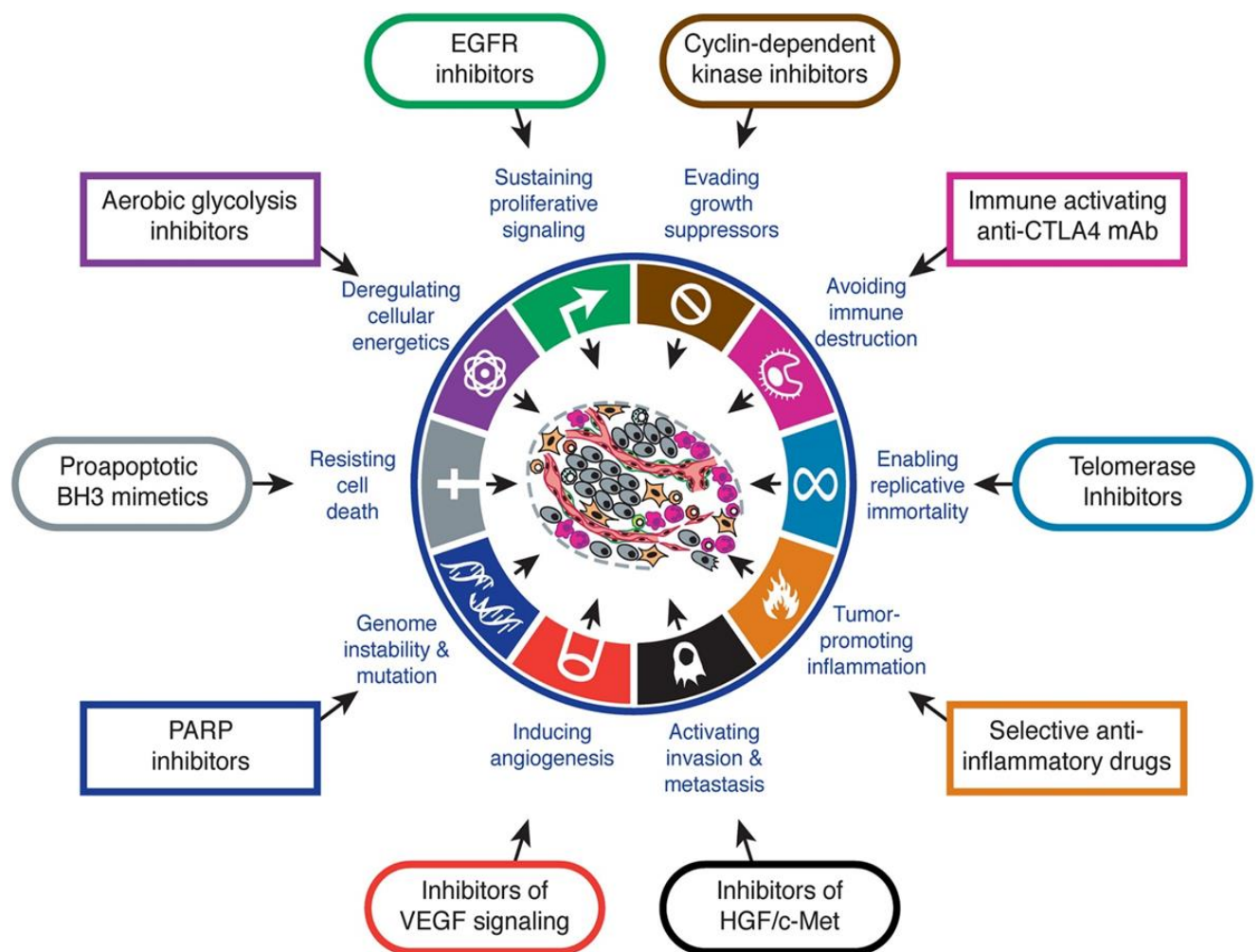


Figure 1-1 Hallmarks of cancer and their therapeutic targeting (Hanahan and Weinberg, 2011)

1.3 Ovarian cancer

Ovarian cancer, with its high rate of mortality, is one of the most clinically significant gynaecological cancers. In the UK from 2013 to 2016, there were on average 20 women diagnosed with ovarian cancer every day, and 11 registered fatalities (Cancer Research UK, 2015). The low morbidity, asymptomatic nature or displayed symptoms including bloating, abdominal pain or loss of appetite, which is similar to gastrointestinal, genitourinary and gynaecological disorders, allows ovarian cancer to go undetected; this contributes to the high fatality ratio (Colombo et al., 2006). There is more than a 90% reoccurrence within 18 months of diagnosis with approximately a 30% mortality rate after 5 years of treatment; this makes ovarian cancer a leading cause of death in cases of gynaecological malignancies (Schmid and Oehler, 2014)

The initial research on ovarian cancer could not find the primary site of tumour origin due to the lack of glandular epithelial cells in the ovarian system. Glandular epithelial cells are believed to be the common precursor for most the cancers, however later research found that ovarian cancers could have originated from three potential sites including ovarian coelomic epithelial cells, the fallopian tubes and the peritoneal cavity lined by mesothelium (Bast et al., 2009).

Besides the lack of distinct symptoms, the heterogeneous nature of ovarian cancer makes it difficult to treat. Cellular grade, proliferative index and histotypes are the factors that contribute to the heterogeneity of ovarian cancer. However, the adaptation of such changes by ovarian cancer cells yet to be determined (Bast et al., 2009).

1.3.1 Risk factors and pathogenesis

Epidemiology studies show that the risk of ovarian cancer is correlated with the number of ovulatory cycles a woman has in her lifetime. The incessant ovulation results in over expression of p53, successive bouts of apoptosis and oxidative damage of DNA in ovarian surface epithelium (OSE) at ovulation site induce trauma and genome instability which further contributes to the carcinogenesis (Ho., 2003). The factors responsible for reduction in ovulatory cycles such as pregnancy and usage of contraceptive pills are being associated with protective effect against ovarian cancer (Sundar et al., 2015). Genetic mutations are also increases the risk of causing ovarian cancer in women. The risk of ovarian cancer for women aged over 70, with BRCA1 mutation, and BRCA2 mutations are as much as 63% and 27% respectively (Sundar et al., 2015).

The wide differentiation in the histology correlates with the molecular and clinical behaviour of the ovarian cancer types (Sundar et al., 2015). Based on the factors mentioned earlier, ovarian cancer can be broadly classified into two categories; Type 1 and Type 2. Type 1 tumours include low-grade serous (LGSC), endometrioid (EC), mucinous (MC), and clear cell (CCC). Type 1 tumours are behave to be indolent with distinct morphological and molecular features, often confined to the ovaries. Type 1 ovarian cancers are tend to grow slow, and detected in early stages by ultrasonography, and show a relatively stable genome without TP53 mutations (Koshiyama et al., 2014).

Type 2 tumours include High- grade Serous (HGSC) and undifferentiated ovarian carcinoma, and are tend to be more aggressive and spreads beyond ovaries. Genetically unstable nature makes the tumours to be detected only in advanced stages. Most of Type 2 tumours have TP53 mutations and more than half of them exhibit BRCA1/2 mutations. However, Type 1

tumours are more challenging to treat due to their adamant clinical response to chemotherapy drugs (Sundar et al., 2015, Koshiyama et al., 2014)

1.3.1.1 Role of Oestrogen and Hormone Replacement Therapy in ovarian cancer

Ovaries are the main source of oestrogen in premenopausal women as Estrone (E1) and Estradiol (E2) are produced in follicular theca of ovarian cells. Oestrogen receptors (α and β) are highly expressed in OSE also indicates that ovaries are vital targets. Studies suggested that EOC is an oestrogen dependant as it could affect the tumour progression by involving proliferation, invasion and mobility of cells (**Figure 1-2**). The inhibition of EOC proliferation in the presence of tamoxifen (antioestrogen) supported the earlier statement.

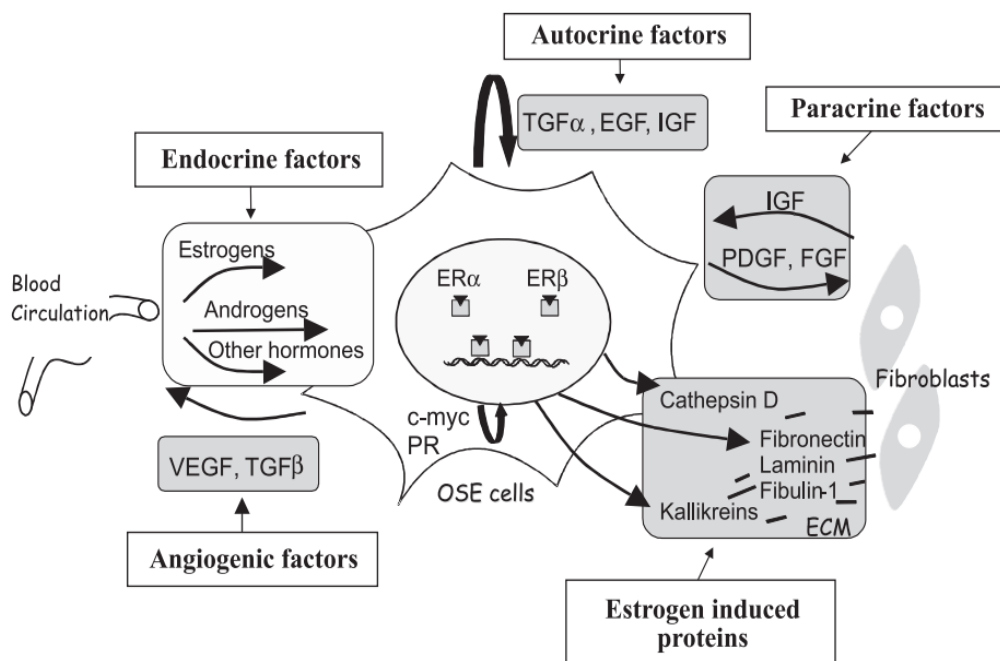


Figure 1-2. Oestrogen induced growth factors results tumour progression in ovarian cancer (Cunat et al., 2004)

Ovarian cancer is commonly diagnosed in either advanced or delayed menopausal women. Most of the women expected to spend one third of their life in post-menopausal stage due to increase in the life expectancy. Oestrogen based Hormonal Replacement Therapy (HRT) is often used by women to relieve from the persistent symptoms (vasomotor flashes and

sweats) associated with menopause state and age-related diseases including osteoporosis, dementia, and myocardial infraction (Ho., 2003). However, the studies shown that HRT increases the risk of epithelial ovarian cancer in postmenopausal women (Colombo et al., 2006, Cunat et al., 2004).

1.3.2 Screening techniques

As mentioned earlier, non- specific symptoms are the major challenge in the early detection of ovarian cancer. In a survey conducted in the UK, more than 36% of women who were subsequently diagnosed with ovarian cancer, had consulted general practitioners with the non-specific symptoms for more than three times before the diagnosis (Error! Reference source not found.). According to the National Institute for Health and Care Excellence (NICE) recommendations, patients with the symptoms related to ovarian cancer should be initially tested for cancer antigen (serum CA125) levels. If the CA125 levels are ≥ 35 IU/mL the patients are recommended to undergo ultrasonography; it is used to detect malignant tumours in the pelvis and abdomen region (Sundar et al., 2015, Gilbert et al., 2012).

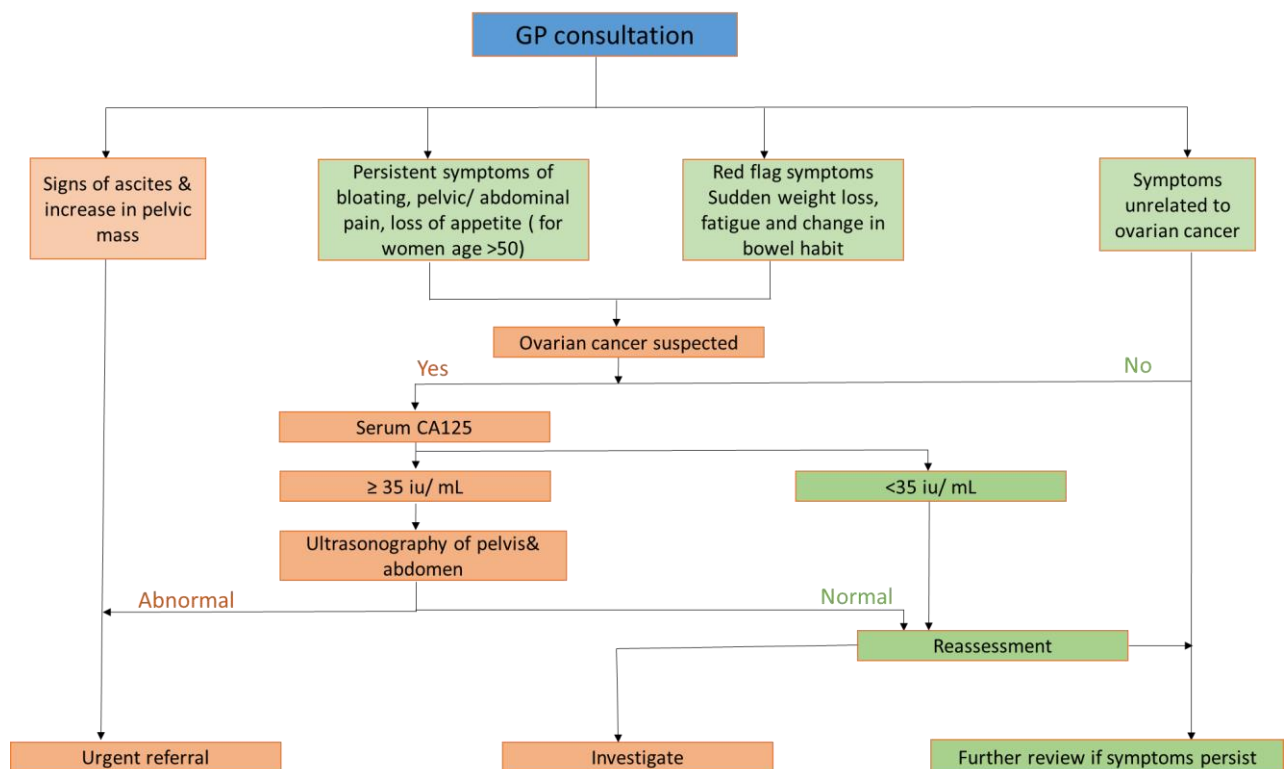


Figure 1-3 Symptoms and diagnosis of ovarian cancer. Adapted from (Sundar et al., 2015)

CA125 is a membrane-bound glycoprotein, which shows increased in levels during benign processes due to inflammation. It is widely used as a biomarker for the detection of ovarian cancer. However, the increase in the levels of CA125 is not ovarian cancer-specific; it is often associated with menstruation and endometriosis. Another drawback is that only 50% of stage 1 and 75%- 80% of advanced ovarian cancers show increased levels of CA125 (Rauh-Hain et al., 2011, Moss et al., 2013, Sundar et al., 2015).

Ultrasonography is another current screening technique involves in the detection of morphological changes that may contribute to the malignancy by the detailed imaging of the ovaries. Morphologic index- based criteria, Risk of Malignancy index (RMI), is used to analyse ultrasound images, which helps to differentiate benign masses from ovarian cancer. However, there are no universal guidelines for morphological index analysis. The sensitivity and

specificity of Ultrasonography screening towards ovarian cancer is 89% and 70% respectively (Rauh-Hain et al., 2011, Natarajan et al., 2018).

Recent studies have shown that new possible biomarkers HE4 or OVA1, in conjunction with CA125 can improve the screening of ovarian cancer. Both biomarkers are still under clinical studies. Plasma circulating tumour DNA is another promising screening technique. It is a complex genomic technology; designed to detect specific mutations in DNA in the plasma released from ovarian cancer cells. The ability to identify the small loads of ovarian tumours is the significant advantage (Forsheew et al., 2012, Sundar et al., 2015).

1.3.3 Ovarian cancer histology

Ovarian cancers are mainly classified in to two types- epithelial ovarian cancer and non-epithelial ovarian cancer based on precursor histotypes (Figure 1-4). (Barlette, 2000, Bast et al., 2009)

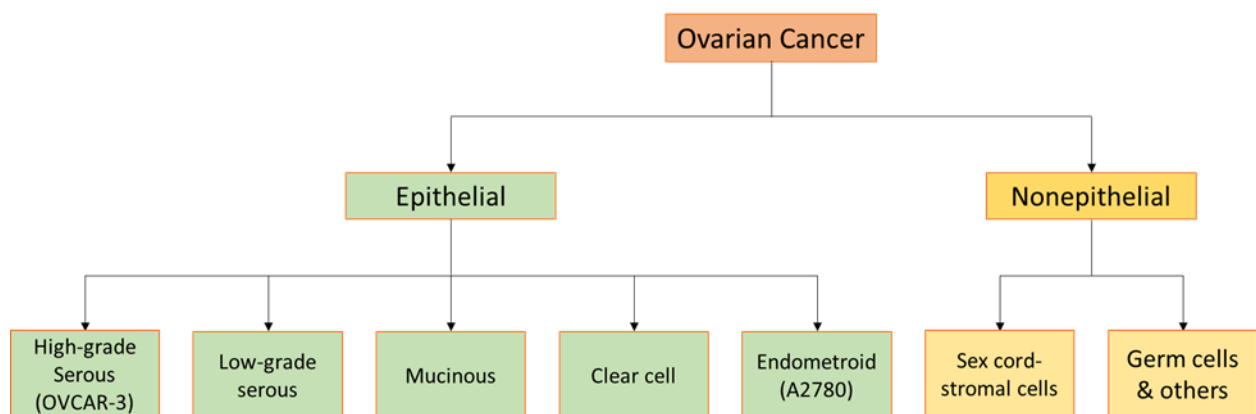


Figure 1-4. The classification of subtypes of ovarian carcinoma based on histologic subtypes. Adopted from (Banerjee and Kaye., 2013)

1.3.3.1 Epithelial Ovarian Cancer (EOC)

Ovaries are surrounded by epithelial cells that are involved in the exchange of molecules between the ovaries and the peritoneal cavity, and are involved in the rupture and repair of an ovarian surface during ovulation. The morphologically indistinctive and histologically

simple nature of the epithelial cells are the barriers in understanding the transformation of the normal cells into tumours. EOC account for over 90% of the cases of all ovarian cancers (Gubbels et al., 2010).

Epithelial Ovarian Cancer (EOC) can be further classified into five distinctive histologic subtypes. High- grade Serous (HGSC), endometrioid (EC), mucinous (MC), Low-grade serous (LGSC) and clear cell (CCC) ovarian cancers (**Error! Reference source not found.**). All EOC were believed to originate from the ovarian surface epithelium (OSE) however, and recent findings suggest distinct sites of origin for different EOC histotypes. HGSC have shown to be originated from the fallopian tube. Endometrioid, mucinous and clear cell ovarian cancers originates from endometrioid, endocervix and endovaginal cells respectively. LGSC Origins are unclear and still believed to originate from OSE (Mackenzie et al., 2015, Bast et al., 2009).

HGSC are most common type of ovarian cancer (70%), which occur in advanced stages of ovarian cancer and metastases. HGSC exhibit p53 (70%), BRCA1/2 (35- 40%), WT1 and p16 mutations (Rescigno et al., 2013). LGSC accounts for less than 5% of all cases of ovarian cancers. LGSC acquire mutations in BRAF, NRAS and KRAS. However, but show stable p53 and BRCA1/2. Mucinous cancer represents 3 – 4% of all cases of OC. They are usually larger and confined to the ovaries. Mutations in KRAS and HER2 enables the progression of tumorigenesis in mucinous cancer. Endometrioid cancer (10%) frequently occur at perimenopausal age in women. EC often have ARIDA1, PIK3CA and PTEN mutations. Clear cell cancers (10%) often diagnosed in patients at earlier stages of OC. Similar to EC, CCC express mutations in ARIDA1, PIK3CA and PTEN genes (Banerjee and Kaye., 2013, Rescigno et al., 2013)

All EOC subtypes distinctly differ from each other with many clinicopathological features including the degree of responses to chemotherapy, different patterns in metastasis and survival mechanisms (Banerjee and Kaye., 2013).

1.3.3.2 Non-Epithelial Ovarian Cancer (NOC)

The non-epithelial OC can be further divided into germ cell and sex-cord stromal ovarian cancer. Non-epithelial OC are very rare and are found in approximately six women per million women per year. Germ cell OC generally occurs in young and adolescent women with high incidents at 15-19 years age whereas sex-cord stromal carcinoma is more like epithelial OC occurs in elderly women. The risk profile and cancer biology of non- epithelial OC is not fully understood due to rare occurrence (Barlette, 2000).

1.3.4 Hallmarks of Ovarian cancer

For different cancers, or cancer subtypes, particular genetic mutations are more common than others. As such, the oncogenic drivers responsible for the acquisition of the individual hallmarks and enabling characteristics of cancer can differ for different cancers. In this subsection, key oncogenic drivers responsible for acquisition of different hallmarks in ovarian cancer are discussed. Among the hallmarks, genome instability, inflammation and angiogenesis in OC has been widely investigated due to their clinical significance.

1.3.4.1 Genome instability and mutations in OC

Genome instability plays a vital role in the development and progression of ovarian cancer. 35- 40% women with HGSC carry germline BRCA 1/2 mutations and over 70% patients acquire p53 mutations. DNA damage induced by UV radaitions, inappropriate activation of proto-oncogene, hypoxia, and mitogenic are common cause of the gene mutation. EOC exhibit the p53 mutations at the locus 17p13.1. P53 involves in growth arrest, in response to DNA

damage by regulating G1/S transition, and allows the repair. If the damage is irreversible, p53 activates apoptosis by regulating both proapoptotic and anti-apoptotic proteins of BCL-2 family (Ozaki and Nakagawara, 2011, Zhang. et al., 2016). Studies have shown that p53 mutated cancer types show higher resistance to platinum-based chemotherapy. The chemo resistance nature of High-grade ovarian cancer is because 97% of HGSC acquire p53 mutation. Small molecules capable of restoring p53 function can be a potential therapeutic approach in HGSC treatment (Hientz. et al., 2017). BRCA 1/2 play important role in homologous recombination repair. BRCA acts a checkpoint in response to DNA damage. BRCA 1 involves in the survey of double strand breaks (DSB) whereas BRCA 2 involves in the repair of DSB by enabling the RAD51 complex to attach at the repair site (Neff. et al., 2017). Germline mutation of either BRCA1 or BRCA 2 increases the susceptibility to ovarian cancer due to loss of self-protection of cells in response to DNA damage (Neff. et al., 2017). EOC with homologous recombination deficiency (BRCA 1/2 mutations) rely on PARP for DNA repair. PARP is an enzyme involves in the repair of single strand DNA breaks by base excision repair whereas BRCA 1/2 proteins involve in repair of double strand DNA breaks through homologous recombination repair pathway. Since most of the ovarian cancer types exhibit BRCA mutations, PARP inhibitors can cause accumulation of DNA damage in BRCA defected ovarian cancers (Monk and Anastasia., 2016) Hence, synthetic PARP inhibitors are a potential targeted approach for the OC with BRCA mutations (Petrillo et al., 2016). PTEN genes mutations also contribute to the ovarian carcinogenesis. The mutations in PTEN gene results in alterations in PI3K/AKT pathway, which results in survival of cancer cells by evasion of apoptosis (Saad. et al., 2010). Besides BRCA, p53, and PTEN mutations, ovarian cancer often exhibit BRAF, RAS, ARID1A mutations (Banerjee and Kaye., 2013, Rescigno et al., 2013)

1.3.4.2 Promoting inflammation in OC

The correlation between severe inflammation and OC progression is well understood over the years. Upregulation of several pro-inflammatory mediators and cytokines, which are produced by TNF- α , and interleukins (IL-6 and IL-8) were observed in EOC (Macciò and Madeddu., 2012, Petrillo et al., 2016). Several pro-inflammatory mediators are released during the ovulation process, and repair process followed by the release of ovum. The incessant ovulation results in exposure of OSE to inflammatory environment, which may leads to the carcinogenesis (Figure 1-5) (Macciò and Madeddu., 2012). COX enzymes are responsible in maintaining the inflammatory status in ovarian cancer. Particularly COX-2 is highly expressed in non-mucinous ovarian cancer cancer. Therefore targeting COX enzymes could be a potential target for inflammation in advanced stages of OC (Macciò and Madeddu., 2012).

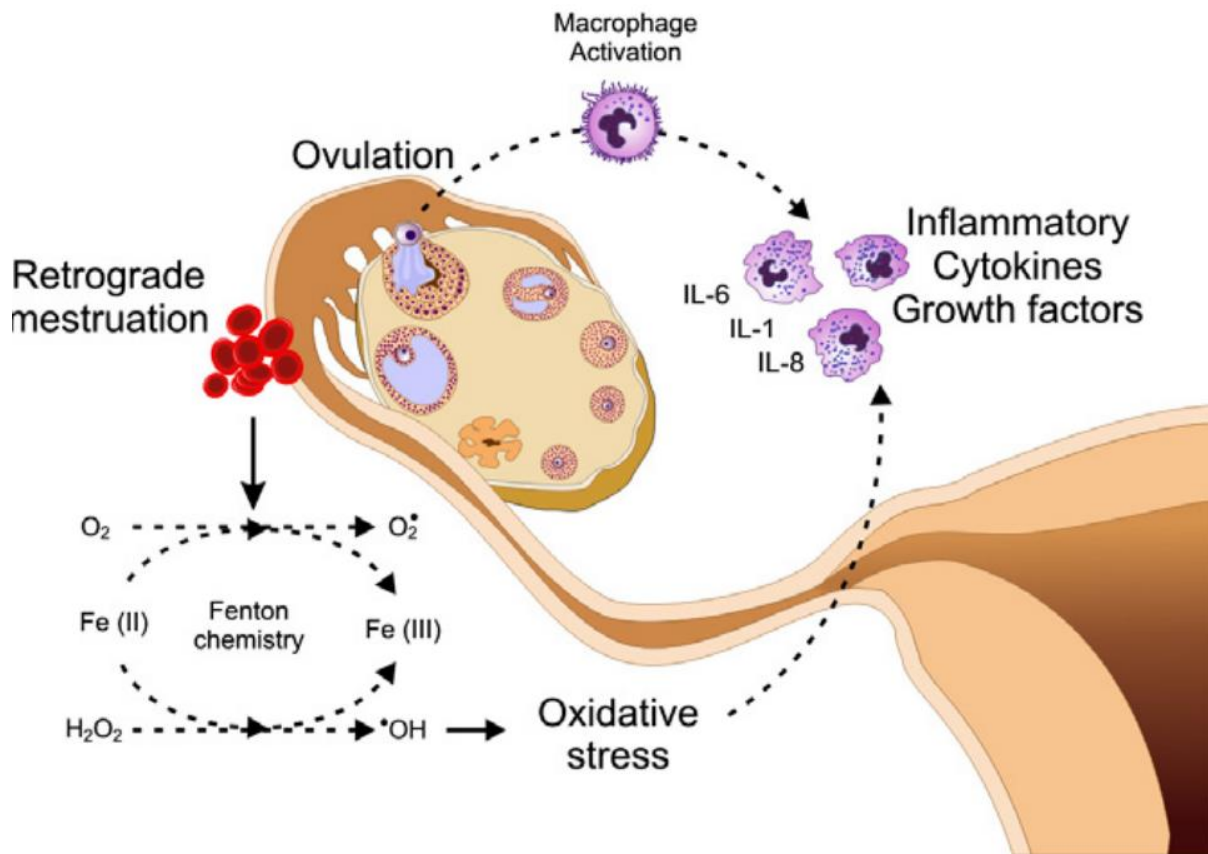


Figure 1-5. The role of inflammation in the development of ovarian cancer (Macciò and Madeddu., 2012)

1.3.4.3 Evading immune destruction

Ovarian cancer creates tumour microenvironment with immunosuppressive factors to evade immune system. Studies has shown that mutation in PTEN and BRCA2 leads to loss of T cells, which contributes to immunodeficiency in ovarian cancer (Jeong et al., 2015). The upregulation of immunosuppressive cytokines such as TGF- β and IL-10, PD-L1 (Programmed Death- Ligand1), and VEGF was observed in peritoneal cavity of ovarian cancer patients. Targeting the immunosuppressive factors could be a potential pharmacological strategy to restore immune system competence in OC (Latha. et al., 2014, Petrillo et al., 2016).

1.3.4.4 Angiogenesis and metastases in OC

OC induces angiogenesis by upregulating the angiogenetic stimulator VEGF. Studies have shown an increase VEGF expression in ovarian tumour tissue, cystic and ascites fluids, and serum of EOC patients. Mutated p53 in ovarian cancer upregulates hypoxia induced factor-1

(HIF-1). The upregulated HIF-1 increases the expression of VEGF. Studies also showed that mutations in KRAs and HRAS genes in ovarian cancer also responsible for over expression of VEGF (Brown et al., 2000, Lengyel., 2010)

The ovarian cancer initiates the invasion and metastases by detaching from primary site of origin and form multi- cellular aggregates. The cellular aggregates travel through peritoneal cavity by ascites. Membrane protein type 1 and 2 are proteolytic enzymes, which enable the detachment of OC cells from site of origin. Omentum, right diaphragm and small bowel mesentery of peritoneum are the most common secondary sites of ovarian metastasis. Integrins and CD44 produced by OC cells helps in binding of OC cells to mesothelium basement membrane of metastatic site. Fas ligands secreted by OC tumour enables the invasion into mesothelial cells. Once OC cells invade through mesothelial cells, they binds to collagen-I of the sub-mesothelial membrane, which enables the tumour to invade extracellular matrix (Lengyel., 2010). Targeting VEGF, Fas ligands, and collagen 1 by using antibodies such as $\alpha 2\beta 1$ could be potential approaches for treating advanced stages of ovarian cancer.

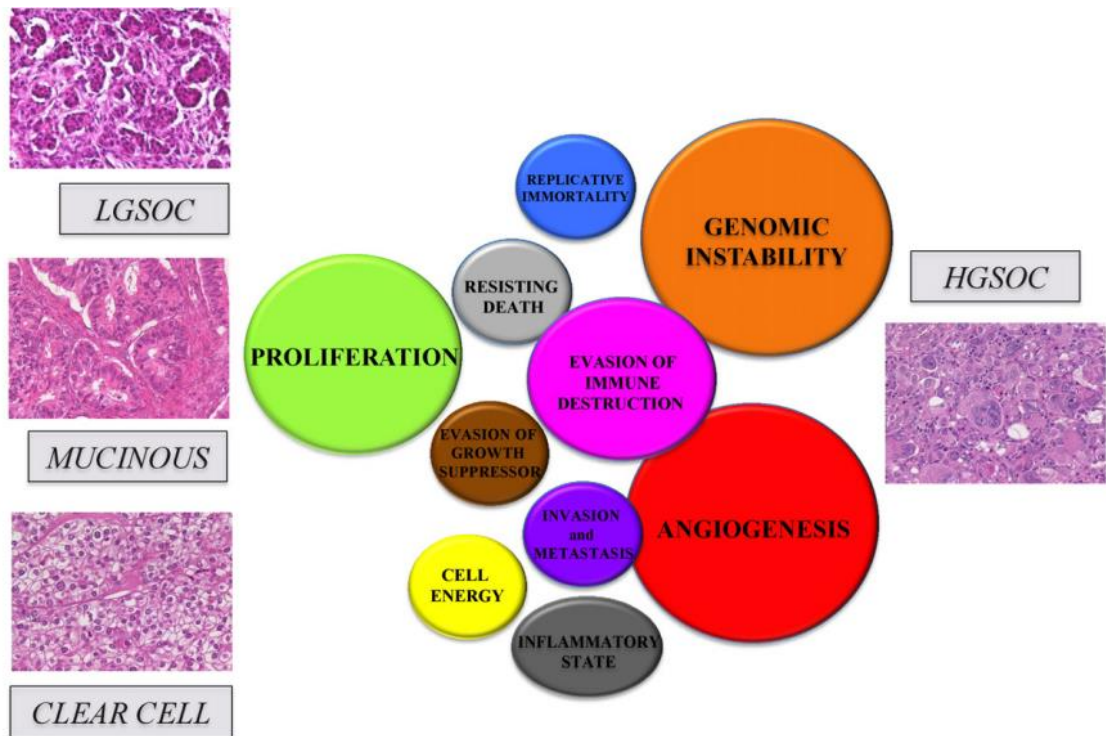


Figure 1-6 Relevance of cancer hallmarks in biology to epithelial ovarian cancer histotypes (Petrillo et al., 2016)

1.3.5 Surgical stages of ovarian cancer

Ovarian cancer is a surgically staged disease; the stages of ovarian carcinoma are classified based on the extent of metastasis by a tumour examined surgically. Stage I is confined to one or both the ovaries, stage II affects organs in the pelvic region, in stage III metastasis occurs beyond the pelvic region into the upper abdomen cavity, and stage IV involves the spread of tumour cells outside the peritoneal cavity which generally affects the liver and lungs. Metastases can occur through blood vessels to the parenchyma of the liver or lung, through the lymphatic system to nodes at the renal hilus or by merely shredding tumour cells into the peritoneal cavity. The absence of an anatomical barrier in the peritoneal cavity allows the widespread of metastasis. (Gubbels et al., 2010, Bast et al., 2009).

1.3.6 Treatment

Patients diagnosed with early stage (stage I) ovarian cancer is generally treated surgically with bilateral oophorectomy, hysterectomy and lymph node dissections. Chemotherapy is usually used for stages II, III and IV (Gubbels et al., 2010). Stages II and III of ovarian cancer are typically treated with platinum-based chemotherapy, for those diagnosed in advanced stages cytoreductive surgery followed by platinum- paclitaxel-based chemotherapy is suggested (Colombo et al., 2006). Carboplatin and paclitaxel are currently used as primary adjuvant therapy for over 95% women diagnosed with ovarian cancer (Boyd and Muggia., 2018).

Carboplatin is an alkylating agent involves in DNA damage. It covalently binds DNA to create adducts that forms both intra and inter crosslinks (Romero and Bast., 2012). Carboplatin was developed in 1980s to overcome the toxicities of cisplatin (Boyd and Muggia., 2018). Paclitaxel stabilises microtubules independent of energy (GTP independent) which results in unusual microtubule stability. This results in accumulation of disorganised microtubule array, which leads to G2/M cell cycle arrest (2010). Carboplatin (5-6 AUC) is administered to patients by intravenous (IV) fusion for 30- 60 minutes followed by IV infusion of 175-185 mg/m² paclitaxel over 3 hours (Bukowska et al., 2016).

The initial response of primary chemotherapy is very positive, but relapse can commonly occur within 2 years with the development of resistance. The platinum- resistant and recurrent patients have been treated by various agents including paclitaxel, docetaxel, topotecan and doxorubicin but none of them has proven to show more than 20% efficacy yet. A recombinant monoclonal antibody, Bevacizumab, is currently used along with carboplatin

and paclitaxel for stage III/IV relapsed cancer patients with platinum resistance. (Llauradó et al., 2014, Bukowska et al., 2016).

1.3.7 Chemotherapy challenges

Many chemotherapeutic drugs are used to treat ovarian cancer, but none of them has been found to be completely effective and safe because of de novo and acquired chemo resistance combined with the expression of immunosuppressive factors. The possible mechanisms for acquired resistance involved in the alteration of membrane transport, target enzymes and target molecules, enhanced DNA repair system and failure to apoptosis (Luqmani, 2005). The toxicity of established drugs is also one of the major problems in cancer chemotherapy. In case of ovarian cancer treatment, carboplatin/ paclitaxel has shown better effects compared to previously used chemotherapeutic combination cisplatin/ paclitaxel, but it did not solve the reoccurrence issue (Ozols, 2006). Besides the fact that carboplatin reduced ototoxicity and nephrotoxicity associated with cisplatin it increased the risk of haematological toxicities (Boyd and Muggia., 2018). The high fatality in advanced stages of ovarian cancer after reoccurrence is due to a small number of tumour cells, which survived during chemotherapy; remain dominant in the peritoneal cavity and grow progressively which may lead to further metastasis and the death of the patient despite the treatment (Ozols, 2006). Another challenge with carboplatin/ paclitaxel chemotherapy is significant induction of toxicities which include neuropathy, alopecia (hair loss) and myelosuppression(Ozols, 2006, Bast et al., 2009).

1.3.8 Current research in ovarian cancer treatment

Ovarian cancers have shown multidrug resistance; besides significant toxicities involved with current drugs indicates the importance of new approaches for the treatment of ovarian

cancer. Some of the potential new chemotherapeutic drugs, which are in under clinical research are listed below:

Olaparib (Lynparza) is a PARP inhibitor; it has shown antitumour activity in high-grade serous ovarian cancer cells independent of BRCA mutations. FDA approved Olaparib as oral medicine for recurrent ovarian cancers (Ledermann et al., 2012, FDA, 2017).

Bevacizumab commercially known as Avastin is a recombinant monoclonal antibody Ig1. It targets VEGF- A (Vascular endothelial growth factor). It has previously indicated anticancer effects on lung, colon and glioblastoma. Recently FDA approved it as a front-line chemotherapeutic drug for ovarian cancer. Bevacizumab is used in combination with paclitaxel and carboplatin for early stages of ovarian cancer. Bevacizumab as a single chemotherapeutic agent for the treatment of stage III and IV ovarian cancer patients (Natarajan et al., 2018, FDA, 2018). Cediranib and nintedanib are other VEGF inhibitors which are currently in clinical use (Natarajan et al., 2018).

Metformin is a potential chemotherapeutic drug for ovarian cancer, which is under phase II clinical trials. It is currently used for the treatment of type 2 diabetes (Buckanovich et al., 2017). Both preclinical and epidemiological studies have shown antitumor effects of metformin on breast, endometrial and gynaecological cancers. The clinical studies have shown that metformin regulates tumour growth by activating AMPK, which involves in inhibition of mTOR pathway. However, detailed mechanism of the drug action still to be elucidated (Irie et al., 2016)

VAL-083 is another drug which in clinical trials for ovarian cancer treatment. Preclinical results have shown positive results on cisplatin resistant ovarian cancer cells (Steino et al., 2013)

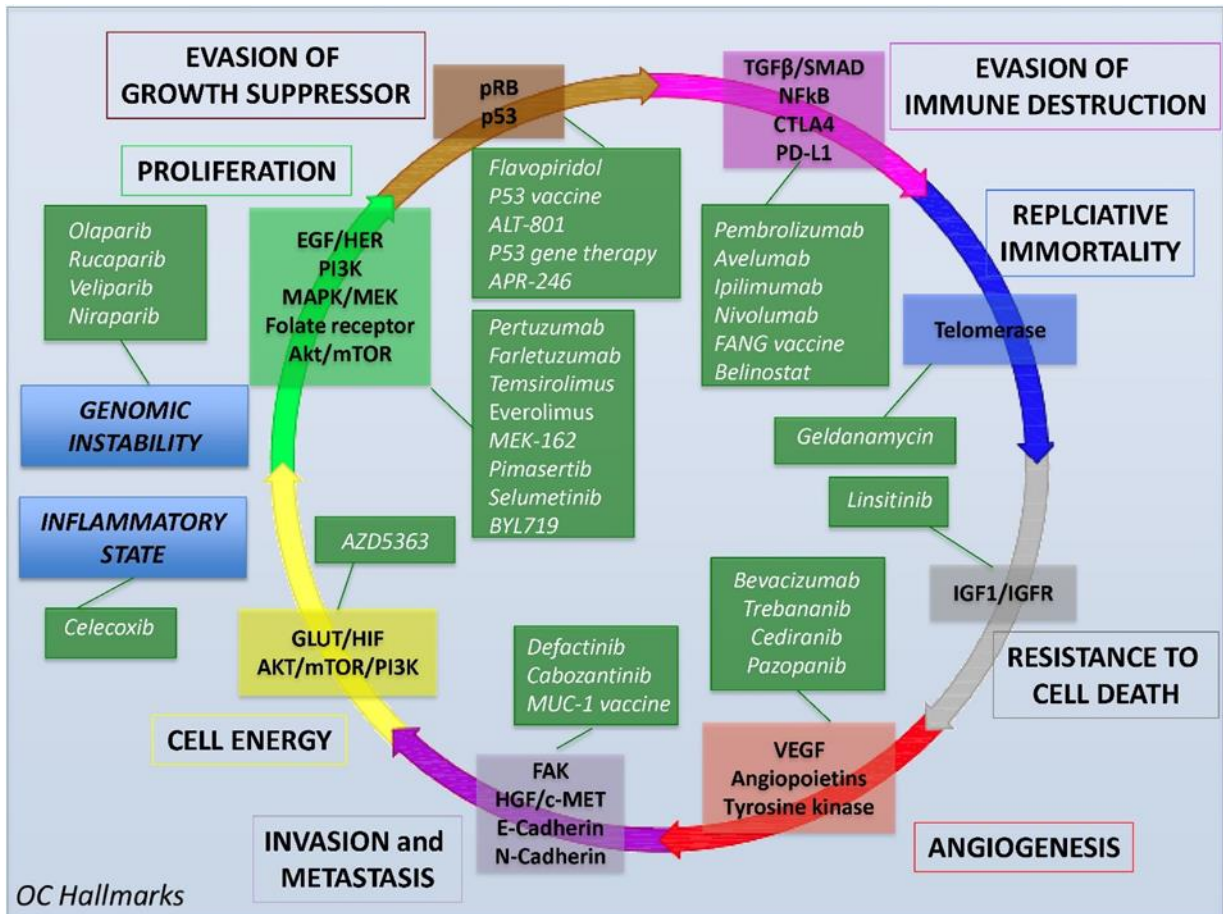


Figure 1-7. Current molecular target drugs (approved or under clinical investigation) based on hallmarks of ovarian cancer (Petrillo et al., 2016)

1.4 Cannabinoids

Cannabis has been used as a medicinal plant for many centuries by Asian and African countries for diseases such as malaria, rheumatic pains, constipation, diseases related to female reproductive organs, and also as an anaesthetic (Alexander et al., 2009) (Dariš et al., 2018). An example of the use of Marijuana in traditional therapy can be seen in Ayurvedic medicine in India, where it was used for neurological, respiratory, gastrointestinal, and infectious diseases (Dariš et al., 2018). However, lack of pharmacological investigations on toxicity meant that it did not become a mainstream medicine in the western world until the 19th century (Alexander et al., 2009, ASHTON, 1999). In the mid-19th century, the analgesic, antiemetic and antispasmodic effects of cannabis extracts were reported for the first time in

Europe (Shevyrin. and Morzherin., 2015, Dariš et al., 2018). In 1851, the cannabis extracts, and resin glands from the plant were accepted as a medicine by the US Pharmacopoeia. However, due to increased use of cannabis for recreational purposes, lack of consistency in the preparation of the extracts, poor investigation in isolating medically active compounds from the cannabis, and extensive research in alternative forms of medicine, the progression of cannabis as a mainstream medicine was aborted (Dariš et al., 2018). Studies conducted in the late 20th century on cannabis lead to the identification, and extraction of the pharmacologically active components, named cannabinoids (ASHTON, 1999). The identification of significant medical cannabinoids and recent legislative changes have improved the possibility of drugs derived from cannabis been approved for use by regulatory bodies (Dariš et al., 2018).

Cannabinoids are the unique family of chemically active components derived from resin glands of *Cannabis* plant. There are over 100 cannabinoids, which have been identified in *Cannabis sativa* (Reekie et al., 2017). Cannabinoids are classified into three main subtypes, i) phytocannabinoids, which are produced in plants, ii) synthetic cannabinoids which are chemically related analogues, and activate similar primary targets of phytocannabinoids, and iii) endogenous cannabinoids, which are naturally produced in humans and animals, and are a derivate of arachidonic acid (Alexander et al., 2009, Caffarel et al., 2012, Sarfaraz et al., 2008)

1.4.1 Endocannabinoids

Endocannabinoids are structural analogues of THC produced biologically in mammals. Endocannabinoids are endogenous ligands that often binds to cannabinoid receptors (Hanuš et al., 2016). Endocannabinoids are structurally saturated or unsaturated amides found in

mammals. Anandamide and 2-arachidonoylglycerol are the major endocannabinoids, which are widely studied.

The biosynthesis, transportation, biological activity, and degradation of endocannabinoids collectively referred to as the endocannabinoid system (Pertwee, 2006, Shevyrin and Morzherin., 2015). ECS consists of endogenous ligands, cannabinoid receptors, and the enzymes involved in the metabolism of the ligands. Fatty acid amide hydrolase (FAAH), and monoacylglyceride lipase (MAGL) are the metabolic enzymes known to degrade the AEA and 2-AG respectively (Izzo et al., 2009, Dariš et al., 2018). The endocannabinoids function by binding and activating cannabinoid receptors of the central nervous system as a retrograde messenger and involved in inhibition of neurotransmitter. Most of the endocannabinoids discovered act as agonist for cannabinoid receptors. However, virdhamine has shown antagonistic effects on CB1 receptors (Pertwee, 2006)

The regulation of food intake, emotional homeostasis, inflammatory and stress related responses, immune system are other functions performed by ECS. ECS also reported engaging in cancer cell signalling. ECS gained the attention of pharmacologists as a potential therapeutic target due to the ability to regulate many biological functions. Targeting the cannabinoid receptors and inhibiting the enzymes involved in degradation of endocannabinoids are viable strategies for ECS based therapies for neuropsychiatric conditions (Pertwee, 2006, Dariš et al., 2018, Shi et al., 2017).

Most of the endocannabinoids discovered act as agonist for cannabinoid receptors. However, virdhamine has shown antagonistic effects on CB1 receptors (Pertwee, 2006)

1.4.2 Cannabinoid Receptors:

The pharmacological activity of cannabinoids can be defined by their ability to activate receptors and its action depends on concentration, duration of exposure and type of the cells and their ligands (Cridge and Rosengren, 2013)

The lipophilic nature of cannabinoids made researchers to assume that the biophysical activity of cannabinoids exerted by direct interaction with lipid bilayer membrane of targeted cells. In 1990, an orphan G- coupled protein receptor named SKR6 (obtained from rat cerebral cortex cDNA library) was found to be a receptor for Δ^9 -tetrahydrocannabinol (Δ^9 -THC) pharmacological activity. This discovery of first cannabinoid receptor SKR6 was later named CB1. Three years later another G- coupled protein receptor named CX5 (later renamed CB2) was identified as cannabinoid receptor in human promyelocytic leukemic cell line HL60 (Pertwee et al., 2010, Pertwee, 2006).

CB1 receptors are mainly expressed in the central nervous system at high levels in basal ganglia, cerebellum, hippocampus and cerebral cortex. The activation of CB1 can affect the process of cognition and memory, induce analgesia and controls the motor function. It is also found in peripheral nervous system and extra- neural tissues include spleen, eyes, testis and uterus, adipocytes and ileum where its activation also mediates the psychotropic properties (Bifulco et al., 2006).

CB2 receptors are mainly expressed in cells and organs of immune system includes spleen marginal zone, lymph node cortex, secondary follicles in tonsils. The activation of CB2 receptors involved in differentiation and migration of immune cells and cytokines suggesting its role in immune responses. CB2 receptors are unrelated to psychotropic properties of cannabinoid agonists (Bifulco et al., 2006; Pertwee et al., 2010). Both receptors act on

secondary messenger system of cells by regulating Ca⁺ and K⁺ ion channels and involves in formation of cAMP (ASHTON, 1999).

Cannabinoid agonists were found to exert pharmacological activities beyond CB1 and CB2 receptors suggested the possibility of other receptors. However, IUPHAR committee proposed a set of guidelines to classify a receptor as a cannabinoid receptor. The five essential criteria for nomenclature of a new cannabinoid receptor include: i) the receptor should be activated by established CB1/ CB2 ligand at its orthosteric site, ii) the receptor should be show sequence amino acid homology with CB1 or CB2 receptors if it is a GPCR, iii) an established CB1/ CB2 agonist should activate the receptor at a physiological concentration, iv) it should not be an established non CB receptor, and it should not show higher potency and intrinsic affinity to a non-cannabinoid receptor compared to endocannabinoid, and V) it should be expressed in mammalian cells that express active endogenous ligands (Console-Bram et al., 2012, Pertwee et al., 2010)

GPR55 is potential cannabinoid receptors from G- coupled protein receptor (GPR) family. It has larger evidence as a cannabinoid receptor because of its ability to mediate the pharmacological responses of many phytocannabinoids, synthetic cannabinoids and endocannabinoid ligands. GPR55 receptors are highly abundant in posterior root ganglion of neurons, involves in upregulation of intracellular calcium upon activation by various cannabinoids (Leyva-Illades and DeMorrow, 2013, Lauckner et al., 2008). *In vivo* studies have shown that GPR55 mediates the anxiolytic effects in mice by down regulating the glutamate receptors GluA1 and GluN2A expression (Shi et al., 2017). GPR55 associated with various physiological activities, and the dysfunction can lead to several diseases. GPR55 involve in regulation of vasculature, regulation of motility in gastrointestinal tract, anti- inflammatory

responses in acute pancreatitis and pro-inflammatory in colitis. GPR55 upregulates insulin secretion and regulate glucose tolerance in pancreases. The physiological function of GPR55 was reported in various cancers including ovarian, breast, prostate, glioblastoma and cholangiocarcinoma (Figure 1-8) (Leyva-Illades and DeMorrow, 2013). Studies have shown that autocrine release of endocannabinoid L- α -lipophosphatidylinositol (LPI) mediates tumour invasion and metastasis to mediate cancer proliferation and angiogenesis in ovarian cancer through putative cannabinoid receptor GPR55 in ovarian cancer cells (Leyva-Illades and DeMorrow, 2013).

Although GPR55 lack CB binding pocket, and insufficient amino acid sequence homology with both CB1 (13.5%) and CB2 (14.4%) receptors, cannabinoids still able to activate the receptor and mediates physiological functions makes GPR55 an atypical cannabinoid receptor (Pertwee et al., 2010).

GPR18 and GPR119 are G-coupled receptors reported to activate by cannabinoids, however, lack of sufficient evidences robust to rename them as cannabinoid receptor isoforms. Transient receptor potential cation channel V family member 1 (TRPV 1) discovered as another potent cannabinoid receptor activated by endogenous cannabinoids AEA (Anandamide) and NADA (N- Archidonoyl dopamine) (Cridge and Rosengren, 2013).

The involvement of ECS in cancer progression is not illustrated completely (Javid et al., 2016). However, both the upregulation of endocannabinoids and cannabinoid receptors, and the down regulation by activating endocannabinoid degrading enzymes were observed in various tumours pathogenesis. Pre-clinical studies on anti- cancer properties of cannabinoids have shown that cannabinoids induce apoptosis by activating cannabinoid receptors in many cancers (Chakravarti et al., 2014, Dariš et al., 2018).

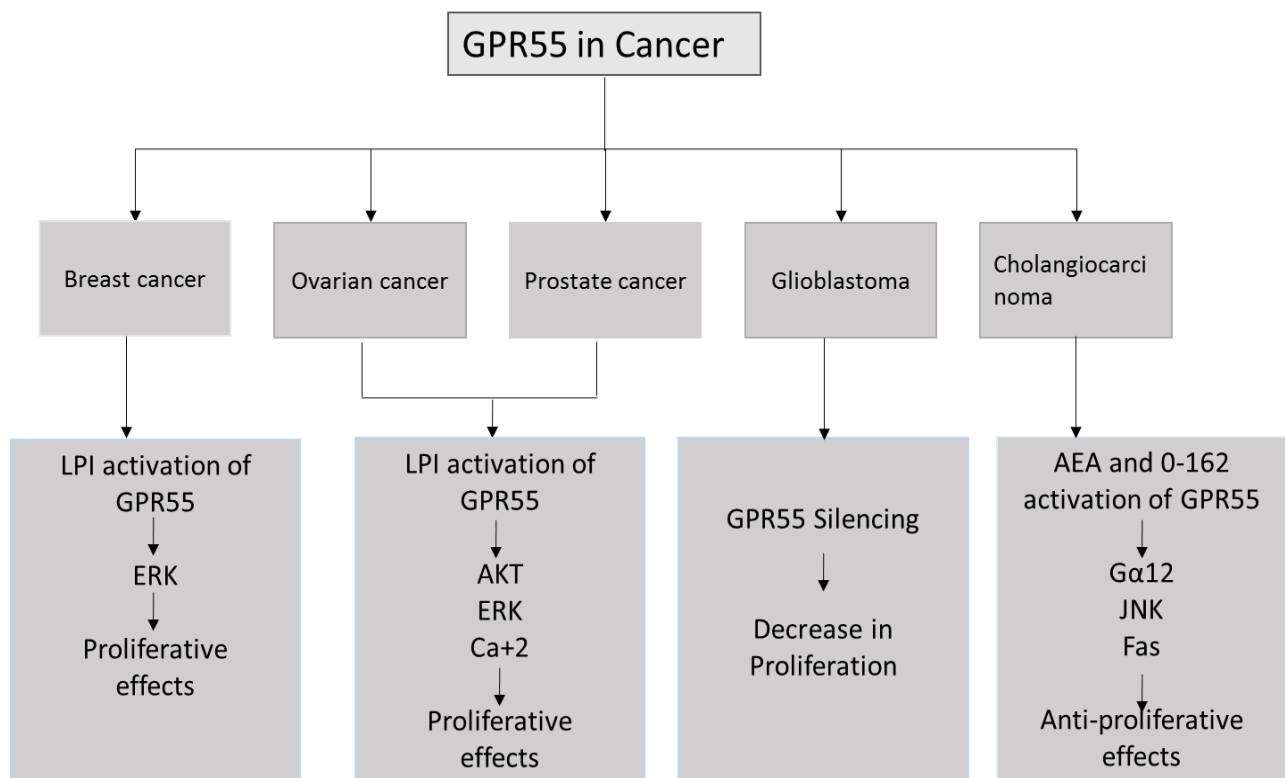


Figure 1-8. The known physiological role of GPR55 in cancer. Adapted from (Leyva-Illades and DeMorrow, 2013)

1.4.3 Phytocannabinoids:

Phytocannabinoids are a group of C₂₁ terpenophenolic compounds derived from cannabis plant that exert the pharmacological effects by binding to the cannabinoid receptors. Among the phytocannabinoids discovered so far, Δ^9 – tetrahydrocannabinol (THC), and CBD are the most abundant phytocannabinoids, followed by cannabiol (CBN), cannabichromene (CBC), Δ^8 – tetrahydrocannabinol (THC), cannabidiolic acid (CBDA), cannabidivarin (CBDV), and cannabigerol (CBG) (Dariš et al., 2018, Reekie et al., 2017).

THC exerts many neuropathological functions through cannabinoid receptors, which includes the modulation of neuro transmitter release, regulation of pain perception, and many gastrointestinal, cardiovascular activities. The anti- cancer properties of THC also been reported in human breast, prostate and glioma cells (Dariš et al., 2018). Although, THC has

shown many medicinal properties, it was limited to clinic use due to its well-known psychotropic activities. CBD is a structural analogue to THC however; it does not have any psychotropic activities. Both the compounds have been widely studied for their medicinal properties. The combination of THC and CBD has shown analgesic efficacy related to neuropathic pain. It currently used as an oral spray to treat spasticity and pain resulting from multiple sclerosis under commercial name Sativex (Reekie et al., 2017, Alexander et al., 2009, Caffarel et al., 2012, Sarfaraz et al., 2008, Portenoy et al., 2012).

1.4.4 Synthetic cannabinoids

Synthetic cannabinoids gained the attention of pharmaceutical companies in the late 1970s. In 1979, Pfizer synthesised a THC analogous called CP47497 as a potential analgesic drug. The clinical studies showed that CP47497 as an effective analgesic compound. However, later studies have shown the higher narcotic effects of CP47497. The same company synthesised another THC analogue (CP55940). However, this compound exhibited even higher narcotic activities. Although CP55940 was failed to use as an analgesic drug, the research on this compound later lead to the finding of the cannabinoid receptor 1 (CB1). Besides the above compounds, nabilone was another synthetic THC analogue, which was used as an antiemetic drug under chemotherapy for cancer treatment, despite its narcotic effects (Shevyrin. and Morzherin., 2015). HU- 210 is another synthetic cannabinoid tested as an analgesic drug that had failed in clinical trials due to psychoactive nature, later a stereoisomer was developed from HU-210 called HU- 211, which has no affinity for CB1 receptor meaning no psychoactive properties. This drug is currently under clinical trials (Shevyrin. and Morzherin., 2015).

Despite the attempts to use synthetic cannabinoids in medical pharmacology, it has gained popularity for the drug abuse in Europe, Russia, and North America. In early 2000, synthetic

drugs CP47497, and JWH- 018 were sold as online herbal smoking blends under the commercial name 'k2' or 'spice'. Over the years, many countries including Germany and Russia tried to implement legal restrictions to control misuse of synthetic cannabinoids. However, it did not wholly restrict the illegal drug trade. Therefore, identification and development of medically significant synthetic cannabinoids with less psychoactive effects remain challenging (Shevyrin. and Morzherin., 2015, Tai and Fantegrossi, 2014).

1.4.5 Cannabinoids and their anti- cancer activity:

Cannabinoids have been used in cancer therapy to reduce the side effects include nausea, alleviate pain, and lack of appetite. However, pre- clinical studies have shown anti- cancer properties of cannabinoids for many cancers in mammalian cells and biological models (Dariš et al., 2018).

Cannabinoids have been attracting a great deal of interest as a source of anti- cancer drugs since the early 1970s because of their ability to regulate cell growth, invasion, and cell death (Guzmán et al., 2001, Dariš et al., 2018). The anti- tumour ability of cannabinoids was first reported by Munson et al. in 1975 where cannabinoids were found to be involved in the inhibition of tumours and prolonged life of mice bearing Lewis lung adenocarcinoma. The involvement of cannabinoid receptors in antitumor genic effect of cannabinoids was described by Galve- Ropreh in 2000, subsequently many independent studies have reported anti- tumour activity in vitro on different cancer cell lines including lung, glioma, pancreas, lymphoma, prostate, uterus and breast carcinoma cells (Alexander et al., 2009).

Cannabinoids have to be shown to be involved in inhibiting tumour cells by altering the cell signalling receptors further inducing apoptosis or inhibiting angiogenesis of tumour cell

(Velasco et al., 2007), it also has been reported that cannabinoids inhibits the tumour metastasis and induce growth arrest (Blázquez et al., 2008).

1.4.6 Non-psychoactive cannabinoids as potential anticancer drugs:

Psychotropic cannabinoids such as Δ^9 - tetrahydrocannabinol (THC) have shown a wide range of medicinal properties including antiemetic effects and tumour inhibition (Alexander et al, 2009). However, the psychoactive properties, and the possible risk of the emergence of dependency and tolerance challenge its practical use in cancer treatment. Other than psychoactive properties, there were no significant side effects with cannabinoids has been observed, so far the general side effects seen include dry mouth, tiredness, and dizziness. However, tolerance to the common side effects is observed within a short period. This gives hope for non-psychoactive cannabinoids as a potential therapeutic approach for cancer treatment (Ostadhadi et al., 2015, Dariš et al., 2018).

Table 1-1. Different types of drug- receptor interactions.

Drug-Receptor Interactions	Pharmacological definition
Agonist	A molecule or drug that can activate a receptor and induce a cellular change
Full Agonist	An agonist that can produce maximum amount of response that the tissue capable of producing
Partial Agonist	An agonist that that cannot produce full response even with maximum concentration
Inverse Agonist	A molecule or drug that can binds receptor and induces the opposite effect from known agonist
Antagonist	A molecule or drug that can binds to receptor and attenuates the effect of an agonist
Competitive Antagonist	An antagonist that can reversibly binds to receptor with no efficacy
Insurmountable Antagonist	An antagonist that irreversibly binds to receptor and reduces the efficacy of agonist

1.4.7 Cannabidiol (CBD)

CBD (CBD) is one of the major non-psychoactive phytocannabinoids, highly abundant in cannabis plant with no psychotomimetic properties. It was first isolated by Adam and colleagues in 1940. In 1963, Mechulam and Shvo determined the stereo chemical structure of CBD (**Figure 1-9**). The research carried out in 1970s showed CBD to have the antiepileptic action. However, clinical trials were not progressed further as the preliminary screening results showed uncertain efficacy even with a large dose. The strong antioxidant effect and Ca^{+2} homeostasis nature of CBD has many proven pharmacological effects include anti-inflammatory, analgesic, neuroprotective, anxiolytic, antipsychotic and anti-ischemic effects (**Figure 1-11**) (Izzo et al., 2009, Zuardi, 2008).

Unlike many cannabinoids, CBD has low affinity for CB1 and CB2 receptors. The studies have shown CBD acts as an antagonist towards the CB1, and inverse agonist towards CB2. CBD has been shown to have multiple molecular targets. The ability of CBD to regulate endocannabinoid system has gained the attention as a therapeutically potential compound. CBD has shown biphasic effects on oxidative stress, immune system, which indeed demonstrated the anti-tumour and neuroprotective nature of the compound. Regulation of Ca^{+2} levels, induction of ROS, regulating ATP and proton leak suggest that the involvement of mitochondria is CBD cellular mechanism (Dariš et al., 2018, Kosgodage et al., 2018b).

The anticancer properties of CBD were first examined in 2000 on glioma cells, which later extended to human meroblastic leukaemia cells (Blázquez et al., 2008, Caffarel et al., 2012). CBD has shown to induce cytotoxicity in human leukaemia cells by a caspase-dependant apoptosis pathway. It was also involved in oxidative stress by enhancing NOX4 (NADPH oxidase) and p22phox proteins levels in cytoplasm (Blázquez et al., 2008, Izzo et al., 2009)

Among 8 non-psychotropic phytocannabinoids tested, CBD has shown higher anti-proliferative/ pro-apoptotic properties, and highest potency with IC₅₀ values between 6 µM and 10.6 µM on MCF7 breast cancer cells. CBD exerted concentration dependant autophagy, and apoptosis induction in breast cancer cells. The inhibition of breast tumour metastasis by regulating the Id1 genes was also observed (Izzo et al., 2009, Shrivastava et al., 2011, Ligresti et al., 2006, Caffarel et al., 2012)

CBD has shown anti- cancer effects in prostate cancer cell lines at a concentration where it has shown significantly less cytotoxicity to non-cancer cells. Further investigation of CBD cytotoxic mechanism on prostate cancer cells has shown the down regulation of CB1, and CB2 receptors. The down regulation of pro- inflammatory interleukins (IL-6& IL-8), vascular endothelial growth factor (VEGF) and prostate specific antigens were observed (Kosgodage et al., 2018a, Sharma et al., 2014, Dariš et al., 2018).

CBD has shown to regulate Exosomes and macrovesicles (EMV). EMVs are extracellular vesicles, which involve in various physiological and pathological pathways including cell migration, and angiogenesis. CBD has shown anti- cancer activity on prostate, breast and hepatocellular cancer cells by inhibiting the EMV (Kosgodage et al., 2018a). Although CBD exerted cytotoxicity towards cancer cells in multiple pathways, the molecular mechanisms responsible for CBD selective cytotoxicity on different tumour cells has yet to be discovered (Massi et al, 2012).

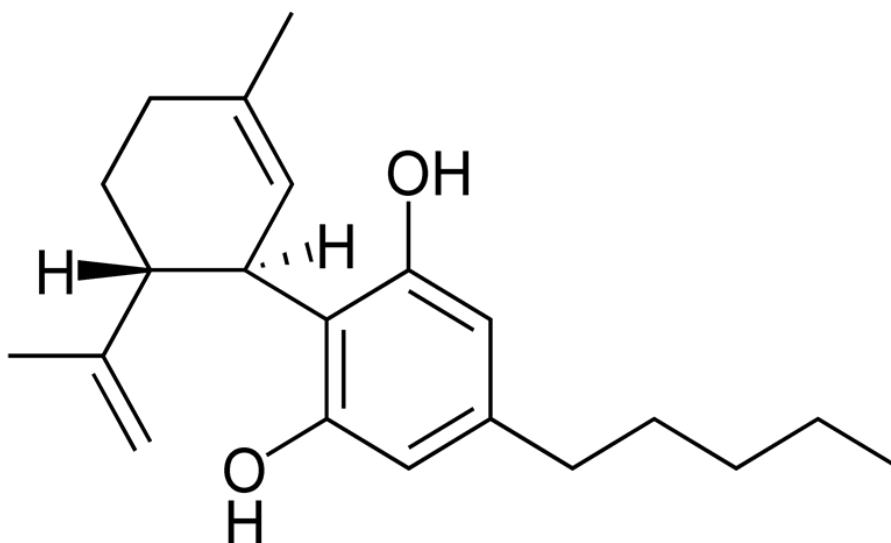


Figure 1-9. Chemical structure of Cannabidiol (CBD)

1.4.8 Cannabigerol (CBG)

CBG is a non-psychoactive phytocannabinoid. It was isolated by Goani and Mechulam in 1964 when they separated hexane extract of hashish on florisil (**Figure 1-10**). Similar to CBD, CBG does not exert any psychoactive properties (**Figure 1-11**). CBG was shown to have antibacterial and antiglaucoma properties (Figure 1-11) (Borrelli et al., 2013). CBG has shown to antagonise the antiemetic effects of CBD (Rock et al., 2011). CBG has weak affinity for cannabinoid receptors CB1 and CB2. CBG is believed to exert its mechanism of action through TRP receptor channels. It has shown weak agonistic effects to TRPV1 and TRPV2, a potent agonist to TRPA1 and antagonist to 5-HTA1 and TRPM8 receptors (Borrelli et al., 2014).

CBG exerted beneficial effects on Inflammatory Bowel Disease (IBD) *in vivo*. The mechanistic studies of such effects showed that CBG possibly is involved in the reduction of oxidative stress in the intestinal mucosa. The destruction of intestinal mucosa through oxidative stress has been shown to be a significant factor in the cause of IBD (Borrelli et al., 2013). *In vivo* studies on a mouse model reported the neuroprotection nature of CBG in Huntington disease.

CBG reduced the aggregation of mutant Huntington in an in vivo model by up-regulating peroxisome proliferator-activated receptor and brain-derived neurotrophic factor (BDNF) (Valdeolivas et al., 2015)

The cytotoxic effect of CBG is also reported in breast cancer cells with better IC50 values next to CBD. Recent studies have shown that CBG also inhibits colon carcinogenesis by acting as TRPM8 antagonists. The mechanistic studies of cytotoxicity of CBG on colorectal cells have shown ROS production, ER stress-related caspase-dependent apoptosis (Nishitoh, 2012, Borrelli et al., 2014, Ligresti et al., 2006). Although CBG was identified and extracted around same time as other cannabinoids, the pharmacological activity of CBG is poorly investigated compared to CBD, and THC. However recent advancement in the identification of CBG pharmacological activities have been gained the attention of the scientific community (Borrelli et al., 2014, Ligresti et al., 2006, Navarro et al., 2018)

Non-psychoactive nature, ability to regulate endocannabinoids, induction of ROS, apoptosis and potentially targeting the transient receptor channels TRP channels indicates that CBG is one the potential cannabinoid for cancer treatment, which requires further investigation.

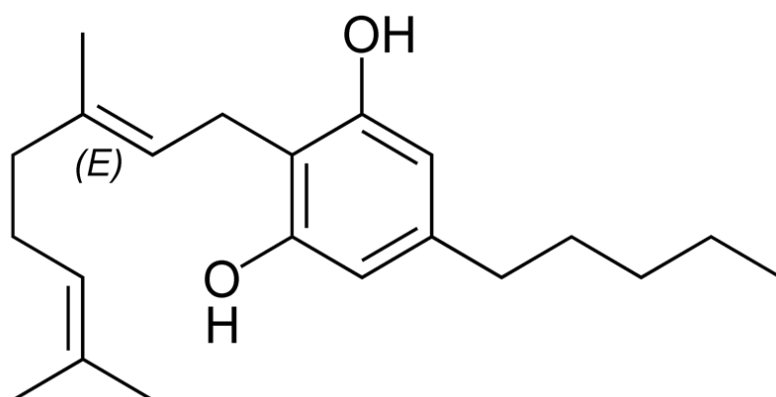


Figure 1-10. Chemical structure of Cannabigerol (CBG)

Table 1-2. Pharmacological effects of CBD and CBG discovered so far

Pharmacological effect	CBD	CBG
Antibacterial	✓	✓
Antiproliferative Anti- cancer	✓	✓
Antiemetic	✓	
Antispasmodic	✓	
Anti- epileptic	✓	
Antipsychotic	✓	
Anti- ischemic	✓	
Anxiolytic	✓	
Antidiabetic	✓	
Antipsoriatic	✓	
Analgesic	✓	✓
Anti-inflammatory	✓	
Bone- stimulant	✓	✓
Immunosuppressive	✓	
Intestinal anti- prokinetic	✓	
Neuroprotective	✓	✓
Vasolorelaxant	✓	

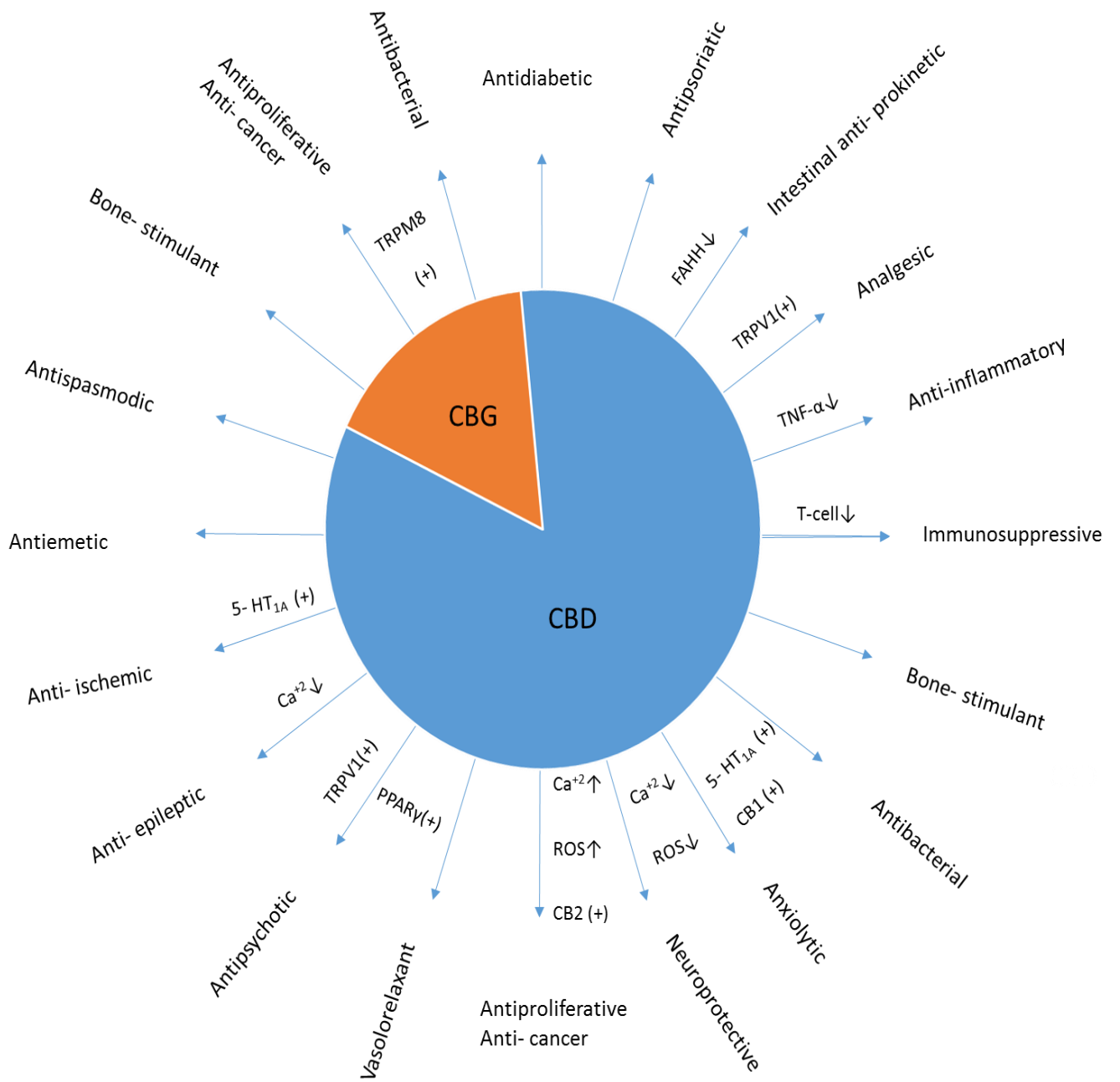


Figure 1-11 pharmacological effects of CBD & CBG, and their proposed mechanism of action. Adapted from (Izzo et al., 2009). ↑ indicates increase levels, ↓ indicates decrease in levels, + indicates activation of the receptor.

1.5 Mechanisms associated with anticancer activity of cannabinoids

Evading apoptosis and alterations in cell cycle are critical hallmarks in tumour progression.

The mechanism studies of anti-cancer activity of the cannabinoids have reported the induction of apoptosis, oxidative stress and inhibition of cell proliferation by cell cycle arrest (Dariš et al., 2018, Xu et al., 2015)

1.5.1 Apoptosis

Apoptosis is a highly conserved mechanism where a cell intentionally undergoes programmed death. It has a vital role in various physiological processes including embryonic development, regulation of the immune system, and cell turnover. Apoptosis generally functions to maintain homeostasis of the cell population in a tissue; it also works as a defensive mechanism when irreversible damage has occurred to cell by diseases or the noxious agents. The imbalance in apoptosis can lead to many diseases including neurodegenerative diseases, ischemic damage, and autoimmune disorder where uncontrolled apoptosis occurs- Too little or no apoptosis would lead to cancer (Elmore., 2007)

Morphological changes involved in apoptosis are cell shrinkage, where cell reduces in size with dense cytoplasm, pyknosis (irreversible condensation of chromatin) followed by membrane blebbing. Membrane blebbing associated with a process called budding which is involved in karyohexis (disruption of nuclear membrane) followed by distribution of cell fragments to apoptotic bodies. Later these apoptotic bodies are subsequently engulfed by tingled body macrophages, parenchymal cells and neoplastic cells and digested by phagolysosomes. Unlike necrosis, where cells undergo energy independent sudden death, apoptosis does not induce any inflammatory reactions. Apoptotic bodies are quickly engulfed

by phagolysosomes avoids secondary necrosis and lysosomes avoid activation of inflammatory cytokines (Elmore., 2007, Hengartner., 2000)

Apoptosis is a highly sophisticated mechanism, which is mainly classified in to two types: extrinsic or death receptor pathway and intrinsic or mitochondrial pathway. Both involve in activation of a set of cysteine proteases called caspases. Caspases are pro- apoptotic enzymes; possessing cysteine active site that target Asp- xxx substrate in a protein. Caspases target cytoskeletal proteins and disrupt cell integration thus inactivating the biological activity leading to cell death. Later studies have shown apoptosis follows another pathway independent of caspases called T- cell mediated cytotoxicity and perforin- granzyme mediated cell death. All the pathways lead to same terminal called execution pathway, which is mediated by caspase 3, 6, and 7 activation (Hengartner., 2000, Elmore., 2007)

1.5.1.1 Extrinsic/ Death receptor pathway

The extrinsic pathway of apoptosis is involved in trans-membrane death receptor mediated interactions. Extrinsic pathway events are initiated by the binding of clustering receptors with homologous ligands. Fas ligand bind to the Fas receptor which further binds to adapter protein containing death receptor domain FADD, TNF ligand bind to the TNF receptor which further binds to adapter protein containing death receptor domain TRADD. They further associate with procaspase- 8 to form the death receptor signalling complex (DISC), resulting in formation of caspase-8 by autocatalytic activation of procaspase 8. The activated caspase 8 triggers the execution pathway. C-FLIP and Toso are the proteins, which regulates extrinsic apoptotic pathway (Elmore., 2007, Locksley et al., 2001).

1.5.1.2 Intrinsic/Mitochondrial pathway

The mitochondrial pathway is a non-receptor based mechanism based on intracellular signals. These signals can be either positive or negative. Negative signals include lack of growth factors, cytokines or hormones whereas positive signals include hypoxia, hyperthermia, toxicity and radiations, infections and free radicals.

The intracellular signals initiate the pathway by depolarising the mitochondrial membrane, this forms mitochondrial membrane permeable transition (MPT) pores. MPT pores result in the release of two sets of proteins into cytosol, which results in apoptosis. The first set of proteins include cytochrome c, smac/ DIABLO and a serine protease H2rA2/omi (Saelens et al., 2004). Cytochrome c binds and activates apaf-1 and procaspase 9 forms apoptosome, which leads to activation of caspase 9. Caspase 9 further triggers the execution pathway. smac/ DIABLO and H2rA2/omi inhibits the IAP (inhibitor of apoptotic proteins) and promotes apoptosis(Elmore., 2007)

The second set of pro- apoptotic proteins includes endonuclease G, CAD and AIF, which are released only after caspase-9 activation. AIF released from mitochondrial membrane translocated to the nucleus, results in DNA fragmentation and condensation of chromatin. Chromatin is further cleaved into oligonucleosomal DNA fragments by endonuclease G. The oligonucleosomal G is further cleaved into small DNA fragments by CAD proteins (Elmore., 2007, Susin et al., 2000).

The mitochondrial apoptotic pathway is regulated by proteins belong to the BC-2 family. Bcl-2 family contain both pro-apoptotic and anti- apoptotic proteins. Tumour suppressor protein p53 involves in regulation of Bcl-2 family proteins(Elmore., 2007).

1.5.1.3 Execution pathway

The execution pathway is the terminal phase of both the intrinsic and extrinsic pathways. Caspase-3, 6 and 7 are activated during the execution phase and acts as effector or executioner proteins. They cleave various substrates include poly (ADP- ribose) polymerase (PARP), cytokeratins, cytoskeletal (fordrin and gelsolin) and nuclear (NuMA) proteins by activating endonuclease proteins which results in degradation of nucleus and cytoskeleton (Slee et al., 2000).

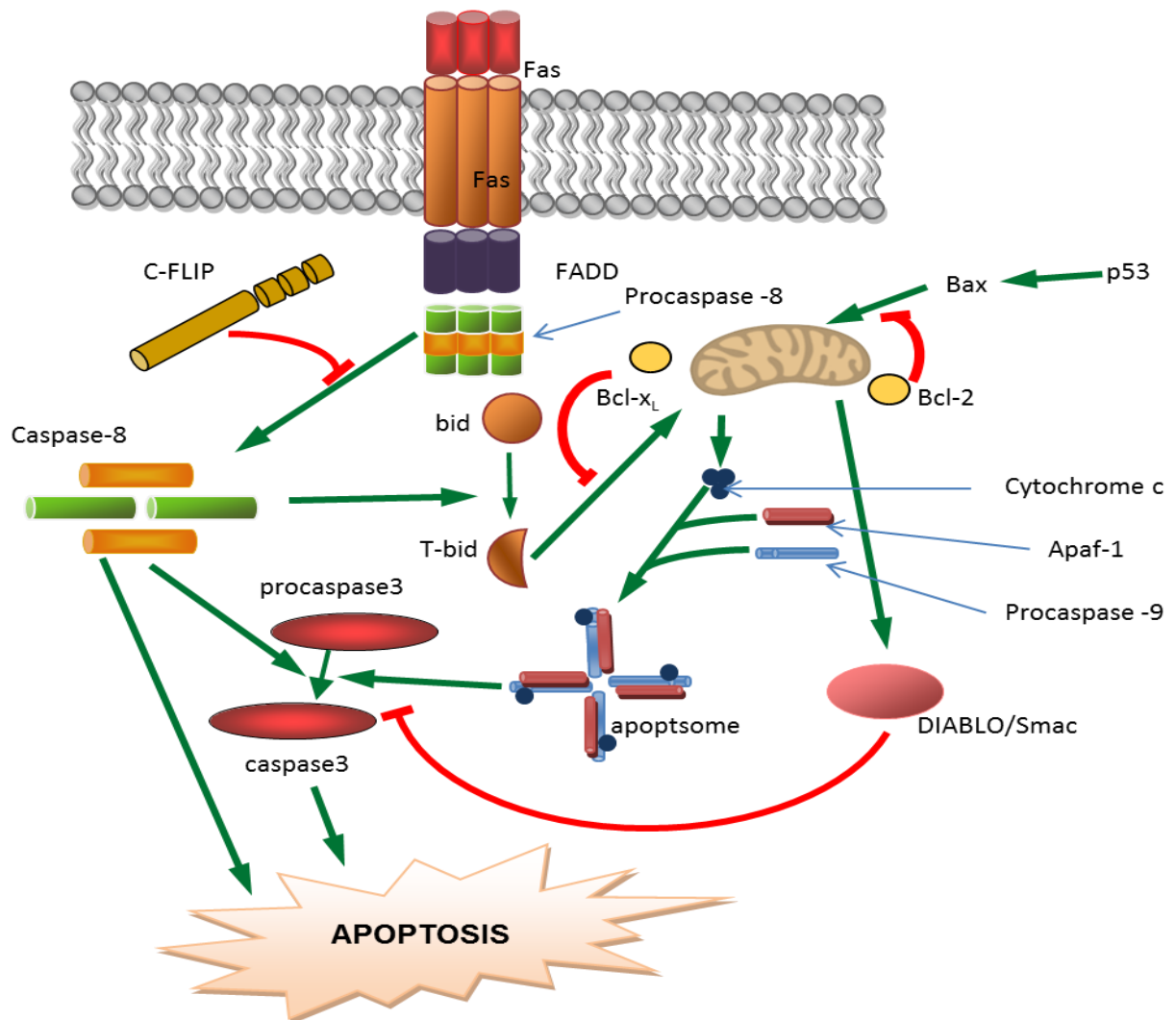


Figure 1-12 schematic representation of Apoptosis. Adopted from (Robinson., 2016)

Ovarian cancer survive apoptosis by multiple mechanisms of actions. p53 mutations exerted by 70% of EOC leads to dysregulation of proapoptotic proteins results in cancer survival. Over 30% ovarian cancers exhibit PTEN mutations, which results in alteration of PI3-kinase/Akt pathway. The alteration involves in inhibition of PIP3 dephosphorylation, which leads to evasion of apoptosis. Over 80% ovarian cancers overcome apoptosis by enhancing the immortality of cells (Saad. et al., 2010)

1.5.2 Cell cycle

The cell cycle in a conserved mechanism involved in duplication of cells by transferring genetic information from one generation to the next. Cell cycle machinery helps to maintain tissue homeostasis. The transformation of genetic information requires replication of the cell genome, which occurs in s-phase (synthesis phase), once s-phase is completely finished, the cell enters a division phase called M-phase (mitotic phase) where cell undergo division to form identical duplicates. The gap between s-phase and M- phase is called G2-phase, and M- phase to S-phase is called G1- phase. A cell enters from G1 to G0 phase, which is a quiescent state when it undergoes differentiation (Elmore., 2007, Pucci et al., 2000).

Cell cycle is regulated by checkpoints that occur during G1/ S phase transition, in s-phase and during G2/M phase. The checkpoints are generally enabled for cell proliferation by growth factors. DNA damage and misalignment of chromosomes during mitotic spindle formation can also involve in activation of checkpoints results in growth arrest. During growth arrest, checkpoints allow cell to repair the damage and resume cell cycle if the damage is irreversible cell undergoes apoptosis(Pucci et al., 2000).

The progression of cell cycle is dependent on activity of cdks (cyclin dependant kinases), which activated by cyclin subunits. Cdks are mainly regulated by pRb and p53. pRB is a

retinoblastoma tumour suppressor protein, which acts as a negative regulator for cell growth. Phosphorylation of pRb is required for a cell to transit from G1 to s-phase. It is mutated or deleted in many cancers such as retinoblastoma carcinoma of lung, prostate, breast, and bladder. P53 is a nuclear binding phosphoprotein, which regulates cell division by predominantly influencing G1 phase of cell cycle. DNA damage by UV radiation, hypoxia or chemotherapeutic drugs can activate p53. As a result, p53 expresses p21 which inhibits cdk5 to phosphorylate pRb results in cell cycle arrest at G1 phase(Schneider et al., 1998, Pucci et al., 2000).

1.5.3 Reactive oxygen species (ROS) inducing apoptosis

Reactive oxygen species is the collective term for radicals, ions, or molecules, which have unpaired electrons in its outermost shell. They are products of normal cellular metabolism or xenobiotic exposure; based on the concentrations it can be beneficial or harmful to cells. The low physiological levels of ROS can acts as a messenger for intracellular signalling and regulation. The excess levels of ROS create oxidative stress on cellular macromolecules and leads to dysfunction of proteins and results in cell cycle arrest, senescence and apoptosis (Circu and Aw., 2010, Liou and Storz., 2010).

ROS are over expressed in most of the cancers. The high levels of ROS in cancer cells may be due to increased metabolism, increased cellular signalling, mitochondrial dysfunction, peroxisome activity or oncogene activity (Liou and Storz., 2010, Storz., 2005). During ovulation, the increased levels ROS can trigger the biochemical events, which involves in remodelling of follicle or OSE cells thus results in ovulation impairment. This can further leads to ovarian carcinogenesis. ROS has shown to contribute tumour proliferation and chemo resistance in ovarian cancer (Calaf et al., 2018, Kim et al., 2017)

The superoxide form of ROS is produced in mitochondrial membrane as an inevitable by-product of oxidative phosphorylation. Superoxide is released into the cytosol through mitochondrial membrane permeable transition pore (MPTP) of outer mitochondrial membrane. The superoxide is generally dismutated to H₂O₂ either in cytosol or in mitochondrial matrix. But the loss of mitochondrial membrane potential results in increase leakage of superoxide into cytosol results in apoptosis by DNA fragmentation (Liou and Storz., 2010, Wen et al., 2013).

1.6 Rationale and aims of the project

The heterogeneity amongst the ovarian cancer types and acquired resistance to the current chemotherapy drugs indicate the importance of new approaches for the treatment of ovarian cancer. Pre-clinical studies have shown the antitumor activities of cannabinoids in different cancer cells. Endocannabinoid system play important role in ovulation process. The autocrine release of endocannabinoid L- α -lipophosphatidylionitol (LPI) mediates tumour invasion and metastasis to mediate cancer proliferation and angiogenesis in ovarian cancer through putative cannabinoid receptor GPR55 in ovarian cancer cells (Leyva-Illades and DeMorrow, 2013). Besides, the upregulation of cannabinoid receptors CB1, CB2 and GPR55 has been observed in human ovarian cancer cells, and associated with regulation of tumour proliferation (Afaq et al., 2006a, Natarajan et al., 2018, Bast et al., 2009). As cannabinoids can potentially target CB receptors, this raises the possibility of cannabinoids as potential anticancer drugs for ovarian cancer treatment. Among the cannabinoids, non-psychoactive cannabinoids have gained interest amongst the scientific community due to their pharmacological activities without psychoactive effects. *In vitro* studies have demonstrated the anticancer properties of CBD and CBG in various cancer cells (Dariš et al., 2018, Borrelli et al., 2013, Kosgodage et al., 2018a).

The aims of this project are to evaluate potential dose-dependent and time-dependent cytotoxic effects of CBD and CBG on human ovarian cancer cells, *in vitro*. This project will investigate the cytotoxic effects of the cannabinoids on *cisplatin* sensitive and *cisplatin* resistant ovarian cancer cells, and the selective cytotoxicity towards ovarian cancer cells will be determined by comparing the cytotoxic effects towards non-cancer cells. The combination effects of CBD or CBG in combination with current chemotherapeutic drugs will also be evaluated, and the combination effect will be determined by the calculation of the combination index. The potential mechanism of actions of CBD and CBG on ovarian cancer cells will be investigated, alongside investigations into the involvement of cannabinoid receptor GPR55 activity in CBD and CBG cytotoxicity on ovarian cancer cells.

1.7 Hypothesis

Based on studies of CBD and CBG in other cancer cell types and involvement of CB receptors in promoting cancer cell survival, it was hypothesised that CBD and CBG may show anti-cancer effects in ovarian cancer as CB receptors have been overexpressed in different ovarian cancer types. In particular, given identification of GPR55 as a putative CB receptor in ovarian cancer, it was hypothesised that CBD and CBG might mediate their effects through GPR55 or one of the canonical CB receptors CB1 or CB2.

CHAPTER 2: Materials and Methods

2.1 Materials

All the materials supplied by Sigma Aldrich, UK unless otherwise stated

2.1.1 General materials

Product	supplier
ApoTox-Glo™ Triplex Assay	Promega, UK
BLUeye pre-stained protein ladder	Geneflow Ltd., Lichfield, UK
Bradford reagent coomassie blue	Life Technologies, UK
CBD	Tocris, UK & GW Pharmaceuticals, UK
CBG	Tocris, UK & GW Pharmaceuticals, UK
Carboplatin	Tocris, UK
Paclitaxel	Tocris, UK
Pathscan® Stress and Apoptosis Signalling Antibody Array Kit (Fluorescent Readout)	Cell Signalling Technology, USA
Solution 7 (JC-1 200 µg/mL)	Chemometec, Denmark
Solution 8 (1µg/mL DAPI).	Chemometec, Denmark
Solution 10 (Lysis buffer)	Chemometec, Denmark
Solution 11 (stabilising buffer)	Chemometec, Denmark
Solution 12 (10mg/mL DAPI)	Chemometec, Denmark
Solution 16 (Propodeum Iodide)	Chemometec, Denmark

2.1.2 Primary antibodies for western blot

Antibody	Supplier	Cat. no	Dilution	Secondary
GpR55 1 ^o antibody	Cayman chemical, USA	10224	1:500	Rabbit
Beta actin 1 ^o antibody	Merck, UK	mab1501	1: 80,000	Mouse

2.1.3 SiRNA for RNAi mediated transfection

siRNA	Supplier	Cat. no
Silencer Selective Negative Control	Thermo fisher, UK	4390844
ON- TARGET Plus SMART Human GpR55	Dharamacon, UK	L-005581-00

2.1.4 Taqman probes for qPCR

TaqMan Probe	Supplier	Cat. No.
GPR55 (FAM TM /MGB probe, non-primer limited)	Thermo Scientific, UK	4331182 (Hs00271662_s1)
Human GAPD (GAPDH) Endogenous Control (FAM TM /MGB probe, non-primer limited)	Thermo Scientific, UK	4333764F
GUSB (FAM TM /MGB probe, non-primer limited)	Thermo Scientific, UK	4331182 (Hs9999908_m1)
CNR1 FAM TM /MGB probe, non-primer limited	Thermo Scientific, UK	4331182 (Hs00275634_m1)
CNR2 FAM TM /MGB probe, non-primer limited	Thermo Scientific, UK	4331182 (Hs00361490_m1)

2.2 Cell culture methods:

Human ovarian cancer cells include A2780 (Sigma Aldrich, UK), A2780 cis (CP70)(Allison et al., 2017) OVCAR3(Hamilton et al., 1983) and IGROV-1 (Erba et al., 2000); a colorectal cancer cell line HCT116 p53++; non-cancerous cells include PNT2 (normal prostate epithelial cell line) (Sigma Aldrich, UK), and ARPE19 (human retinal pigment cell line) (Dunn et al., 1996) were maintained according to the ATCC guidelines.

Cell Line	Complete media
A2780, IGROV-1 and PNT2	RPMI 1640 + 10 % (v/v) fetal bovine serum (FBS) + 1% (v/v) sodium pyruvate + 1%(v/v) L-glutamine
A2780/CP70	RPMI 1640 + 10 % (v/v) fetal bovine serum (FBS) + 1% (v/v) sodium pyruvate + 1%(v/v) L-glutamine (1 μ M cisplatin for every two passages to maintain the resistance)
OVCAR 3	RPMI 1640 + 20 % (v/v) fetal bovine serum (FBS) + 1% (v/v) sodium pyruvate + 1%(v/v) L-glutamine
HCT116 p53++	DMEM+ 10 % (v/v) fetal bovine serum (FBS) + 1% (v/v) sodium pyruvate + 1%(v/v) L-glutamine
ARPE19	DMEM: DMEM F12 (1:1) 10 % (v/v) fetal bovine serum (FBS) + 1% (v/v) sodium pyruvate + 1%(v/v) L-glutamine

All the cells were grown in an incubator, which was maintained with 5 % CO₂ at 37°C under humidified conditions. The cells were sub- cultured when reached 70% confluence.

2.3 Sub- culturing of cells by trypsinisation

Sub- culturing was carried out either to set up an experiment or to maintain the cells for future use. The media was removed and, washed with 8mL of 1x PBS supplemented with 1 % (v/v)

EDTA. 2mL of trypsin (0.05%) - EDTA (0.02%) (Sigma Aldrich, UK) solution was used to detach cells from flask. After 2 minutes of incubation, complete media was added to inactivate trypsin. Cells were transferred to 50mL conical flasks and centrifuged at 1200 rpm for 5 minutes. Following centrifugation, the supernatant was removed, and cells were suspended in complete media. Cells were added according to a recommended ratio, to a fresh, labelled T75 flask and transferred to incubator.

2.3.1 Cell counting by haemocytometer:

The cells were counted using haemocytometer (sigma Aldrich, UK). Trypan blue was used to distinguish the viable cells from dead. The total number of viable cells were calculated according to **Equation 1**

$$T = (N \div S) \times D \times 10^4 \quad (\text{Eq.1})$$

T= Total number of viable cells/ mL

N= Total number of viable cells counted

S= Total number of squares (1mm²) counted

D= Dilution factor

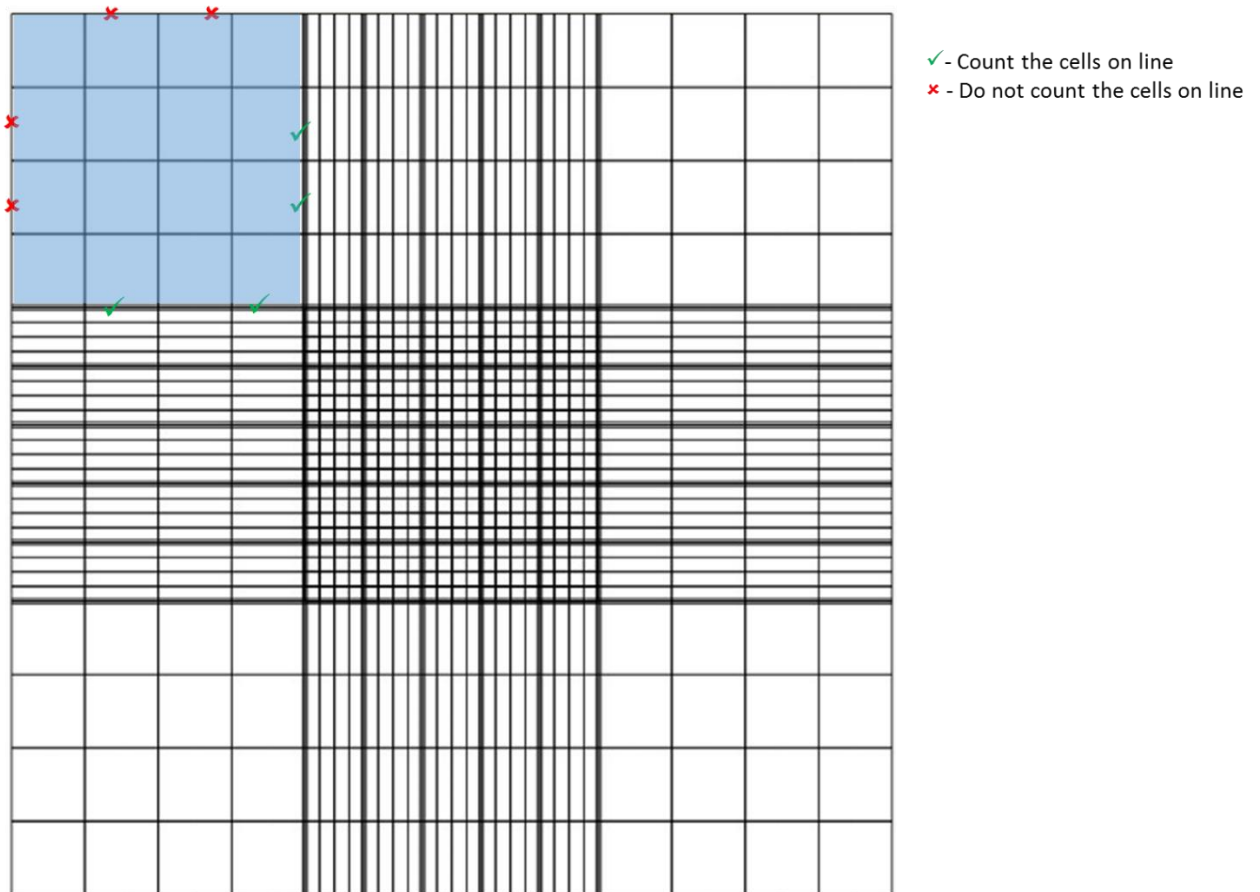


Figure 2-1. General representation of haemocytometer grid with a square highlighted

2.4 Cryo-preservation of cells:

The cells were detached from flasks as described in **section 2.3**. Cells were suspended in complete media supplemented with 10% DMSO (dimethyl sulfoxide) and 20% FBS. These were aliquoted to cryovials (3 to 4 vials per T75), and placed in a cryopreservation box (Nalgene® “Mr. Frosty®”) containing isopropanol. Cryopreservation box avoids ice crystal formation of cells by allowing it to cool down 1° per min. The box was immediately transferred to -20°C freezer, and then transferred to -80°C. After overnight storage, the vials were transferred liquid nitrogen storage (-196°C) for long term storage.

2.5 Chemo sensitivity assay

2.5.1 Preparation of MTT solution:

MTT (sigma Aldrich, UK) was dissolved in ultra-pure water with 5% (w/v) final concentration. The solution was sterile filtered and stored at 4°C (protected from light). The final concentration of 0.5 % MTT (w/v) solution was added to each well in a 96 well plate.

2.5.2 Drug addition

All drugs or compounds were dissolved in ethanol (1% final concentration), DMSO (0.1% final concentration) or ultrapure water. All the concentrations mentioned in experiments were the final concentrations. Repetman pipette (Gilson, UK) was used for the addition of drugs.

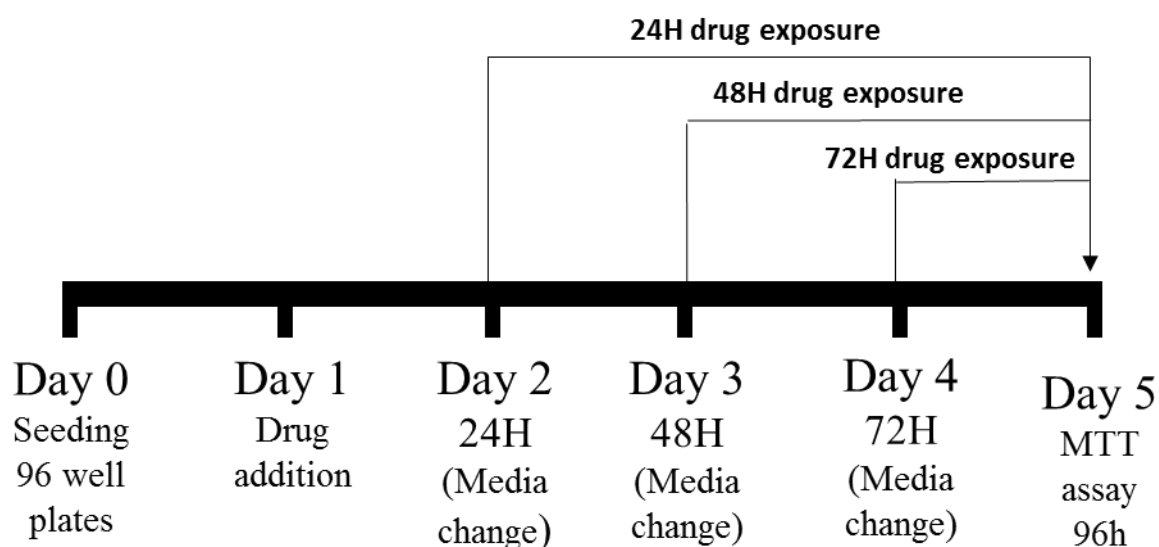
2.5.3 MTT assay:

The cells were detached from flasks as described in **section 2.3**. Cells were seeded at a density of 1500 cells per well for A2780 and A2780 CP70, 2000 cells per well for ARPE19 19 and 3000cells per well for OVCAR3 and PNT2 in 96 well plates. The final volume in each was kept constant (200 µL media per well), and cells were incubated for 24 h before drug treatment. After 24 h, 2 µL of drug (1 nM – 100 µM) or vehicle was added to wells, and incubated for a further 24 h, 48 h, 72 h or 96 h. After the allocated contact time had elapsed, the media was removed and 0.5 % (w/v) MTT solution diluted in complete media (200 µL) was added to each well. Following a 4 h incubation, the supernatants were removed, and the formazan crystals were dissolved in dimethylsulfoxide (150µL). The absorbance was read at 540 nm on a Tecan Infinite 50 plate UV reader.

2.5.4 Chemo sensitivity assay with drug washout

The seeding of cells and addition of drugs in 96 well plates were performed as described in **section 2.5.3**. After the allocated contact time had elapsed, the media was removed, washed

with PBS. 200 μ L of complete media was added to each well to allow the cells to recover. At 96 h time point (since the drug added) MTT assay was performed as described in **section 2.5.3**.



2.5.5 IC₅₀ determination:

Cytotoxicity was expressed as a relative percentage of the absorbance measured at 540 nm in the control and drug-treated cells. Data were presented as the mean \pm standard error of the mean. At least 3 independent experiments were carried out to determine the IC₅₀ ($n \geq 3$).

2.5.6 Selectivity Index:

Preferential cytotoxicity of CBD and CBG towards cancer cells were determined by selective index. The Selective index (SI) is the ratio of mean IC₅₀ values on non-cancer cells to cancer cells. If $SI > 1$, this means drug shows preferential cytotoxicity towards cancer cells, if $SI = 1$, means it is equally toxic to both cancer and non- cancer cells. If $SI < 1$, this means it is more toxic to non- cancer cells than cancer cells (Allison et al., 2018).

$$SI = N \div C \quad (\text{Eq.2})$$

SI = Selectivity Index

N= Mean IC₅₀ on non- cancer cells

C= Mean IC₅₀ on cancer cells

2.5.7 Combination Index:

The combination Index (CI) for drug A (CBD or CBG), when they were combined with drug B (Carboplatin or Paclitaxel) was calculated by the ratio of the applied concentration of drug A (100 nM) in the combination to the IC₅₀ of A when it was applied individually, the ratio of the applied concentration of drug B in the combination (combination IC₅₀ – concentration of drug A), to IC₅₀ of B on the cells (Liang Zhao, 2004)

$$CI_{A+B} = (C_A \div IC_{50} A) + (C_B \div IC_{50} B) \quad (\text{Eq.3})$$

CI_{A+B} = Combination index of A and B

C_A = Concentration of A applied in the combination

C_B = Concentration of B applied in the combination

IC₅₀ A = IC₅₀ of drug A when it was applied individually to the cells

IC₅₀ B = IC₅₀ of drug B when it was applied individually to the cells

Table 2-1. Indication of combination effects relative to combination index values. Adopted from (Bijnsdorp et al., 2011)

CI value	Combination effect
>0.1	Very strong synergism
0.1–0.3	Strong synergism
0.3–0.7	Synergism
0.7–0.85	Moderate synergism
0.85–0.9	Slight synergism
0.9–1.1	Nearly additive
1.1–1.2	Slight antagonism
1.2–1.45	Moderate antagonism
1.45–3.3	Antagonism
3.3–10	Strong antagonism

2.6 Viability Assay:

Viability of cells were determined by NucleoCounter NC-3000 image cytometry using Via1 cassettes (Chemometec, Denmark). Via1 cassettes are preloaded with acridine orange and DAPI. Acridine orange stains all the cells whereas DAPI differentiate dead cells from viable by staining DNA of dead cells. Following the preparation of cell suspension in 1X PBS, cells were drawn into cassettes by inserting the tip of cassette into cell suspension and pressing the piston. The cassettes were immediately paced on NC3000 for analysis. Cell density should be in between 5×10^4 cells/mL – 5×10^6 cells/mL for ideal results.

2.7 Mitochondrial membrane potential assay:

The mitochondrial membrane potential assay was performed to detect the loss in mitochondrial potential (de-polarisation), which is a vital step in apoptosis. Cells were seeded in T25 flasks at 4×10^5 cells per flask, and were incubated for 48 h. the incubation time was sufficient for the flasks to reach ideal confluency to carry out the assay. After incubation time elapsed. Drug concentrations 10 μM , 30 μM and 50 μM were added to the flasks, and further incubated for 24 h. Following incubation, cells were harvested and suspended in PBS. Cell viability and number were determined by the cell viability assay using via1 cassettes on NC 3000 system. The samples were diluted in PBS to 1×10^6 cells/mL. 2.5 $\mu\text{g}/\text{mL}$ of JC-1 (Chemometec, Denmark) was added to each sample. JC-1 is a negatively charged dye, which stains as a fluorescent red as it aggregates in the mitochondrial matrix. In the absence of mitochondrial membrane potential, JC-1 localises in the cytosol in its fluorescent green form. Following the addition of JC-1 the cells were incubated for 10-30 minutes at 37°C . After the incubation, cells were washed twice with 1x PBS without disturbing the pellet, and the pellet was re-suspended in 0.25mL of $1\mu\text{g}/\text{mL}$ DAPI (Chemometec, Denmark). DAPI stains as florescent blue in late apoptotic and necrotic cells by binding to the DNA. 12.5 μL of samples were loaded on to an A-8 slide (Chemometec, Denmark) ensuring that no air bubbles formed. The samples were analysed immediately using the NC-3000 image cytometry. The degree of apoptosis (in proportional to loss in mitochondrial membrane potential) was measured using a scatter plot of JC-1 red fluorescence vs JC-1 green fluorescence.

2.8 Annexin- V assay

The Annexin- V assay was performed to differentiate healthy cells from early and late apoptotic cells. Cells were seeded in T25 flasks at 2.75×10^5 cells per flask and were incubated for 24 h. Drugs were added as described in **section 2.7**. Cells were suspended in PBS at a

density of 4×10^5 cells/mL, followed by centrifugation at 400 g for 5 minutes. The supernatant was removed and replaced with 100 μ L of Annexin V mix (94 μ L of Roche buffer (BD Bioscience), 2 μ L of Annexin V-CF488A (Santa Cruz Biotechnology, UK), 2 μ L of 10 μ g/mL of Propidium Iodide (PI) (Chemometec, Denmark), and 2 μ L of Hoechst 33342 buffer (Thermo-Scientific, UK)). Hoechst 33342 buffer in the Annexin V mix binds to all the nuclei in the sample and fluoresces violet. The early apoptotic cells are stained with Annexin V-CF488A, which fluoresces, green. The non-viable cells are stained by PI, and the late apoptotic cells are stained by both PI and Annexin V-CF488A, which fluoresces red, and green respectively. Following the addition of Annexin V mix, samples were incubated at 37°C for 20mins in the dark with regular mixing to keep the cells in suspension. After the incubation time elapsed, 40 μ L of samples were loaded on to an A-2 slide (Chemometec, Denmark) ensuring that no air bubbles formed. The samples were analysed immediately using the NC 3000 system. The scatter plot of the fluorescence intensity of Annexin V-CF488A vs the fluorescence intensity of PI was used as a representation of cells in different stages of apoptosis.

2.9 Cell cycle analysis

Cells were seeded, and drugs were added to the flasks as described in **section 2.7**. Cells were suspended in PBS with density closer to 1×10^6 cells mL^{-1} . The cells were washed twice with 1x PBS before the addition of 250 μ L of lysis buffer (solution 10, Chemometec) supplemented with 10 μ g/mL DAPI (solution 12, Chemometec) was added to the samples and incubated for 5 minutes at 37°C. After incubation, 250 μ L of stabilisation buffer (solution 11, Chemometec) was added. 12.5 μ L of Samples were loaded on to an A-8 slide ensuring that no air bubbles formed. The samples were analysed immediately using the NC 3000 system.

2.10 Caspase 3/7 assay

Caspase 3/7 assay was carried out to determine the involvement of caspase in execution of apoptosis induced by CBD and CBG on ovarian cancer cells.

2.10.1 Sensolyte homogenous caspase 3/7 assay:

Sensolyte homogenous caspase 3/7 assay kit (Anaspec, UK) was used to determine the caspase activity in ovarian cancer cells when treated with CBG. Cells were seeded in 96 well plate at 6×10^3 cells per well, and were incubated for 24 h. CBG was added in concentrations of 10 μ M, 20 μ M, 30 μ M and 50 μ M and incubated for 24 h. After the incubation time elapsed, the media was removed and replaced with 150 μ L/well of fresh complete media. Caspase 3/7 solution was prepared by diluting the caspase substrate 1:100 with DTT- containing assay buffer. 50 μ L/well caspase substrate was added to the plates, and the cells were incubated for 30 mins. Ac-DEVD-AMC serves as the fluorogenic indicator for assaying caspase-3/7 activities. AcDEVD-AMC generates the AMC fluorophore, in the presence of caspase 3/7, which produces bright blue fluorescence. The fluorescence was measured by the FLOUstar OPTIMA plate reader with the excitation at 354nm and emission at 442nm.

2.10.2 ApoTox-Glo™ Triplex Assay (caspase 3/7 activity)

Cells were seeded and drugs were added as described in **section 2.10.1**. After 24 h incubation, caspase 3/7 reagent was prepared by mixing caspase buffer and substrate (Promega, UK) and 100 μ L of reagent was added to each well for 30 minutes incubation at room temperature. The pro luminescent substrate DEVD- Aminoluciferin would be activated in presence of caspase3/7 enzyme. The luminescence was measured by the FLOUstar OPTIMA plate reader.

2.11 H2DCFDA- ROS assay

Cells were seeded in 96 well plate at 6000 cells per well and were incubated for 24 h. Drugs were dissolved in ethanol, and added in concentrations ranging 10 μ M, 30 μ M and 50 μ M (two rows for each concentration) 100 μ M hydrogen peroxide was used as positive control incubated for 2 h, 3 h and 6 h time points. At each time point, media was removed from 96 well plates and replaced with 100 μ L of PBS. 10 μ M DCFDA (2', 7'-dichlorodihydrofluorescein diacetate) reagent was added to one row each concentration and incubated for 30 minutes. After incubation PBS containing H2DCFDA reagent was removed and replaced with fresh 100 μ L of PBS. Fluorescence was observed at maximum excitation 492nm and emission 520nm spectra using FLUOstar OPTIMA micro plate reader.

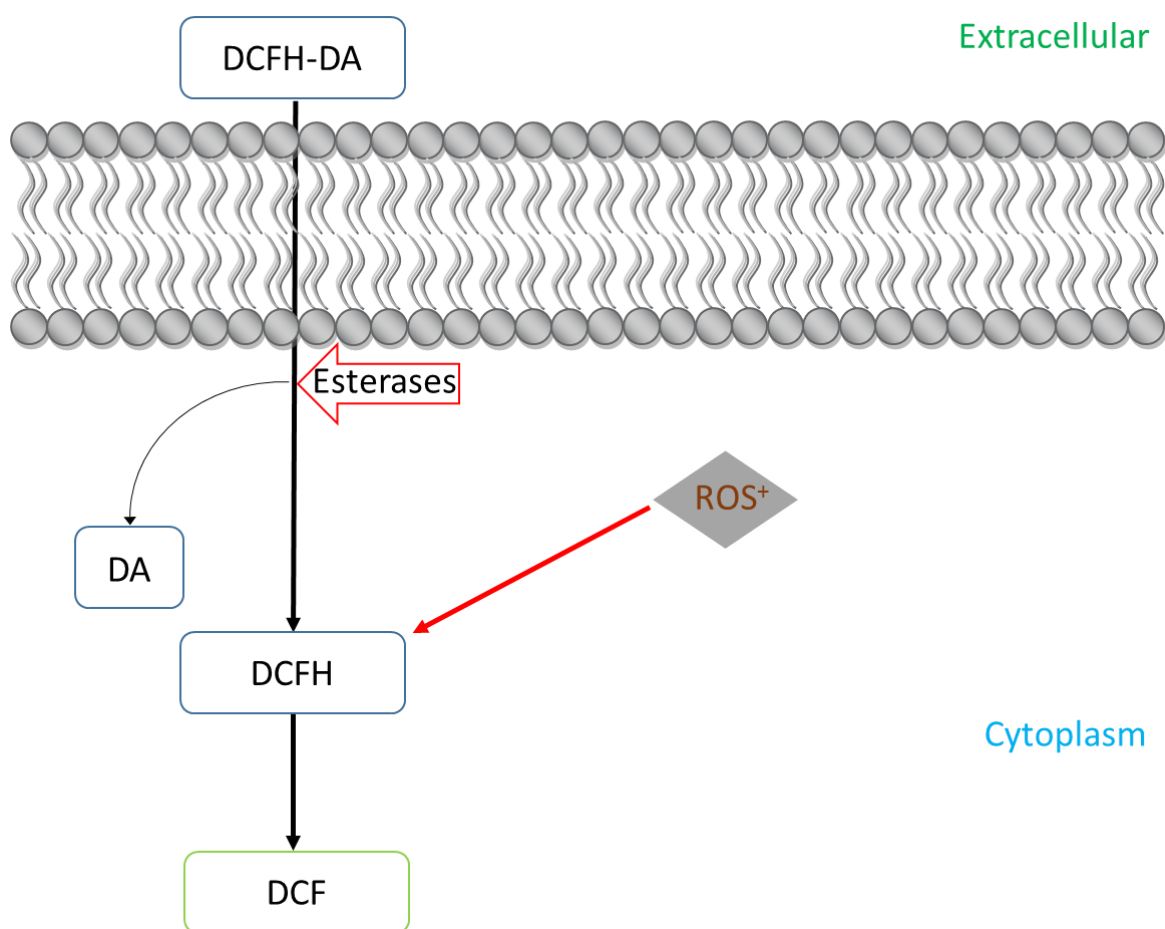


Figure 2-2 Schematic representation of the concept of H2DCFDA- ROS assay

2.12 Western Blot analysis

Cells were seeded and drugs were added as described in **section 2.7**. Following the drug incubation, cells were harvested by trypsinisation. Cells were washed twice with 5mL of 1X PBS. The cell pellets were homogenised in RIPA lysis buffer (100 μ L) containing protease inhibitors (2% v/v) and incubated for 30 minutes on wet ice with occasional sonication. Cell homogenates were centrifuged at 13500 rpm and 4°C for 15 minutes to remove cell debris. The cell lysate supernatants were collected and stored at -80°C.

Bradford assay was used to determine the concentration of proteins. Cell lysates were diluted using ultra-pure water. Protein standards ranging from 250 μ g/ μ L - 1500 μ g/ μ L (Thermo fisher scientific, UK), and diluted lysate samples were added to 96 well plates. 250 μ L Bradford Reagent (Life Technologies, Paisley, UK) and incubated at room temperature for 5mins. The absorbance was read on a Tecan Infinite 50 plate UV reader at 595 nm.

Protein concentration was calculated, and 20 μ g of protein sample was supplemented with 1 M DTT (2 μ L), LDS sample buffer (5 μ L) and ultra-pure water to bring the total volume up to 20 μ L. The samples were then heated for 5 minutes at 95°C.

The samples were resolved on polyacrylamide pre-cast gels (4-12 % tris-bis) (Thermo fisher scientific, UK) using Running Buffer (1X) (Thermo fisher scientific, UK) at 180 V, 400 mA for 50mins. The gels were then, electro transferred to nitrocellulose membranes at 25 V, 400 mA for 2 h on wet ice using transfer buffer (1X) (Thermo fisher scientific, UK). The membranes were blocked in 5 % Skimmed Milk in TBST for 1 hour at room temperature. After incubation, the primary (1°) antibody (diluted in 5 % Skimmed Milk/ TBST) was added. The blots were then, incubated at 4°C on slow rotor overnight. The unbound primary antibody was washed by TBST (3 times with 5 minutes wash each time). The appropriate 2° antibody (1:5000

dilution) was added to blots and incubated for 1 hour at room temperature (in the dark). The blots were washed again with TBST (3 X). A Li-cor Odyssey infrared imaging system was used to analyse the blots. The contrast wavelength was chosen according to the fluorescent dye conjugated to secondary antibody (700nm/ 800nm). The image quality of blots were optimised by adjusting the intensity, brightness and contrast.

2.13 ELISA Pathscan® Apoptosis and Stress assay

Cells were seeded, and drugs were added to the flasks as described in **section 2.7**. Following the drug incubation, cells were harvested and cell lysates were collected using RIPA lysis buffer (100 µL) containing protease inhibitors (2 % v/v) as described in **section 2.12**

Bradford assay was used to determine the concentration of proteins. Pathscan® stress and apoptosis signalling antibody array kit (Cell Signalling, USA) (**Error! Reference source not found.**) was assembled according to the manufacturer instructions. Before the addition of lysates to the wells, the blocking buffer (100 µL/well) was added to block non-specific binding, and the wells were incubated for 15 mins at 22.5°C using orbital shaking at 50 rpm. After the incubation, the blocking buffer was decanted, and 75 µL of lysates (500 µg/mL) were added to the wells, and incubated for 18 h at 4°C, 50 rpm on an orbital shaker. Following the incubation time elapsed, the lysates were decanted, and the wells were washed using 1x array wash buffer (5 x 100 µL, 5 minutes, and 22.5 °C). Followed by the washing steps, 1 x DyLight™ detection antibody cocktail was added to the wells, and incubated 1 hour at 22.5 °C. After the incubation, the wells were washed using 1x array wash buffer (5 x 100 µL, 5 minutes at 22.5 °C). Followed by the washing steps, 1 x DyLight™ 680-linked Streptavidin solution was added, and incubated for 30 minutes at 22.5°C in darkness. After the incubation, the wells were washed using 1x array wash buffer (5 x 100 µL, 5 minutes, and 22.5 °C). The multi- well

gasket slide was removed from the pads, and the slide was washed with 10 mL ultra-pure water. The slide was allowed to dry. The Images were captured using LI-COR® Biosciences Odyssey® infrared imaging system.

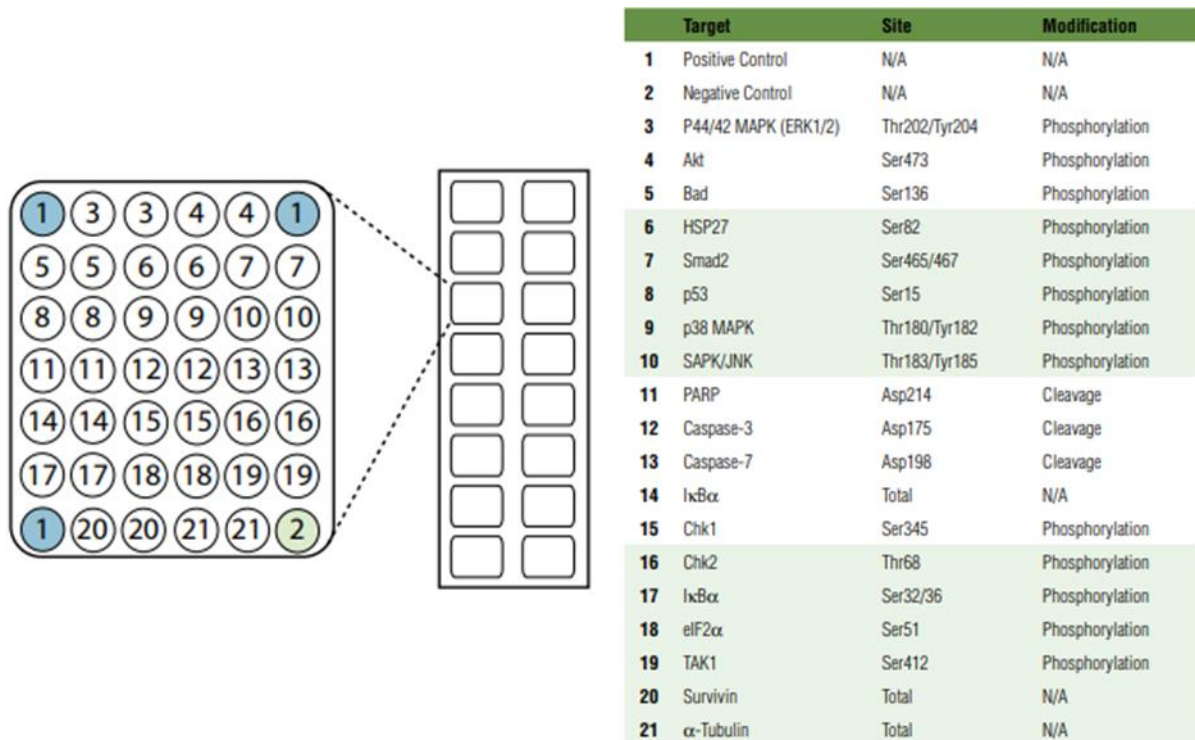


Figure 2-3 The plan of Pathscan® stress and apoptosis signalling antibody array kit (Cell Signaling Technology, 2015)

2.14 siRNA mediated RNAi transfection

Low passage cells were used for siRNA transfection. A2780 cells were seeded with a density of 2.5×10^5 cells per T25 flask where as HCT116 p53^{+/+} cells were seeded at a density of 2.75×10^5 cells/ flask. The cells were incubated for 24 h. Before transfection, siRNA was diluted (200nM) with OPTIMEM (Thermo fisher scientific, UK), mixed with Oligofectamine (Thermo fisher scientific, UK) for a liposomal siRNA formation. The flasks were washed two times with 3mL of OPTIMEM, followed by the addition of 2mL of OPTIMEM to each flask with dispenser. 0.5mL of siRNA and mix was added to each flask drop by drop. The flask was moved zigzag

manner (keeping it flat) to increase the efficiency of transfection. The flasks were incubated for 5 h. After the incubation time elapsed, 2.5mL of feed media (2X complete media) was added to flask using dispenser (final volume of media in flask was 5mL) and incubated further for 48 h and 72 h.

After the incubation time elapsed, the cells were harvested using trypsin, and the cells were washed twice with ice cold PBS. The PBS was carefully removed and cell pellets were stored at -80°C.

2.15 mRNA extraction

Total mRNA was extracted from the cell pellets using a RNeasy mini kit (Qiagen, UK). The cells were disrupted by adding 600 µL of RLT buffer (0.1% beta mercaptoethanol). Lysates were transferred onto QIAshredders (Qiagen, UK), centrifuged for 2min at 16000g for homogenisation. 600 µL of 70% ethanol was added to lysates. 700 µL sample was transferred into RNeasy column placed in a 2mL collection tube. It was spun down at 9000g for 15s. The flow through was discarded. 350 µL of RW1 was added to spin column and centrifuged for 15s at 9000g. The flow through was discarded. Each sample was treated with 10 µL DNAase in 70 µL of RDD buffer solution to digest the residues of cellular DNA, and incubated at room temperature for 30 mins. The columns were treated with 350 µL of RW1 and centrifuged for 15s at 9000g. 500 µL of RPE buffer was added to RNeasy column and, centrifuged at 9000g for 15s. Column was washed again with RPE buffer and centrifuged for 2mins. The flow through was discarded. RNeasy column was placed in a new 2mL collection tube and centrifuged at 16000g for 2mins. RNeasy column was placed in a new 2mL collection tube, followed by addition of 50 µL of RNase- free water. RNeasy column was centrifuged for 1 min at 9000g. RNA from collection tube was carefully transferred into new 1.5mL centrifuge tube.

mRNA was quantified by using the nanodrop2000 (Thermo fisher scientific, UK), a sample retention spectrophotometer.

2.16 Reverse transcription (cDNA synthesis):

cDNA was synthesised from the mRNA using a Precision nanoScript2 reverse transcription Kit (Primer Design, UK). 2µg of RNA template was used for reverse transcription. The dilutions were made with DNase/ RNase free water to make the final volume of 8µL. 1µL of oligo-dT primers and 1µL of random nanoprimers were added to each of the samples. Samples (10µL) were then transferred to the thermocycler, and incubated at 65°C for 5 mins. This step is called the annealing step, in which the RT primers are annealed to the denatured RNA. Following the annealing step, samples were immediately transferred onto wet ice to avoid RNA degradation. 10µL of reverse transcription mix containing 5µL of 4x nanoscript buffer, 3µL of RNase- free water, 1µL of 10mM dNTP mix, and 1µL nanoscript enzyme was added to each sample. The samples (20µL) were then transferred to thermocycler for 'extension step'. During the extension step, samples were incubated at 25°C for 5 min, followed by the incubation at 42°C for 20mins. The reaction was heat inactivated by incubating samples at 72°C for 10 mins. cDNA samples were collected, and stored at -20°C.

2.17 Real-Time qPCR

A Precision FAST qPCR Master Mix was used for the real-time qPCR. 50ng of cDNA was used as a template for the reaction. DNase/ RNase free water was used as a control, and mRNA with no RT (reverse transcription) was used as a negative control. 5 µL of cDNA (diluted using DNase/ RNase free water) was added to each well in a 96 well plate. 15 µL of master mix containing 10 µL of precision FAST mix, 4 µL of DNase/ RNase free water and 1 µL of 20X TaqMan probe (GAPDH/ GUSB/GPR55/ CB1/ CB2) was added to each well. The Step one real

time qPCR system was used for amplification. Plate design was edited according to the experimental plan. The steps involved in the amplification protocol were activation of the enzyme by hot start for 2min at 95°C, denaturation step at 95°C for 5sec followed by annealing and extension steps at 60°C for 20 sec, where the data was collected after each cycle. The final data was collected after 40 cycles, and it was analysed using a Stepone v2.3 software and Microsoft excel.

2.18 Statistical Analysis

Statistical analysis were carried out using Graph pad 7, one-way ANOVA with Dennett's multi comparison test. P values of <0.05 were considered to be statistically significant compared to control values.

CHAPTER 3: Evaluation of CBD and CBG cytotoxicity towards ovarian cancer cells *in vitro*

3.1 Introduction

CBD and CBG have been shown to exert *in vitro* anticancer activity on breast, prostate and colon cancer cell lines (Dariš et al., 2018). The purpose of this chapter is to evaluate the activity against ovarian cancer cells A2780, cisplatin resistant A2780/CP70 cells, and OVCAR-3 cells. Selective cytotoxicity of CBD and CBG towards ovarian cancer is determined by comparing their cytotoxicity towards non- cancer cells ARPE19 and PNT2. Cytotoxicity and selectivity is compared to that of the palatinate carboplatin, which is in use for treatment of ovarian cancer.

3.2 Results

3.2.1 Solvent/ Vehicle effect on A2780 viability:

Cannabinoids are highly soluble in ethanol so it was used as a solvent to dissolve CBD and CBG. Whilst a solvent control was used in all experiments, it was important to determine the toxicity of ethanol at different concentration to identify non- toxic concentrations on ovarian cancer cells.

A2780 cells were seeded at 1500 cells per well (7500cells mL^{-1}), and incubated for 24 h. After incubation time elapsed, ethanol (1%, 0.1% and 0.01%) or media were added to the corresponding wells. The plates were then incubated for a further 24 h, 48 h, and 72 h. After the allocated contact time had elapsed, MTT assays were carried out as described in **section 2.5.3** to determine the viability of cells.

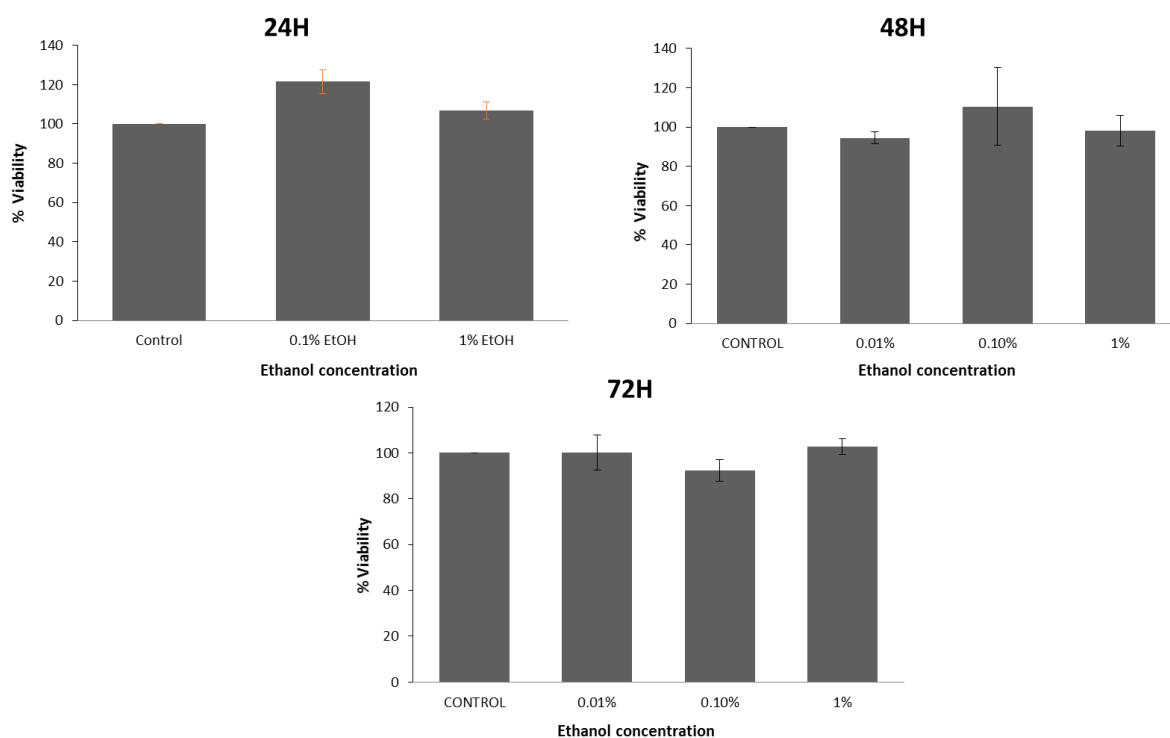


Figure 3-1 Solvent or vehicle effect on A2780 cell viability: Viability of A2780 Cells treated with 0.01%, 0.1% and 1% ethanol compared to control cells (cells with complete media) at 24 h, 48 h and 72 h. Data represents the mean \pm standard error of mean of $n=3$, n is the number of independent biological experiments.

The viability of A2780 cells were unaffected by ethanol up to a concentration of 1% (**Figure 3-1**). The effect of ethanol concentration above 1% on ovarian cancer cells was not tested, as it was the maximum concentration of solvent control required which was added to the cells.

3.2.1.1 Effect of vehicle/solvent concentration on CBD cytotoxicity:

The solubility of CBD in ethanol and its cytotoxic effect when it was dissolved in pure ethanol and 10% ethanol was tested on A2780 cells. A2780 cells were seeded at 1500 cells per well (7500cells mL^{-1}) and, incubated for 24 h. After 24 h, CBD was serially diluted separately in absolute and 10% ethanol (90% complete media) to prepare a concentration range from 100 nM to 10 mM. 2 μL of different concentrations of CBD (1nM to 100 μM final concentrations) diluted in absolute and 10% ethanol were added to corresponding wells in each plate. The

plates were incubated further for 24 h, 48 h, 72 h and 96 h. After the allocated contact time had elapsed, MTT assay was carried out to determine the viability of cells

CBD diluted in absolute ethanol had shown the IC₅₀ values ranged from 3.46 μM to 12.3 μM whereas CBD diluted in 10% ethanol was ranged from 9.09±0.83 μM to 18.88± 0.7 μM. Despite the fact that CBD diluted in both absolute and 10% ethanol did not form any detected precipitation, the above results had shown that CBD has more potency when pure ethanol is used as a vehicle. This could be due to undetected precipitation or the instability of compound when dissolved in 10% ethanol compared to absolute ethanol. Based on the results obtained (**Figure 3-1, Table 3-1**), 1% ethanol was used as vehicle for further experiments.

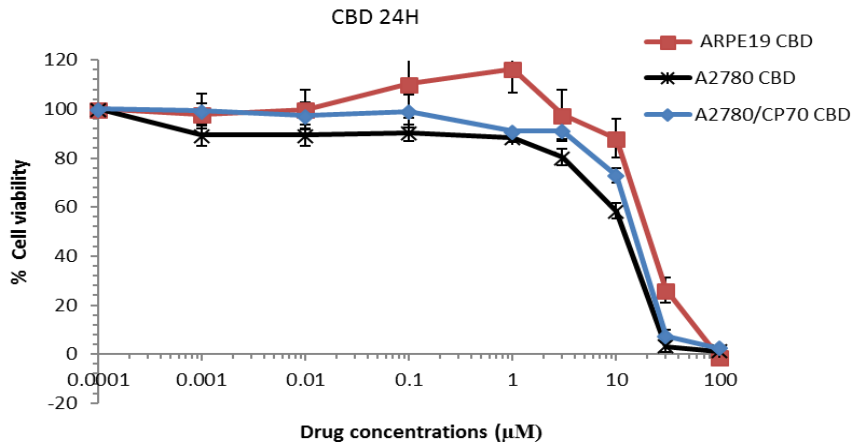
Table 3-1. The mean IC₅₀ values of CBD on A2780 cells with 0.1% and 1% ethanol respectively

IC ₅₀	24 h	48 h	72 h	96 h
CBD (0.1%ETOH)	18.88±0.01 μM	14.11±0.5 μM	13.47±0.78 μM	9.09±0.83 μM
CBD (1%ETOH)	12.3± 0.7 μM	6.84± 1.07 μM	4.4±0.15 μM	3.46±0.17 μM

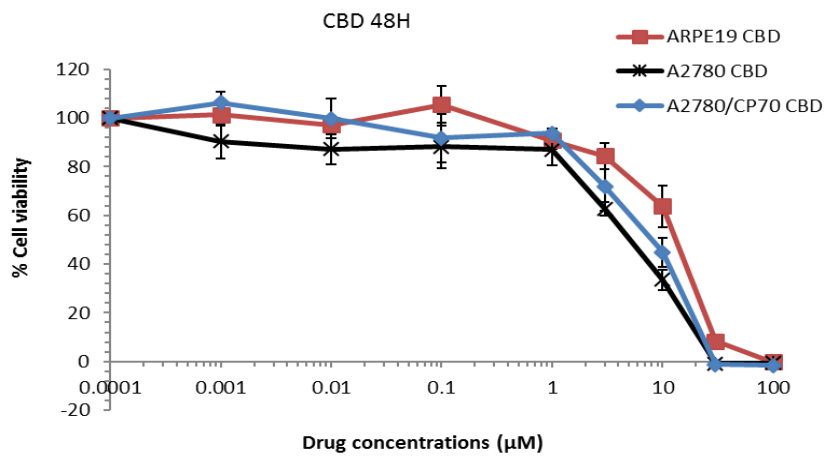
3.2.2 *In vitro* anticancer activity of CBD:

The effects of CBD were investigated on ovarian cancer cell lines (A2780, A2780 CP70, IGROV and OVCAR 3) and non- cancer cells include PNT2 (prostate cells) and ARPE19 (retinal epithelial cells). A2780 and A2780/CP70 cells were seeded at density of 1500 cells per well, IGROV and ARPE19 were seeded at density of 2000 cells per well whereas OVCAR-3 and PNT2 were seeded at 3000 cells per well. After 24 h incubation, different concentrations of CBD or vehicle were added to corresponding wells. The plates were further incubated for 24 h, 48 h, 72 h and 96 h contact points.

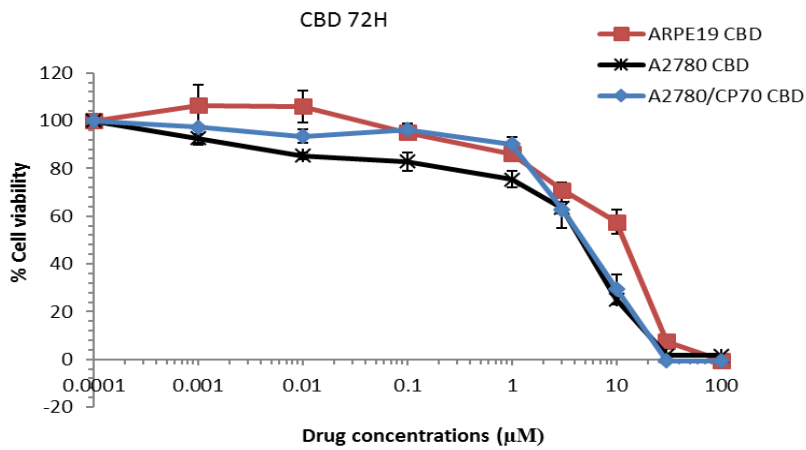
a)



b)



c)



d)

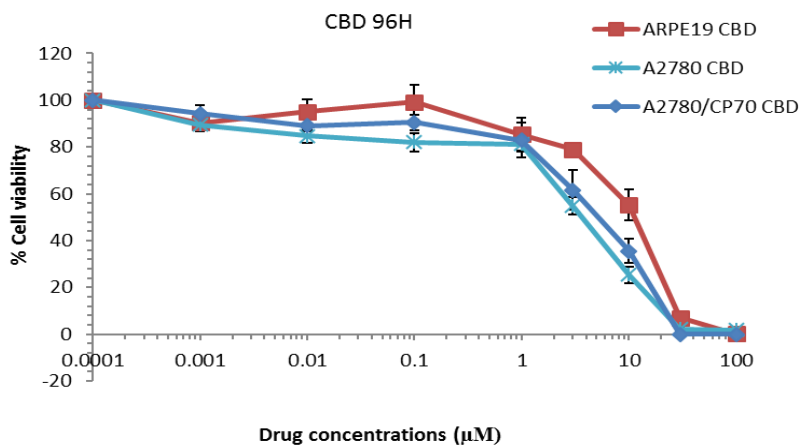


Figure 3-2. **In vitro cytotoxicity of CBD.** The effect of CBD (1 nM to 100 μ M) on ovarian cancer cells A2780, A2780/CP70 and non- cancer cells ARPE19 (retinal epithelial) and at 24 h (a), 48 h(b), and 72 h (c), and 96 (d) hour time points. The effect of CBD on cell viability as indicated by absorbance at 540 from dissolved formazan crystals compared to vehicle control. Data represents the mean \pm standard error of $n=4$, n is the number of independent biological experiments.

CBD (1 nM- 100 μ M) induced dose-dependent cytotoxicity in the ovarian cancer cells. CBD exerted cytotoxic effects evidently from 1 μ M on all the cell lines tested (**Figure 3-2**). The dose-response curves to CBD on ovarian cancer cells (A2780, A2780 CP70) compared ARPE19 and PNT2 cells after 24 h, 48 h, 72 h and 96 h exposure indicated increase in activity towards the cancer cells. CBD was shown to be more potent in inducing cytotoxicity in A2780 cells compared cisplatin resistant A2780/CP70 cells at all the time points tested.

Table 3-2 IC_{50} values for CBD induced cytotoxicity on ovarian cancer A2780, A2780/CP70, OVACAR-3 cells and non-cancer ARPE19 and PNT2 cells

CBD	24h	48h	72h	96h
A2780	12.3 \pm 0.7 μ M	6.84 \pm 1.07 μ M	4.47 \pm 0.15 μ M	3.46 \pm 0.17 μ M
CP70	16.10 \pm 0.59 μ M	11.2 \pm 0.65 μ M	7.3 \pm 0.4 μ M	5.79 \pm 0.82 μ M
OVACAR3	37.232 \pm 3.53 μ M	21.12 \pm 1.6 μ M	17.71 \pm 0.5 μ M	8.97 \pm 1.19 μ M
ARPE19	25.29 \pm 1.83 μ M	14.40 \pm 0.9 μ M	13.01 \pm 0.2 μ M	11.71 \pm 1.15 μ M
PNT2	40.61 \pm 2.27 μ M	17.73 \pm 2.42 μ M	17.18 \pm 0.57 μ M	14.39 \pm 1.6 μ M

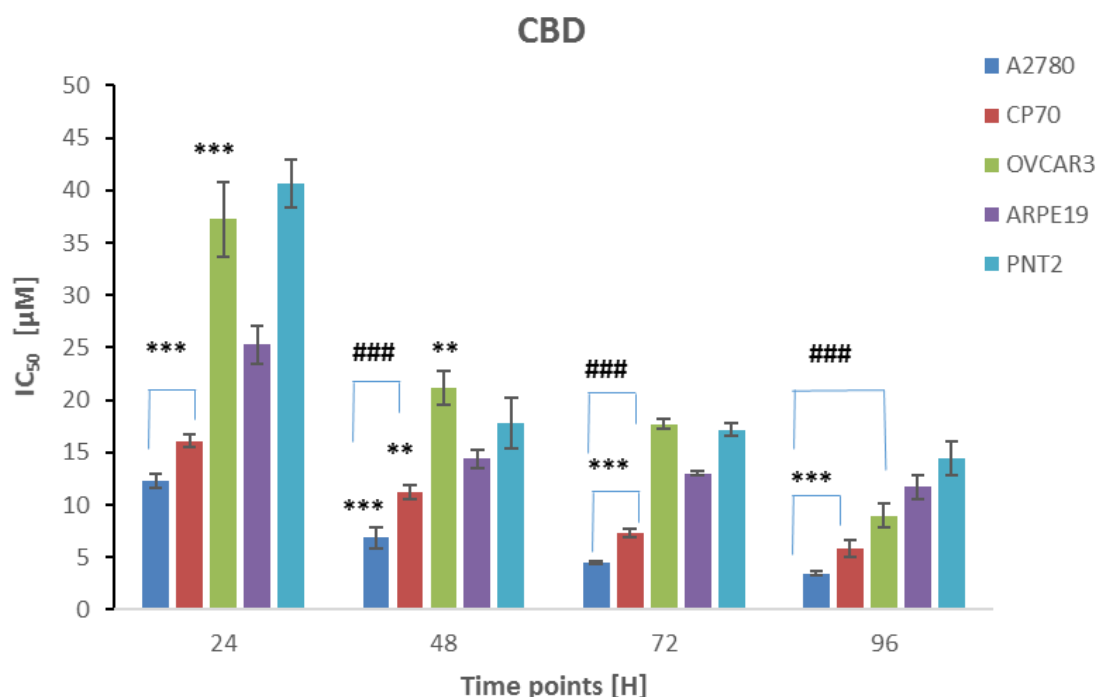


Figure 3-3 **The IC₅₀ values of CBD.** IC₅₀ values of CBD on A2780, A2780/CP70, ARPE19 and PNT2 cells at 24 h, 48 h, and 72 h, and 96 h time points. Data represents the mean ± standard error of mean of n=4. n is the number of independent biological experiments. **P<0.01 and ***P<0.001 (AREPE19), ###P<0.001 (PNT2).

The cytotoxicity of CBD increased with exposure time on all the cell lines tested. Amongst the cell lines tested, CBD was shown the highest potency on A2780 ovarian cells with lower IC₅₀ values (12.3 ± 0.7 µM, 6.84± 1.07 µM, 4.47± 0.15 µM and 3.46± 0.17 µM). Furthermore, CBD was shown lower IC₅₀ values in ovarian cancer A2780 and A2780/CP70 cells to non-cancer cells at all the time points tested. At 96 h contact time, the IC₅₀ values were significantly lower on ovarian cancer cells compared to PNT2 non- cancer cells.

3.2.2.1 Preferential Cytotoxicity of CBD:

Any preferential cytotoxicity of CBD cancer cells was compared to non-cancer cells by calculation of the selectivity index. Mean IC₅₀ values (n=4) on each ovarian cell lines were

compared with non- cancer cells ARPE19 and PNT2 separately for 24 h, 48 h, 72 h and 96 h time points.

$$SI = N \div C$$

(Section 2.5.6)

SI = Selectivity Index

N= Mean IC₅₀ on non- cancer cells

C= Mean IC₅₀ on cancer cells

If SI > 1, this means the drug shows preferential cytotoxicity towards cancer cells, if SI= 1, it means it is equally toxic to both cancer and non- cancer cells. If SI<1, this means it is more toxic to non- cancer cells than cancer cells (Allison et al., 2018)

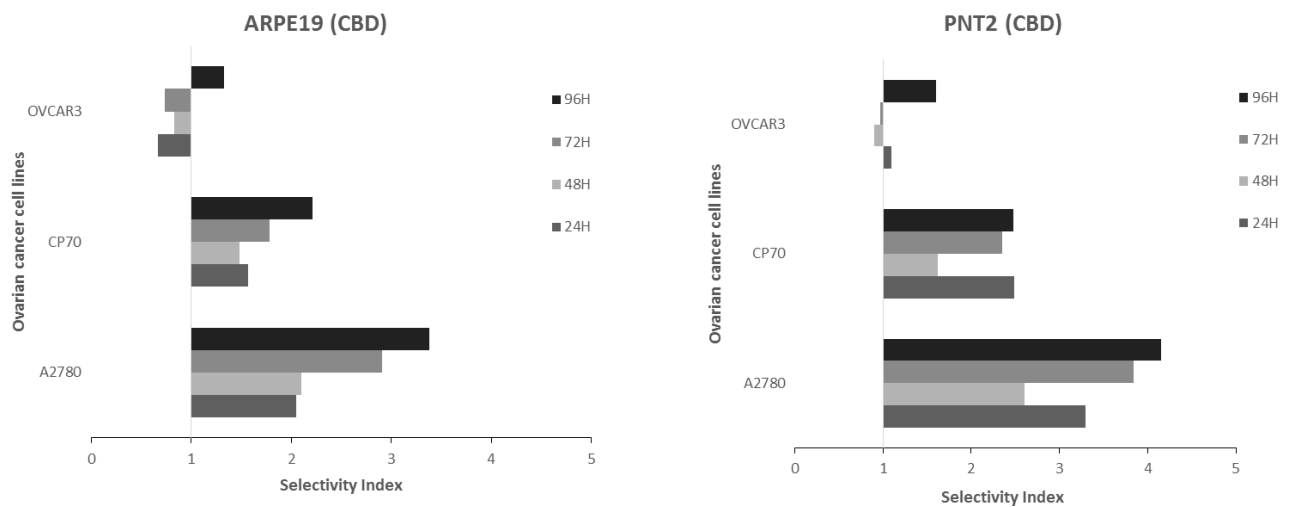


Figure 3-4. **The selective index of CBD against ARPE19 and PNT2.** The selectivity index values of CBD on ovarian cancer cells A2780, A2780 CP70, OVCAR 3 (based on mean IC₅₀ values) against non- cancerous cells ARPE19 and PNT2 after 24 h, 48 h, 72 h, and 96 h time points. Data represents the mean of n=4, n is the number of independent biological experiments.

CBD was shown to induce the preferential cytotoxicity in ovarian cancer cells A2780 and A2780/CP70 cells compared to ARPE19 and PNT2 at all the time points tested. The cancer

selectivity of CBD increased with increasing exposure time. CBD was shown selectivity towards OVACAR-3 only after 96 h exposure.

3.2.3 *In vitro* anticancer activity of CBG:

Similar experiments were performed to evaluate the activity of CBG on ovarian cancer and non-cancer cells as described in **section 3.2.2** IC₅₀ values were achieved from dose response of CBG (1 nM- 100 µM) on the cell lines. The results are summarised (**Figure 3-5, Figure 3-6, and Table 3-3**).

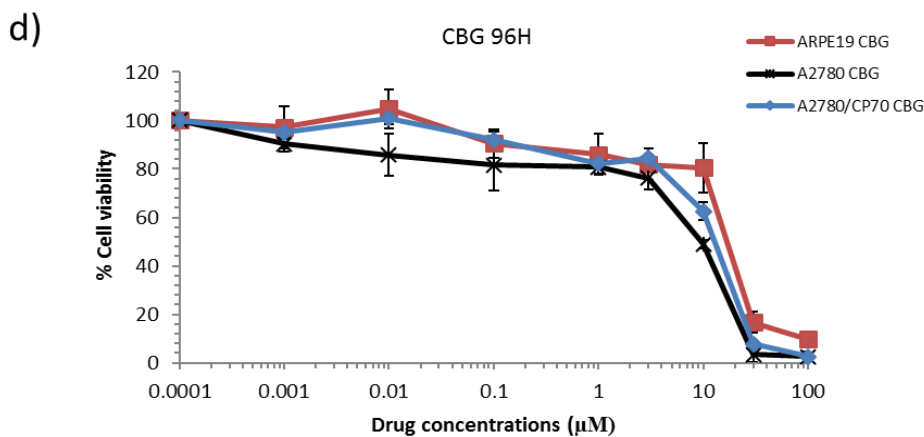
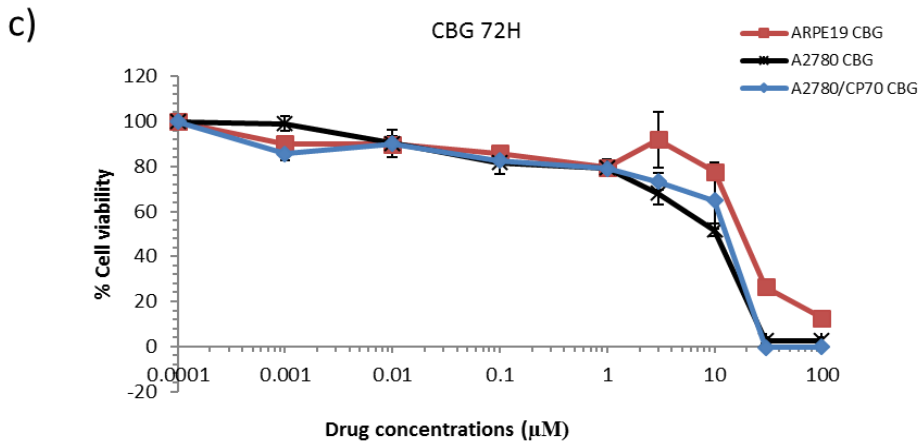
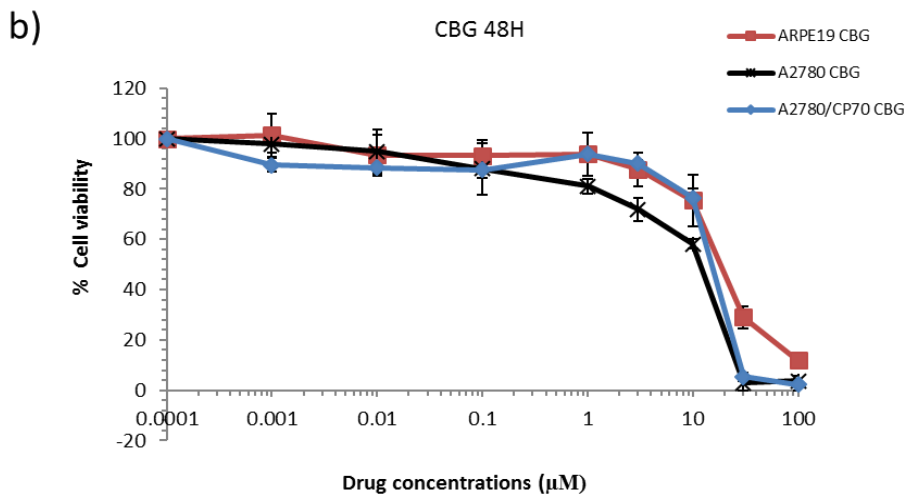
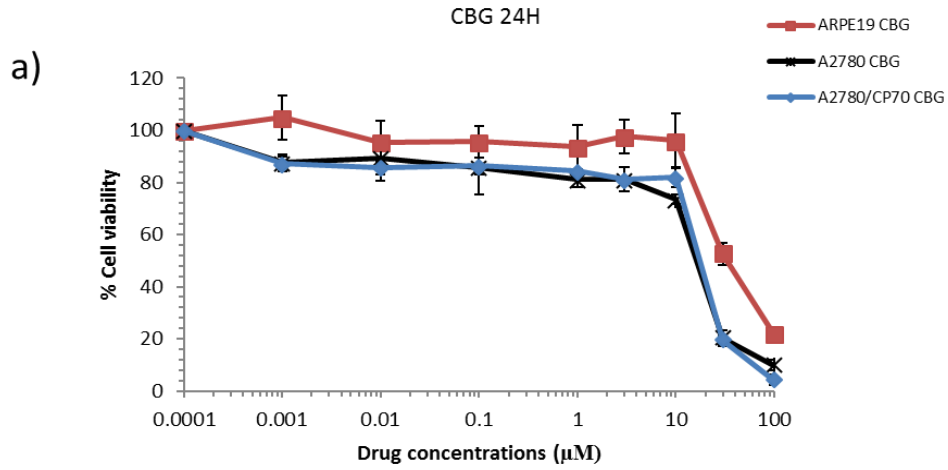


Figure 3-5. **In vitro cytotoxicity of CBG.** The effect of CBG (1 nM to 100 μ M) on ovarian cancer cells A2780, A2780/CP70 and non- cancer cells ARPE19 (retinal epithelial) and at 24 h (a), 48 h(b), and 72 h (c), and 96 (d) hour time points. The effect of CBG on cell viability as indicated by absorbance at 540 from dissolved formazan crystals compared to vehicle control. Data represents the mean \pm standard error of n=4, n is the number of independent biological experiments.

CBG has induced cytotoxicity in a dose-dependent manner in all cells. The cytotoxicity effects of CBG increases with drug exposure time (**Figure 3-5**). The pattern of CBG cytotoxicity towards all the cells tested was also similar to CBD, where A2780 cells were the most sensitivity followed by A2780/CP70, OVCAR-3 cells were the least sensitive ovarian cancer cells when treated with CBG (**Figure 3-5**).

Table 3-3 IC_{50} values for CBG induced cytotoxicity

CBG	24h	48h	72h	96h
A2780	15.26 \pm 0.31 μ M	13.86 \pm 0.55 μ M	9.39 \pm 0.80 μ M	5.69 \pm 0.21 μ M
CP70	17.73 \pm 0.05 μ M	15.42 \pm 0.8 μ M	12.25 \pm 1.44 μ M	7.12 \pm 0.75 μ M
OVCAR3	43.22 \pm 2.12 μ M	30.06 \pm 1.01 μ M	23.04. \pm 2.5 μ M	17.35 \pm 1.19 μ M
ARPE19	32.08 \pm 1.83 μ M	21.18 \pm 2.74 μ M	19.23 \pm 1.01 μ M	17.35. \pm 2.36 μ M
PNT2	37.18 \pm 2.06 μ M	22.88 \pm 1.52 μ M	19.95 \pm 0.32 μ M	18.26 \pm 1.3 μ M

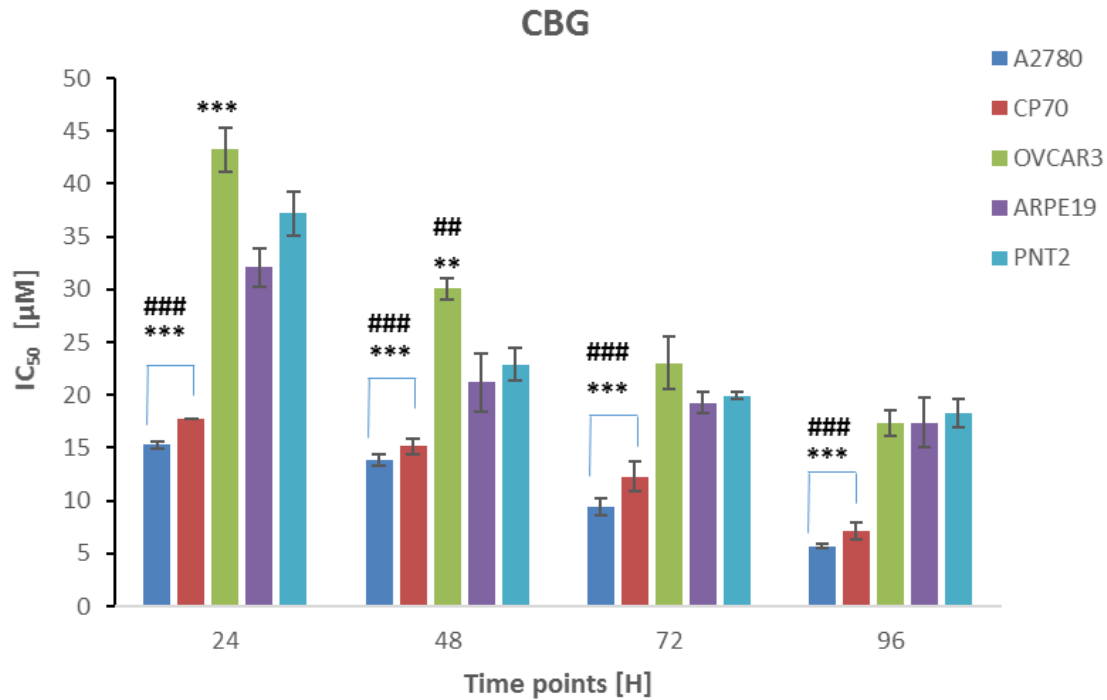


Figure 3-6 **The IC₅₀ values of CBG.** IC₅₀ values of CBG on A2780, A2780 CP70, ARPE19 and PNT2 cells at 24 h, 48 h, and 72 h, and 96 hour time point (a& b). It represents the mean \pm standard error of n=4, n is the number of independent biological experiments. **P<0.01 and ***P<0.001 (AREPE19). ##P<0.01 and ###P<0.001 (PNT2)

The IC₅₀ values of CBG are lower in ovarian cancer cells A2780 and A2780/ CP70 cells compared to non- cancerous cells except for OVCAR-3 cells where IC₅₀ values are close to both ARPE19 and PNT2 cells at all the time points tested (**Figure 3-6**).

3.2.3.1 Preferential Cytotoxicity of CBG:

Any preferential cytotoxicity exerted by CBG towards ovarian cancer cells when compared to non-cancer cells was determined by calculation of the selective index.

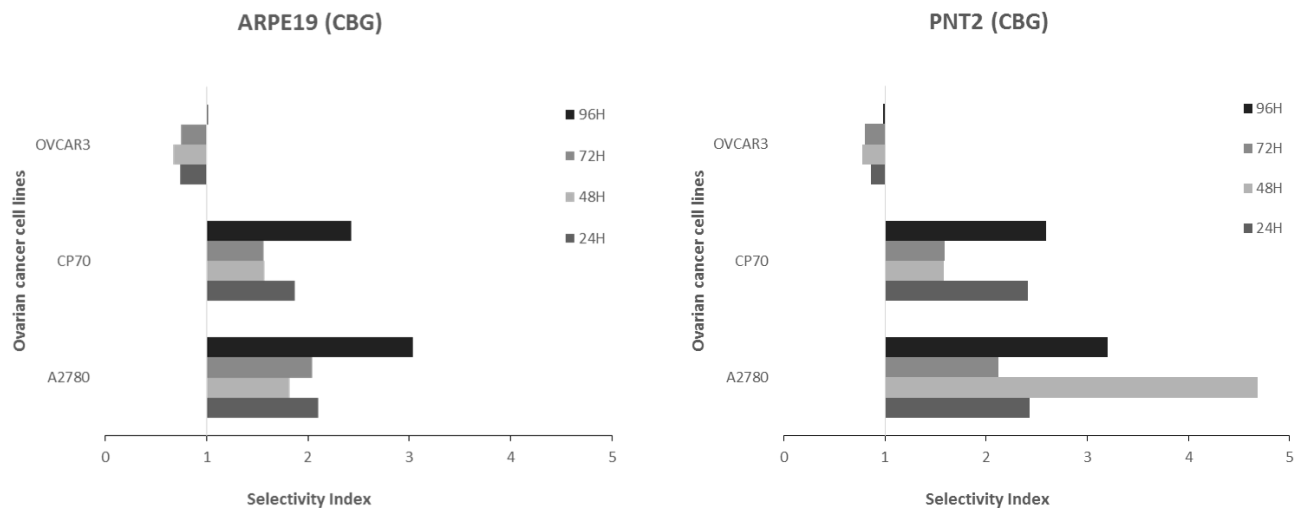


Figure 3-7. **The selective index of CBG against ARPE19 and PNT2.** The selectivity index values CBG on ovarian cancer cells A2780, A2780 CP70, OVCAR 3 (based on mean IC50 values) against non- cancerous cells ARPE19 and PNT2, after 24 h, 48 h and 72 and 96 h time points. Data represents the mean of n=4, n is the number of independent biological experiments

Similar to CBD, CBG was shown the preferential cytotoxicity towards ovarian cancer cells A2780 and A2780/CP70 compared to ARPE19 and PNT2 at all the time points tested. After 96 h exposure, CBG was equally toxic to OVCAR-3 and non-cancer cells with selective index value closer to 1.

In comparing the cytotoxicity of CBD and CBG, CBD induced greater cytotoxicity with lower IC₅₀ values towards the ovarian cancer cells tested compared to CBG. CBD and CBG both were shown their preferential cytotoxicity towards ovarian cancer cells A2780 and A2780/CP70 compared to ARPE19 and PNT2. Among all the time points tested, CBD and CBG were shown their highest selectivity towards cancer cells after 96 h exposure. However, OVACAR 3 seemed to be resistant to both cannabinoids. There was not any significant difference in preferential cytotoxicity between CBD and CBG. However, CBD is appeared to be preferable because of its lower IC₅₀ values and slightly better selective indices.

3.2.4 Cytotoxicity of CBD and CBG with drug washout experiments:

It was important to investigate whether the anticancer activities of CBD or CBG are due to rapid toxicity or anti-proliferative effects, which for example growth arrest of cells. So further investigations were carried out where both A2780 and A2780/CP70 cells were treated with CBD and CBG, and cells were allowed to recover from drug exposure after each time point by washing out the drug and replacing with complete media as described in **section 2.5.4**.

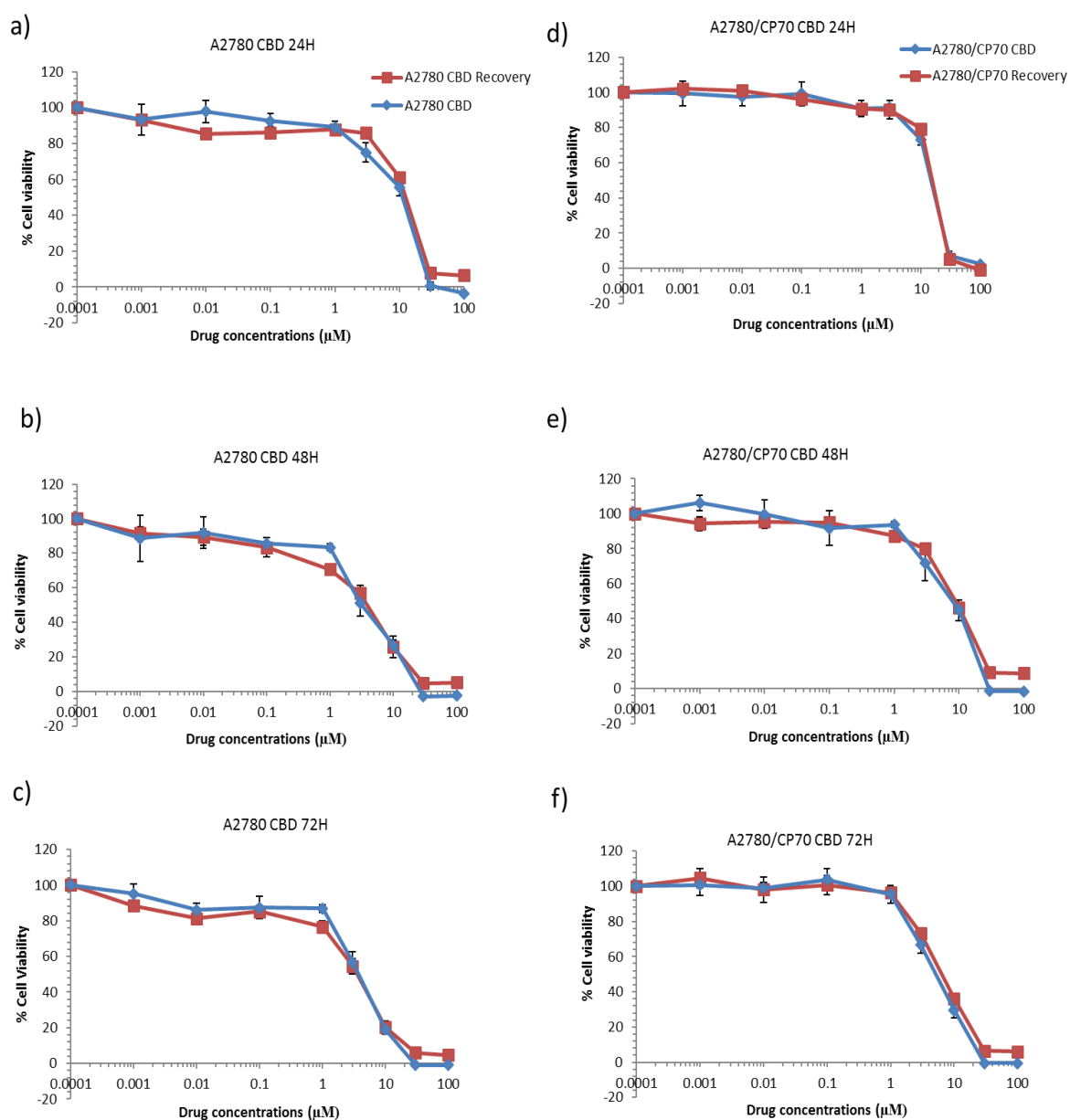


Figure 3-8 **Comparison of cytotoxic effects of CBD in normal vs drug washout MTT assays.** MTT assays were used to compare the cytotoxic effects induced by CBD after each time point and the cytotoxic effects of CBD when the cells were allowed to recover from drug exposure; the time points assayed were 24, 48 and 72 h. Graph a& d represents the 24 h exposure of CBD whereas b& e represents 48 h and, c& f represents 72 h on A2780 and A2780 CP70 cells respectively (n=4)

Table 3-4. The comparison between the IC50 values of CBD on A2780 cells, when cells were allowed to recover after each time point, and instant MTT viability assay after 24 h, 48 h and 72 h drug exposure.

A2780 CBD	24h	48h	72h
Instant MTT	11.72± 1.5µM	6.05± 1.0µM	4.54± 0.3 µM
Recovery assay	12.26± 0.9µM	7.4± 0.9µM	4.33± 0.1 µM

Table 3-5. The comparison between the IC50 values of CBD on A2780/CP70 cells, when cells were allowed to recover after each time point, and instant MTT viability assay after 24 h, 48 h and 72 h drug exposure

A2780 CP70 CBD	24h	48h	72h
Instant MTT	14.95± 0.6 µM	12.2± 1.1µM	7.11± 1.0µM
Recovery assay	16.62± 0.3 µM	10.74± 0.5µM	7.64± 0.4 µM

There was no significant difference observed in dose-responses of CBD between the MTT assay performed after each time point to the drug washout experiments, where the cells were allowed to recover from drug exposure, on both ovarian cancer cells at all the time points tested (**Figure 3-8, Table 3-4,& Table 3-5**)

Similar experiments were carried out with CBG on A2780 and A2780/CP70 cells. Results are summarised below in **Figure 3-9, Table 3-6& Table 3-7.**

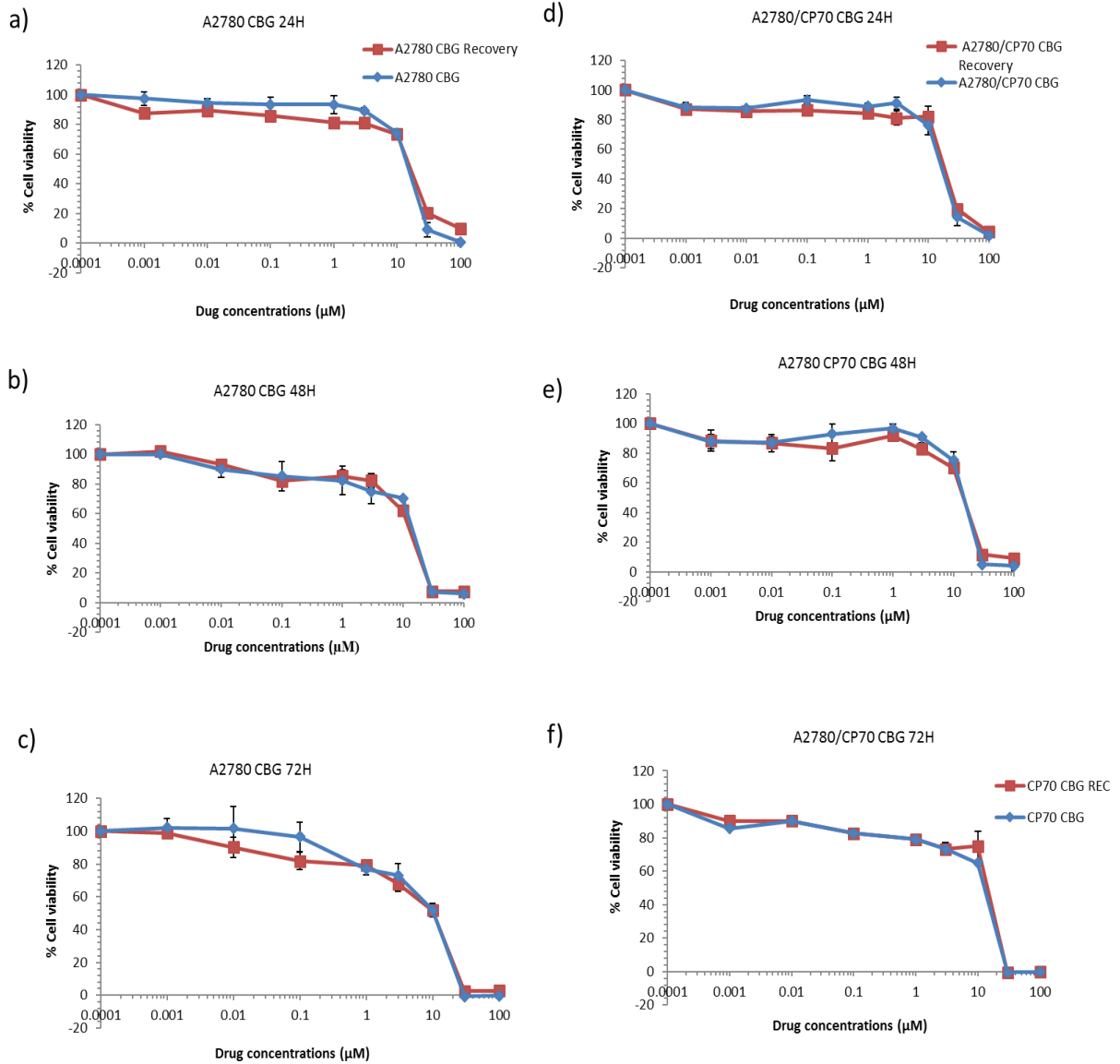


Figure 3-9 Comparison of cytotoxic effects of CBG in normal vs drug washout MTT assays. MTT assays were used to compare the cytotoxic effects induced by CBG after each time point and the cytotoxic effects of CBG when the cells were allowed to recover from drug exposure; the time points assayed were 24, 48 and 72 h. Graph a & d represents the 24 h exposure of CBG whereas b & e represents 48 h and, c & f represents 72 h on A2780 and A2780/CP70 cells respectively (n=4)

Table 3-6 The comparison between the IC₅₀ values of CBG on A2780 cells, when cells were allowed to recover after each time point, and instant MTT viability assay after 24 h, 48 h and 72 h drug exposure.

A2780 CBG	24h	48h	72h
Instant MTT	15.4± 0.3 µM	14.0± 0.5µM	10.01± 1.0µM
Recovery assay	14.9± 0.7 µM	12.72± 1.71µM	9.1± 1.39 µM

Table 3-7. The comparison between the IC₅₀ values of CBG on A2780/CP70 cells, when cells were allowed to recover after each time point, and instant MTT viability assay after 24 h, 48 h and 72 h drug exposure.

A2780 CP70 CBG	24h	48h	72h
Instant MTT	17.73± 1.0 µM	15.40± 0.6 µM	12.82± 1.0 µM
Recovery assay	17.72± 1.1 µM	14.84± 0.3 µM	11.78± 0.4 µM

Similar to CBD, the IC₅₀ values achieved by CBG with the instant MTT assays, and the cell recovery chemo sensitive assays were not significantly different from each other at 24 h, 48 h and 72 h exposure on both A2780 and A2780 CP70 (**Table 3-6** and **Table 3-7**).

There was no significant difference in the dose-responses data generated by the drug washout chemo sensitive assays and the instant MTT assays with CBD and CBG treatment. These results indicate that both cannabinoids exert irreversible cytotoxic effects on ovarian cancer cells.

3.2.5 Cytotoxicity of Carboplatin:

Carboplatin is one of the currently using chemotherapeutic drugs for ovarian cancer treatment. It was important to compare the effects of carboplatin with CBD and CBG on

ovarian cancer cells. The cytotoxic effects of carboplatin were investigated with different drug exposure times (24 h, 48 h, 72 h and 96 h) on A2780 and A2780/CP70 cells. Both normal MTT assays (**section 2.5.3**), and drug washout assays (**section 2.5.4**) were carried to investigate the difference in dose responses of carboplatin.

Carboplatin did not induce cytotoxicity when MTT assay was performed immediately after 24 h exposure in both the cell lines tested. However, the drug washout experiments where carboplatin was removed after 24 h, and cells were left in fresh complete media, and MTT was carried out after 72 h showed the greater cytotoxicity at concentrations higher than 1 μM . The maximum viability occurred around 5% at the highest concentration of 100 μM . Similar profile of response was observed when carboplatin was intact for 48 h. However, there was no significant difference between cytotoxicity induced by carboplatin at all the concentrations tested when cells were exposed to 72 h in both the conditions, and cytotoxicity response curves of carboplatin were superimposable after 72 h exposure (**Figure 3-10**).

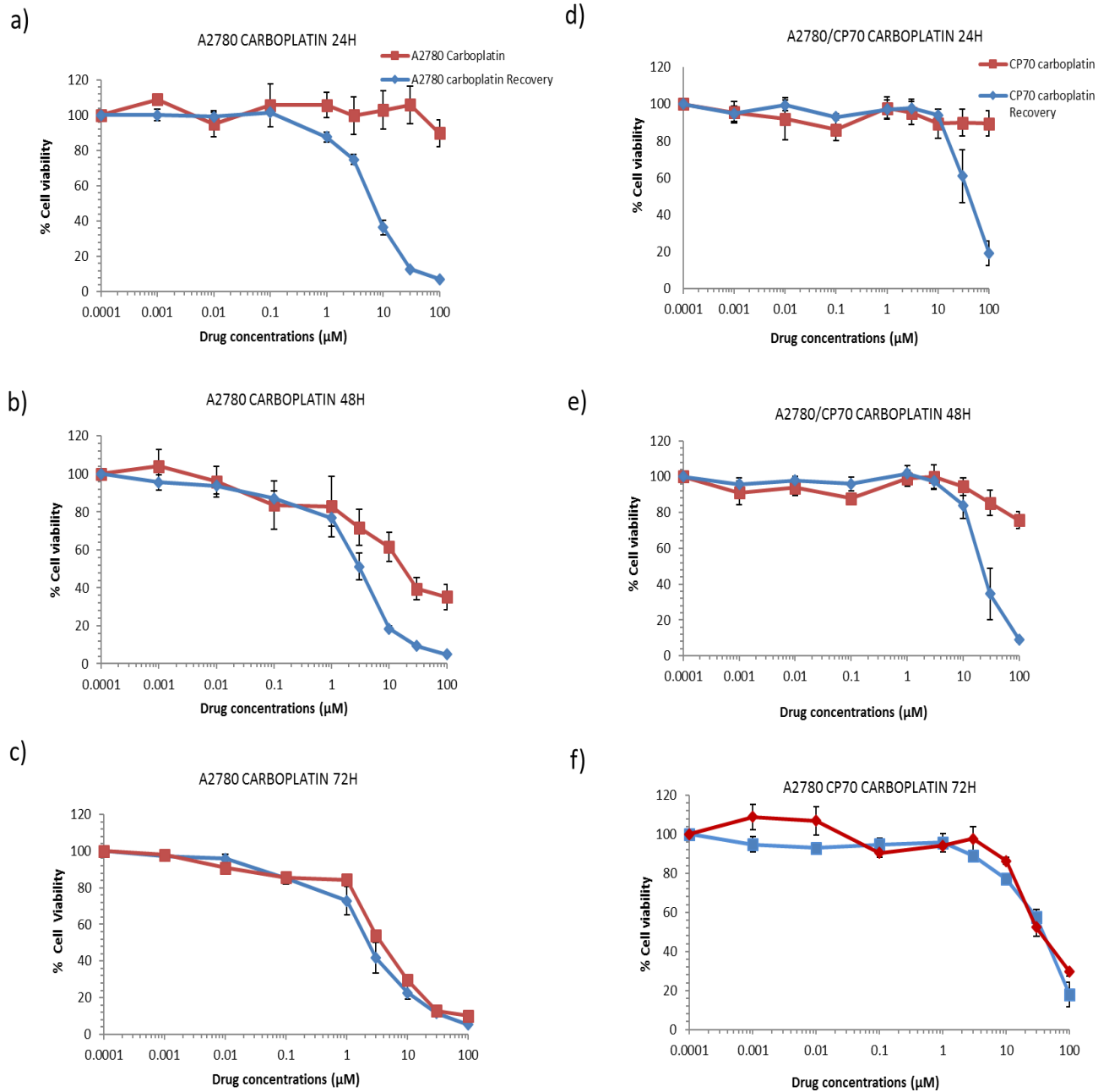


Figure 3-10. **Chemosensitive dose-response curves of A2780 and A2780/CP70 to carboplatin.** The difference in cytotoxic effects of carboplatin (1 nM to 100 μM) on A2780 and A2780 CP70 when MTTs were performed normally after each time point to drug washout experiments. Graph a& d represents the 24 h exposure of carboplatin whereas b& e represents 48 h and, c& f represents 72 h on A2780 and A2780/CP70 cells respectively (n=4)

Table 3-8 The comparison between the IC₅₀ values of carboplatin on A2780 cells, when cells were allowed to recover after each time point, and instant MTT viability assay after 24 h, 48 h and 72 h drug exposure.

A2780	24h	48h	72h
Carboplatin	>100µM	17.3±0.6µM	4.28±0.7µM
Carboplatin recovery	7.9±0.51µM	4.79±0.24µM	2.64±0.5µM

Table 3-9. The comparison between the IC₅₀ values of carboplatin on A2780 CP70 cells, when cells were allowed to recover after each time point, and instant MTT viability assay after 24 h, 48 h and 72 h drug exposure.

A2780 CP70	24h	48h	72h
Carboplatin	>100µM	>100µM	48.03±1.9µM
Carboplatin recovery	66.5±3.35µM	48.7±0.4µM	45.5±2.6µM

Chemo sensitivity assays carried out immediately after each time point showed that the IC₅₀ values of carboplatin were higher than 100 µM on both A2780 and A2780/CP70 cells after 24 h and 48 h. However, after similar exposure times where the cells were allowed to recover, carboplatin exerted cytotoxicity on A2780 with IC₅₀ values 7.95±0.51 µM and 4.79±0.24 µM, on A2780/CP70 cells with 66.5 ±0.35 µM and 48.7 ±0.4 µM respectively with drug washout chemo sensitivity assay. This might be because of the mechanism of action of carboplatin, which will be analysed further in discussion (**Table 3-8** and **Table 3-9**).

3.2.6 Comparison of carboplatin selectivity towards ovarian cancer cells compared to CBD and CBG:

The preferential cytotoxicity of carboplatin towards ovarian cancer cells against ARPE19 cells were investigated. The results were compared against CBD and CBG. **Figure 3-11, Figure 3-12& Figure 3-13**

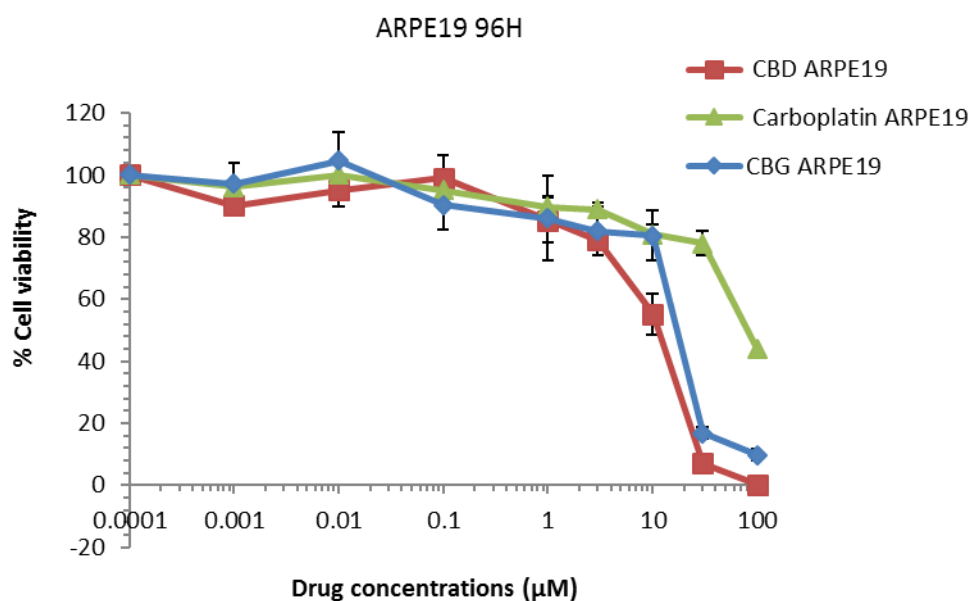


Figure 3-11. *The comparison of chemosensitivity of carboplatin against CBD and CBG on ARPE19 cells. The difference in dose-response curves of carboplatin on ARPE19 cells after 96 h exposure was compared with dose responses of CBD and CBG against ARPE19 cells. Each point represents mean ± s.e mean of n=4.*

The cytotoxicity effects of carboplatin on ARPE19 cells exerted an IC_{50} value of $83.62 \pm 0.4 \mu M$ after 96 h exposure. This was higher to the IC_{50} value exerted by carboplatin on A2780 ($2.57 \pm 0.3 \mu M$) and A2780/ CP70 cells ($44.9 \pm 3.5 \mu M$).

The preferential selectivity of carboplatin towards ovarian cancer cells against ARPE19 was calculated using Selectivity Index. The results were summarised and compared with CBD and CBG below.

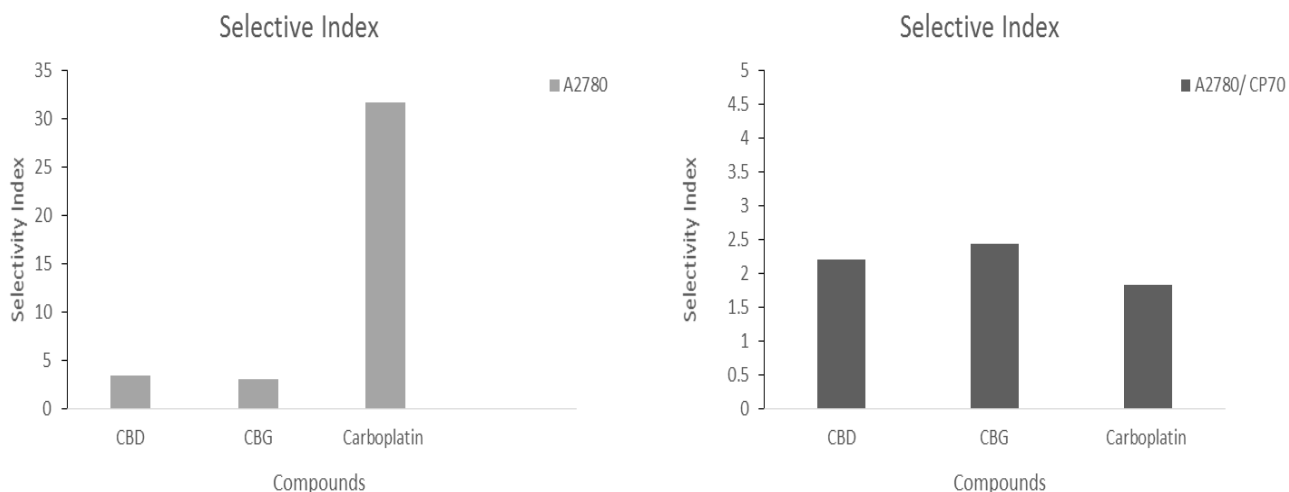


Figure 3-12 **Comparison of Selectivity Index.** The selectivity index of carboplatin on A2780 (left) and A2780/CP70 (right) cells against ARPE19 cells were compared with selectivity index of CBD and CBG after 96 h exposure.

Carboplatin was shown better preferential cytotoxicity towards A2780 cells when compared to CBD and CBG. However, CBD and CBG were shown better selectivity index towards cisplatin resistant A2780/ CP70 cells compared to carboplatin after 96 h exposure (**Figure 3-12**).

3.2.7 Comparison of carboplatin resistance factor with CBD and CBG in ovarian cancer cells

The resistant factor values for carboplatin, CBD and CBG were calculated by using the ratio of the mean IC₅₀ values of the compounds on cisplatin resistant A2780/ CP70 cells to the mean IC₅₀ values of the compounds on cisplatin sensitive A2780 cells. The cross resistance towards cisplatin resistance cells was determined by resistance factor calculation (McDermott et al., 2014)

$$RF = R \div S \quad (\text{Eq. 4})$$

RF= Resistant factor

S= Mean IC₅₀ values of the compounds on sensitive cell line

R= Mean IC₅₀ values of the compounds on resistant cell line

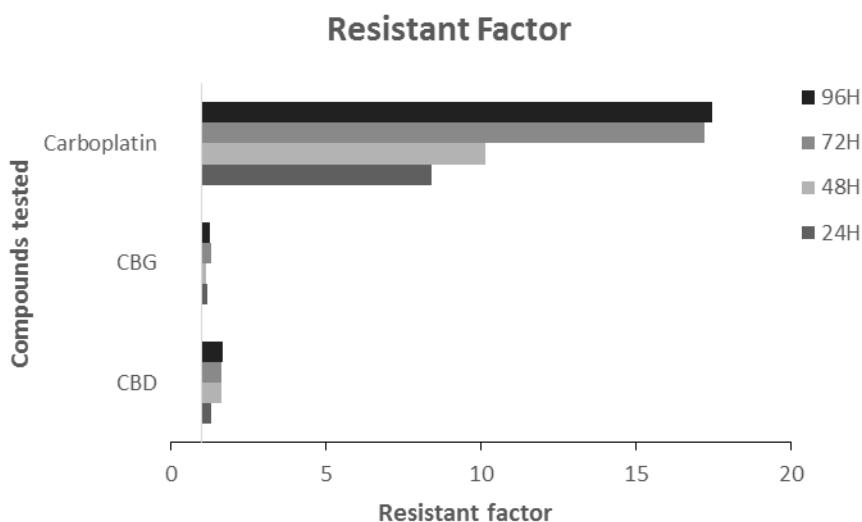


Figure 3-13. **Comparison of Resistant factor.** The difference between the resistance factor values of carboplatin, CBD and CBG after 24 h, 48 h, 72 h and 96 h contact times. Each value represents the mean \pm s.e mean of $n=4$.

The resistant factor values for carboplatin, CBD and CBG indicated that all the compounds were less sensitive towards cisplatin resistant cells. CBD and CBG exerted RF values <2 at all the time points tested. However, carboplatin was shown much higher RF values with maximum up to 17.83 (**Figure 3-13**). Even though carboplatin seemed to be more potent on A2780 cells with higher selectivity index, CBD and CBG exerted almost similar cytotoxic effects on both cisplatin-sensitive and cisplatin resistant cells.

3.3 Discussion

The results from chemosensitivity experiments indicated that both CBD and CBG have micromolar potency towards all three human ovarian cancer cell lines tested which included the cisplatin- and carboplatin- resistant line A2780/CP70. The IC_{50} values of CBD and CBG on A2780, A2780/CP70, and OVACAR 3 ovarian cancer cells are consistent with other published reports of activity against breast and prostate cancer cells at similar doses (Izzo et al., 2009, Ligresti et al., 2006)

IC₅₀ values for CBD were slightly lower than for CBG for the three ovarian cancer cell lines tested at all the time points indicating that CBD is more potent compared to CBG against A2780, A2780/CP70, and OVACAR-3. This is similar to studies in MCF-7 and breast cancer cell lines, which also indicated CBD to be the more potent cannabinoid (Ligresti et al., 2006). CBG induced selective cytotoxicity towards oestrogen receptor positive MCF-7 ($9.8 \pm 3.4 \mu\text{M}$) cells compared to oestrogen negative cells, MDA-MB-231 ($16.2 \pm 2.1 \mu\text{M}$) whereas CBD induced similar cytotoxicity in both MCF-7 ($8.2 \pm 0.3 \mu\text{M}$) and MDA-MB-231 ($10.6 \pm 1.8 \mu\text{M}$) cell lines. This suggests CBG can be a potential anti-cancer compound for oestrogen positive ovarian carcinoma (Ligresti et al., 2006).

CBD and CBG on ovarian cancer cells showed their highest selectivity towards cancer cells after 96 h exposure, suggesting the cancer selective cytotoxic effects of CBD and CBG increased with exposure that is more prolonged. However, both cannabinoids were much less active against OVACAR-3 cancer cells with IC₅₀ values similar to those of CBD and CBG towards the two non-cancer cell lines tested. OVACAR-3 cells were developed from malignant ascites of a patient with progressive adenocarcinoma of the ovary, which was refractory to the combination of Adriamycin, melphalan and cisplatin chemotherapy drugs used as treatment, so the cross-resistance could be a possible reason for the lower potency of the cannabinoids towards OVACAR-3 cells (Hamilton et al., 1983).

MTT assay is considered the gold standard cell sensitivity assay by many researchers. Since mitochondrial dysfunction considered as a common indicator for many cellular pathological processes. MTT assay rely on intracellular NAD (P) dependant oxidoreductases, which are produced by functional mitochondria. The production of NAD (P) dependant oxidoreductases also affected in a viable cell with reduced mitochondrial activity (Jaszczyszyn and

Gasiorowski., 2008, Surin. et al., 2017). However, microscopic observation of ovarian cancer cells treated with CBD/CBG in well plates developed for MTT, were shown 50% of growth inhibition at a concentration range similar to the IC_{50} values obtained by MTT assay.

The drug washout chemosensitivity assays showed that both CBD and CBG exerted similar IC_{50} values to the values generated by normal MTT assay after the corresponding time points. This indicates that the effects of CBD and CBG did not change with the cell recovery time, suggesting irreversible cytotoxic effects of the cannabinoids on the ovarian cancer cells.

IC_{50} values exerted by carboplatin by drug washout chemosensitivity assay were significantly lower than the values generated by conventional MTT assay at 24 h and 48 h: this could be because of carboplatin mechanism of action. The cytotoxicity mechanism of carboplatin involves its binding to DNA thus inhibiting transcription and replication as well as the generation of DNA damage which may result in cell cycle arrest or if the damage is not repaired cell death by apoptosis or other mechanisms. This complex mechanism would take a longer time to effect on mitochondrial function (Sousa et al., 2014).

The selectivity index of carboplatin towards the A2780 ovarian cancer cell line compared to the non-cancer ARPE19 cells indicates that carboplatin is more cancer cell selective in its cytotoxicity than CBD or CBG. However, when the relative cytotoxic effects of the drugs on cisplatin resistant A2780/CP70 cells and the parental cisplatin sensitive A2780 cells were tested the resistance factor values of carboplatin, CBD and CBG indicated that carboplatin had a greater than 9 fold resistance factor compared to CBD and CBG. This could be due to the cross-resistance mechanism of cisplatin resistant ovarian cancer cells towards carboplatin (Gore et al., 1989).

The lower resistance factors (< 2) of both CBD and CBG indicate that they exerted similar cytotoxic effects on both cisplatin sensitive and cisplatin resistant cells. Based on these data, further investigations were carried out to determine whether CBD or CBG when combined with current ovarian cancer chemotherapy drugs could increase their efficacy towards ovarian cancer cells.

CHAPTER 4: Evaluation of the combination effects of CBD/ CBG with the chemotherapeutic drugs, *In Vitro*

4.1 Introduction

The development of a malignant tumour is associated with a series of complex genetic mutations and alteration of multiple pathways, which makes cancer a difficult disease to treat. The fact that ovarian cancer associated with a diversity of mutations and histological types, it is difficult to get the desired therapeutic effect with a single drug (Natarajan et al., 2018, Kashif et al., 2015, Humphrey et al., 2011). The combination of drugs that exert different or non-overlapping mechanisms of action could improve the therapeutic effect. The different mechanisms of action also helps to overcome the drug resistance, which is a significant challenge in cancer treatment. Drug combinations can also sometimes reduce the considerable side effects of drugs, as lower, less toxic concentrations are required in the combination compared to single drug treatments (Kashif et al., 2015). However, side effects such as hypersensitive reactions, and the accumulation of toxicities of current combination treatments highlight the need to investigate potential compounds for combination therapies to treat cancer (Kashif et al., 2015, Fotopoulou, 2014).

This chapter will be focused on the combination effects of CBD with CBG, carboplatin, and paclitaxel (Taxol) to determine the most potent combination for ovarian cancer cells. Carboplatin and Taxol are both currently used for ovarian cancer chemotherapy (Fotopoulou, 2014).

4.2 Results

4.2.1 Combination effects of CBD with CBG

CBD and CBG used in this combination experiments were supplied by the GW Pharmaceuticals, UK. The purity of the compounds was tested using LC-MS. The cytotoxic

effects of CBD and CBG were provided by GW Pharmaceuticals, UK was compared against CBD and CBG purchased from Tocris, UK.

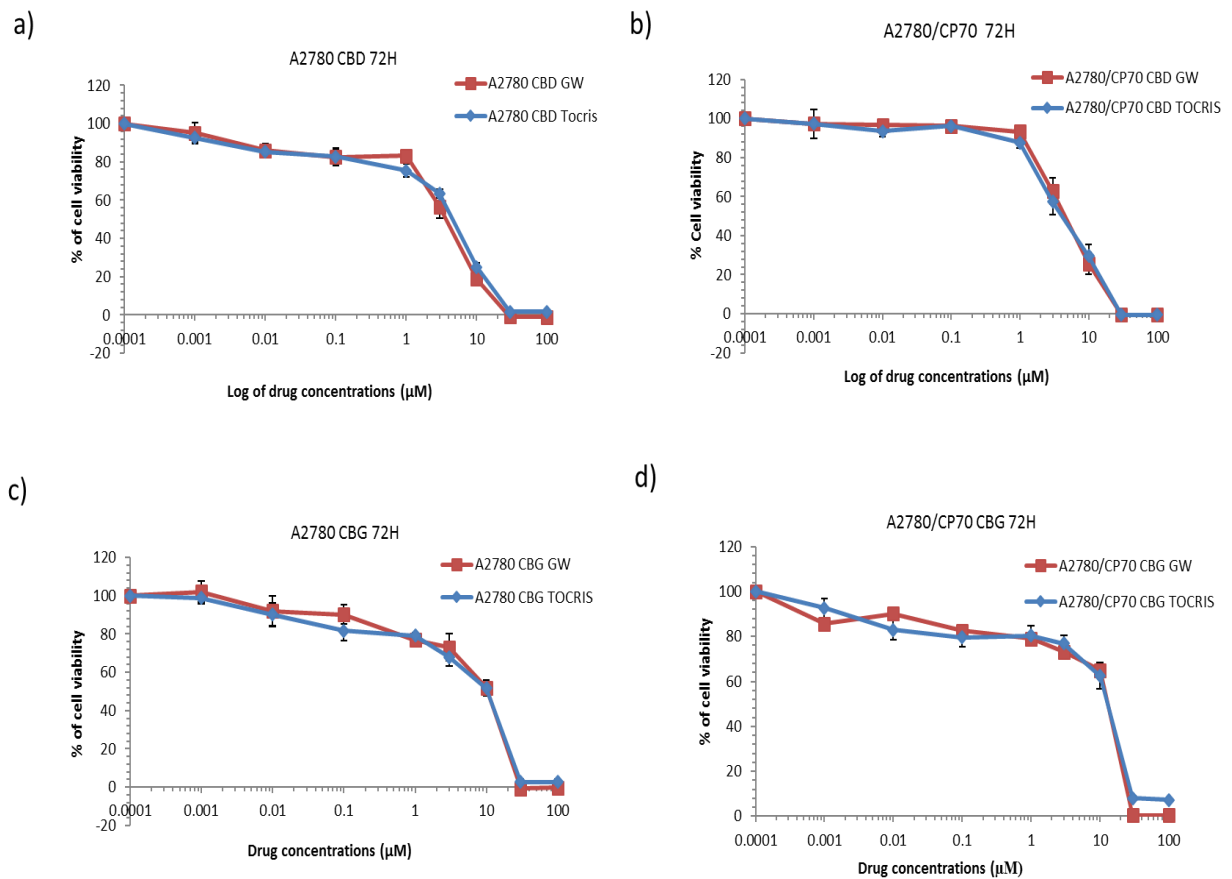


Figure 4-1. Dose- response curves of CBD and CBD after 72 h. The Representative comparison of dose-response curves of CBD, and CBG supplied by GW pharmaceuticals and Tocris on A2780 (a& c) and A2780/CP70 (b& d) cells after 72 h. The effect of CBD on cell viability as indicated by absorbance at 540 from dissolved formazan crystals compared to vehicle control. Data represents the mean \pm standard error of mean of $n=4$, n is the number of independent biological experiments.

As shown in **Figure 4-1**, the dose-response curves of CBD and CBG supplied by Tocris and GW pharmaceutical were overlapping at 72 h contact times tested. Similar results were observed at 24 h, and 48 h indicates that there is no difference in the compounds supplied by both the companies. Therefore, the experiments conducted using CBD and CBG provided by GW pharmaceuticals are comparable to the other experiments where the compounds were purchased from Tocris, UK.

The combination effect of CBD and CBG was investigated on A2780 and A2780/CP70. The cells were seeded in 96 well plates and incubated for 24 h. After incubation, different concentrations of CBD and CBG drugs were prepared at different ratios (1:1, 1:5 and 5:1) of concentration- response curves were constructed for each ratio from 1 nM to 100 μ M. 2 μ L of combination mix was added to corresponding wells. The plates were further incubated for 24 h, 48 h and 72 h. When the allocated time elapsed, MTT assay was performed. IC₅₀ values were achieved from dose response curves.

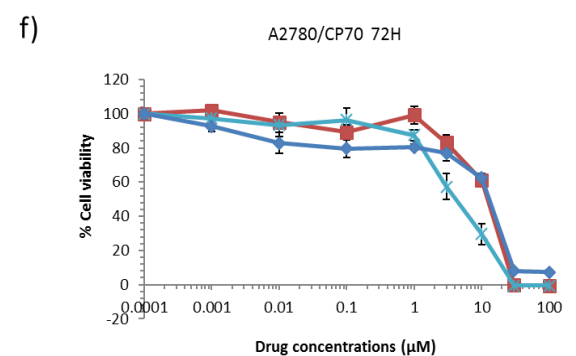
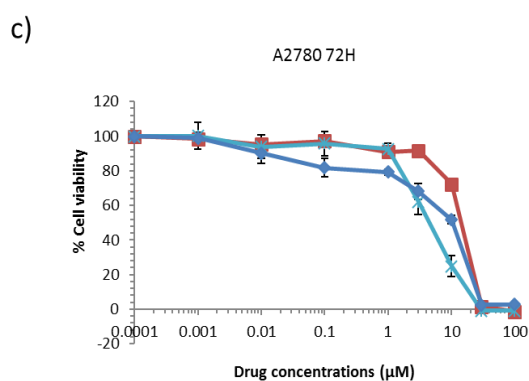
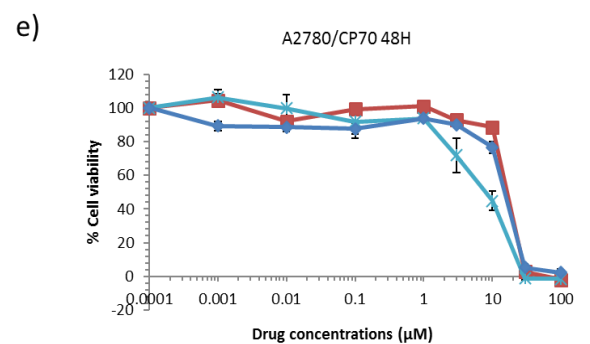
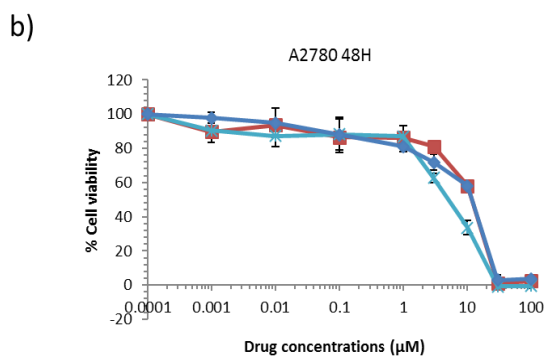
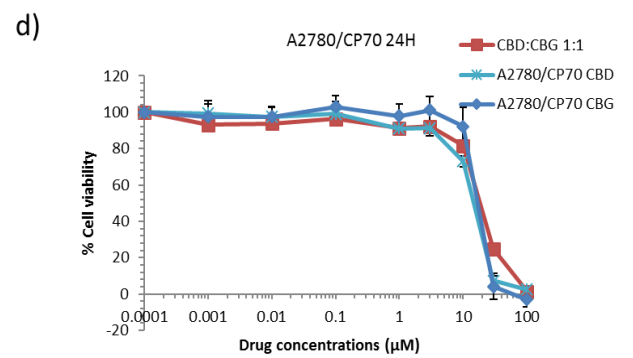
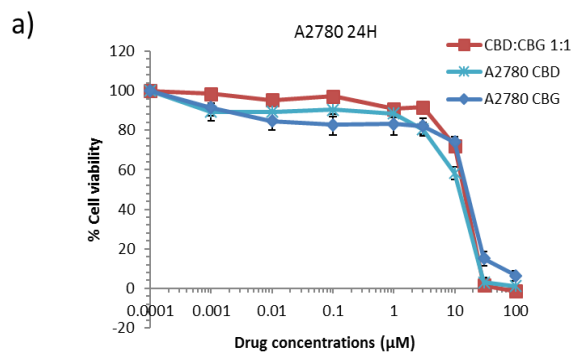


Figure 4-2 **CBD in combination with CBG**. The representative comparison of dose-responses of CBD alone to CBG alone and CBD and CBG in 1:1 combination on A2780 and A2780/CP70 cells after 24 h (a& d), 48 h (b& e) and 72 h (c& f) contact times. Graph a& d represents the 24 h exposure whereas b& e represents 48 h and, c& f represents 72 h on A2780 and A2780 CP70 cells respectively (n=4)

CBD alone on A2780, A2780/CP70 cells was more effective than CBG alone and CBD in combination with CBG (1:1) (**Figure 4-2**). Amongst the combinations tested, CBD: CBG 5:1 showed better cytotoxic effects followed by CBD: CBG 1:1 and 1:5 respectively on both the cell lines.

Table 4-1 The IC_{50} (μM) values of CBD alone, CBG alone and, CBD:CBG (1:1, 1:5, 5:1) on both A2780 and A2780/CP70 cells after 24 after 24 h, 48 h and 72 h contact time

IC_{50} (μM)	24H		48H		72H	
	A2780	CP70	A2780	CP70	A2780	CP70
CBD	12.3± 0.7	16.1± 0.5	6.84± 1.07	11.2± 0.65	4.4±0.15	7.3± 0.4
CBG	15.26±0.05	17.73±0.05	13.86±0.55	15.42±0.8	9.39±0.80	12.25±0.75
CBD:CBG 1:1	14.27±1.6	18.99± 0.1	11.67±1.6	15.74±1.9	5.95±1.06	12.23±1.3
CBD:CBG 1:5	14.57±1.7	21.55±3.06	8.28±2.1	15.88±0.2	4.30±1.5	13.98±0.65
CBD:CBG 5:1	13.58± 1.8	15.84±2.1	7.7±2.3	11.42±1.4	3.08± 0.6	7.16±2.8

The IC_{50} values demonstrated by CBD alone on A2780, and A2780/CP70 cells were lower than CBG alone and all the combinations of the compounds tested. Among the cannabinoid combinations, IC_{50} values of CBD in combination with CBG 5:1 were closer to the IC_{50} values of CBD alone, followed by CBD/CBG 1:1 and 1:5 respectively. Based on the results (**Figure 4-2 & Table 4-1**) it was observed that the combination of CBD and CBG did not increase the potency of CBD.

4.2.2 Carboplatin in Combination with CBD or CBG:

4.2.2.1 *Carboplatin in Combination with CBD or CBG on A2780 cells:*

The combination effects of CBD or CBG on ovarian cancer cells were investigated when combined with carboplatin. The sub-lethal concentrations (100 nM) of CBD or CBG on ovarian cancer cells were taken as a constant in combination to carboplatin (1nM- 100 μ M). The cells were seeded in 96 well plates and incubated for 24 h. The following day the plates were treated with 100 nM CBD or CBG, and incubated for 30 minutes. After the incubation time elapsed, the plates were treated with carboplatin with the dose ranges from 1 nM to 100 μ M to the corresponding wells. The plates were further incubated for 24 h, 48 h, 72 h and 96 h contact times. After each time point (24 h, 48 h and 72 h), the media was removed from 96 well plates, and were washed with PBS to remove any remaining drug. The wells were replaced with 200 μ l of complete media. Cells were allowed to recover up to 96 h from initial drug contact. MTT assay was performed after 96 h.

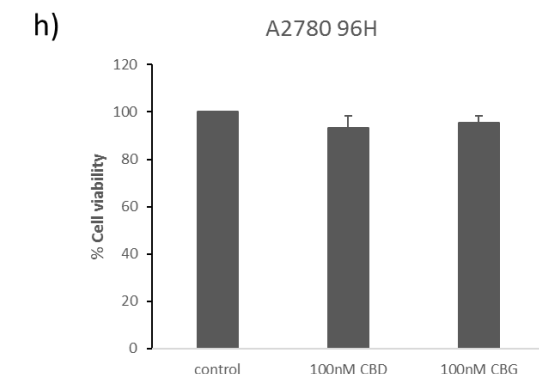
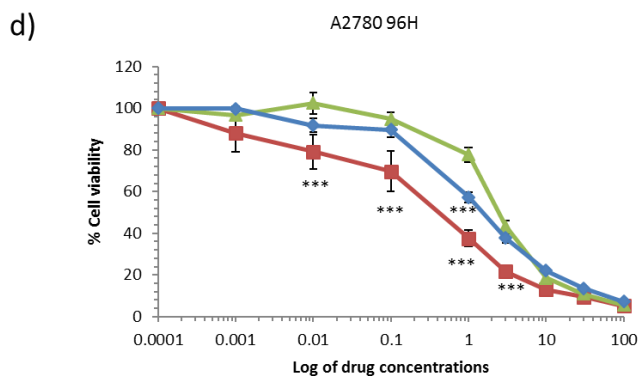
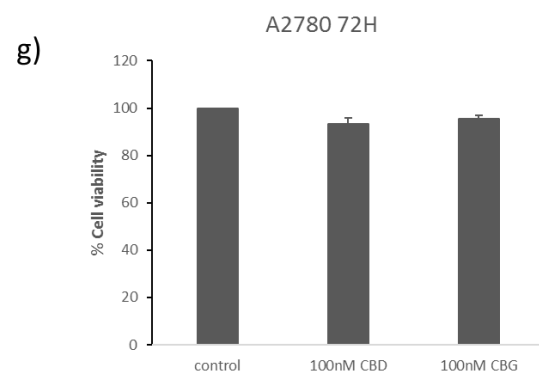
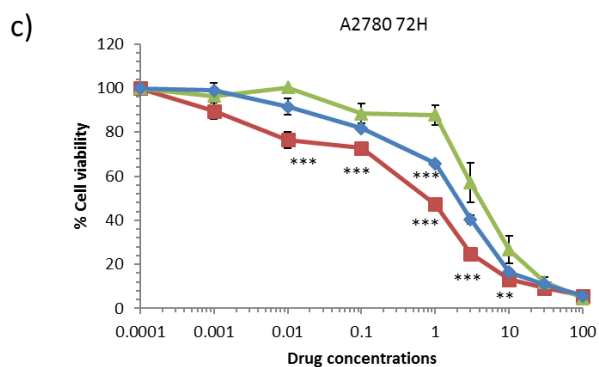
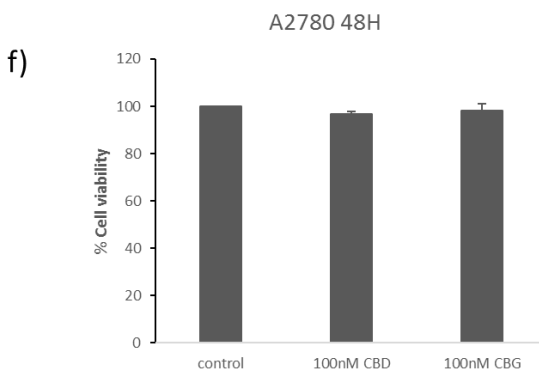
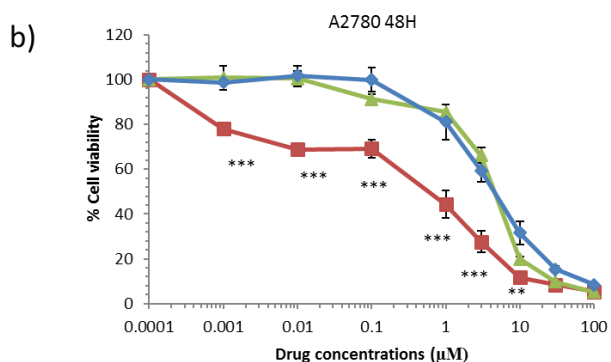
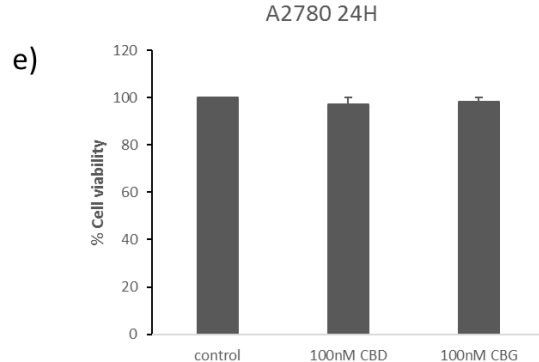
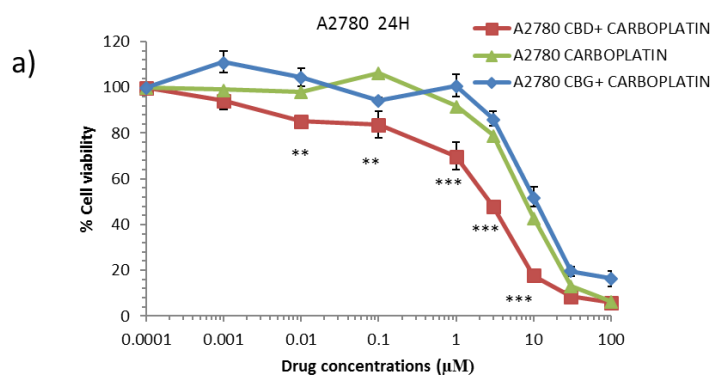


Figure 4-3 Carboplatin in combination with 100 nM CBD or 100 nM CBG on A2780 cells. Comparison between carboplatin alone to carboplatin in combination with 100 nM CBD and carboplatin in combination with 100 nM CBG. 1% ultrapure water was used as a solvent control for carboplatin alone whereas 100 nM CBD and 100 nM CBG were used as a control for combination. Graph a) represents 24 h, b) represents 48 h, c & d represents 72 h and 96 h respectively. The viability of A2780 cells with 1% ethanol (control) were compared to the viability with 100 nM CBD and 100 nM CBG at 24 h (e), 48 h (f), 72 h (g), and 96 h (h). ** $P < 0.01$ and *** $P < 0.001$. (n=4)

As can be seen in **Figure 4-3**, when carboplatin was used in combination with 100 nM CBD the cytotoxic effect of carboplatin was improved at all the time points tested. The combination of 100 nM CBG plus carboplatin induced superimposable concentration response curves. The results indicate that CBD, when used at non-toxic concentrations, in combination with carboplatin induces greater cytotoxicity compared to the effects of carboplatin alone on both the ovarian cancer cells.

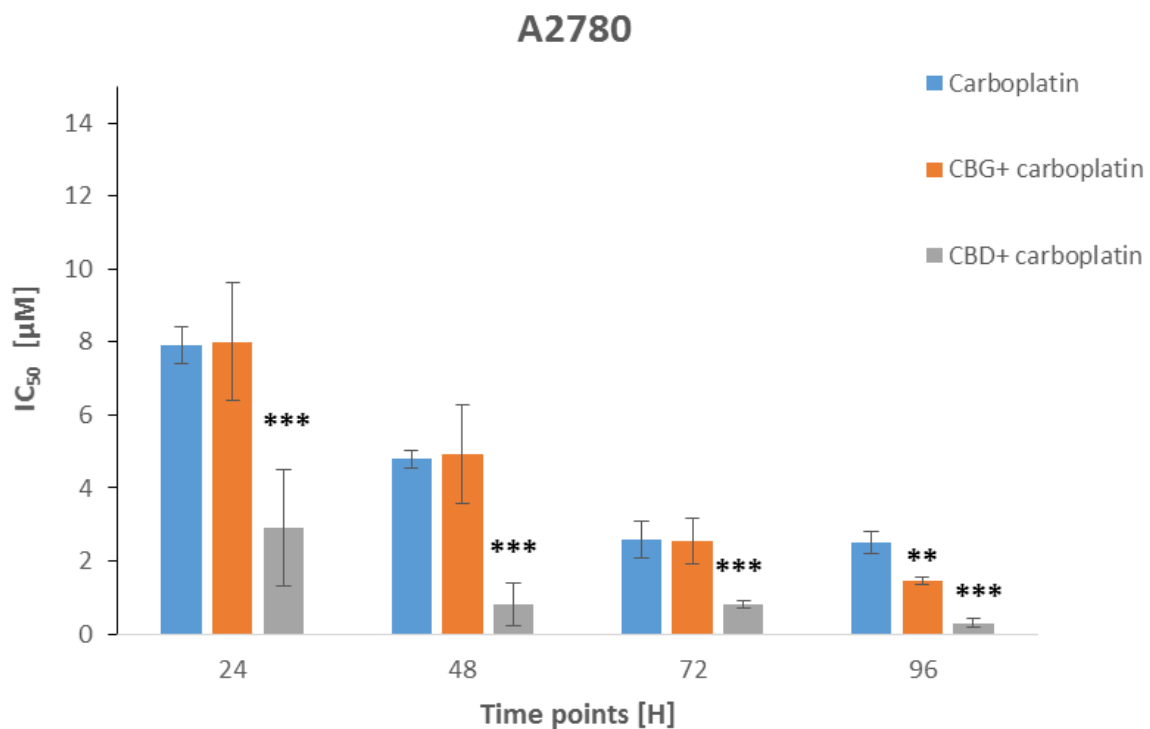


Figure 4-4 IC_{50} values of carboplatin alone, and in combination with CBD or CBG in A2780 cells. The comparison of IC_{50} values of Carboplatin alone, and carboplatin when combined with 100 nM CBD or 100 nM CBG on A2780

cells at 24 h, 48 h, 72 h, and 96 h. It represents the mean \pm standard error of mean of n=4, **P<0.01 and ***P<0.001

That carboplatin in combination with 100 nM CBD shown significantly (P< 0.001) lower the IC₅₀ values (2.91 \pm 1.62 μ M, 0.82 \pm 0.62 μ M, 0.82 \pm 0.13 μ M and 0.23 \pm 0.13 μ M) compared to carboplatin alone (7.9 \pm 0.5 μ M, 4.7 \pm 0.2 μ M, 2.6 \pm 0.5 μ M and 2.5 \pm 0.3 μ M). Carboplatin in combination with 100 nM CBG showed the IC₅₀ value 1.46 \pm 0.5 μ M significantly (p<0.01) lower than carboplatin alone treatment at 96 h exposure (**Figure 4-4**)

In order to investigate CBD or CBG induce additive or synergistic effects when combined with carboplatin, the combination Index was calculated. It has accepted that If CI between 0.90 and 1.10 indicates additivity; CI below this range indicates synergism and above this range indicates antagonism (Liang Zhao, 2004). The combination Index (CI) for CBD or CBG when combined with drug Carboplatin was calculated by the ratio of the applied concentration of CBD or CBG (100 nM) in the combination to the IC₅₀ of CBD or CBG when it was applied individually, the ratio of the applied concentration of carboplatin in the combination (combination IC₅₀ – 100 nM), to IC₅₀ of B on the cells.

$$CI = (100 \text{ nM} \div \text{the IC}_{50} \text{ of CBD or CBG}) + (\text{carboplatin concentration in combination IC}_{50} \div \text{the IC}_{50} \text{ of CBD or CBG})$$

For e.g. The CI of carboplatin in combination with CBD at 24 h contact time on A2780 cells

Concentration of CBD in the IC₅₀ of the combination = 100 nM (0.1 μ M)

Concentration of carboplatin in the IC₅₀ of the combination = 2.91 μ M – 0.1 μ M = 2.8 μ M

The IC₅₀ of CBD on A2780 cells at 24 h = 12.3 μ M

The IC₅₀ of Carboplatin on A2780 cells at 24 h = 7.9 μM

So,

$$CI_{[CBD + CARBOPLATIN]} = (0.1 \div 12.3) + (2.8 \div 7.9) = 0.36$$

The CI values of carboplatin in combination with CBD at 24 h (0.36), 48 h (0.17), 72 h (0.15), and 96 h (0.096) suggested the strong synergism effect. Whilst CBG has shown synergism with carboplatin only after 96 h exposure (CI = 0.55).

4.2.2.2 Carboplatin in Combination with CBD / CBG on A2780/ CP70 cells:

Similar experiments to A2780 cells were carried out on A2780/ CP70 cells. The results were summarised in **Figure 4-5& Figure 4-6**

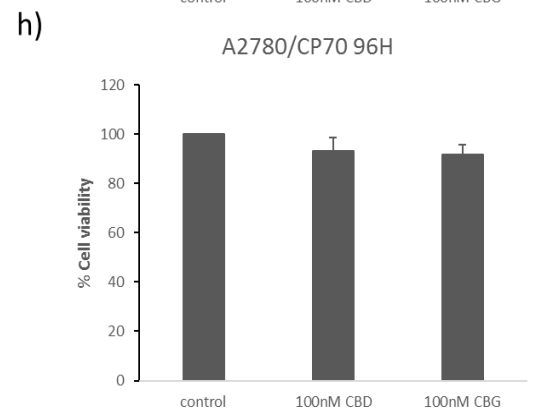
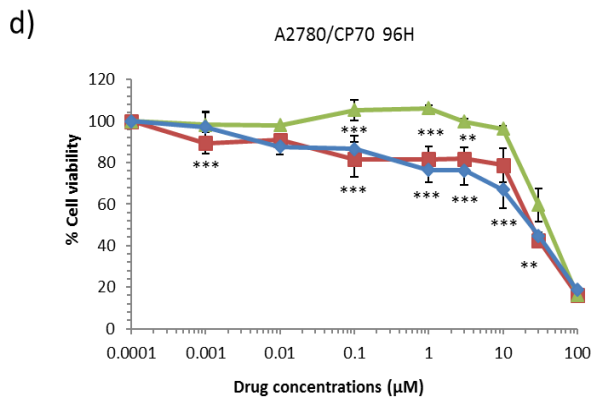
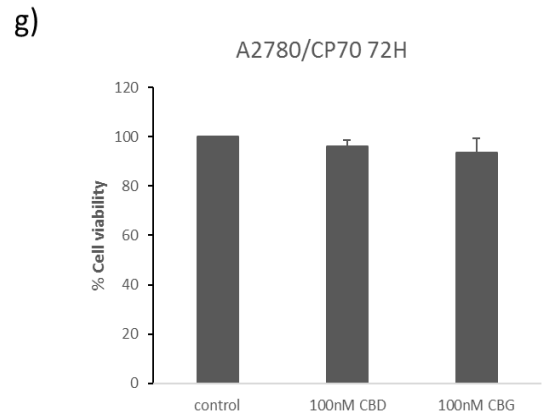
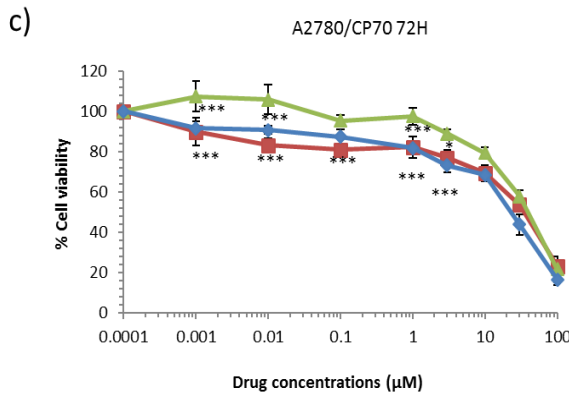
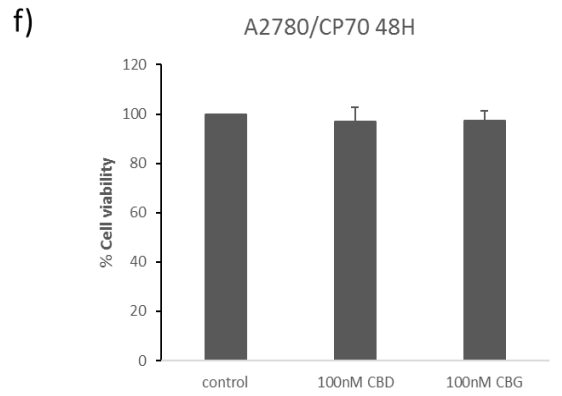
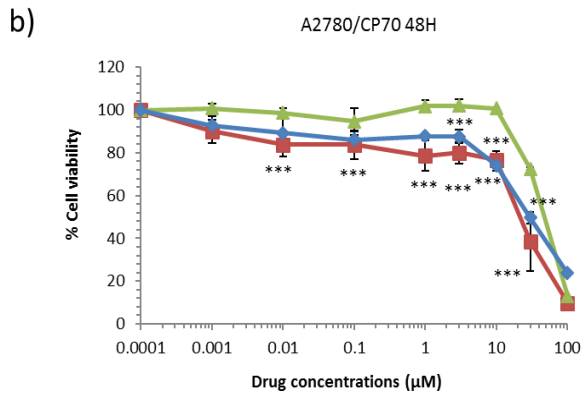
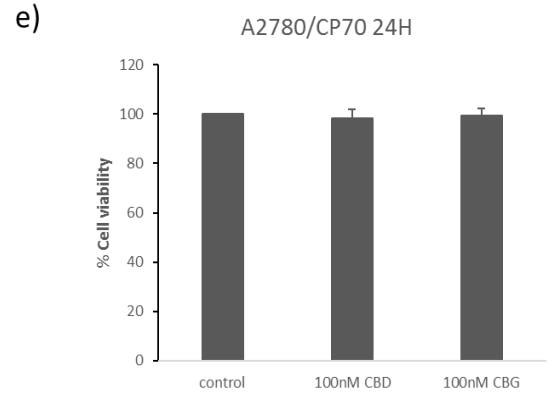
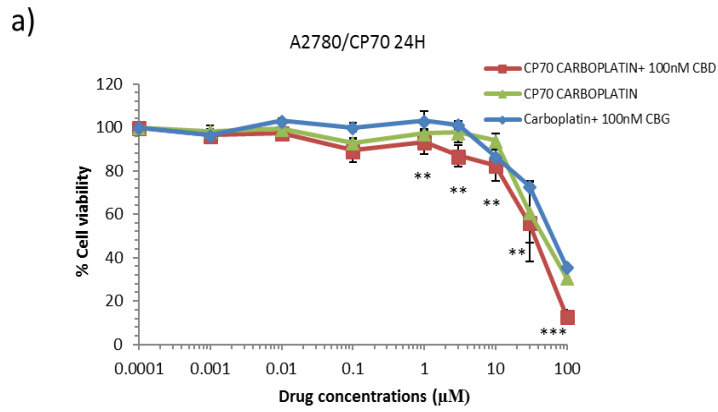


Figure 4-5 Carboplatin in combination with 100 nM CBD or 100 nM CBG on A2780/CP70 cells. The comparison between carboplatin alone to carboplatin in combination with 100 nM CBD and carboplatin in combination with 100 nM CBG. 1% ultrapure water was used as a solvent control for carboplatin alone whereas 100 nM CBD and 100 nM CBG were used as a control for combination. Graph a) represents 24 h, b) represents 48 h, c & d represents 72 h and 96 h respectively. The viability of A2780/CP70 cells with 1% ethanol (control) were compared to the viability with 100 nM CBD and 100 nM CBG at 24 h (e), 48 h (f), 72 h (g), and 96 h (h). * $P < 0.05$, ** $P < 0.01$ and *** $P < 0.001$. ($n=4$)

Carboplatin had shown better cytotoxic effects when combined with CBD and CBG at 48 h, 72 h and 96 h on A2780/CP70 cells. CBD and CBG had shown similar dose-response effects when combined with carboplatin at all-time points except 24 h, where CBD in combination with carboplatin seemed to be more effective.

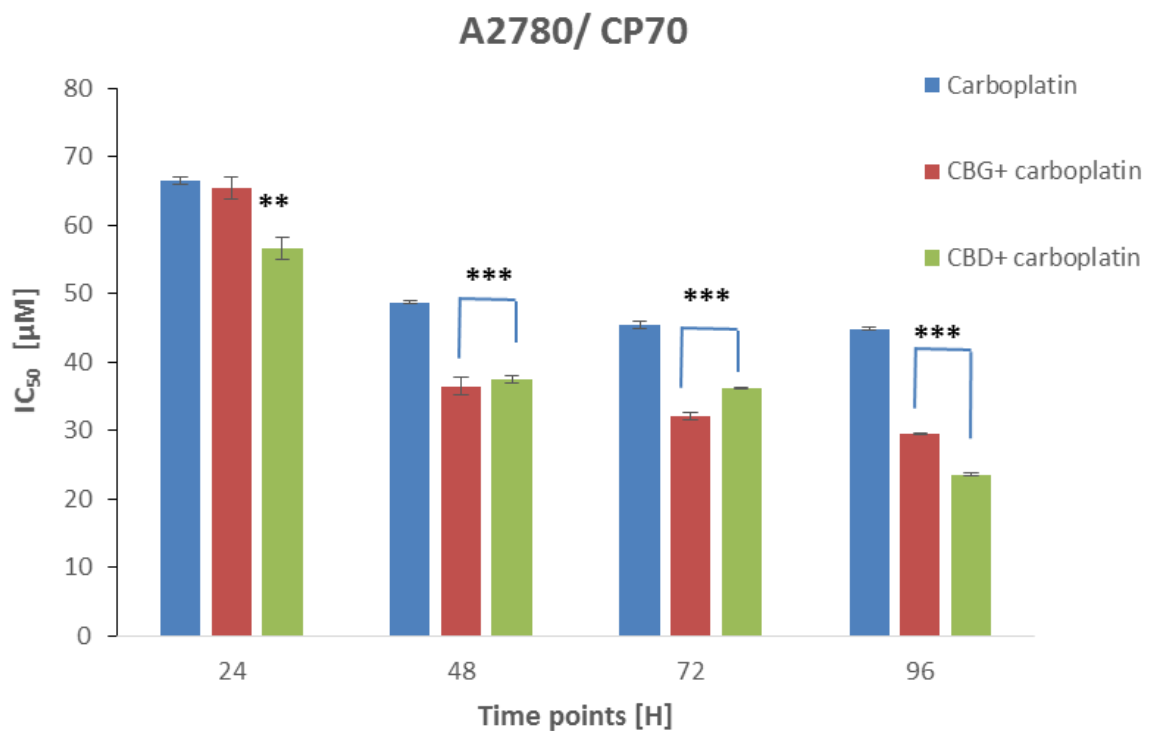


Figure 4-6 IC₅₀ values of carboplatin alone, and in combination with CBD or CBG A2780/CP70 cells. The comparison of IC₅₀ values of Carboplatin alone, and carboplatin when combined with 100 nM CBD or 100 nM CBG on A2780/CP70 at 24 h, 48 h, 72 h, and 96 h. It represents the mean \pm standard error of mean of $n=4$, n represents the number of experiments. ** $P < 0.01$ and *** $P < 0.001$ ($n=4$).

Carboplatin in combination with 100 nM CBD determined significantly ($P < 0.001$) lower IC_{50} values ($56.7 \pm 2.6 \mu\text{M}$, $37.5 \pm 1.2 \mu\text{M}$, $36.1 \pm 1.1 \mu\text{M}$ and $23.6 \pm 0.7 \mu\text{M}$) compared to carboplatin alone ($66.5 \pm 3.3 \mu\text{M}$, $48.7 \pm 0.4 \mu\text{M}$, $45.6 \pm 0.5 \mu\text{M}$ and $44.9 \pm 3.2 \mu\text{M}$). Carboplatin in combination with 100 nM CBG achieved significantly lower ($P < 0.001$) IC_{50} values of $36.5 \pm 3.2 \mu\text{M}$, $32.1 \pm 2.7 \mu\text{M}$, and $29.5 \pm 0.5 \mu\text{M}$ at 48 h, 72 h and 96 h respectively (**Figure 4-6**).

Carboplatin when combined with CBD has demonstrated slightly synergistic effects with CI values 0.85, 0.78, 0.8 and 0.57 after 24 h, 48 h, 72 h, and 96 h respectively. Carboplatin in combination with CBG exerted similar effects at 48 h (0.78), 72 h (0.71), and 96 h (0.65).

Both the cannabinoids demonstrated synergistic effects when combined with carboplatin on A2780, and cisplatin resistant A2780/CP70 cells. Further combination experiments were carried out on ARPE19 cells to determine whether the synergetic effects demonstrated by the cannabinoids in combination with carboplatin were cancer selective as seen in **Figure 4-7**.

4.2.2.3 Carboplatin in Combination with CBD /CBG on ARPE19 cells:

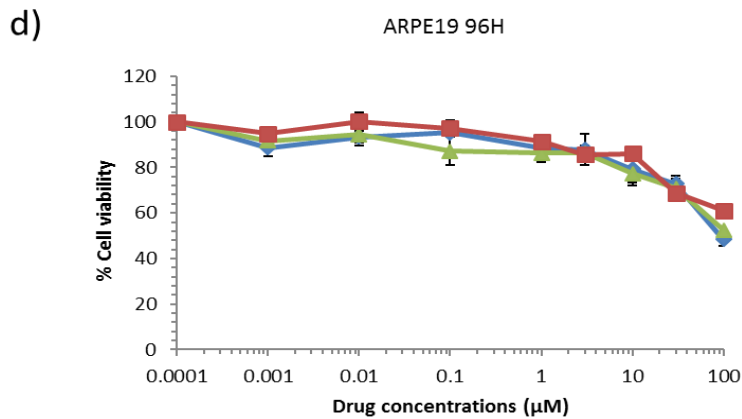
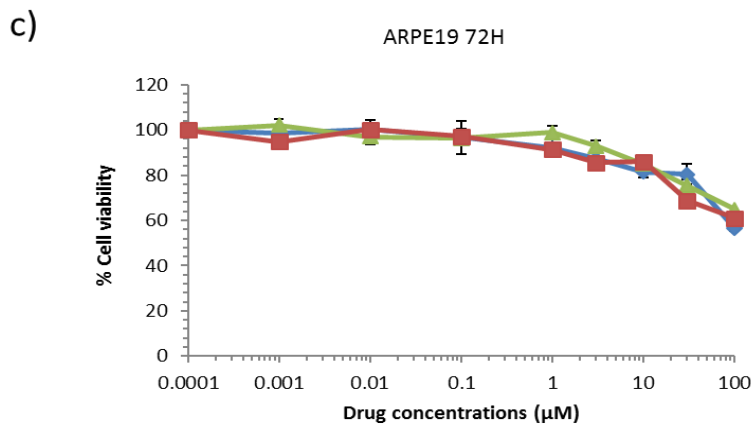
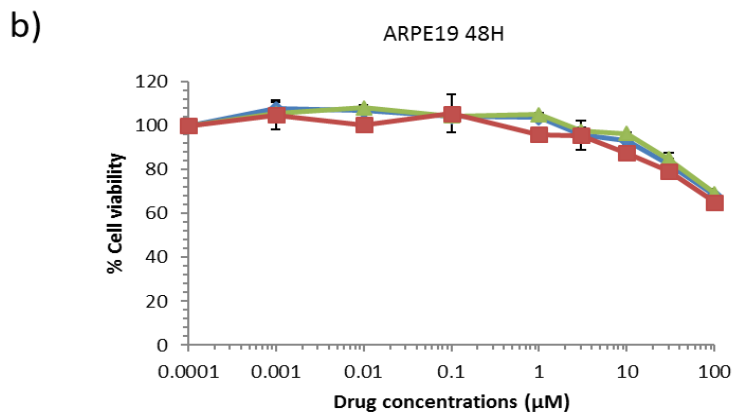
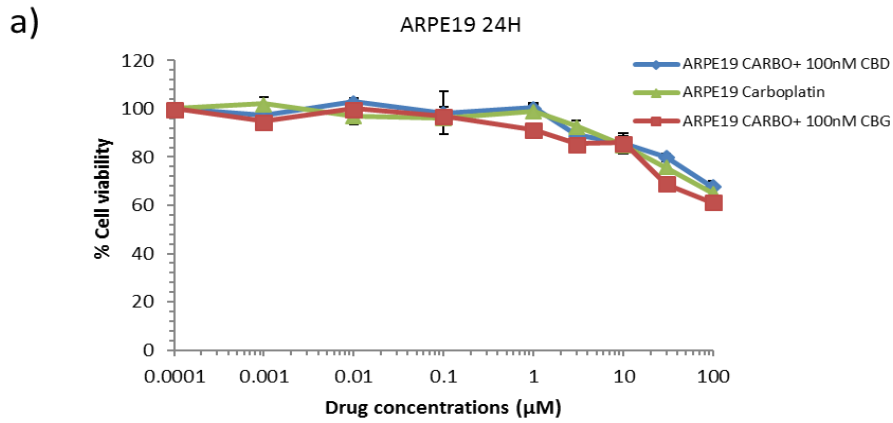


Figure 4-7. Carboplatin in combination with 100 nM CBD or 100 nM CBG on ARPE19 cells. The comparison between carboplatin alone to carboplatin in combination with 100 nM CBD and carboplatin in combination with 100 nM CBG. 1% ultrapure water was used as a solvent control for carboplatin alone whereas 100 nM CBD was used as a control for combination. Graph a) represents 24 h, b) represents 48 h, c & d represents 72 h and 96 h respectively. (n=4).

Unlike in the ovarian cancer cells, CBD or CBG did not show any significant difference in carboplatin cytotoxicity on ARPE19 cells when used in the combination. The results suggested that synergetic effects of the cannabinoids in combination with carboplatin were cancer selective (**Figure 4-7**).

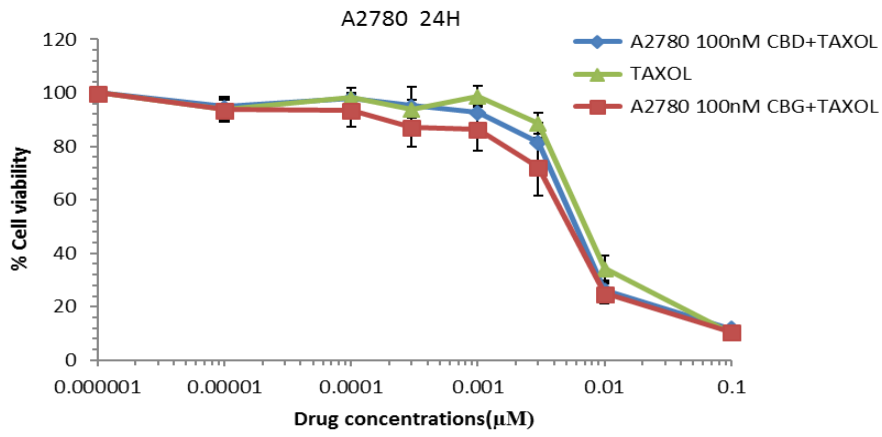
4.2.3 Paclitaxel (Taxol) in combination with CBD or CBG

4.2.3.1 Taxol in combination with CBD or CBG on A2780 cells

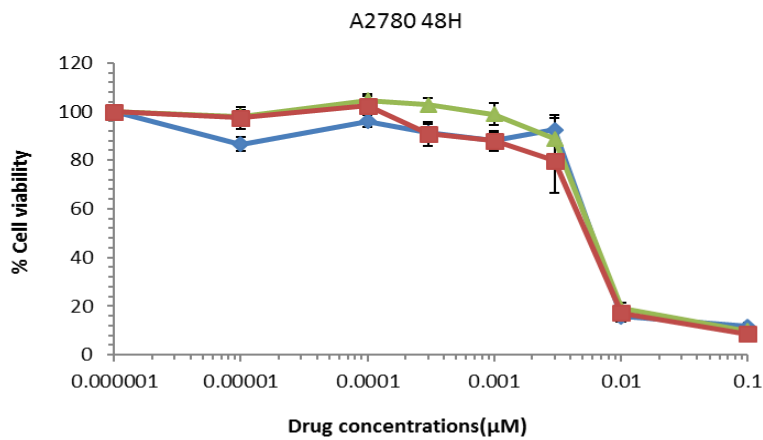
Paclitaxel, commonly known as Taxol, is a standard drug used in combination with carboplatin in the treatment of ovarian cancer. Therefore, the combination effects of the cannabinoids CBD or CBG with Taxol was investigated on A2780 and A2780/CP70 cells. The sub-lethal concentrations (100 nM) of CBD or CBG on ovarian cancer cells were taken as a constant in combination to Taxol (10 pM- 100 nM). Experiments were carried out as described in **section**

4.2.2.1.

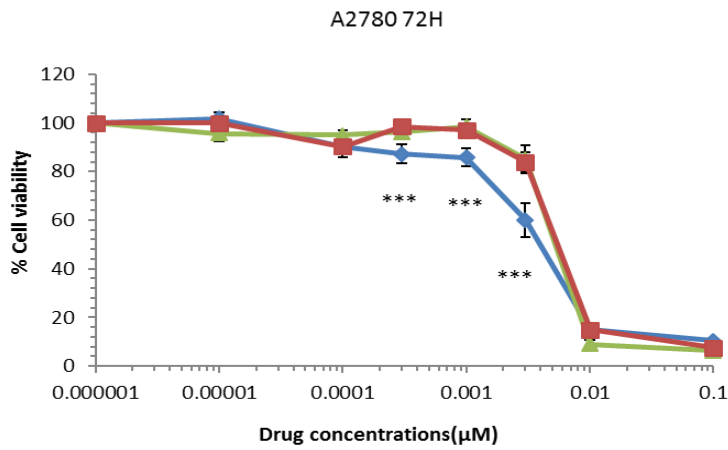
a)



b)



c)



d)

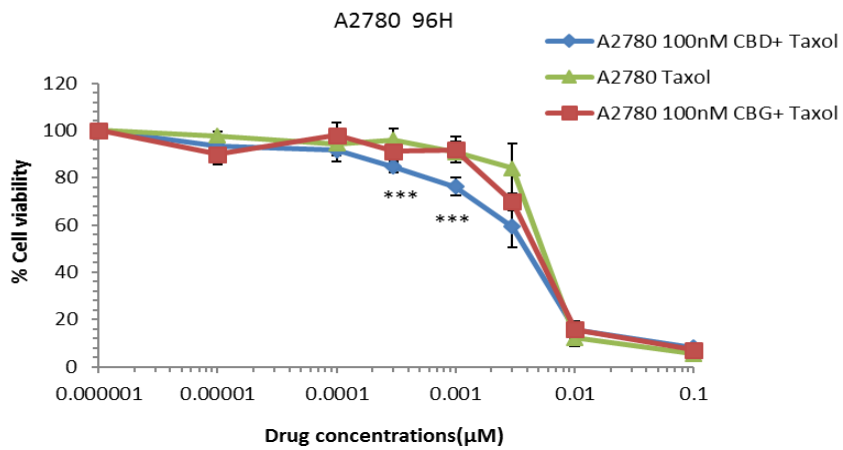


Figure 4-8. **Taxol in combination with 100 nM CBD/ 100 nM CBG on A2780 cells.** The comparison between Taxol alone to Taxol in combination with 100 nM CBD, and Taxol in combination with 100 nM CBG. 0.1% DMSO was used as a solvent control for Taxol alone whereas 100 nM CBD or 100 nM CBG were used as a control for combination. Graph a) represents 24 h, b) represents 48 h, c & d represents 72 h and 96 h respectively. * $P < 0.05$, ** $P < 0.01$ and *** $P < 0.001$. ($n=4$)

Taxol (10 pM- 100 nM) induced a greater cytotoxicity when cells were pre-treated with 100 nM CBD following 72 h and 96 h contact times. However, pre-treated with CBG was shown a very little effects on the dose response curves of Taxol on A2780 cells at all the time points tested as shown in **Figure 4-8**

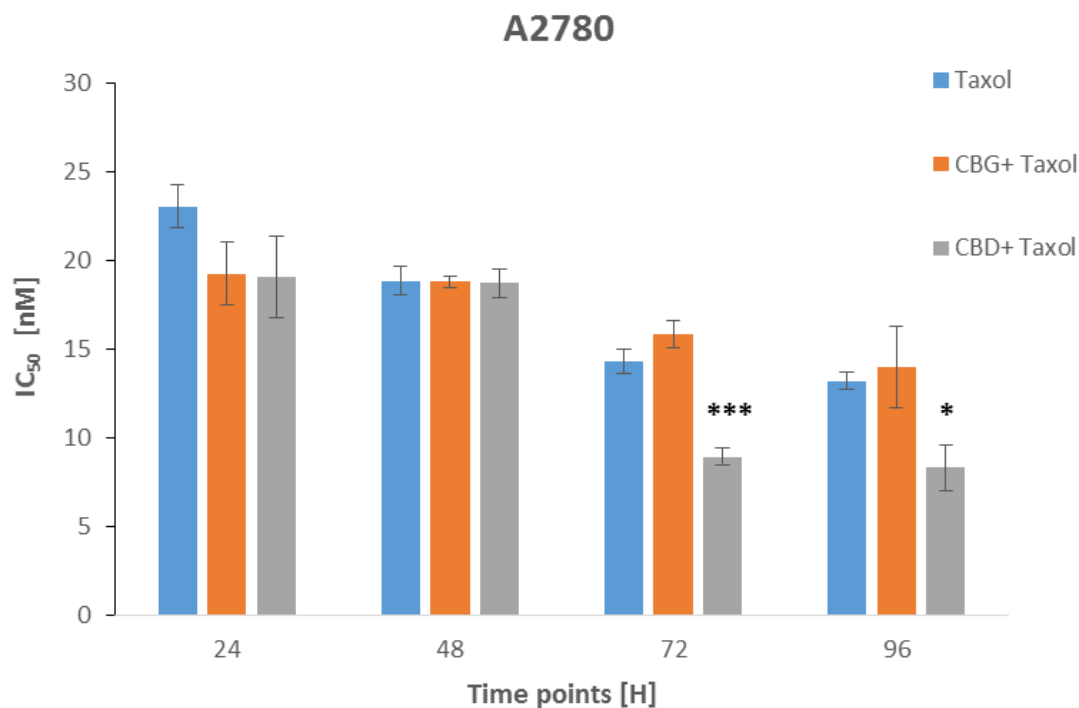


Figure 4-9. **IC₅₀ values of Taxol alone, and in combination with CBD or CBG in A2780 cells.** The comparison of IC₅₀ values of Taxol alone, and Taxol when combined with 100 nM CBD or 100 nM CBG on A2780 cells at 24 h, 48 h, 72 h, and 96 h. Data represents the mean \pm standard error of $n=4$, n represents the number of experiments. * $P < 0.05$, ** $P < 0.01$ and *** $P < 0.001$

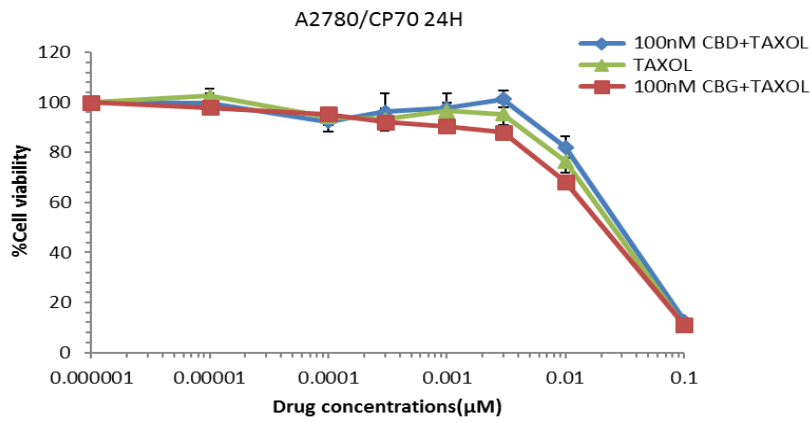
Taxol in combination with 100 nM CBD afforded lower IC₅₀ values (19.12± 2.3 nM, 18.75± 0.8 nM, 8.94± 0.5 nM and 8.32± 1.3 nM) compared when Taxol was used in combination with 100 nM CBG (19.25± 1.6 nM, 18.8± 0.3 nM, 16.86± 0.8 nM and 14.01± 2.3 nM) and Taxol alone (23.5± 1.2nM, 18.87± 0.8 nM, 14.33± 0.7 nM and 13.23± 0.5 nM). The results were significant only after 72 h exposure (**Figure 4-9**).

The CI values of CBD in combination with Taxol at 72 h (0.54) and 96 h (0.6) demonstrated a synergistic effect on A2780 cells.

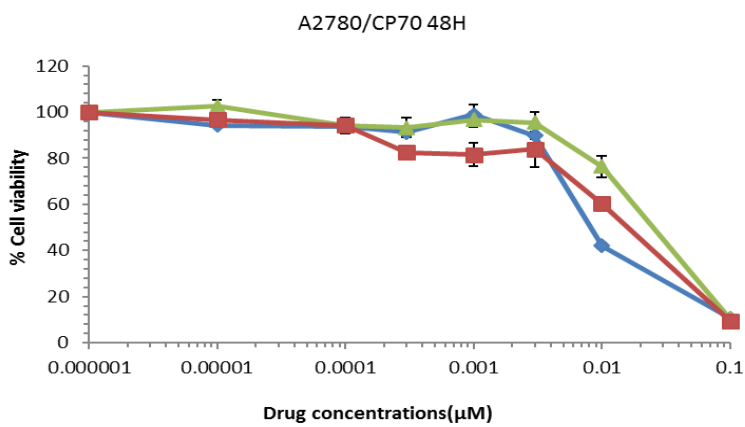
4.2.3.2 Taxol in combination with CBD or CBG on A2780/CP70 cells

Similar experiments (**section 4.2.3.1**) were carried out on A2780/CP70 cells. The results were summarised below

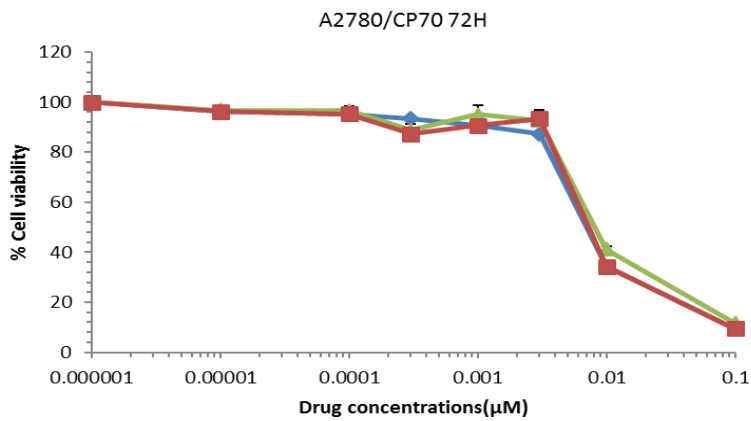
a)



b)



c)



d)

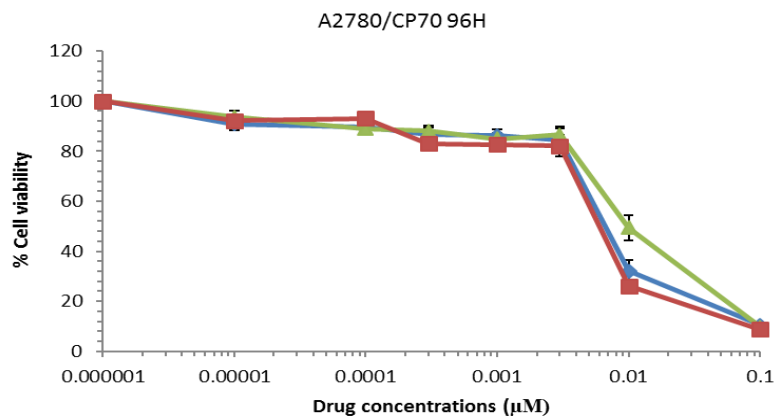


Figure 4-10. **Taxol in combination with 100 nM CBD or 100 nM CBG on A2780/CP70 cells.** The comparison between Taxol alone to Taxol in combination with 100 nM CBD and 100 nM CBG on A2780/CP70 cells. 0.1% DMSO was used as a solvent control for Taxol alone whereas 100 nM CBD and 100 nM CBG were used as a control for combination. Graph a) represents 24 h, b) represents 48 h, c & d represents 72 h and 96 h respectively. * $P < 0.05$, ** $P < 0.01$ and *** $P < 0.001$. ($n=4$)

Pre-treatment of CBD or CBG in combination with Taxol induced the difference in the dose – response curves compared to Taxol alone at 24 h, 48 h and 72 h contact times on cisplatin resistant A2780/ CP70 cells. There was a difference observed at 96 h at 30 nM concentration, where combination of Taxol with CBD, and CBG showed significant ($p < 0.01$) dose- responses compared to Taxol alone (**Figure 4-10**)

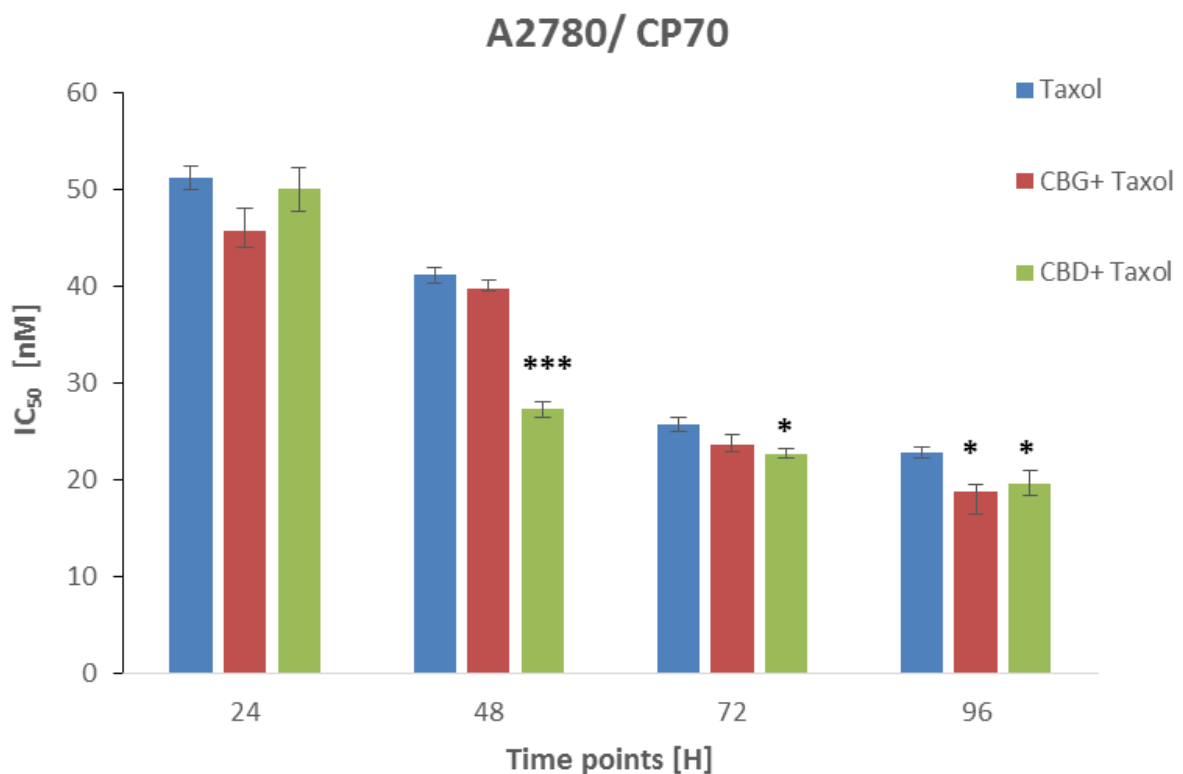


Figure 4-11. **IC₅₀ values of Taxol alone, and in combination with CBD or CBG in A2780/CP70 cells.** The comparison of IC₅₀ values of Taxol alone, and Taxol when combined with CBD or CBG on cisplatin resistant A2780/ CP70 cells at 24 h, 48 h, 72 h, and 96 h. Data represents the mean \pm standard error of $n=4$, n represents the number of experiments. * $P < 0.05$, ** $P < 0.01$ and *** $P < 0.001$

Taxol in combination with 100 nM CBD significantly induced the cytotoxicity with lower IC₅₀ values (27.35± 0.8 nM, and 22.75± 0.9 nM) compared to Taxol in combination with 100 nM CBG (39.88± 2.3 nM and 23.75± 1 nM), and Taxol alone (41.26± 2.3 nM, 25.74± 0.6 nM, and 22.89± 0.6 nM) at 48 h (P<0.001), 72 h (P<0.05) and 96 h (P<0.05) on A2780/ CP70 cells. Taxol in combination with 100 nM CBG demonstrated significantly lower IC₅₀ values (18.73± 0.6nM) (*P<0.05) compared Taxol alone (22.89± 0.6nM) at 96 h contact time. The combination index was calculated for the above time points to determine the combination effects of CBD or CBG when combined with Taxol (**Figure 4-11**).

CI values of Taxol with CBD at 48 h (0.69), 72 h (0.88) and 96 h (0.87) demonstrated slightly synergistic effects of the combination on A2780/CP70. CBG in combination with Taxol also shown slight synergism with CI value 0.83 on A2780/CP70 at 96 h.

CBD in combination with Taxol on A2780 cells showed synergism after 72 h exposure and whereas it was showed, slight synergistic on A2780/CP70 cells. CBG in combination with Taxol showed additive effect on both A2780 and CP70 cells. Based on the combination results, Taxol seemed to be more effective when combined with CBD than CBG. Pre- treatment of CBD in combination with Taxol showed to be more effective in A2780 cells compared to cisplatin resistant A2780/ CP70 cells.

4.3 Discussion

There was no increase observed in the cytotoxicity towards ovarian cancer cells of CBD when combined with CBG (1:1,1:5 and 5:1). The IC₅₀ values of the combinations tested were in-between the values generated by CBD and CBG. Amongst all of them, CBD generated the lowest IC₅₀ values followed by 5:1, 1:1, 1:5 (CBD:CBG), and CBG alone. This is consistent with earlier results (Chapter 3) indicating that CBD is more potent than CBG against these cells. As

the proportion of CBD decreased, the IC₅₀ values of the combinations increased. Indicates that CBD alone is more potent than when in combination with CBG. This could be due to them sharing the same receptor targets for their mechanism of action but having different receptor affinities or stability. , In prostate cancer cells (LnCaP) both CBD and CBG induced cytotoxicity effects by targeting the TRM8 receptor (De Petrocellis et al., 2013). The results in this study suggest that the combination of CBD and CBG does not improve cytotoxicity of CBD as a single agent.

Carboplatin potency towards ovarian cancer cells was increased when combined with sub-lethal doses of CBD and CBG. In A2780 cells, CBD has shown strong synergistic effects after 24 h (CI 0.36), 48 h (CI 0.17), 72 h (CI 0.15), and 96 h (CI 0.096) contact time. However, carboplatin, when combined with CBG was only able to achieve a significant synergistic effect after 96 h (CI 0.55). In cisplatin resistant A2780/CP70 cells, CBD was shown similar effects; however, in this cell line, CBG demonstrated synergistic effects from 24 h although synergy overall was less pronounced. Overall, CBD is the preferable cannabinoid for carboplatin combination based on the synergism observed. CBD or CBG, when combined with carboplatin, did not show any synergistic effects on non- cancer ARPE19 cells, indicating that the synergistic effects of the cannabinoids with carboplatin are ovarian cancer selective.

In A2780 cells, Taxol, when combined with CBD, was shown to have synergistic effects after 72 h (CI 0.54), and 96 h (CI 0.6) contact times. However, CBG in combination with Taxol was shown to have no or a very little effect on the dose responses of Taxol at all the time points tested. In A2780/CP70 cells, the combination index analysis of Taxol when combined with CBD demonstrated slightly synergistic effects at 48 h (0.69), 72 h (0.88) and 96 h (0.87). Unlike

in A2780 cells, CBG in combination with Taxol also was shown to have slight synergism with CI value 0.83 on A2780/CP70 at 96 h.

Both CBD and CBG has shown effects at sub-lethal concentrations when combined with carboplatin or paclitaxel. This could be due to the effects of the cannabinoids on growth factor inhibition of cells that may not cause cell death as measure by the MTT assay. Overall, greater synergy was observed with CBD than with CBG whether in combination with carboplatin or Taxol. The synergistic effects were more pronounced with carboplatin than Taxol, which may relate to the different mechanisms of action of carboplatin and Taxol as well as that of the cannabinoids themselves. Importantly, CBD and CBG did not synergise with carboplatin in the non-cancer ARPE19 cells, however, this has yet to be tested for combinations with Taxol.

CHAPTER 5 Mechanistic studies of CBD and CBG on ovarian cancer cells

5.1 Introduction

In vitro and *in vivo* pre-clinical studies indicate that the anti-cancer mechanism of action of cannabinoids can differ depending on the type of cancer, and also that the effects are highly dependent on dose and the specific cannabinoid itself (Dariš et al., 2018). To better understand how cannabinoids might exert anti-tumour activity in context of ovarian cancer, it is essential to understand the effects of cannabinoids on important cellular processes that contribute to tumorigenesis (Dariš et al., 2018). At present, there are no reports in the literature testing CBD or CBG against human ovarian cancer cells either *in vitro* or *in vivo*. In this chapter, mode of action studies are carried out to assess possible effects of CBD or CBG on, a) the cell cycle and, b) apoptosis. Based on studies against other cancer tissue types, effects of CBD and CBG on levels of reactive oxygen species (ROS) in the ovarian cancer cells and their possible contribution to cytotoxicity are also investigated. Results of a protein array focused on cellular stress signalling proteins are also presented which indicate differences in the molecular response to CBD and CBG as well as differences between the cisplatin-resistant and cisplatin-sensitive ovarian cancer cells.

5.2 Results

5.2.1 Cycle analysis of A2780 and A2780/CP70 cells following CBD or CBG treatment

Experiments were carried out to investigate the effects of CBD and CBG on the cell cycle in cisplatin sensitive and parental A2780 cells.

The experiments were carried out as described in **section 2.9**. The effects of CBD and CBG on the cell cycle were analysed by NC3000 image cytometry using DAPI, a fluorescent stain that

binds to DNA. The changes in DNA content at different stages of cell cycle was observed by variation in DAPI fluorescence.

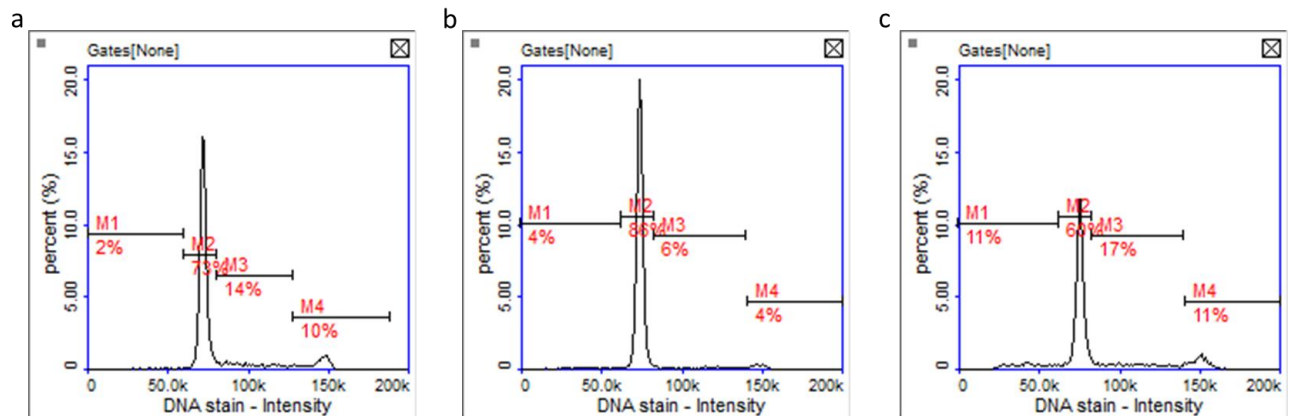


Figure 5-1 Cell cycle analysis of A2780 cells treated with CBD. Representative analysis of the DNA content in different stages of cell cycle when A2780 cells were treated with CBD for 48h. M2 represents G₀/G₁ Phase, M3 represents S phase, M4 represents G₂/M phase and M1 represents Sub G₀ phase. a) A2780 cells treated with vehicle b) A2780 cells treated with 30 μM CBD c) A2780 cells treated with 50 μM CBD.

The DNA content at each stage of the cell cycle was quantified using manual gating (Figure 5-1). The control sample was gated according to the NC3000 cell cycle analysis protocol. Drug treated samples were applied similar gating systems to the control using the NC3000 software. Three biological independent replicates were carried out and the mean with standard error of each phase were summarised below.

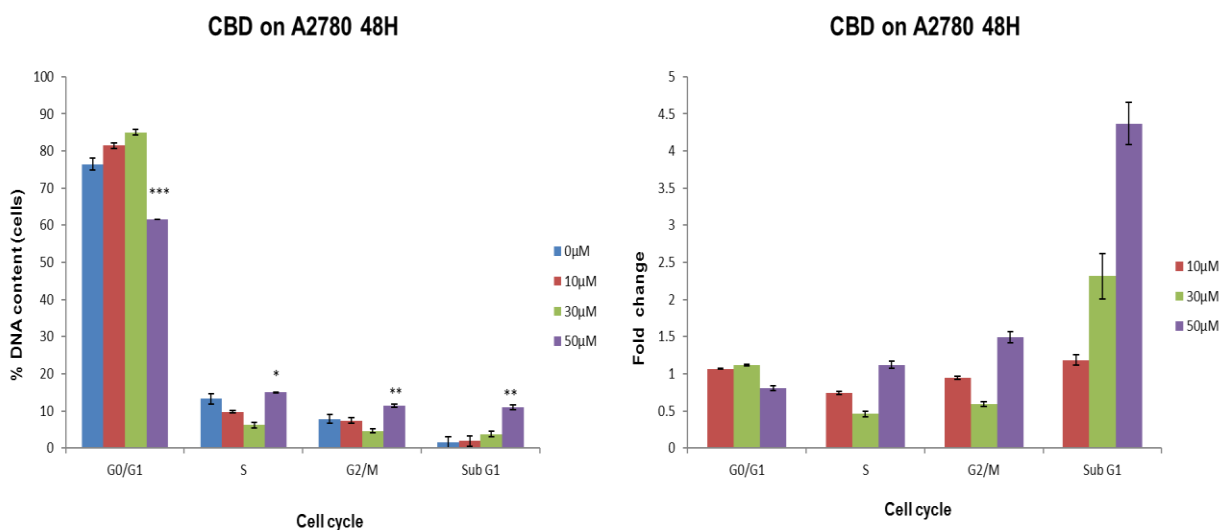


Figure 5-2. **Cell cycle analysis of A2780 cells treated with CBD.** The Comparison of different stages of A2780 cell cycle when cells were exposed to CBD (10 μ M, 30 μ M and 50 μ M) for 48 h. 1% ethanol treated cells were used as a control. The percentage of DNA content among CBD treated cells as a relative factor for different stages of cell cycle (left), the fold change compared to control (right). It represents the mean \pm standard error of mean of n=3, *P<0.05 and **P<0.01

A2780 cells when treated with CBD for 48h, there was increase in G0/G1 phase from control (76.4 \pm 2.5%) at 10 μ M (81.4 \pm 1.3%) and 30 μ M CBD (85 \pm 1.5%) is observed (**Figure 5-2**). The increase in the G0/G1 phase correlates with a decrease in the S phase population from control (13.3 \pm 1.9) at 30 μ M CBD (6 \pm 1.5%). The decrease in the G0/G1 at 50 μ M CBD (61.6 \pm 1.4%) was explained by significant increase in subG1 phase (P<0.01) from control (1.6 \pm 0.4%) to 50 μ M CBD (11.1 \pm 1.02%); this suggests that 50 μ M was too high concentration and exerted the cytotoxic effect on cells leading to DNA fragmentation which further lead to induction of cell death.

The increase in G0/G1 correlated by decrease in S phase when A2780 cells treated with CBD, indicates the possibility of G1 growth arrest however, the changes observed were not significant (**Figure 5-2**).

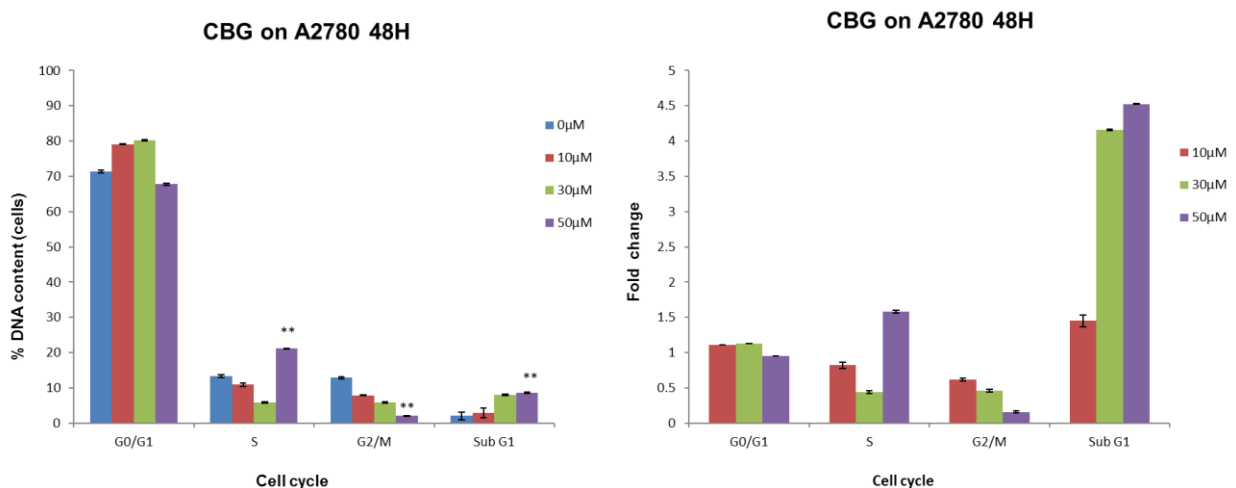


Figure 5-3 **Cell cycle analysis of A2780 cells treated with CBG.** Comparison of different stages of A2780 cell cycle when cells were exposed to CBG (10 μ M, 30 μ M and 50 μ M) for 48 h. 1% ethanol treated cells were used as a

control. The percentage of DNA content among CBG treated cells as a relative factor for different stages of cell cycle (left), the fold change compared to control (right). Data represents the mean \pm standard error of $n=3$, N represents the number of experiments. * $P<0.05$, ** $P<0.01$ and *** $P<0.001$

Similar to CBD, when A2780 cells treated with CBG, the increase in G0/G1 phase from control (71.3 \pm 0.5%) to 10 μ M (79.1 \pm 0.4%) and 30 μ M CBG (80.2 \pm 1.3%) was observed. The increase in G0/G1 phase was correlated by decrease in S phase from control to 30 μ M CBG (**Figure 5-3**). The decrease in G0/G1 A2780 cells treated with of 50 μ M CBG (67.6 \pm 1.1%) was explained by significant increase in subG1 phase ($P<0.01$) from control (2 \pm 1.2%) to 50 μ M CBD (8.7 \pm 0.6); indicates DNA fragmentation. However at 50 μ M CBD there was a significant increase ($P<0.01$) in S phase and a significant decrease ($P<0.01$) in G2/M compared to the control; this suggests the possibility of growth arrest at S phase (**Figure 5-3**).

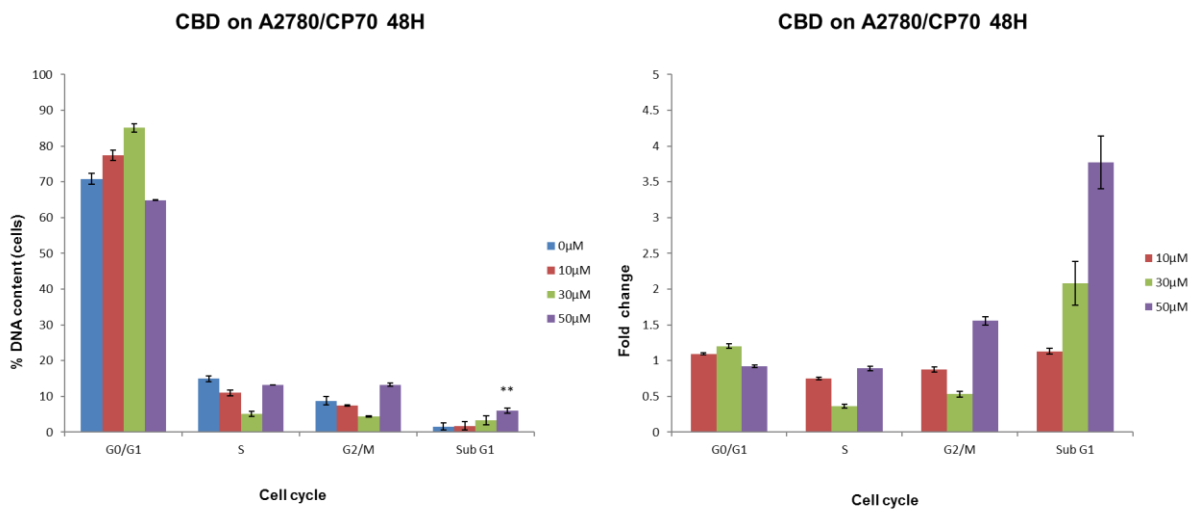
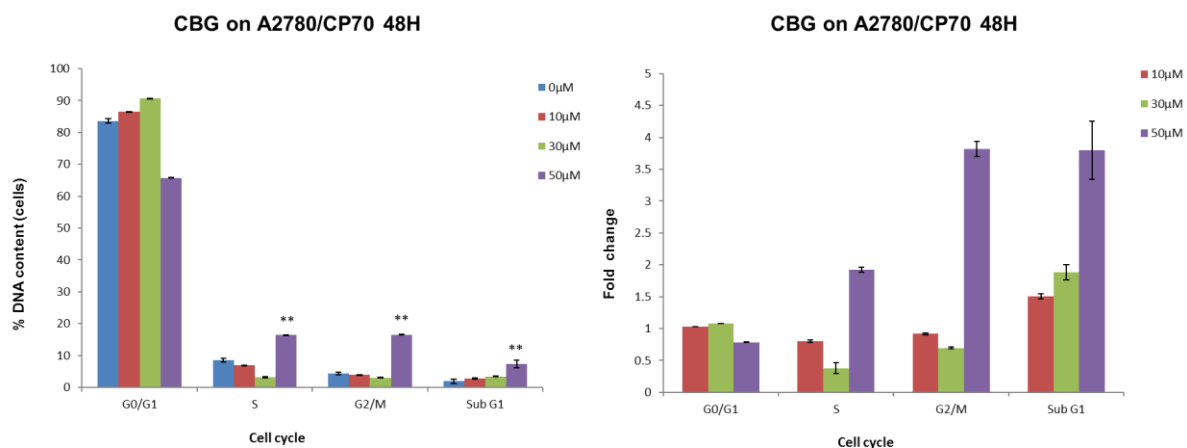


Figure 5-4 Cell cycle analysis of A2780/CP70 cells treated with CBD. Comparison of different stages of A2780 CP70 cell cycle when cells were exposed to CBD (10 μ M, 30 μ M and 50 μ M) for 48 h. 1% ethanol treated cells were used as a control. The percentage of DNA content among CBD treated cells as a relative factor for different stages of cell cycle (left), the fold change compared to control (right). It represents the mean \pm standard error of $n=3$, N represents the number of experiments. ** $P<0.01$

CBD exerted similar effects on cisplatin resistant A2780/CP70 cells compared to parental A2780 cells. The increase in G0/G1 phase from control (70.8 \pm 1.4%) at 10 μ M (77.4 \pm 1.3%) and

30 μM CBD ($85.1\pm 1.1\%$) along with a decrease in the S phase were observed. The decrease in G0/G1 of 50 μM CBD treated A2780 C70 cells ($64.9\pm 0.9\%$) was explained by significance increase in subG1 phase ($P < 0.01$) from control ($1.5\pm 0.06\%$) at 50 μM CBD ($6\pm 0.9\%$) suggest that 50 μM was too high concentration and exerted cytotoxic effect on cells lead to DNA fragmentation (**Figure 5-4**).



*Figure 5-5 Cell cycle analysis of A2780/CP70 cells treated with CBG. Comparison of different stages of A2780 CP70 cell cycle when cells were exposed to CBG (10 μM , 30 μM and 50 μM) for 48 h. 1% ethanol treated cells were used as a control. The percentage of DNA content among CBG treated cells as a relative factor for different stages of cell cycle (left), the fold change compared to control (right). It represents the mean \pm standard error of mean of $N=3$, N represents the number of experiments. * $P < 0.05$, ** $P < 0.01$ and *** $P < 0.001$*

After 48 h, there was increase in G0/G1 from control ($83.6\pm 0.6\%$) to 10 μM ($86.4\pm 0.5\%$) and 30 μM CBG ($90.6\pm 0.4\%$) was observed in A2780/CP70 cells. The decrease in S phase was observed from control ($13.3\pm 0.6\%$) to 30 μM CBG ($5.6\pm 0.6\%$) followed by the significant increase at 50 μM CBG. Similar to S phase, significant increase ($P < 0.01$) in G2/M phase observed at 50 μM CBG (16.4 ± 1.9). SubG1 phase increased ($P < 0.01$) from control ($1.9\pm 0.14\%$) to 50 μM CBD ($7.4\pm 0.6\%$) suggest the DNA fragmentation, and induction of cell death (**Figure 5-5**).

The results demonstrate that CBG at highest concentration tested (50 μ M CBG) possibly induce partial growth arrest in S phase and G2/M phase in cisplatin resistant A2780/CP70 cells at 48 h time point (**Figure 5-5**).

The cell cycle analysis of A2780 and A2780/CP70 when treated with CBD has shown the possibility of G0/G1 growth arrest. The cell cycle analysis of A2780 treated with CBG demonstrated possible growth arrest at S phase whilst partial growth arrest in both S phase and G2/M phase was observed in cisplatin resistant A2780/CP70 cells.

Having observed the cell cycle analysis of ovarian cancer cells when treated with CBD/ CBG, the cytotoxicity mechanism of both the cannabinoids were investigated to determine the involvement of apoptosis. This was assessed by two different methodologies: mitochondrial membrane potential assay and Annexin V assay.

5.2.2 Mechanistic investigation of CBD/ CBG cytotoxicity on ovarian cancer cells by mitochondrial membrane potential assay

The disruption of mitochondrial membrane potential ($\Delta\psi_m$) leads to mitochondrial dysfunction, which results in apoptosis. Mitochondrial membrane potential assay can be used to assess the early apoptosis in a cell (Ly et al., 2003). The assay was performed on the NC3000 imaging analysis system using JC-1 (5,5',6,6'-tetrachloro-1,1',3,3'-tetraethylbenzimidazol-carbocyanine iodide). JC-1 is a lipophilic cation dye, which can penetrate through healthy mitochondrial membrane. At low concentrations, JC-1 exists as green fluorescent monomer whereas it forms red fluorescent aggregates in healthy mitochondrial membrane. The decrease in red to green fluorescent ratio indicates the disruption of mitochondrial membrane potential ($\Delta\psi_m$)(Galluzzi et al., 2007). DAPI (4', 6- diamidino-2- phenylindole) stain was also used, which gives blue stain for late apoptotic and dead cells.

The percentage of healthy and early apoptotic cells were estimated by excluding DAPI stained dead cells using NC3000 image analysis software.

The experiment was carried out as described in **section 2.7**. The results were summarised below.

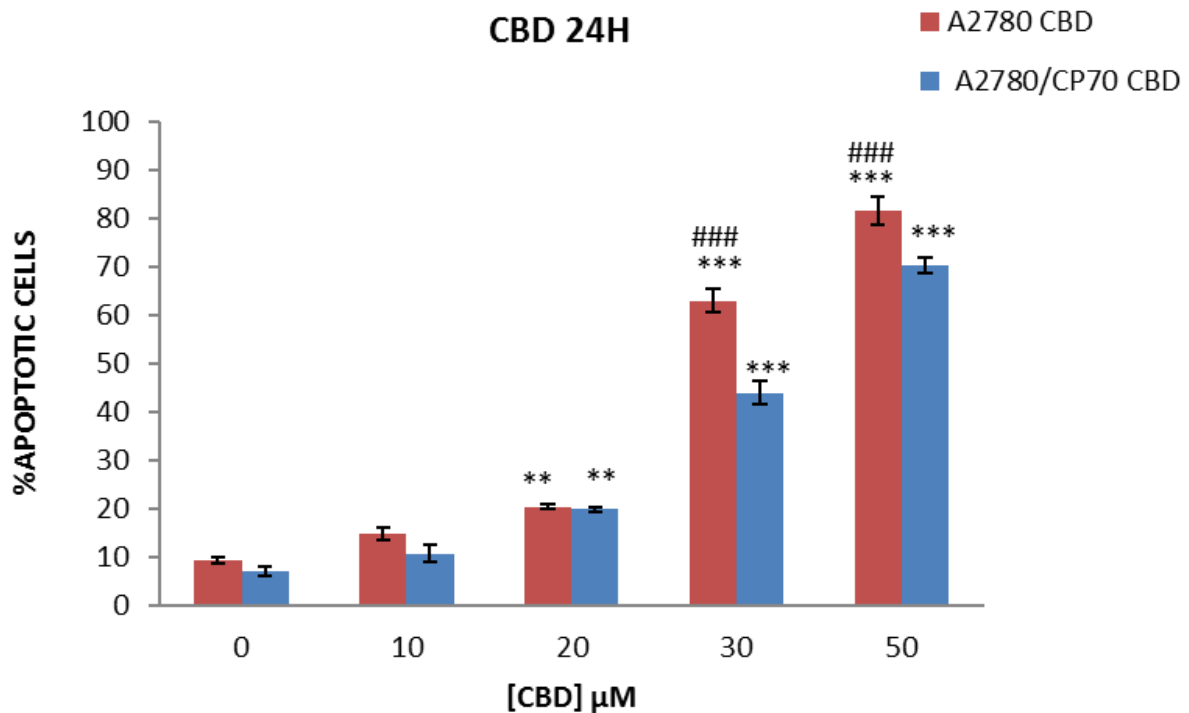
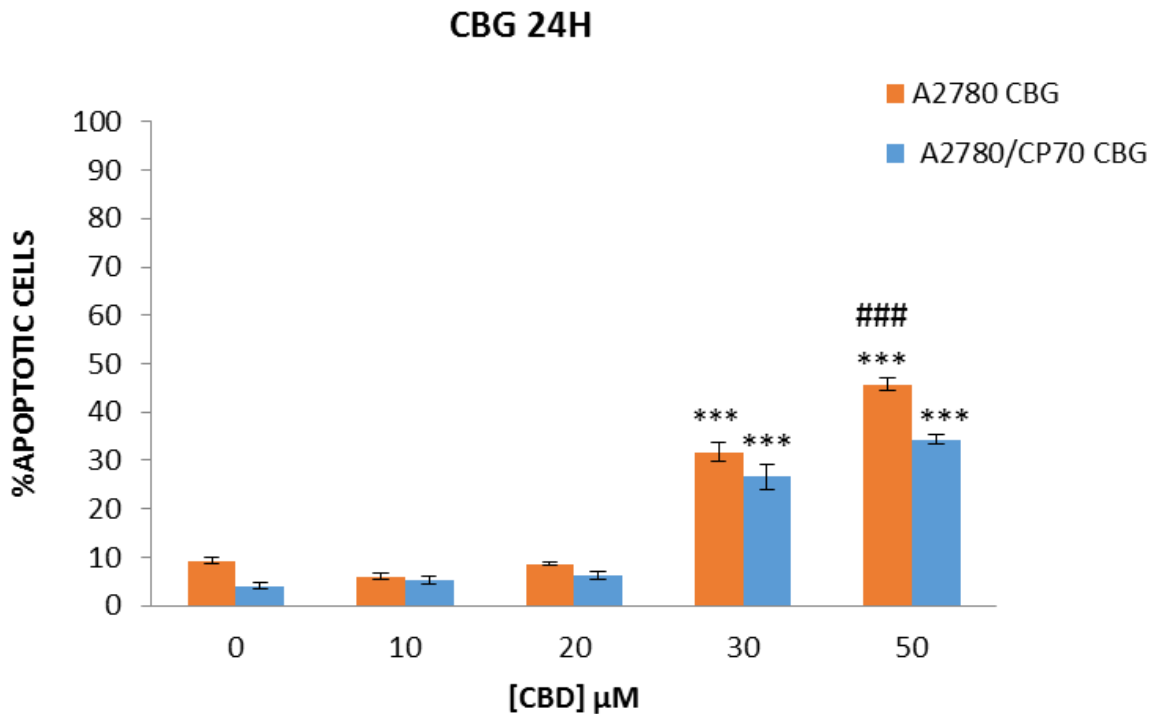


Figure 5-6 **Mitochondrial membrane potential assay on A2780 cells treated with CBD.** The percentage of apoptotic cells of non-treated to CBD treated with 10 μM , 20 μM , 30 μM and 50 μM on A2780 and A2780 CP70 respectively after 24 h contact time. 1% ethanol treated cells were used as a control. It represents the mean \pm standard error of mean of $N=3$, N represents the number of experiments. $**P<0.01$ and $***P<0.001$ (relative to controls), and $###P<0.001$ (relative to each other cell line at the concentration).

CBD induced an increase in the percentage of apoptotic cells in a dose-dependent manner in both the cell lines (**Figure 5-6**). Those achieved significance ($p<0.01$, $p<0.001$) at 20 μM , 30 μM , and 50 μM CBD. Pre-treatment with 30 μM , and 50 μM CBD induced significantly ($p<0.001$) greater percentage of apoptotic cells in A2780 as compared to cisplatin resistant

A2780/CP70. This correlates with greater cytotoxic effects of CBD on cisplatin sensitive compared to cisplatin resistant ovarian cancer cells, which was previously observed.



*Figure 5-7 Mitochondrial membrane potential assay on A2780 and A2780/CP70 cells treated with CBG. The percentage of apoptotic cells of non-treated to CBG treated with 10 μM , 20 μM , 30 μM and 50 μM on A2780 and A2780/CP70 respectively after 24 h contact time. 1% ethanol treated cells were used as a control. It represents the mean \pm standard error of mean of $N=3$, N represents the number of experiments. * $P<0.05$, ** $P<0.01$ and *** $P<0.001$ (relative to controls) # $P<0.05$, ## $P<0.01$ and ### $P<0.001$ (relative to each other cell line at the concentration).*

CBG induced an increase in the percentage of apoptotic cells in a dose-dependent manner in both the cell lines after 24 h (**Figure 5-7**). Those achieved significance ($p < 0.01$, $p < 0.001$) at 30 μM , and 50 μM CBG. CBG at 50 μM induced significantly ($p < 0.001$) greater percentage of apoptotic cells in A2780 as compared to cisplatin resistant A2780/CP70. This correlates with greater cytotoxic effects of CBG on cisplatin sensitive compared to cisplatin resistant ovarian cancer cells, which was previously observed.

The results indicated that both CBD and CBG affect mitochondrial membrane potential to induce apoptosis. CBD was shown to induce apoptosis at lower concentrations compared to CBG on both ovarian cancer cells correlates with the IC₅₀ values demonstrated earlier.

5.2.3 Mechanistic investigation of CBD/ CBG induced apoptosis by Annexin V assay

Annexin V is a cell impermeable protein, which has a high affinity for phosphatidylserine. Phosphatidylserine is located on the cytoplasmic surface of a cell membrane in a normal functioning cell. However, in apoptotic cells, it is translocated to the outer surface of the plasma membrane, which makes it available for Annexin v binding. In this experiment, Annexin v conjugated with a green fluorescent dye CF™488A was used. When Annexin V binds to Phosphatidylserine, it releases CF™488A (Ex/Em = 490/515 nm), which was analysed by NC3000 image cytometry.

The experiments were carried out on ovarian cancer cells A2780 and A2780/CP70, and non-cancer cell line ARPE19 with CBD and CBG as described in **section 2.8**

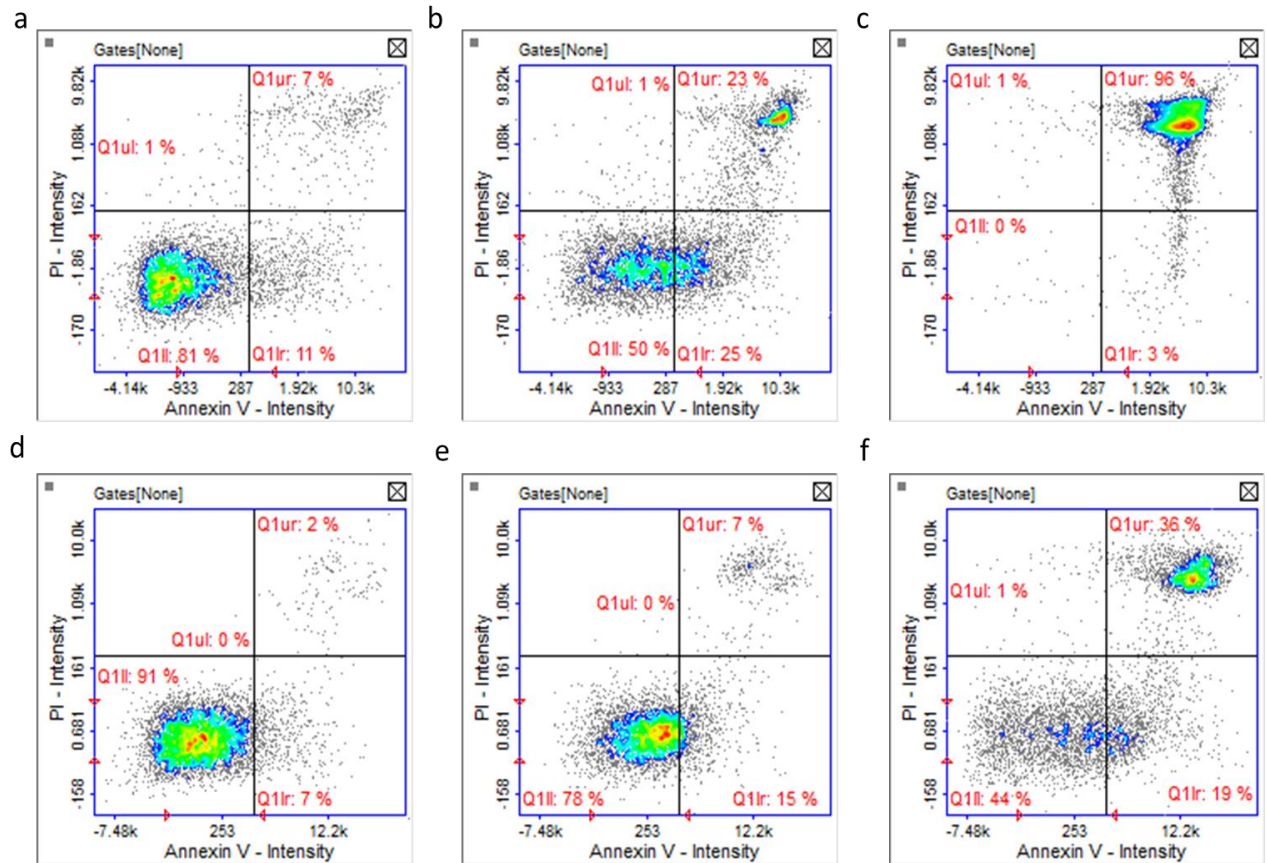


Figure 5-8. **Representation of Annexin V assay analysis.** The representative results of Annexin V analysis in A2780 cells and ARPE19 cells treated with CBD for 24 h. a, b & c represents A2780 cells treated with vehicle, 30 μM CBD and 50 μM CBD respectively, and d, e & f represents ARPE19 cells treated with vehicle, 30 μM CBD and 50 μM CBD respectively.

The scatter plot of the fluorescence intensity of Annexin V-CF488A vs the fluorescence intensity of PI was used as a representation of cells in different stages of apoptosis. The percentage of cells were quantified using manual gating (**Figure 5-8**). The control sample was gated according to the NC3000 Annexin V protocol. Drug treated samples were applied similar gating systems to control using the NC3000 software. Three biological independent replicates were carried out and the mean values with standard errors were summarised below

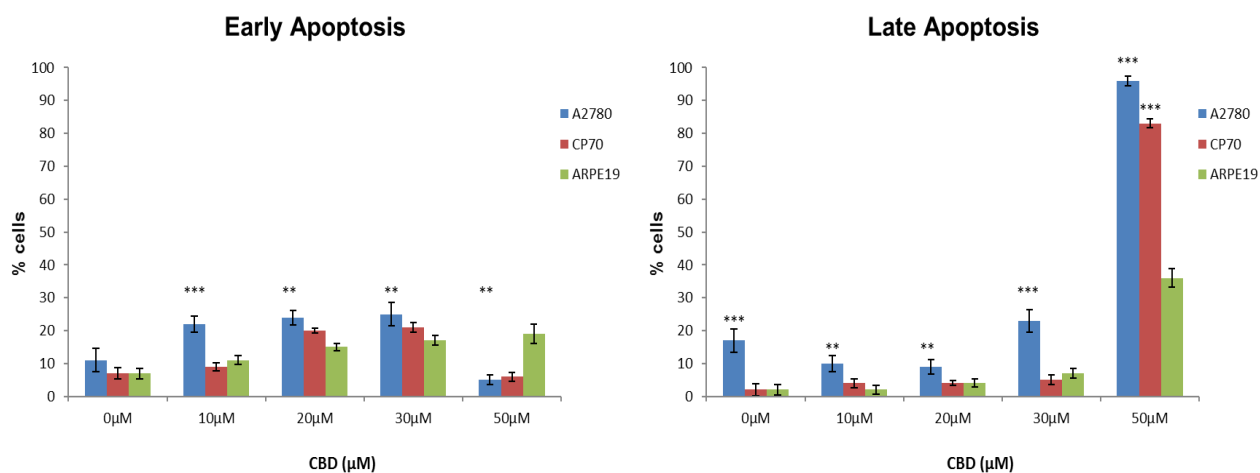


Figure 5-9. **CBD Annexin V assay at 24 h.** The percentage of cells in early apoptosis (left) and late apoptosis (right) when A2780, A2780 CP70 and ARPE19 were treated with 10 μM, 20 μM 30 μM and 50 μM of CBD. 1% ethanol treated cells were used as a control. It represents the mean ± standard error of mean of n=3, n represents the number of biological experiments. *P<0.05, **P<0.01 and ***P<0.001 (relative to ARPE19 cells)

CBD at 10-30 μM induced early apoptosis in A2780 cells at 24 h. However, at 50 μM of CBD higher percentage of cells were in late apoptotic phase. Similar profile of action was observed in A2780/CP70 cells. Both ovarian cancer cells shown significantly (P<0.001) less percentage of apoptotic cells compared to non-cancer ARPE19 cells correlates with the selective cytotoxicity of CBD towards ovarian cancer cells (**Figure 5-9**).

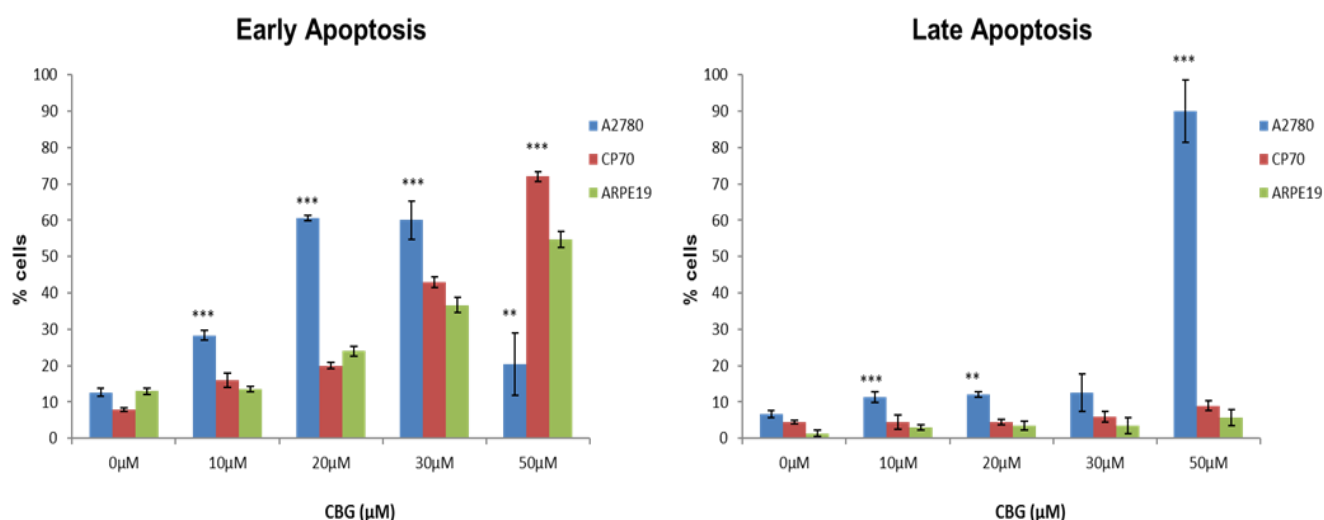


Figure 5-10. **CBG Annexin V assay at 24 h.** The percentage of cells in early apoptosis (left) and late apoptosis (right) when A2780, A2780 CP70 and ARPE19 were treated with 10 μM, 20 μM 30 μM and 50 μM of CBG. 1% ethanol treated cells were used as a control. It represents the mean ± standard error of mean of n=3, n represents the number of biological experiments. *P<0.05, **P<0.01 and ***P<0.001(relative to ARPE19 cells)

Similar to CBD, The percentage of apoptotic cells in A2780 cells were higher than A2780/CP70 and ARPE19 cells when treated with CBG for 24 h. A2780 showed 20±6.4%, 90±8.3 % of cells in early apoptosis and late apoptosis whereas A2780 CP70 72±1.4%, 9±1.4 % and ARPE19 54±2.1%, 5.6±1.8 when treated with 50 μM CBG (**Figure 5-10**). At 50 μM CBG, both ovarian cancer cells shown significantly (P<0.001) less percentage of cells in early apoptosis compared to non-cancer ARPE19 cells. CBG also shown selective induction of apoptosis in the ovarian cancer cells tested compared to non- cancer ARPE19 cells.

When compared to CBD, more percentage of the ovarian cancer cells when treated with CBG were in early apoptosis than late apoptosis; it correlates with the earlier results where CBD has shown better cytotoxicity compared to CBG.

The Annexin V assay results suggest that both CBD and CBG induce apoptosis selectively in ovarian cancer cells compared to non-cancer cells. Results showed that cells were in early

apoptosis when treated with 50 μM CBG whereas cells were in late apoptosis when treated with same concentration of CBD.

Mitochondrial membrane potential assay and Annexin V assay demonstrated that CBD and CBG induce apoptosis in the ovarian cancer cells. So further investigations were carried out to understand better the pathways leading to apoptosis. Caspase 3/7 assay was carried out to determine whether the apoptosis induced by CBD or CBG in ovarian cancer cells through a caspase-dependent mechanism. Caspase 3 and caspase 7 are involved in the execution of both intrinsic and extrinsic caspase-dependent pathways hence the quantification of caspase 3/7 in ovarian cancer cells when treated with CBD/ CBG were investigated.

5.2.4 Investigation of Caspase 3/7 Activity in CBD and CBG induced apoptosis

The protease activity of caspase 3/7 was quantified in the ovarian cancer cells in the presence of CBD or CBG. The experiments were carried out as described in **section 2.10.2**. The results are analysed and summarised below.

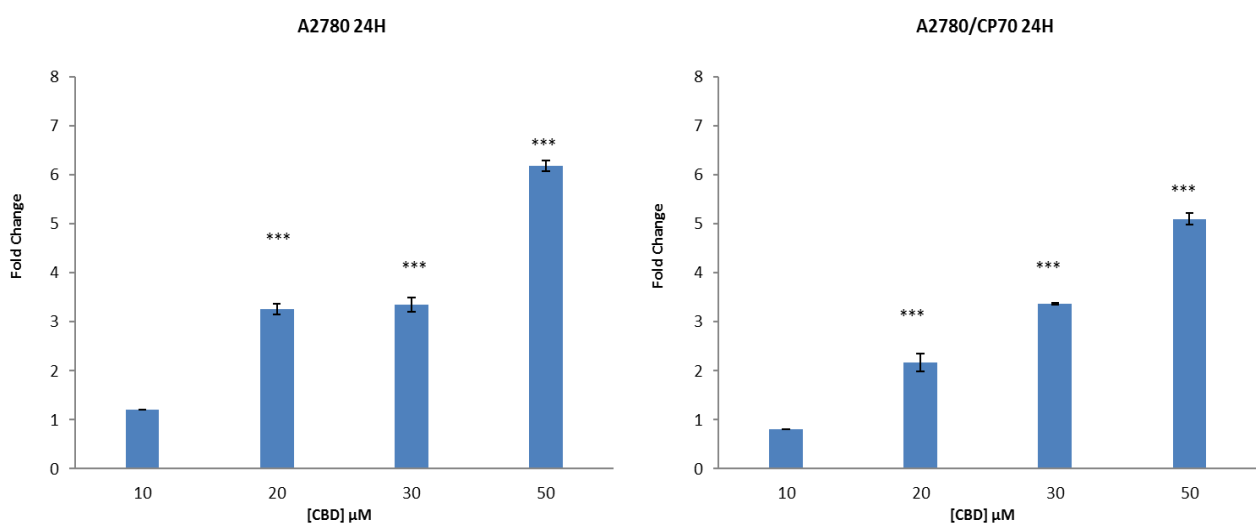


Figure 5-11. *ApoTox-Glo™ Triplex assay of CBD treatment at 24 h. The fold change in caspase3/7 activity of A2780 (left) and A2780 CP70 (right) when treated with CBD of 10 μM , 20 μM , 30 μM and 50 μM respectively. It represents the mean \pm standard error of mean of $n=3$, n represents the number of experiments. *** $P<0.001$*

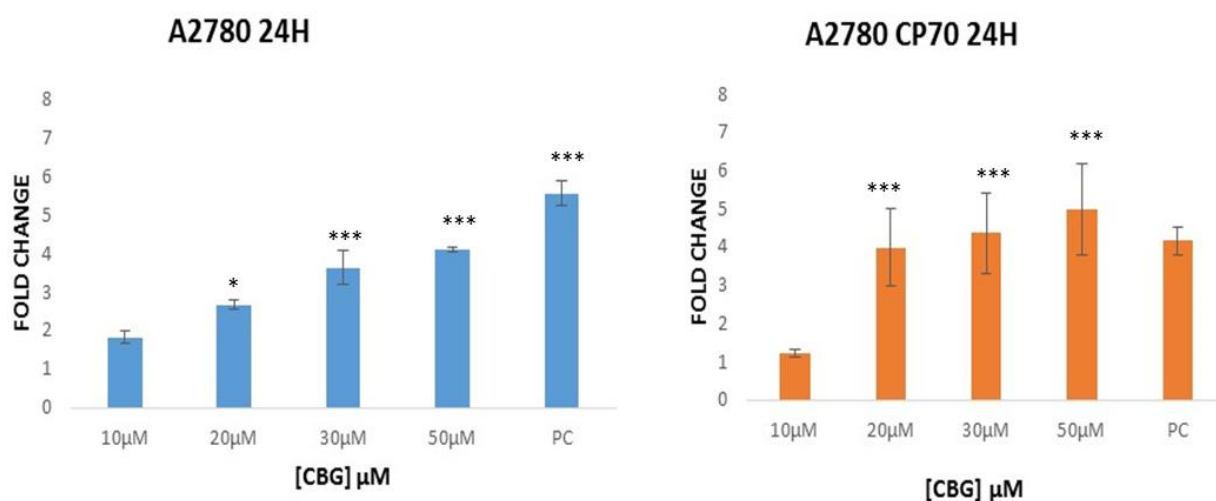


Figure 5-12. *Sensolyte caspase 3/7 assay of CBG treatment 24 h.* The fold change in caspase 3/7 activity of A2780 (left) and A2780 CP70 (right) when treated with CBG of 10 μM, 20 μM 30 μM and 50 μM respectively after 24 h contact time. 1% ethanol treated cells were used as a negative control whereas 50 μM of cisplatin was used as Positive control. It represents the mean ± standard error of mean of N=3, N represents the number of biological experiments. *P<0.05, **P<0.01 and ***P<0.001

As shown in **Figure 5-11** & **Figure 5-12**, Both CBD and CBG increased the caspase 3/7 activity in both A2780 and A2780/CP70 cells in dose-dependent manner at 24 h time point. The significance difference in activity of caspases 3/7 was observed at concentrations higher than 10 μM in both the cells lines treated with CBD or CBG.

Based on the results obtained, both CBD and CBG induce cytotoxicity by caspase-dependant apoptosis in the ovarian cancer cells.

5.2.5 Investigation of reactive oxygen species (ROS) contribution towards CBD and CBG cytotoxicity

Levels of intracellular reactive oxygen species was determined by dichlorodihydrofluorescein diacetate (H₂DCF-DA). 2',7'-dichlorodihydrofluorescein diacetate is a lipophilic, membrane permeable compound. Cellular esterase convert DCFDA to non-fluorescent DCFH, which further oxidised in the presence intracellular reactive oxygen species (H₂O₂) results in production of fluorescent 2',7'-dichlorodihydrofluorescein (DCF) (Gomes et al., 2005)

The experiments were carried as described in **section 2.10**.

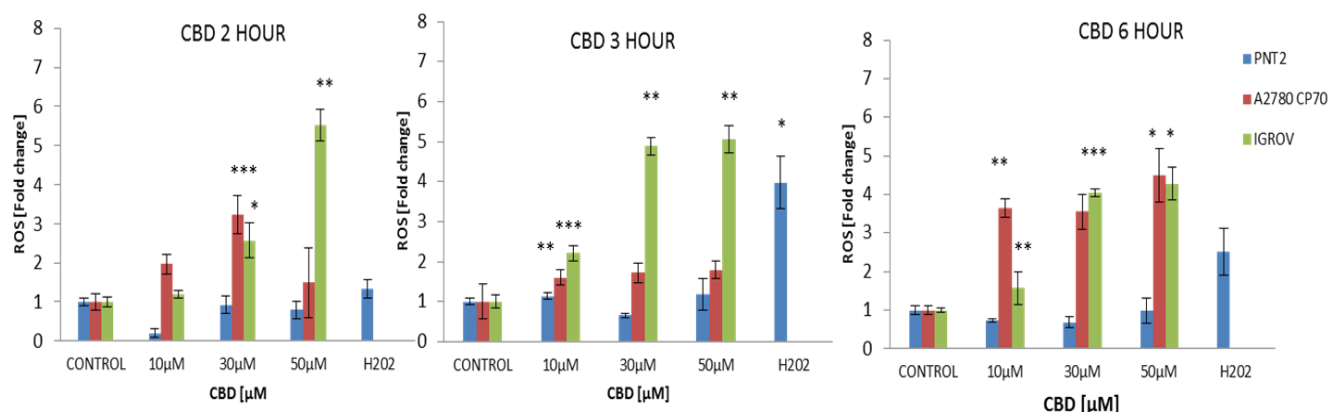


*Figure 5-13 DCF-DA reactive oxygen species (ROS) assay for CBD cytotoxicity. The fold change in fluorescence of 2',7'-dichlorodihydrofluorescein diacetate (H2DCF- DA) compound by CBD (10 μM, 30 μM and 50 μM) on ovarian cancer cells (A2780 CP70 and IGROV) and PNT2 (prostate non-cancer cells) at 2h, 3h and 6h contact points where 100 μM H₂O₂ used as positive control. (n=3) *P<0.05, **P<0.01 and ***P<0.001*

CBD did not show any significant increase in 2',7'-dichlorodihydrofluorescein production in PNT2 at any concentration (10uM, 30uM and 50uM) tested compared to control. The highest concentration of CBD tested (50 μM) did not exert any change in the fluorescence at the time points 2h (0.79±0.23), 3h (1.18± 0.39), and 6h (0.97± 0.32) (**Figure 5-13**).

CBD was shown the concentration-dependant 2',7'-dichlorodihydrofluorescein induced fluorescence in both A2780/CP70 and IGROV ovarian cancer cells. CBD shown to be significantly effective at 6-hour time point on A2780/CP70 where 10 μM, 30 μM and 50 μM showed 3.6, 3.5 and 4.4 fold changes respectively, similar trend was observed in IGROV at 10 μM, 30 μM and 50 μM with the fold changes 1.5, 4.03 and 4.5 respectively(**Figure 5-13**). The results indicate selective induction of ROS in ovarian cancer cells compared to non- cancer PNT2 cells.

Similar experiments were carried out with CBG to determine the involvement of intracellular ROS production in the cytotoxicity exerted by CBG on the ovarian cancer cells.

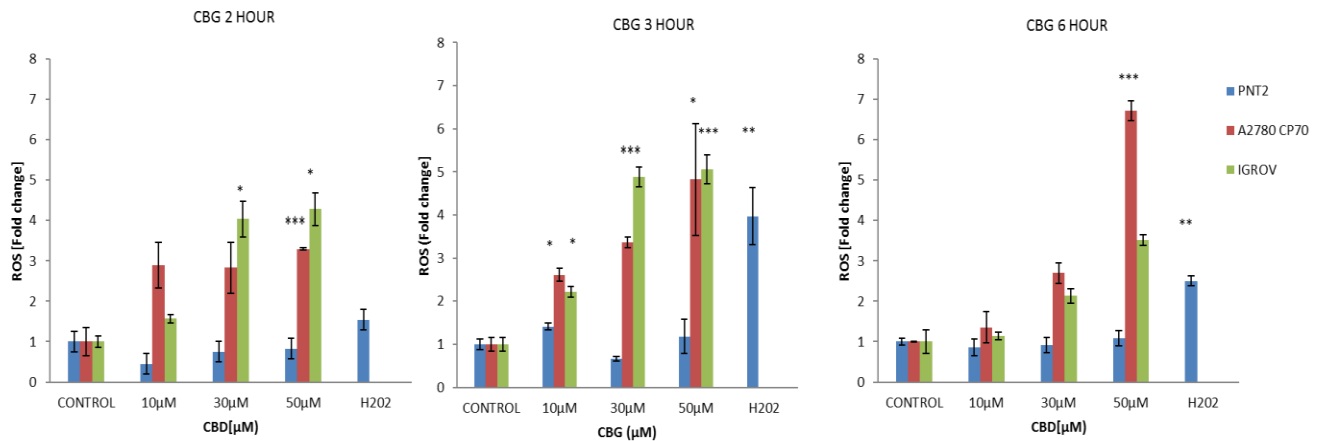


Figure 5-14. *DCF-DA reactive oxygen species (ROS) assay for CBG cytotoxicity.* The fold change in fluorescence of 2',7'-dichlorodihydrofluorescein diacetate (H₂DCF-DA) compound by CBG (10 μM, 30 μM and 50 μM) on ovarian cancer cells (A2780 CP70 and IGROV) and PNT2 (prostate non-cancer cells) at 2h, 3h and 6h contact points. 1% ethanol treated cells were used as a negative control whereas 100 μM H₂O₂ used as positive control. *P<0.05, **P<0.01 and ***P<0.001

Similar to CBD, CBG did not show any significant increase in 2',7'-dichlorodihydrofluorescein production in PNT2 at any given concentration (10 μM, 30 μM and 50 μM) compared to control. The fold change in the fluorescence exerted by 50 μM CBG on PNT2 at 2h (0.82±0.32), 3h (1.14± 0.3) and 6h (1.08± 0.19) were not different from the control (**Figure 5-14**).

CBG has also shown the concentration dependant 2',7'-dichlorodihydrofluorescein induced fluorescence in both A2780 CP70 and IGROV ovarian cancer cells. At all the time points tested, CBG was more effective at 6hour time point on A2780 CP70, and the fold change was directly proportional to the increase in CBG concentration; indicates the dose responsive production of ROS. However, CBG on IGROV was shown to be more effective at 3 h time point. The reduction in the fold change at the 6h time point might be due to the increased toxicity of CBG to IGROV with longer exposure time (**Figure 5-14**).

Both CBD and CBG had induced intracellular ROS in ovarian cancer cells whereas it did not show any effect on PNT2 cells. Cancer selective induction of ROS by CBD and CBG consistent with the he preferential cytotoxic nature of them on ovarian cancer cells compared to non-cancer cells. However, the reason for this selective ROS require further investigation.

Further investigations were performed to investigate the contribution of ROS in CBD induced cytotoxicity.

5.2.6 Rescue of CBD cytotoxicity on ovarian cancer cells by anti- oxidant:

α -tocopherol also known as vitamin- E is an anti-oxidant and scavenger of Reactive Oxygen Species (ROS). Therefore, the cytotoxicity of CBD on the ovarian cancer in the presence of an anti- oxidant was tested to investigate the contribution of ROS in CBD induced cytotoxicity.

Firstly, the cytotoxicity of α - tocopherol on A2780 and A2780/CP70 cells were investigated to by MTT assay.

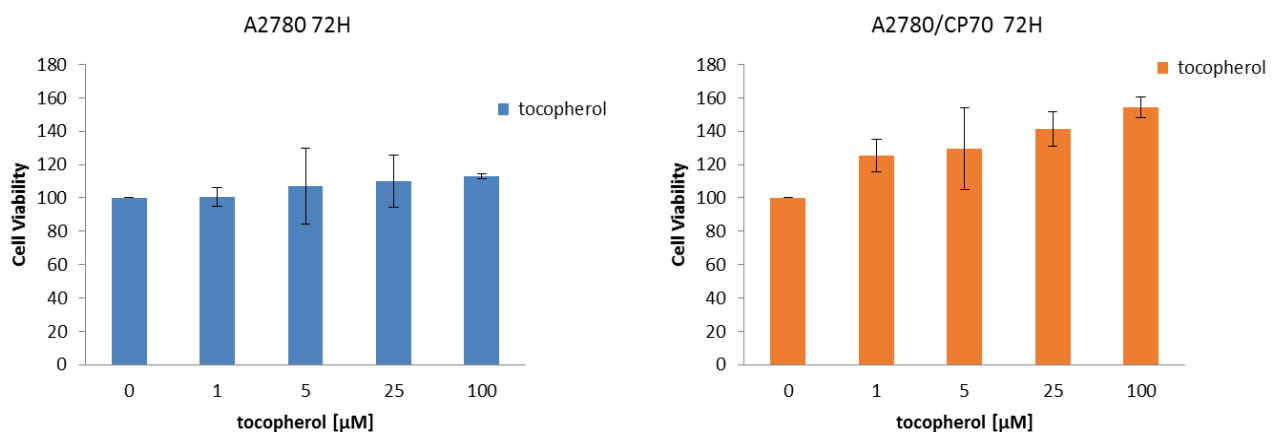
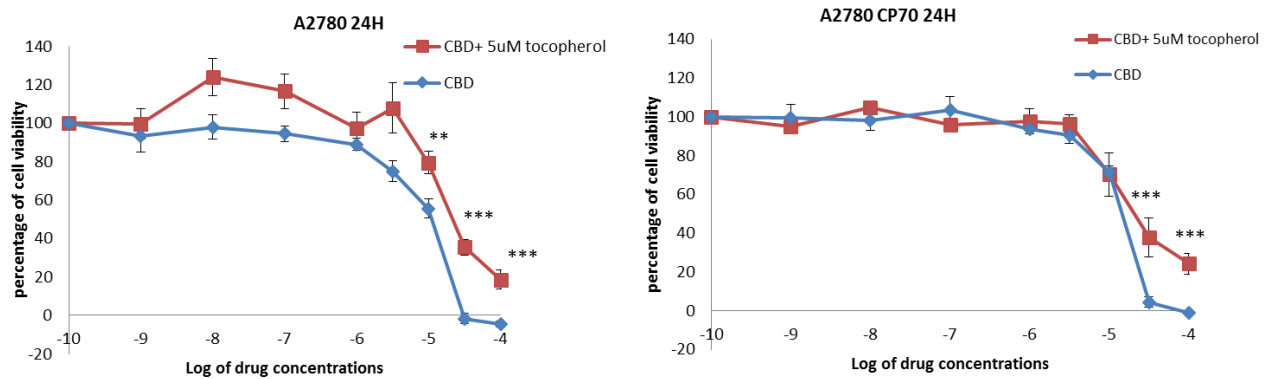


Figure 5-15 Toxicity of α - tocopherol on A2780 cells and A2780/CP70 cells. The cytotoxic effects of α - tocopherol at the concentration 1 μ M, 5 μ M, 25 μ M, and 100 μ M on A2780 (left), and A2780/CP70 (right) at 72h. Data represents the mean \pm standard error of mean of N=3, N represents the number of experiments.

As shown in **Figure 5-15**, α - tocopherol at highest concentration tested (100 μ M) did not induce cytotoxic effects on both A2780 and A2780/CP70 cells after 72 h exposure.

Further experiments were carried out where A2780 and A2780/CP70 cells were treated with CBD (1nM- 100 μ M) in the presence of 5 μ M α - tocopherol.



*Figure 5-16. The effect of 5 μ M α -tocopherol on CBD cytotoxicity. The combination effect of 5 μ M α -tocopherol with CBD compared to CBD alone on A2780(left) and A2780 CP70 (right) after 24 hour exposure. 1% ethanol treated cells were used as a control for CBD alone whereas as 5 μ M α -tocopherol treated cells were used as a control for combination. It represents the mean \pm standard error of mean of N=4, N represents the number of experiments. *P<0.05, **P<0.01 and ***P<0.001*

As shown in **Figure 5-16**, in the presence of 5 μ M α - tocopherol, the cytotoxic effects of CBD was reduced on both A2780 and A2780/CP70 cells. Further experiments were carried out in with 30 μ M CBD in presence of α - tocopherol (1 μ M- 100 μ M). The cell viability was assessed after 24 h, 48 h and 72 h contact times with MTT assay.

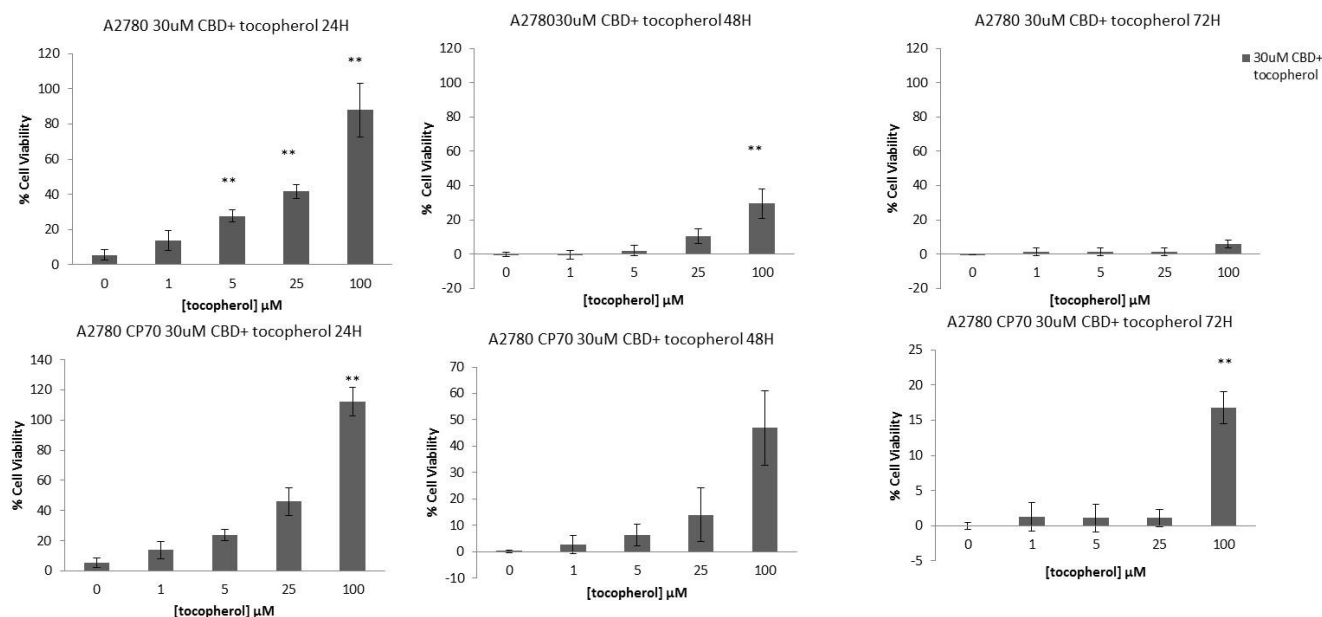


Figure 5-17. **The dose-dependent effect of α -tocopherol on CBD cytotoxicity.** The cytotoxic effect of 30 μ M CBD alone and in combination with tocopherol (1nM to 100 μ M) on A2780 (top) and A2780 CP70 (bottom) cell line after 24 hour, 48 hour and 72 hour contact time. It represents the mean \pm standard error of mean of N=4, N represents the number of experiments. *P<0.05, **P<0.01 and ***P<0.001

The results (Figure 5-17) indicate that CBD cytotoxicity is reduced with increased concentrations of α -tocopherol on the ovarian cancer cells. After 24 h, 30 μ M CBD combined with 100 μ M of α -tocopherol did not induce any cytotoxicity whilst the same concentration of CBD alone induced over 90% cytotoxicity on both A2780 and A2780/CP70 cells. The above results strongly suggest the contribution of ROS in CBD induced cytotoxicity in A2780 and A2780/CP70 ovarian cancer cells.

5.2.7 Effects of CBD or CBG on expression of key proteins involved in apoptosis and stress signalling

ELISA Pathscan® Apoptosis and Stress assays (cell Signalling, US) were performed (as described in section 2.11), and the changes in the expression levels of some of the key proteins were summarised below.

5.2.7.1 Quantification of the expression cell cycle regulators (Chk 1& chk 2)

Chk-1 and chk-2 are serine/ threonine kinases, which regulates the cell cycle. CHK- 1 is a stable protein throughout the cell cycle (predominantly in the G0/G1 phase) whereas chk- 2 is confined to S and G2/M phases. DNA damage is one of the factors involves inactivation chk- 1 and chk-2, which eventually leads to cell cycle arrest (Bartek and Lukas, 2003).

The expression of Chk-1 and chk-2 in regards to increasing concentration of the CBD and CBG were quantified in A2780 and A2780/ CP70 cells.

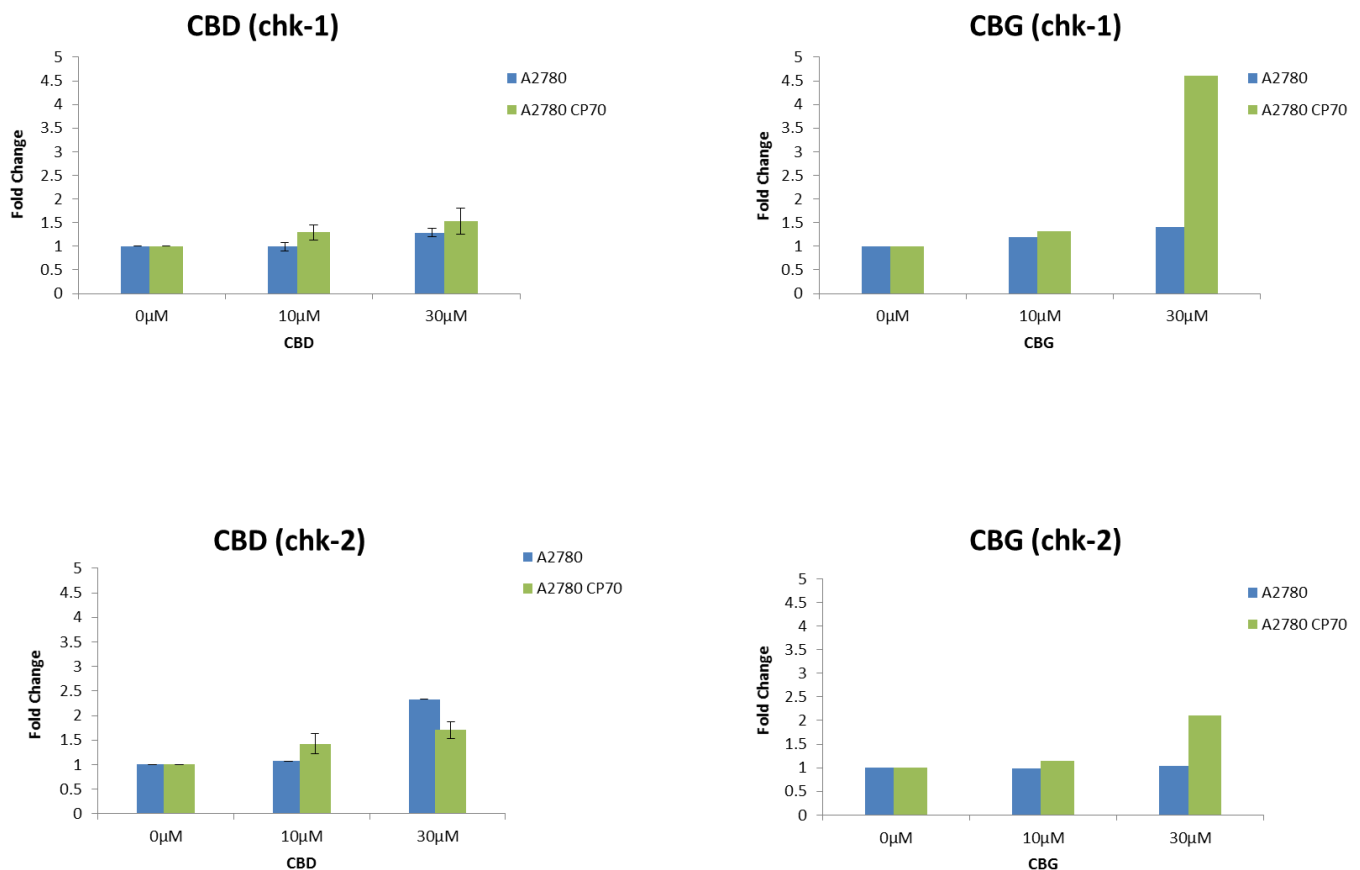


Figure 5-18. **Fold change of Chk 1 & 2 protein in A2780, and A2780/ CP70 cells.** The change in the expression of phosphorylated Chk 1 (Ser345) & chk2 (Thr68) following with CBD or CBG (10 μM or 30 μM) treatment on A2780, and A2780/ CP70 cells for 24 h. CBD on A2780, and A2780/ CP70 cells (n=2); CBG on A2780, and A2780/ CP70 cells (n=1)

As shown in **Figure 5-18**, a little increase in the fold change from control the expression of phosphorylated chk-1 (ser345) from control to 30 μ M CBD on both A2780 cells (1.29), and A2780/ CP70 cells (1.53). Similar to CBD, there was not much difference in chk-1 was observed when A2780 cells treated with CBG. However, the cytotoxicity of CBG resulted in a 4-fold increase in chk-1 levels in the cisplatin-resistant A2780/ CP70 cells. The predominant increase in Chk-1 levels in regards to increased concentrations of CBG in the cisplatin-resistant ovarian cancer cells are consistent with the G2/M cell cycle arrest observed earlier (**Figure 5-5**).

The approximately 2-fold increase in the expression of phosphorylated chk2 (Thr68) observed in A2780 cell treated with 30 μ M CBD whilst CBG induced similar effects in A2780/CP70 cells (**Figure 5-18**).

5.2.7.2 Quantification of the expression of caspase 3& caspase 7

Caspase 3 and caspase 7 are involved in the execution of both intrinsic and extrinsic caspase-dependent pathways hence the expression of cleaved caspases 3& 7 in ovarian cancer cells when treated with CBD/ CBG were investigated

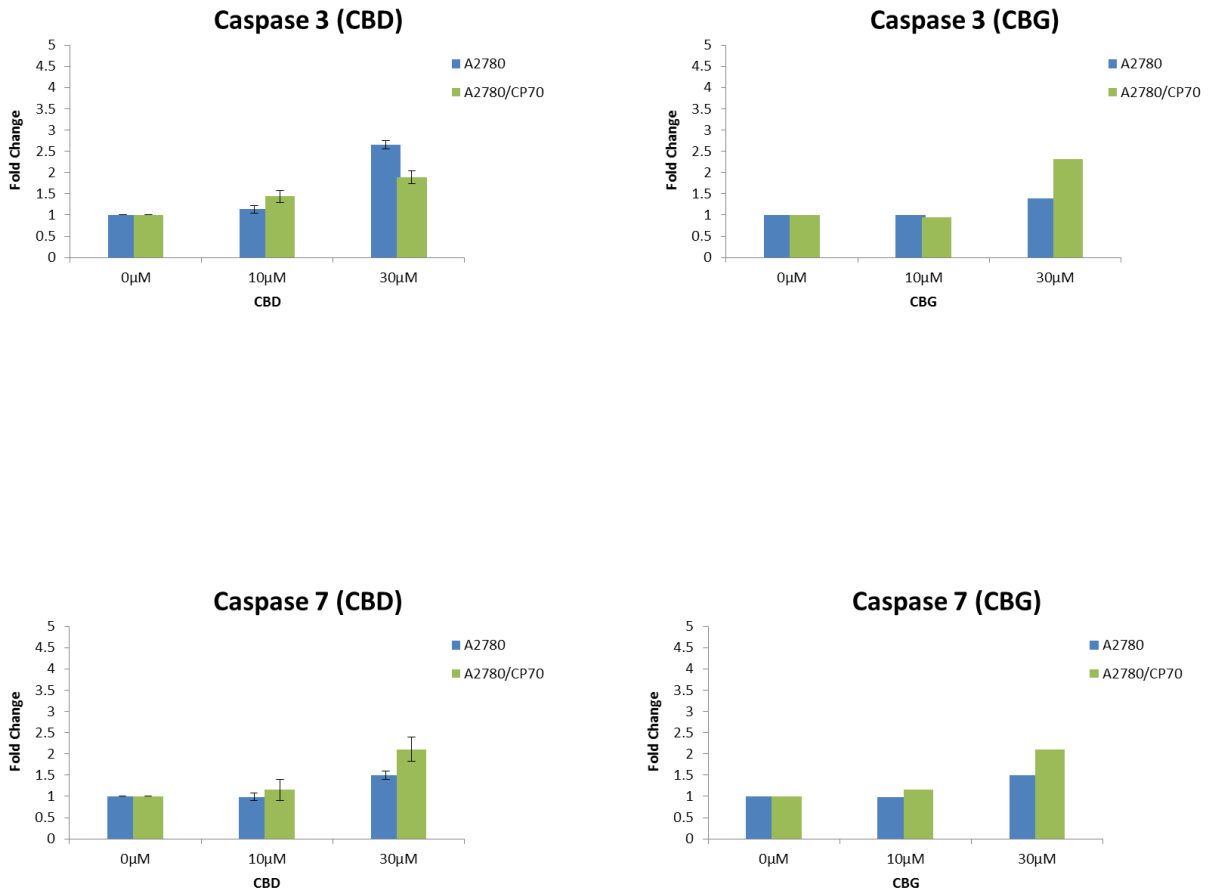


Figure 5-19 **Fold change of caspase 3& caspase7 in A2780, and A2780/ CP70 cells.** The fold change in the expression of cleaved caspase 3 (Asp 175) & caspase 7 (Asp 198) when A2780 and A2780/CP70 cells treated with CBD or CBG (10 μM or 30 μM). CBD on A2780, and A2780/CP70 cells (n=2); CBG on A2780, and A2780/CP70 cells (n=1)

As shown in **Figure 5-19**, increase expression levels of caspase 3 (Asp 175) was observed in A2780 cells at 30 μM CBD (2.63) and 30 μM CBG (1.39). Similar results were exerted by CBD (1.89) and CBG (2.31) in the cisplatin-resistant A2780/CP70 cells. Similar to the caspase 3 expression, there was a slight increase in caspase 7 (Asp 198) was also observed in both A2780 cells and A2780/CP70 cells at 30 μM CBD (1.49; 2.11) and 30 μM CBG (1.34; 2.31). The increase in cleaved caspase 3, caspase 7 consistent with the earlier assays where CBD and CBG have shown a dose-dependent increase in the caspase 3 /7 activity.

5.2.7.3 Quantification of the expression of tumour suppressor gene (p53)

P53 is a tumour suppressor gene, which involves in various biological processes including regulation of cell cycle. In response to DNA damage, p53 involves in the activation of proapoptotic proteins (Ozaki and Nakagawara, 2011). By regulating both proapoptotic, and antiapoptotic proteins of BCL-2 family, p53 plays a crucial role in apoptosis. The expression of p53 in both cell line in the presence of the CBD/ CBG was analysed and quantified as below.

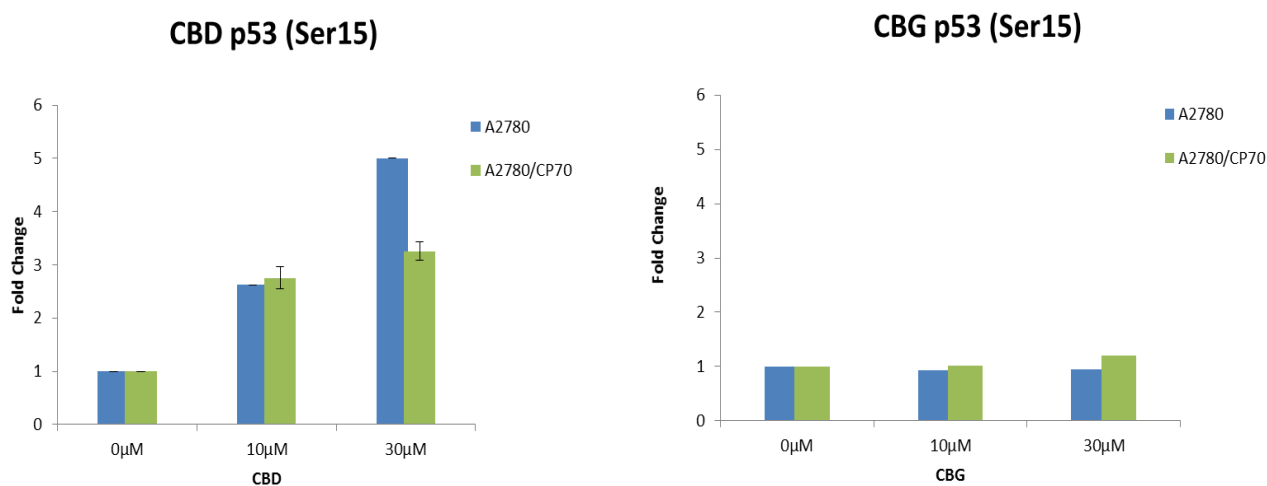


Figure 5-20. **Fold change of phosphorylated p53 in A2780, and A2780/ CP70 cells.** The fold change in the expression of phosphorylated p53 (serine 15) when A2780 and A2780 /CP70 cells treated with CBD or CBG (10 μM and 30 μM). CBD on A2780, and A2780/ CP70 cells (n=2); CBG on A2780, and A2780/ CP70 cells (n=1)

As shown in **Figure 5-20**, there was a 5 fold, and a 3 fold increase in the expression of phosphorylated p53 (ser15) was observed in A2780 and A2780/CP70 respectively when treated with 30 μM CBD. CBG at highest concentration did not alter the expression of p53 (ser15) in A2780 cells however, there was a slight increase was observed A2780/CP70 cells (1.21- folds).

5.2.7.4 Quantification of the expression of Bad and Survivin

Bad is a proapoptotic protein of Bcl- 2 family. It promotes apoptosis by binding to anti-apoptotic proteins. Survivin is an Inhibitory apoptotic protein (IAP) family protein. It involves in inhibition of apoptosis by binding to caspases. The expression of Bad and surviving was analysed and quantified as below.

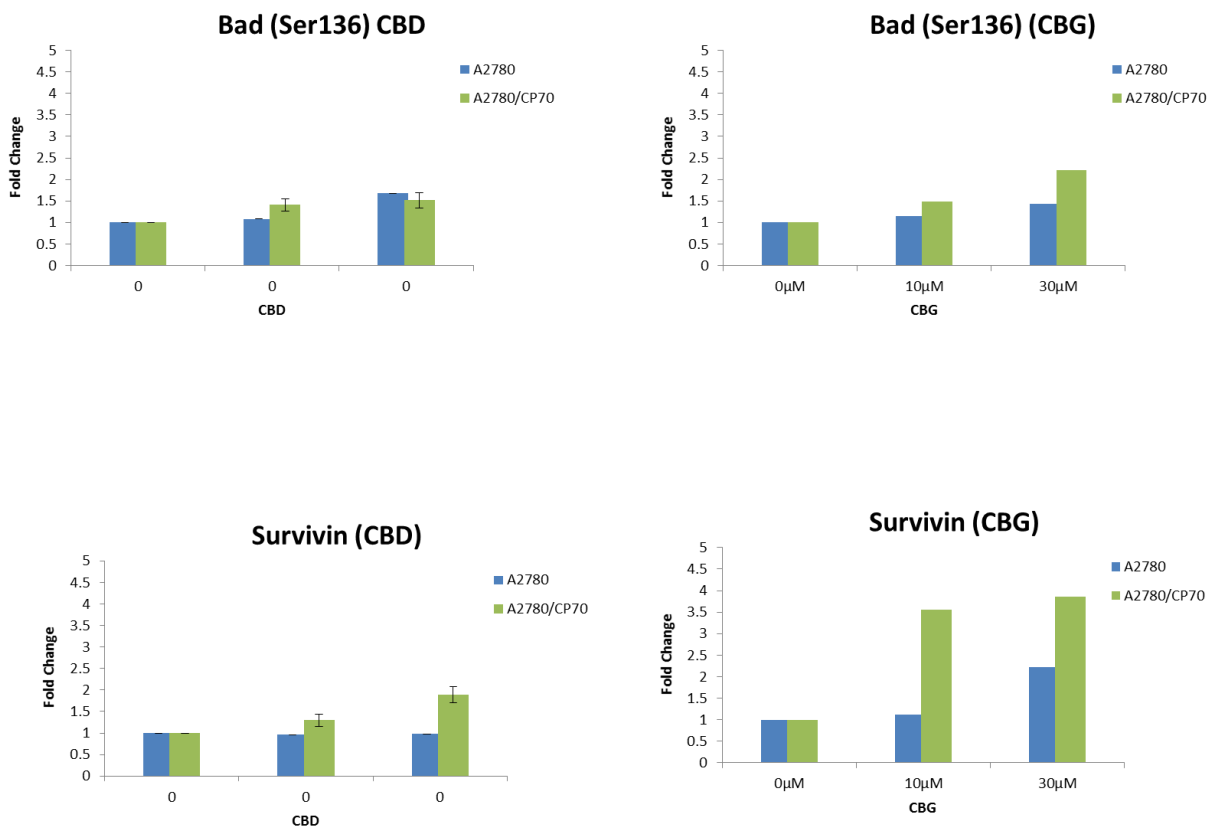


Figure 5-21 . **Fold change of phosphorylated Bad and total survivin in A2780, and A2780/ CP70 cells.** The fold change in the expression of Bad (serine 136) and total survivin when A2780 and A2780 /CP70 cells treated with CBD or CBG (10 μM and 30 μM). CBD on A2780, and A2780/ CP70 cells (n=2); CBG on A2780, and A2780/ CP70 cells (n=1)

As shown in **Figure 5-21**, although an effective increase in the expression of phosphorylated p53 (ser 15) in CBD treated A2780 and A270/CP70 cells, there was only a slight increase in the expression of Bad (ser136) was observed with the highest concentration of CBD tested (1.53;

1.68). At 30 μM , CBG there was a 3.86-fold increase in the survivin expression was observed in A2780/ CP70 cells.

5.2.7.5 Quantification of the expression of Poly (ADP-ribose) polymerase (PARP)

PARP are a family of proteins involves in various cellular functions including transcription, replication and DNA repair. In response to DNA damage, they involve in the regulation of apoptosis by activating Apoptosis-inducing factors (AIF).

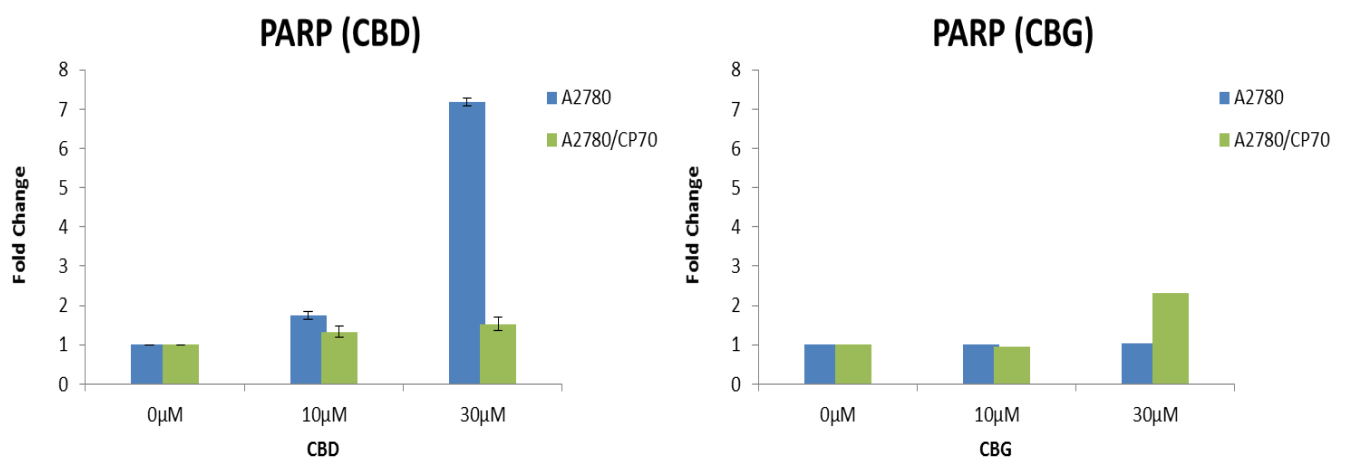


Figure 5-22. **Fold change of PARP in A2780, and A2780/ CP70 cells.** The fold change in the expression of cleaved PARP (Asp214) when A2780 and A2780 /CP70 cells treated with CBD or CBG (10 μM and 30 μM). CBD on A2780, and A2780/ CP70 cells (n=2); CBG on A2780, and A2780/ CP70 cells (n=1)

A2780 cells have shown a 7-fold increase in the expression of cleaved PARP (Asp214) when treated with 30 μM of CBD (Figure 5-22), effective increase in the PARP (Asp214) levels in CBD treated A2780 cells correlates with the p53 increase observed earlier. Compared to A2780 cells, relatively less PARP activity was observed in A2780/CP70 cells (1.53 fold) when treated with 30 μM of CBD. In contrast to CBD, CBG at 30 μM (2.51) has shown an increase in PARP activity in A2780/CP70 cells whereas it did not show any effect at the same concentration in A2780 cells.

5.2.7.6 Expression of stress related proteins.

HSP (heat shock protein) 27 is a stress-related protein. It involves cell survival processes under stress by inhibiting the activation of caspase 9. TAK 1 is another protein involved in cell survival process by activating NF κ B pathway. HSP27 and TAK1 proteins regulate the ROS induced apoptosis. Therefore, the expression levels of both the proteins with increased concentrations of CBD/ CBG on ovarian cancer cells were analysed. The results were summarised below.

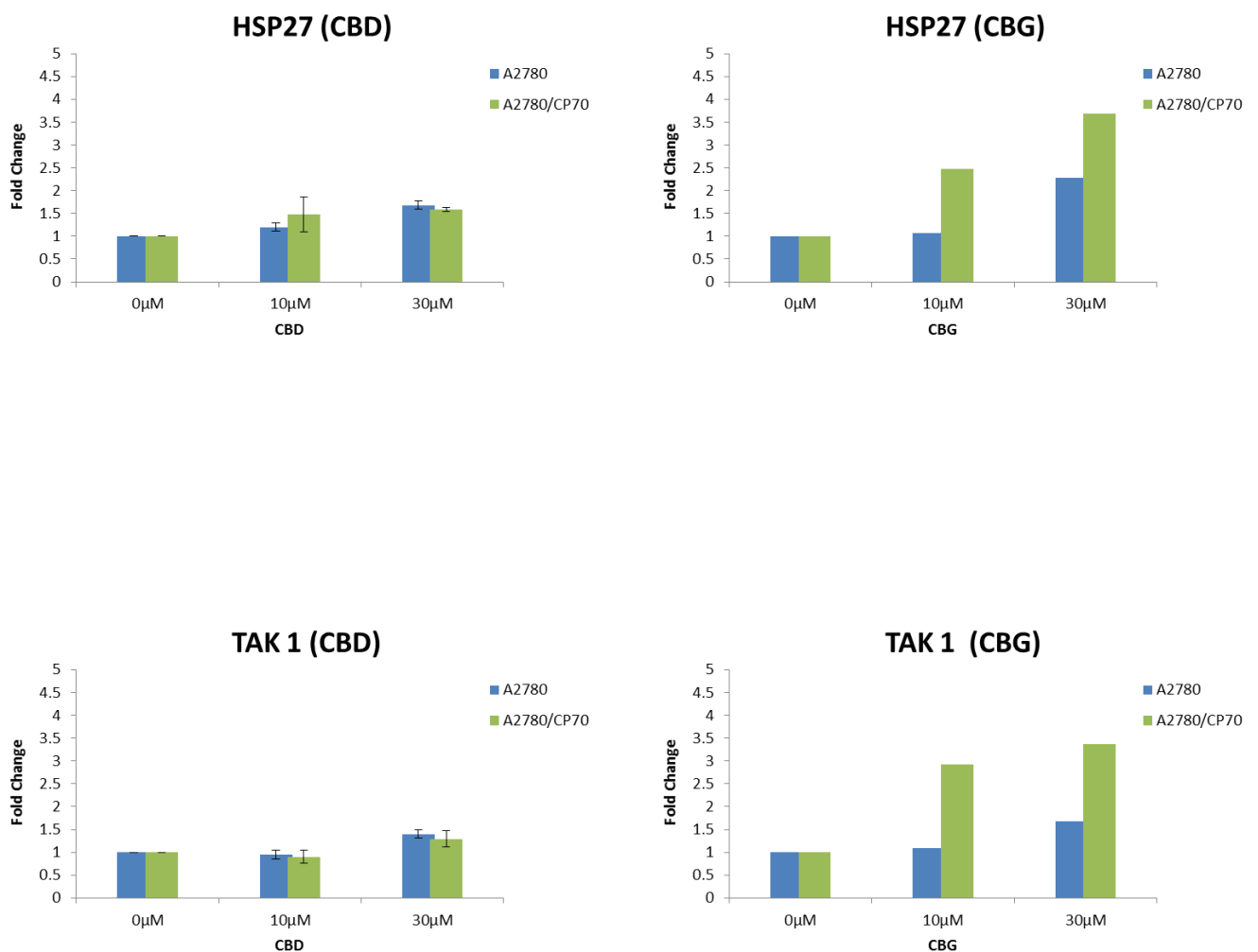


Figure 5-23 **Fold change of phosphorylated HSP27 and TAK 1 in A2780, and A2780/ CP70 cells.** The fold change in the expression of phosphorylated HSP27 (Ser82) and TAK 1 (ser412) when A2780 and A2780/ CP70 cells treated with CBD or CBG (10 μM and 30 μM). CBD on A2780, and A2780/ CP70 cells (n=2); CBG on A2780, and A2780/ CP70 cells (n=1)

As shown in Figure 5-23, 30 μ M CBD has shown 1.68 and 1.58 fold increase in the expression of HSP27 (Ser82) in A2780 and A2780/CP70 cells respectively. Similar to CBD, 30 μ M CBG has shown a 1.48-fold increase on A2780 cells. However, at the same concentration of CBG, there was almost 4-fold (3.68) increase in HSP27 levels were in A2780/CP70 cells. CBD has shown a little increase TAK 1 levels at the 30 μ M concentration on A2780 cells (1.40), and A2780/CP70 cells (1.29). Similar to HSP27, 30 μ M CBG has shown a 3.36-fold increase on A2780/ CP70 cells.

5.3 Discussion

The cell cycle analysis of A2780 cells and A2780/CP70 cells when treated with CBD (10 μ M and 30 μ M) have shown the possibility of G1 growth arrest at 48 h. A small increase in Chk- 2 phosphorylation levels (compared to control) when A2780 cells (2 fold), and A2780/CP70 (1.6 fold) were treated with 30 μ M CBD at 24 h supports the possibility of G1 growth arrest. The significant increase in DNA proportion of Sub G1 phase with increased doses of CBD in both the cell lines suggested the induction of cell death: this was later confirmed by several different apoptosis assays.

Cell cycle analysis of A2780 cells treated with CBG at 50 μ M demonstrated the possible growth arrest at S phase whilst in the A2780/CP70 cells, increased doses of CBG suggested the partial growth arrest in the S phase and G2/M phase. A 4-fold increase in chk-1 levels was observed when A2780/CP70 cells were treated with 30 μ M CBG supports cell cycle checkpoint activation.

The cell cycle analysis was performed only at the 48 h time point. Therefore, the above results are only suggestive of possible cell cycle effects. Cell cycle analysis at later time points would indicate whether cells are accumulating in a particular phase of the cycle and time, indicating

arrest at that phase. The analysis of cell cycle progression with other techniques such as FACS with BrdU labelling would also help to confirm arrest in at particular phase of the cell cycle.

The induction of apoptosis by CBD and CBG has been reported in cancer cells including prostate, breast and colon cancer cells (Dariš et al., 2018). Mitochondria can play a critical role in induction of apoptosis. Disruption in mitochondrial membrane potential ($\Delta\psi_m$) increases the membrane permeability, resulting in release of pro-apoptotic factors, which activates induction of apoptosis (Fleury et al., 2002). Quantifying the loss of $\Delta\psi_m$ is commonly used technique to assess the cellular apoptosis. Both CBD and CBG induced the loss of membrane potential in A2780 and A2780/CP70 cells in a dose-dependent manner suggesting the induction of apoptosis in both the cell lines. The possible induction of apoptosis by CBD and CBG in the ovarian cancer cells was confirmed by quantifying the Annexin V binding with extracellular exposed phosphatidylserine (PS) (Schutte et al., 1998). The Annexin V assay also demonstrated similar results to the mitochondrial membrane assay.

There are several different mechanisms of apoptosis including the extrinsic and intrinsic apoptosis pathways, which are both caspase-dependent, and another mechanism is a caspase-independent mechanism (Elmore., 2007).

CBD has demonstrated to induce caspase-dependent apoptosis in various cancers such as breast, prostate, leukaemia, and CBG has been shown to exert its cytotoxicity in prostate cancer cells by induction of intrinsic apoptotic pathway (Izzo et al., 2009, Dariš et al., 2018, Shrivastava et al., 2011). Quantification of caspase 3/7 enzyme activity in the ovarian cancer cells with increased concentrations of CBD and CBG demonstrated the involvement caspases in apoptosis. The increase in the levels of cleaved caspases 3& 7, using an ELISA assay produced the similar results; the increase in the levels of cleaved PARP (Ser214) is also an

indication of caspase activity. As caspase 3 cleaves PARP to separate, the DNA binding site at amino terminal from catalytic domain, which leads to apoptosis(Nicholson et al., 1995, Lazebnik et al., 1994). The increased in the levels of cleaved PARP and multi fold increase of caspase activity observed in the ovarian cancer cells treated with CBD and CBG indicate that both CBD and CBG exert their cytotoxicity in ovarian cancer cells by caspase-dependant apoptosis.

CBD is reported to be cytotoxic activity towards human glioma cells by induction of ROS whereas CBG induced ROS in colon cancer cells (Singer et al., 2015, Borrelli et al., 2014). Here it is shown that CBD and CBG both induced ROS production in the ovarian cancer cells. Importantly, the same concentration of CBD or CBG did not increase the ROS levels in non-cancer PNT2 cells. The increased expression levels of phosphorylated HSP27 and TAK1 (stress related proteins) in the ovarian cancer cells treated with CBD and CBG also indicate the of ROS production (Omori et al., 2008, Liu et al., 2007). The selective oxidative stress observed in the ovarian cancer cells compared to non- cancer cells can be correlated with the neuroprotective and anticancer nature of the cannabinoids CBD and CBG (Valdeolivas et al., 2015, Dariš et al., 2018, Alvarez et al., 2008)

CHAPTER 6 Investigation of cannabinoids receptors in CBD and CBG induced cytotoxicity on ovarian cancer cells.

6.1 Introduction

Cannabinoid receptors are involved in growth, metastasis and energy metabolism of various cancer types. Both the upregulation and downregulation of cannabinoid receptors were observed in multiple tumours pathogenesis and anti-proliferative effects of cannabinoid in cancer cells are often associated with cannabinoid receptors (Chakravarti et al., 2014, Dariš et al., 2018). Since GPR55 involves in regulation of inflammation, angiogenesis, and tumour invasion and metastases it was important to see whether the cannabinoids CBD and CBG exert their anticancer effects through GPR55 in ovarian cancer (Leyva-Illades and DeMorrow, 2013). In this chapter, the involvement of cannabinoid receptors CB1, CB2, and especially GPR55 in the anticancer activity of CBD and CBG in ovarian cancer cells will be investigated.

6.2 Results

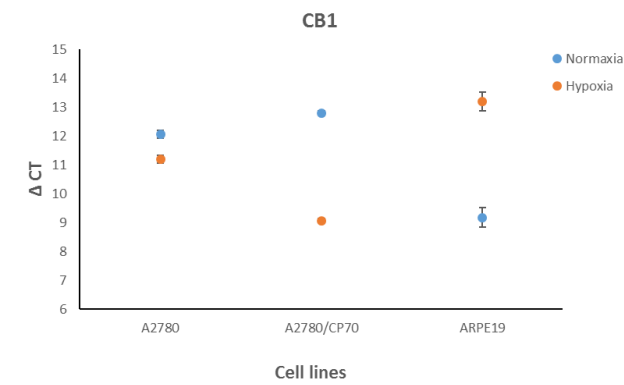
6.2.1 Investigation of expression levels of CB1, CB2 and GPR55 in hypoxia and normoxia conditions.

The abnormality in oxygen tension commonly occurs in malignant tumours. The rapid proliferative nature of tumour cells leads to the expansion of tumour tissue away from vasculature. The distance between vasculature and tumour cells results in a shortage of oxygen supply, which leads to the formation of a hypoxic environment in the tumour. The hypoxic environment advances tumour progression by enabling the tumour to upregulate angiogenesis, anaerobic glycolysis, cell mobility and metastasis. The hypoxic environment also induces the cell quiescence, which helps tumours to increase their resistance to chemotherapy (Muz et al., 2015). Therefore, the experiments were carried out to determine

the expression levels of cannabinoid receptors in the A2780 cells, A2780/CP70 cells, and ARPE19 cells in both normal and hypoxic conditions.

The cells were seeded in T75 flasks as described in **section 2.7**. A flask from each cell line was transferred to normoxia (normal incubator oxygen) and hypoxia condition (hypoxic chamber with 0.1% oxygen). After 6 hours, the media was replaced for the cells in hypoxic chamber with the complete media, which was incubated in hypoxic chamber 24 h prior to the seeding. Similarly, the cells in normal incubator was also replaced with normal complete media. After 72 h (incubated to reach 70% cell confluence in the flasks), the RNA was extracted, cDNA was synthesised and qPCR was performed as described in section 2.15, 2.16, and 2.17.

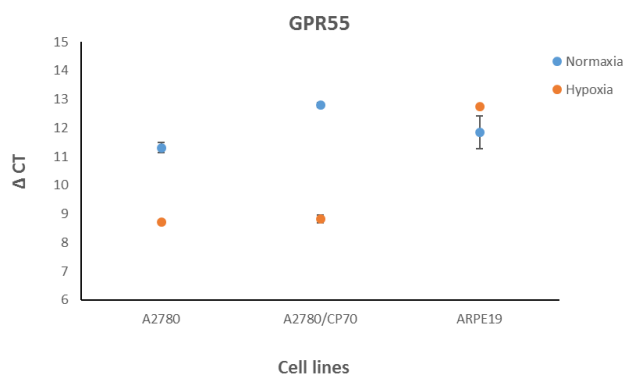
The expression levels of CB1, CB2 and GPR55 were quantified against GUSB. In A2780 cells grown in hypoxia conditions, The A2780 cells did not show any difference in CB2 receptor and CB1 receptors was slightly over expressed ($\Delta\Delta\text{CT} < 1$) where as GPR55 over expressed with $\Delta\Delta\text{CT}$ 2.69 compared to the A2780 cells grown in normal oxygen conditions. In cisplatin resistant A2780/CP70 cells, all the cannabinoid receptors tested CB1, CB2 and GPR55 were over expressed with $\Delta\Delta\text{CT}$ values 3.73, 5.48 and 3.97 respectively. In contrast to the ovarian cancer cells, in hypoxia conditions ARPE19 non-cancer cells under expressed CB1, CB2 and GPR55 receptors with $\Delta\Delta\text{CT}$ -0.89, -4.01 and -0.67 as shown in **Figure 6-1**. The over expression of the cannabinoid receptors in the ovarian cancer cells, and under expression in non-cancer cells under hypoxic conditions is an interesting observation which could be possibly related to the upregulation of cannabinoid receptors in tumour progression. However, the investigation of cytotoxic effects of CBD and CBG and their affinity towards the cannabinoid receptors under hypoxic conditions would be an ideal approach for future research.



CB1	Normoxia (Δ CT)	Hypoxia (Δ CT)
A2780	12.05± 0.26	11.19± 0.38
A2780/CP70	12.79± 0.35	9.06± 0.02
ARPE19	9.17± 0.04	13.18± 0.04



CB2	Normoxia (Δ CT)	Hypoxia (Δ CT)
A2780	11.70± 0.14	11.79± 0.29
A2780/CP70	14.28± 0.07	8.83± 0.14
ARPE19	11.99± 0.33	12.66± 0.33



GPR55	Normoxia (Δ CT)	Hypoxia (Δ CT)
A2780	11.39± 0.17	8.72± 0.02
A2780/CP70	12.79± 0.01	8.82± 0.12
ARPE19	11.85± 0.57	12.74± 0.002

Figure 6-1. **The expression of CB1, CB2 and GPR55 receptors.** Δ CT values of CB1, CB2 and GPR55 compared to housekeeping gene GUSB in A2780, A2780/CP70 and ARPE19 cells under normoxia and hypoxia conditions. GUSB used as a housekeeping gene for data normalisation. Data represents n=1.

Table 6-1 $\Delta\Delta CT$ values of CB1, CB2 and GPR55 receptors in A2780, A2780/CP70, and ARPE19 cells.

$\Delta\Delta CT$ (Normoxia - hypoxia)	CB1 ($\Delta\Delta CT$)	CB2 ($\Delta\Delta CT$)	GPR55($\Delta\Delta CT$)
A2780	0.86	-0.09	2.67
A2780/CP70	3.73	5.45	3.97
ARPE19	-4.01	-0.67	-0.89

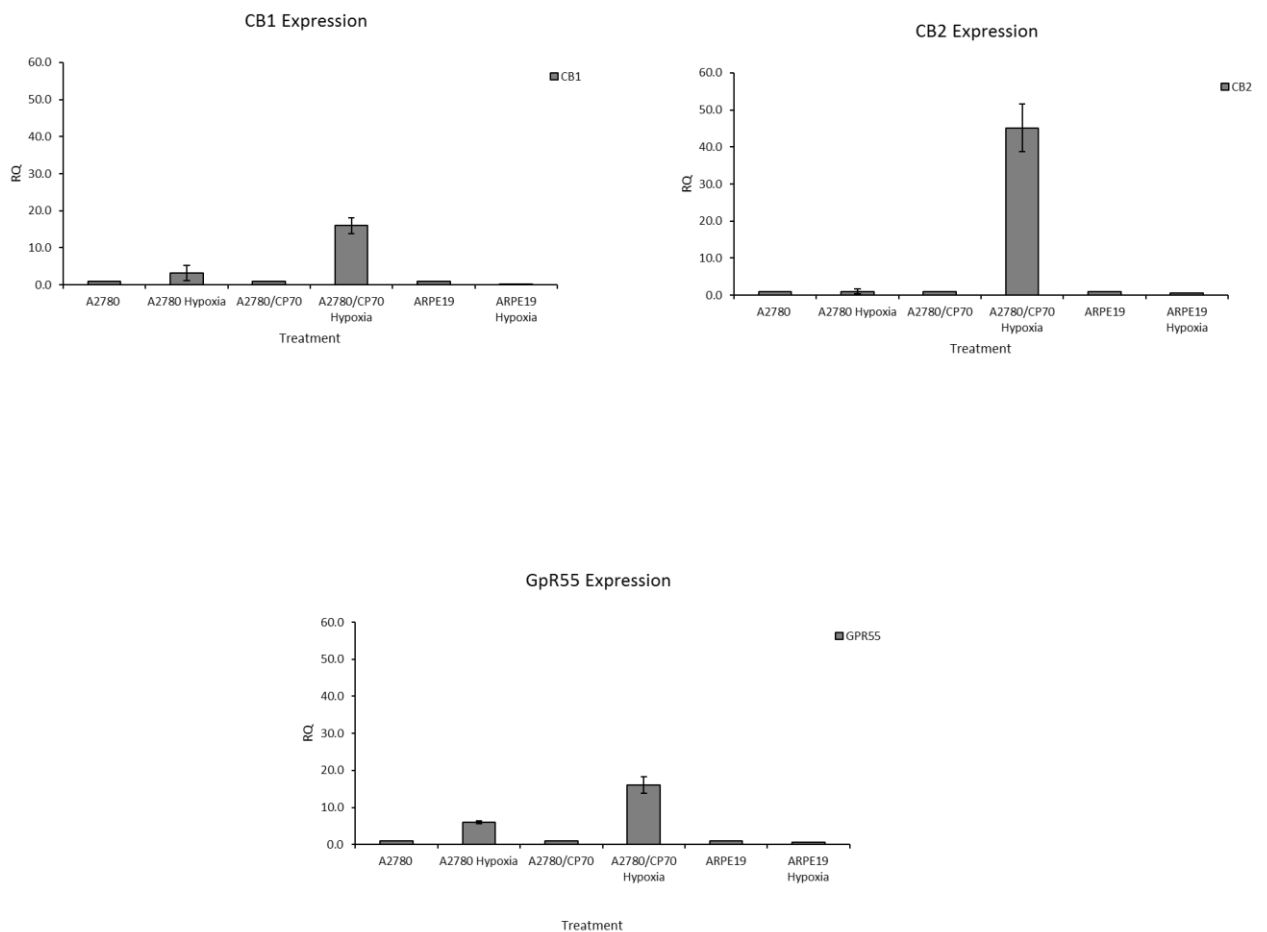


Figure 6-2. **Fold change in the expression of CB1, CB2 and GPR55 receptors.** The increased levels of CB1, CB2 and GPR55 (the fold change in hypoxia conditions compared to normoxia in A2780, A2780/CP70 and ARPE19 cells. GUSB was used as a housekeeping gene. Data represents n=1.

6.2.2 Investigation of the involvement of GPR55 receptor in CBD and CBG induced cytotoxicity.

The expression of GPR55 receptor in CBD and CBG treated A2780 and A2780/CP70 were determined by western blot analysis. The ovarian cancer cells were seeded, and vehicle or CBD (10 μ M, 20 μ M, 30 μ M and 50 μ M) were added as described in section 2.6. After 24 h incubation, the lysates were collected, and western blot analysis was carried out (as described in section 2.11). The expression of the GPR55 receptor in CBD/ CBG treated samples compared to the controls were quantifying against corresponding beta-actin levels.

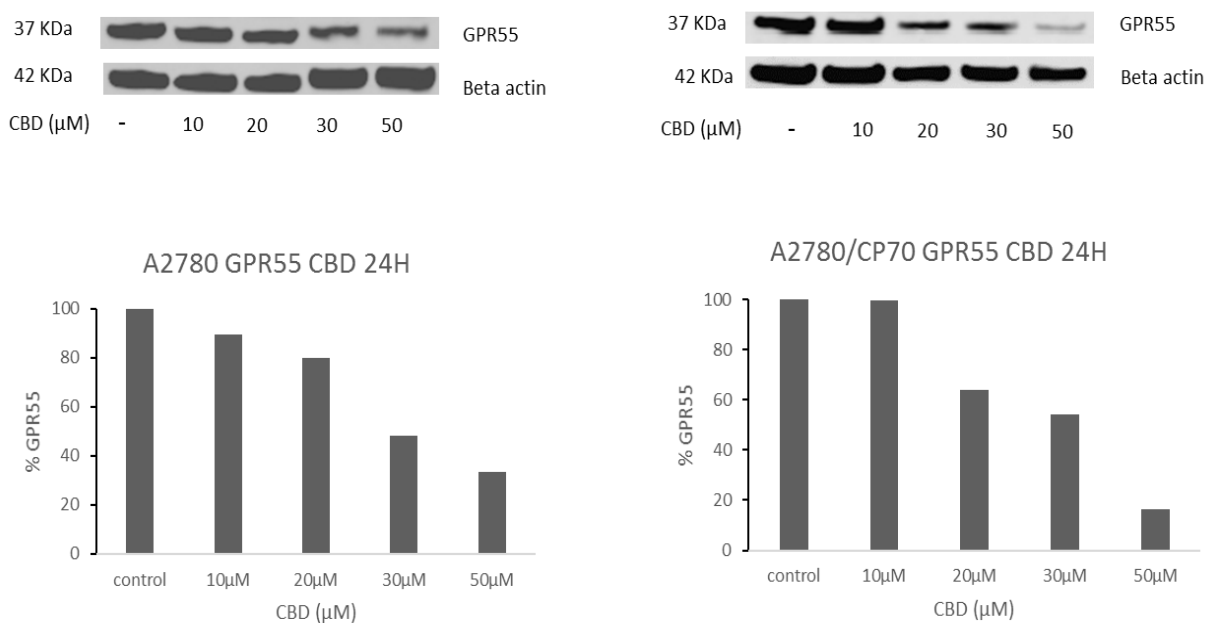


Figure 6-3. GpR55 protein levels in A2780 and A2780/CP70 cells treated with CBD. The levels of GpR55 protein in A2780 cells (left) and A2780/CP70 cells (right) when treated with CBD (10 μ M, 20 μ M, 30 μ M and 50 μ M) were quantified against beta actin. Top left blots represent the protein expression of beta actin and GpR55 in A2780 cells, and top right blots represent the protein expression of beta actin and GpR55 in A2780/CP70 cells. Quantification by densitometry (n=1).

As shown in **Figure 6-3**, GpR55 is expressed in both A2780 and CP70 cells raising the possibility that CBD/CBG might act via this receptor. A dose-dependent reduction of GpR55 receptor expression was observed in both A2780 and A2780/CP70 cells when treated with CBD. At 50

μM CBD, the expression levels of the GpR55 receptor were reduced to 33% and 16% of basal expression levels in A2780 and A2780/CP70 cells respectively. The results indicate the possible involvement of the GpR55 receptor in CBD induced cytotoxicity. Similar experiments were carried out with CBG (10 μM , 30 μM and 50 μM)

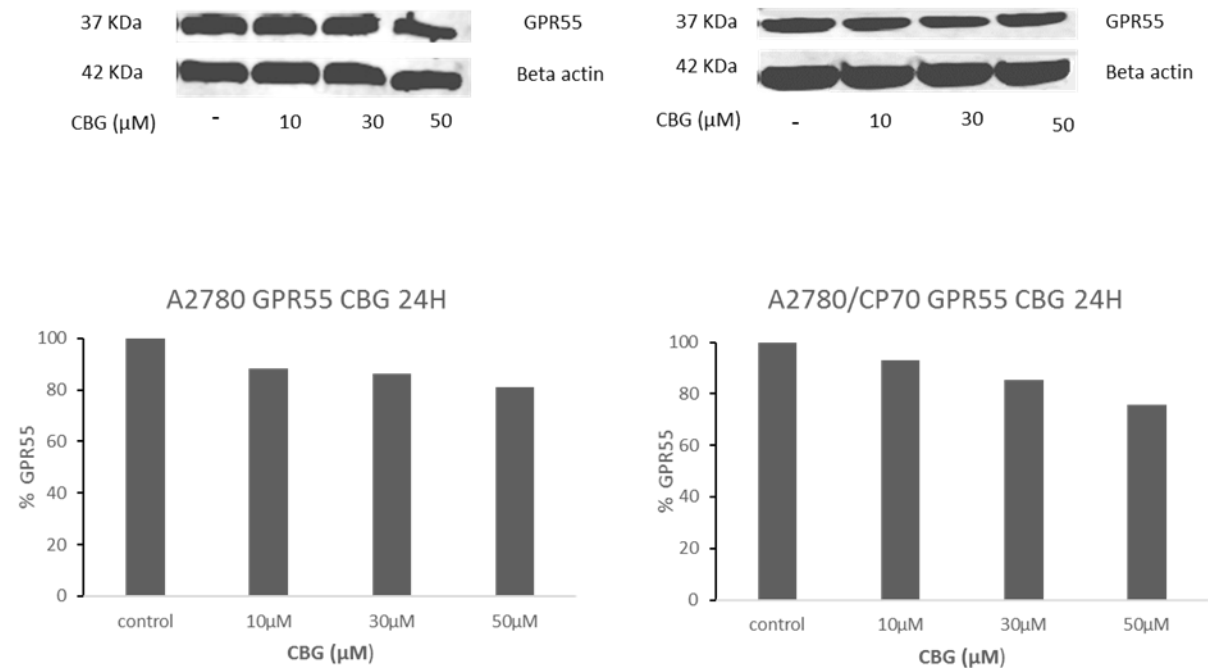


Figure 6-4. **GpR55 protein levels in A2780 and A2780/CP70 cells treated with CBG.** The levels of GpR55 protein in A2780 cells (left) and A2780/CP70 cells (right) when treated with CBG (10 μM , 30 μM and 50 μM) were quantified against beta actin. Top left blots represent the protein expression of beta actin and GpR55 in A2780 cells, and top right blots represent the protein expression of beta actin and GpR55 in A2780/CP70 cells. Quantification by densitometry ($n=1$).

A very small reduction of GpR55 receptor expression was observed in both A2780 and A2780/CP70 cells when treated with 50 μM CBG but this was much less pronounced than the dose-dependent decrease with CBD treatment (**Figure 6-4**). At 50 μM CBG, expression levels of the GpR55 receptor were reduced to 81% and 75% respectively in A2780 and A2780/CP70 cells.

Between the cells lines tested, CBD resulted in a greater reduction of GpR55 in cisplatin resistant A2780/ CP70 compared to A2780 cells. However, the experiment was performed once hence more biological repeats are required to determine whether this is a consistent and reproducible observation.

Further investigations were carried out to investigate the cytotoxicity effects of both the cannabinoids in the presence of a GpR55 antagonist in A2780 and A2780/CP70 cells.

6.2.3 Investigation CBD and CBG cytotoxicity in the presence of GPR55 antagonist CID16020046.

The involvement of the GpR55 receptor in CBD or CBG induced cytotoxicity was further investigated using CID16020046. CID16020046 is a selective antagonist for the GpR55 receptor. Pre-treatment of the ovarian cancer cells with CID16020046 can potentially block the GpR55 receptor. The cytotoxicity of CBD or CBG on A2780 and A2780/CP70 in the presence of CID16020046 was tested to determine the involvement of the GpR55 receptor.

A2780 and A2780/CP70 cells were seeded as described in section 3.2. After 24 h incubation, the cells were treated with 1 μ M of CID16020046, and incubated for 1 h. After 1h, cells were treated with CBD or CBG (1nM to 100 μ M) for 96h and MTT assays were then performed (as described in section 2.5.3).

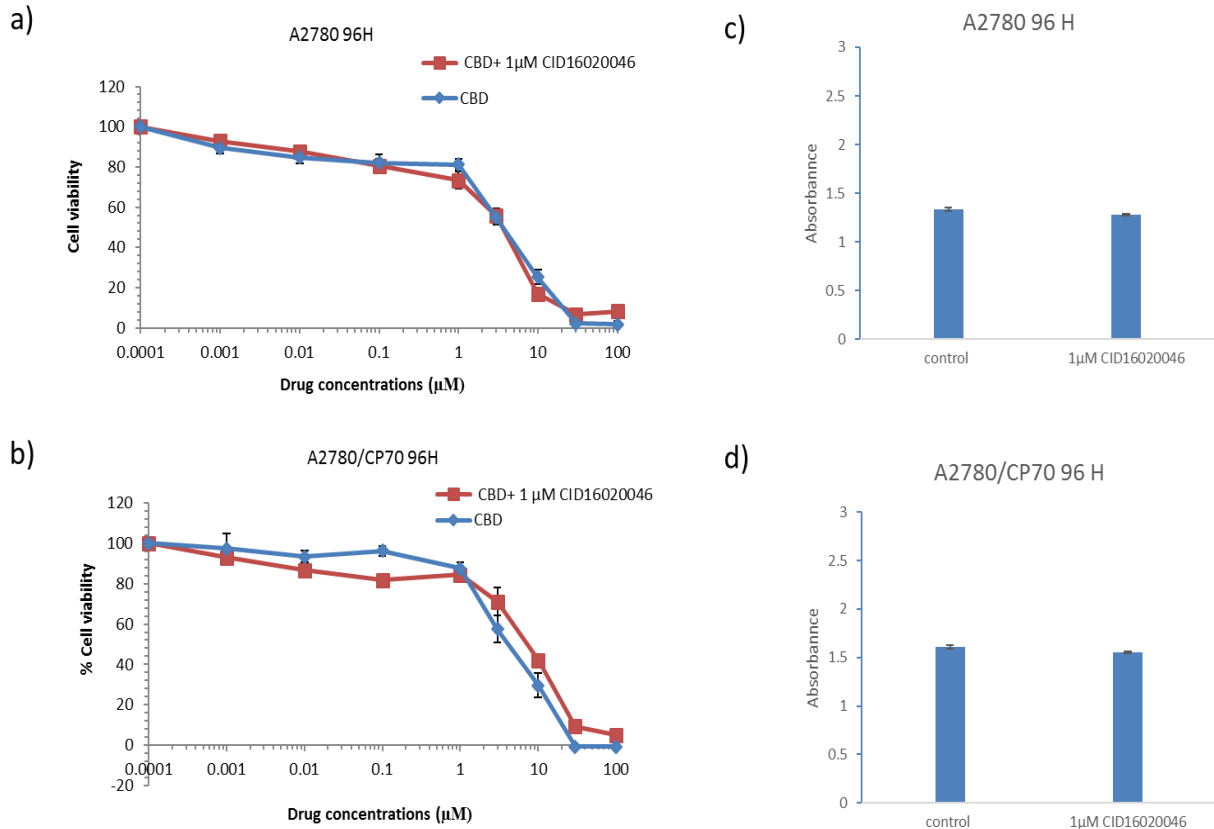


Figure 6-5. Cytotoxicity of CBD in the presence of GpR55 antagonist CID16020046. Comparison of the dose-response of CBD alone and CBD in combination with 1 μM CID16020046 on A2780 and A2780/CP70 cells after 96 h exposure. 1% ethanol was used as a solvent control for CBD alone. For combination experiments, % viability is expressed relative to that of 1 μM CID16020046 (a& b). Effect of 96h 1 μM CID16020046 on cell viability as indicated by absorbance at 540 from dissolved formazan crystals compared to vehicle control (c& d). Data represents the mean \pm standard error of mean of n=3, n is the number of independent biological experiments.

As shown in **Figure 6-5**, the absorbance values of 1 μM of CID16020046 on A2780 (1.28 ± 0.1) and A2780/CP70 (1.55 ± 0.08) were similar to the absorbance values of 1% ethanol (vehicle) on A2780 (1.33 ± 0.1) and A2780/CP70 (1.61 ± 0.2) indicating that 1 μM of CID16020046 alone did not exert any cytotoxicity effects. The IC₅₀ values exerted by CBD when combined with CID16020046 on A2780 ($4.04 \pm 0.35 \mu\text{M}$) was similar to the IC₅₀ values exerted by CBD alone ($3.46 \pm 0.17 \mu\text{M}$). CBD, when combined with CID16020046 on A2780/CP70, has shown higher IC₅₀ values ($7.12 \pm 1.17 \mu\text{M}$) compared to CBD alone ($5.79 \pm 0.82 \mu\text{M}$) however, the difference observed was not significant.

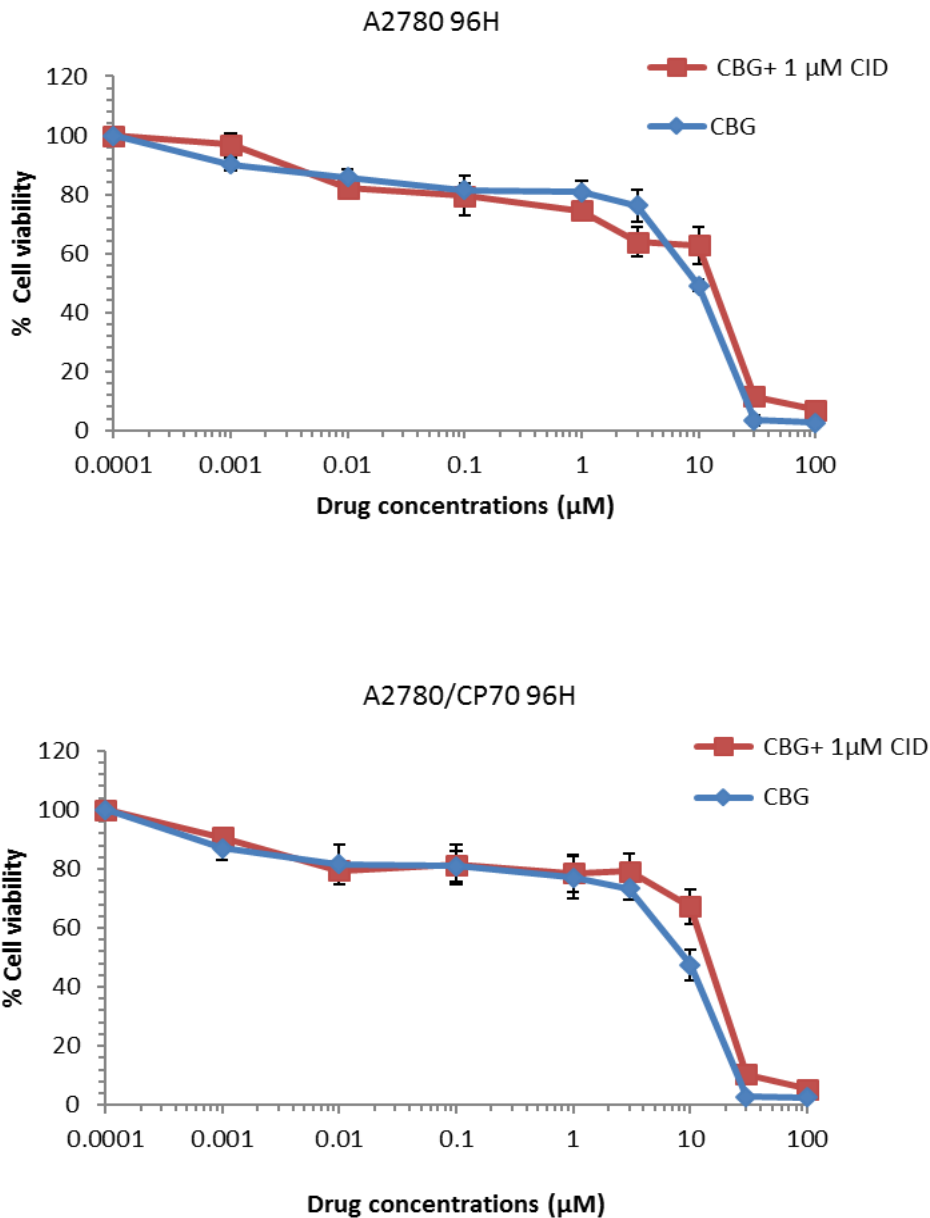


Figure 6-6 **cytotoxicity of CBG in the presence of GPR55 antagonist**. Comparison of the dose-response of CBG alone and CBG in combination with 1 μM CID16020046 on A2780 and A2780/CP70 cells after 96 h exposure. 1% ethanol was used as a solvent control for CBG alone. For combination experiments, % viability is expressed relative to that of 1 μM CID16020046. Data represents the mean ± standard error of mean of N=3, N is the number of independent biological experiments.

Similar to CBD, The IC₅₀ values of CBD when combined with CID16020046 were similar in A2780 cells compared to CBG alone. In A2780/CP70 cells the IC₅₀ values of the combination (13.2 ± 2.8 μM) were significantly (P<0.05) higher than CBG alone (7.1 ± 0.7 μM) (**Figure 6-6**).

Previous pharmacological studies have shown significant GPR55 antagonistic effects of CID16020046 at 20 μ M in ovarian cancer cells (Hofmann et al., 2015a). Further experiments were carried to determine the combination effects of CBD on CID16020046 induced cytotoxicity in A2780 cells

The effects of 10 μ M and 20 μ M CID16020046 alone, and in combination with 10 μ M CBD was investigated on A2780 cells were investigated after 48 h by performing Annexin V assay (as described in **section 2.7**). The results were analysed using the NC3000 software.

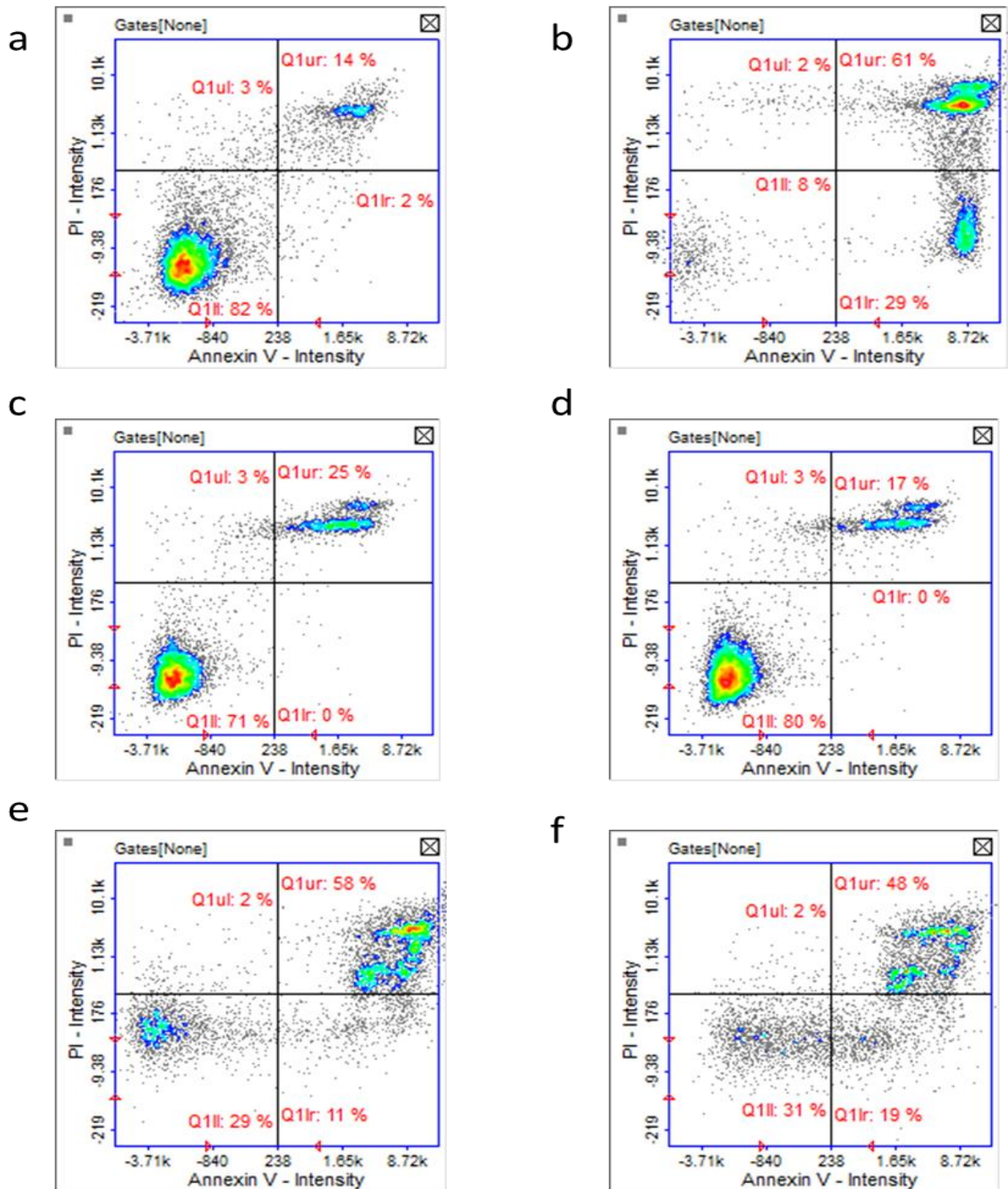


Figure 6-7 Annexin V analysis of CBD in combination with CID16020046 on A2780 cells. The comparison of the percentage apoptotic cells induced by the cytotoxicity of 10 μ M and 20 μ M CID16020046 alone, and in combination with 10 μ M CBD in A2780 cell. a) A2780 cells treated with 1% ethanol b) A2780 cells treated with 10 μ M CBD c& d A2780 cells treated with 10 μ M CID16020046 alone, and 10 μ M CID16020046 in combination with 10 μ M CBD respectively whereas e& f A2780 cells treated with 20 μ M CID16020046 alone, and 20 μ M CID16020046 in combination with 10 μ M CBD respectively. In each scatters plot, the bottom left quadrant represents the percentage of healthy cells, the bottom right quadrant represents the percentage of early apoptotic cells whereas top right represents the late apoptotic or necrotic cells.

As shown in **Figure 6-7**, the cytotoxicity effects of CBD on A2780 cells alone (61%) was rescued when combined with 10 μ M CID16020046 (17%) and 20 μ M CID16020046 alone (48%). The above results indicate that CID16020046 comprised the cytotoxic effects of CBD on A2780 cells meaning the possible involvement of GPR55 receptor in the cytotoxic mechanism of CBD in the ovarian cancer cells.

However, the results are the representation of one biological experiment, which requires further repeats.

6.2.4 GpR55 RNAi-mediated silencing in A2780 and A2780/ CP70 cells

A2780 and A2780/CP70 cells were transfected with Negative Control siRNA and GPR55 siRNA as described in section 2.13. The flasks were incubated for 48 h and 72 h time points. After incubation time elapsed, cells were harvested and lysates were collected for protein analysis.

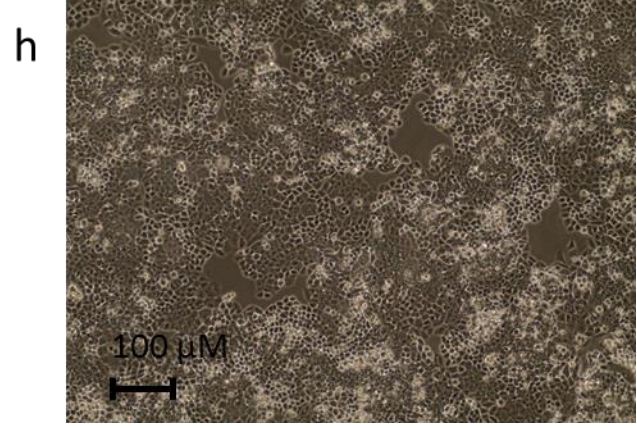
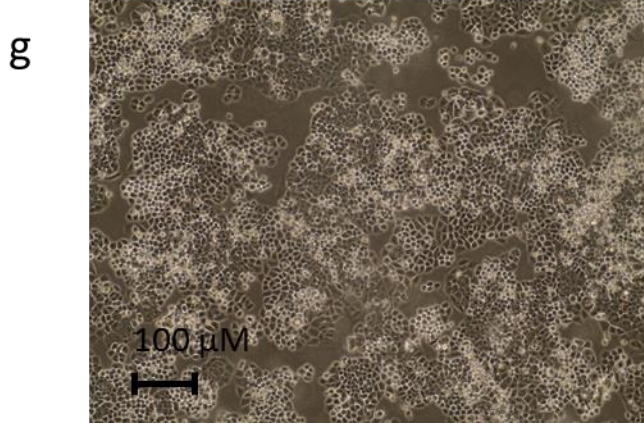
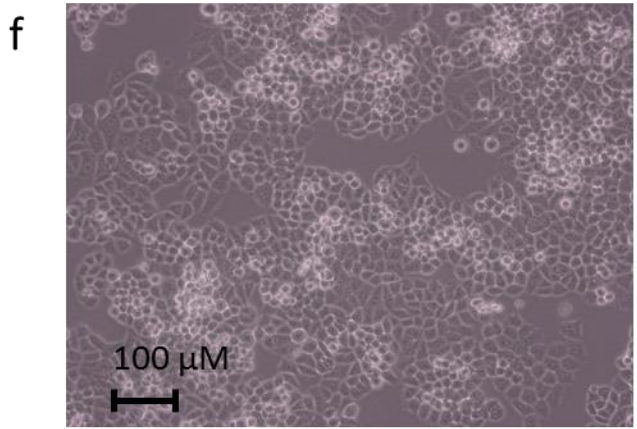
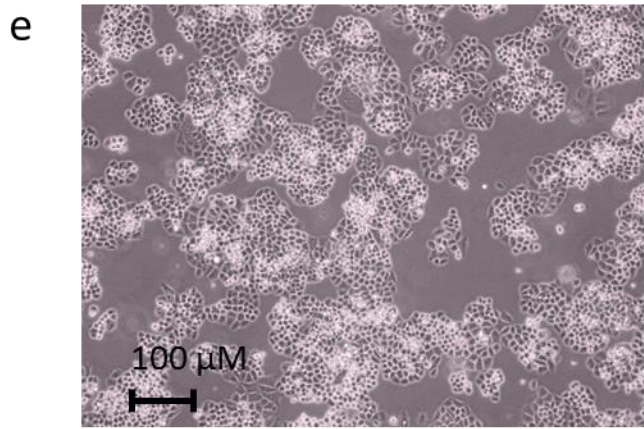
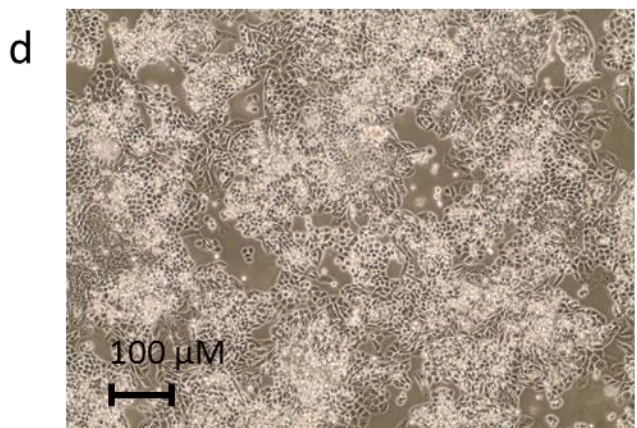
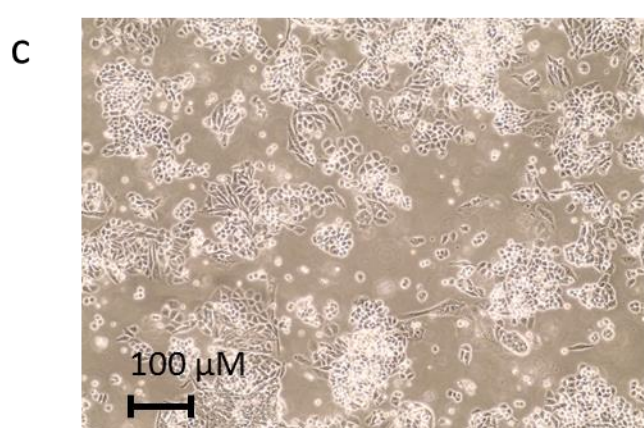
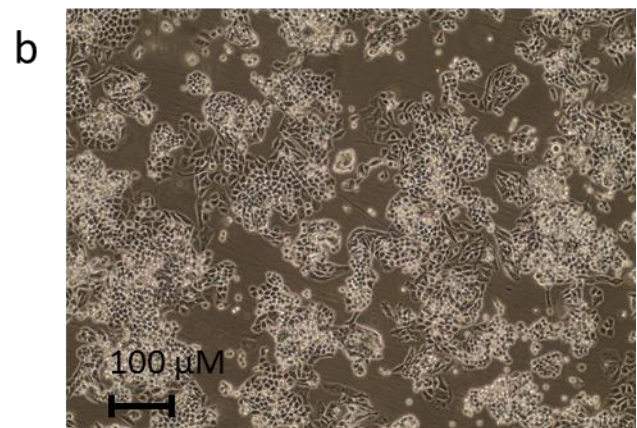
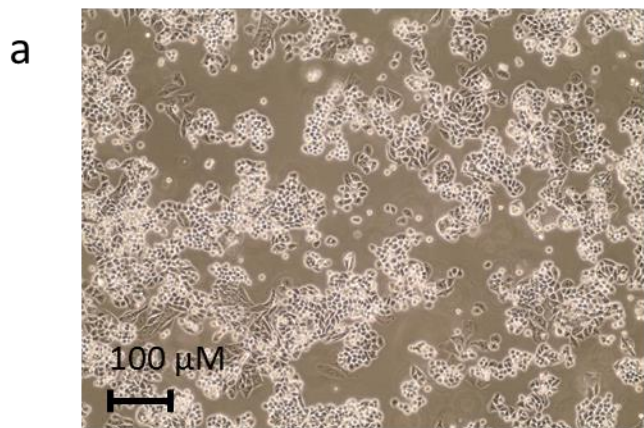


Figure 6-8. **GPR55 RNA silencing in A2780 and A2780/CP70 cells.** The bright field microscopic images of GPR55 RNA silencing in A2780 cells, and A2780/CP70 cells after 48 h and 72 h. a & b represents negative RNAi control, and GPR55 RNA silenced A2780 cells after 48 h; c & d represents negative RNAi control, and GPR55 RNA silenced A2780 cells after 72 h; e & f represents negative RNAi control, and GPR55 RNA silenced A2780/CP70 cells after 48 h; g & h represents negative RNAi control, and GPR55 RNA silenced A2780/CP70 cells after 72 h.

As shown in **Figure 6-8**, there were no morphological differences observed in A2780 cells. In A2780/CP70 cells, GPR55 RNA silenced cells looked slightly larger (**Figure 6-8 f**) compared to negative siRNA control cells (**Figure 6-8 e**). No significant difference in growth rate (the confluence of the cells in a flask) between the cells transfected with GPR55 siRNA and negative control cells was observed in both the ovarian cancer cells.

Further investigation was carried out to determine the efficiency of the transfection. Western blot analysis was used to quantify the expression levels of GPR55 protein in transfected cells.

6.2.5 Analysis of GPR55 RNA silencing by western blot

Western blot analysis was carried out for the transfected cells to determine the GPR55 expression levels as described in section 2.12 .

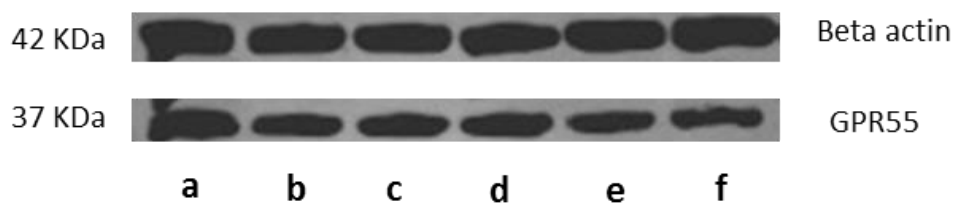


Figure 6-9. **Western blot analysis of GPR55 transfection.** Comparison of GPR55 protein expression GPR55 siRNA transfected samples to the controls. a & b represents the negative control and GPR55 siRNA samples of A2780 cells after 48 h; c & d represents the negative control and GPR55 siRNA samples of A2780 cells after 72 h; e & f represents the negative control and GPR55 siRNA samples of A2780/CP70 cells after 72 h.

As shown in **Figure 6-9**, the western blot results did not show the reduction of GPR55 in transfection samples. This could be due to low or no knockdown at mRNA levels Of

GPR55receptor. The stability or longer half-life of the GPR55 receptor in the cells, and the nonspecific binding of the GPR55 antibody could be other possibilities.

So further experiments were carried out to investigate the levels of target mRNA knockdown by the siRNA transfection of the GPR55 receptor. Based on the literature, HCT116 p53^{+/+} cells were used as positive control for transfection, and preliminary experiments were carried out on A2780 cells.

6.2.6 Analysis of GpR55 RNAi-mediated silencing in A2780 cells by qPCR

A2780 and HCT116 cells were transfected with Negative Control siRNA and GpR55 siRNA as described in section 2.13. The HCT116 cells were incubated for 48 h and 72 h time points following transfection whereas A2780 cells were incubated for 72 h. After incubation time elapsed, cells were harvested, and total mRNA was extracted as described in section 2.14.

Total mRNAs collected from samples were reverse transcribed, and qPCR was carried out as described in section 2.15& 2.16.

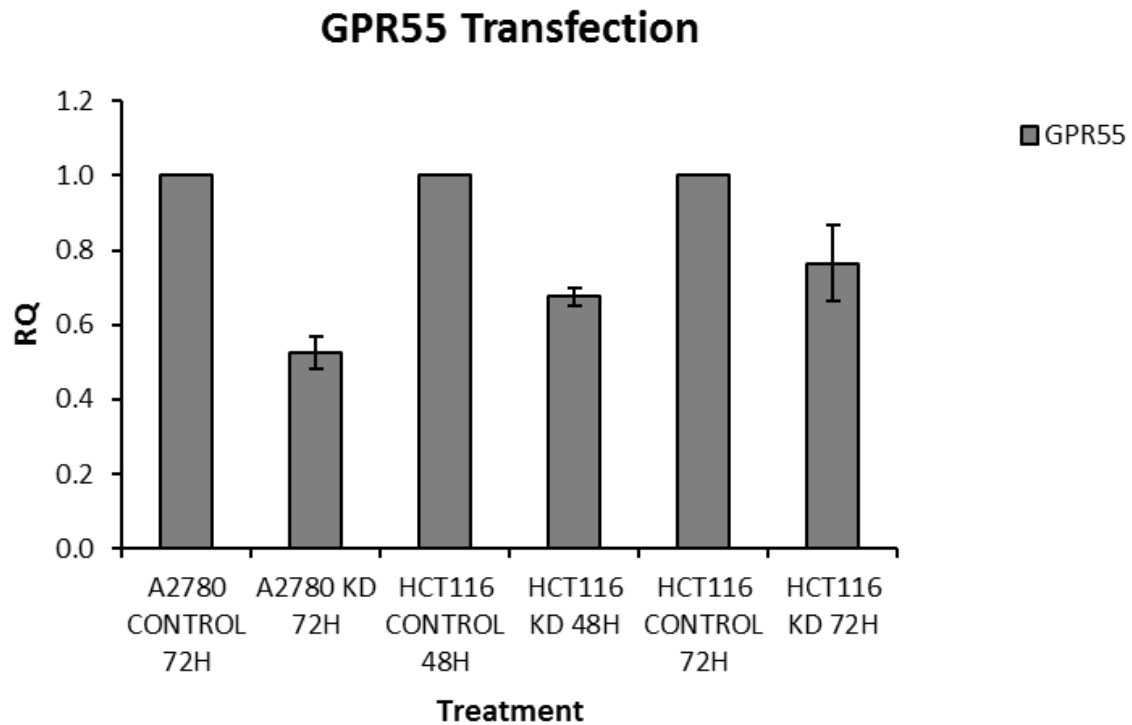


Figure 6-10. *Relative quantification of siRNA knockdown by qPCR. The levels of GPR55Mrna in GPR55 siRNA knockdown and negative siRNA knockdown A2780 cells and HCT116 cells were analysed by qPCR. (KD refers to GPR55 Knockdown samples).*

As shown in **Figure 6-10**, quantitative PCR results indicated the reduction in GPR55 levels in the siRNA transfected cells. After 72 h, The RQ values of A2780 GPR55 knockdown cells were 0.53 ± 0.04 , and the RQ values HCT116 p53++ GPR55 knockdown cells after 48 h and 72 h were 0.67 ± 0.02 and 0.76 ± 0.10 respectively.

Based on the results (Figure 6-10) indicating modest GPR55 mRNA knockdown by approximately 50%. Further experiments were carried out to determine the cytotoxicity effects of CBD and CBG in A2780 GpR55 knockdown cells although due to time constraints it has not been possible to validate reduction in GpR55 protein expression. It is possible that the ~50% reduction in GPR55 mRNA at 72h is not sufficient to cause a decrease in GPR55

protein as suggested by immunoblot analysis (Fig. 6-7). However, GPR55 antibody has also not validated with GPR55 wild type and knockout protein samples extracted from healthy ileum of mice. The results showed non-specific binding of GPR55 antibody in both wild and knockout samples (see appendix)

6.2.7 Evaluation of CBD and CBG cytotoxicity in GPR55 silenced A2780 cells.

A2780 cells were transfected with GPR55 siRNA, and negative silencer RNA, and incubated for 48 h. After incubation time elapsed, 15 μ M CBD or 15 μ M CBG was added to GPR55 siRNA transfected cells, and control cells. The cells were further incubated for 24 h. After incubation time elapsed, Annexin V assay was performed as described in section 2.7.

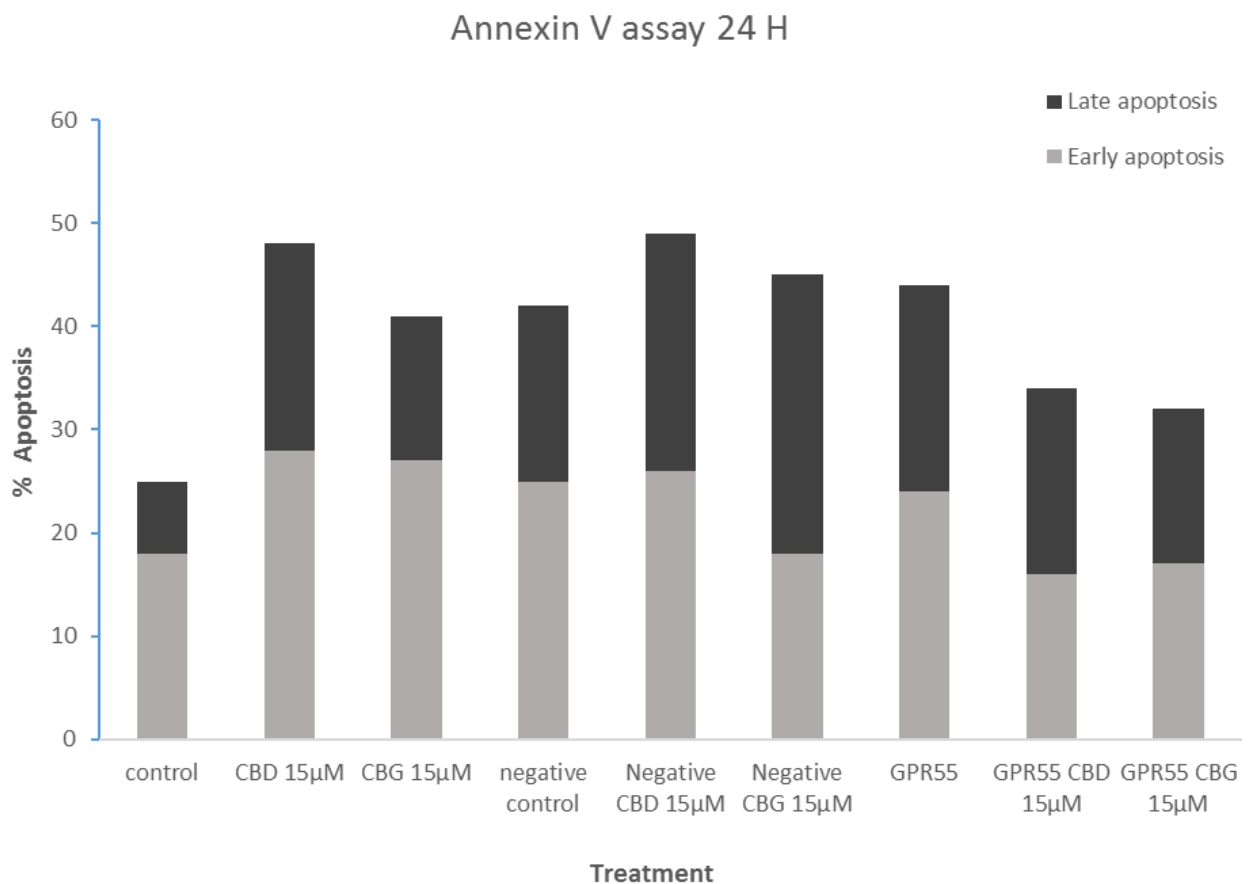


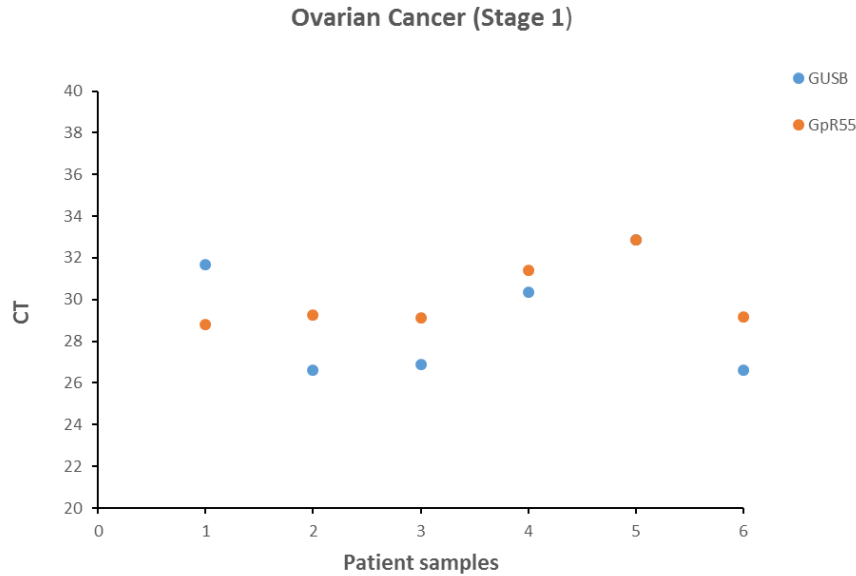
Figure 6-11. CBD/ CBG cytotoxicity on GPR55 KD A2780 cells. Comparison of percentage of apoptotic cells in A2780 normal cells, negative siRNA silenced A2780 cells, and GPR55 siRNA A2780 cells, when cells were treated with 15 μ M of CBG or CBD for 24 h.

As shown in **Figure 6-11**, the total percentage of apoptotic cell in GPR55 KD A2780 cells with when treated with 15 μ M CBD (34%) was lower than normal A2780 cells treated with 15 μ M CBD (48%), and negative siRNA transfected cells treated with 15 μ M CBD (49%). Similar to CBD, GPR55 KD A2780 cells, when treated with CBG, has shown the lower percentage of apoptotic cells (32%) compared to CBG cytotoxicity on both normal A2780 treated cells (41%), and negative siRNA transfected cells (45%). The preliminary results suggest that both CBD and CBG cytotoxicity is compromised in the absence of GPR55, which is also consistent with the rescue of CBD cytotoxicity with GPR55 antagonist. However, the experiment was carried out only once. More biological repetitions, optimisation of GPR55 transfection incubation time, and using another independent siRNA would help to understand the affinity of the cannabinoids in the cytotoxic effects on the ovarian cancer cells.

In parallel to this study, the expression of GPR55 in different ovarian cancer patients was quantified.

6.2.8 GPR55 messenger RNA expression levels in ovarian cancer patients

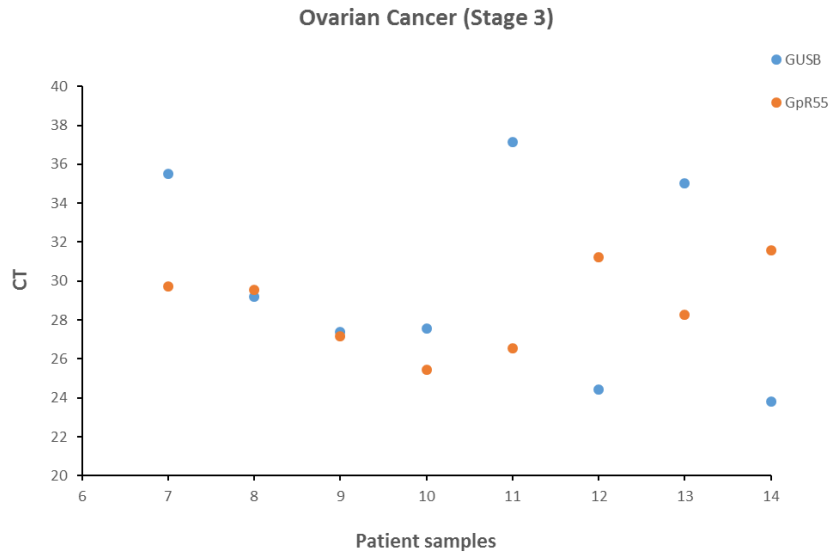
Dr Sandra Bell, a collaborator from the Leeds institute of medical and clinical sciences (LIBACS), UK has kindly provided RNA samples extracted from tissues or ascites of patients with ovarian cancer of different stages and grades. RNA samples were reverse transcribed, and the GpR55 expression levels were quantified by real-time PCR (Figure 6-12)



NO	Stage	Grade	Histology	GUSB (CT)	GPR55 (CT)	Δ CT
1	1a	Null	Granulosa	31.69	28.81± 0.07	-2.88
2	1c	High	Clear cell	26.60	29.23± 0.09	2.63
3	1c	High	Clear cell	26.60	29.15± 0.09	2.55
4	1c	High	Endometria	30.34	31.41± 0.03	1.07
5	1a	Null	Mucinous	32.86	32.88± 0.06	0.02
6	1c	High	Clear cell	26.87	29.10± 0.05	2.27

Figure 6-12 **Expression of GPR55 in stage 1 ovarian carcinoma histotypes.** The expression levels of GPR55 compared to GUSB in different histological types of stage 1 ovarian cancer. Scatter plot shows the CT values of GPR55 and GUSB in each sample (top), detailed information of patients mentioned in the table (below).

As shown in **Figure 6-12**, GPR55 was expressed in all stage 1 ovarian cancers tested. Among the histotypes, Granulosa carcinoma express higher levels of GPR55 (Δ CT -2.88) followed by mucinous (Δ CT 0.02) and endometrial cancers (2.27) compared to GUSB. The samples extracted from 3 patients diagnosed with 1c clear cell carcinoma expressed GPR55 with Δ CT values 2.63, 2.55 and 2.27.



NO	Stage	Grade	Histology	GUSB (CT)	GPR55 (CT)	Δ CT
7	3c	Low	Serous	35.50	29.72± 0.09	-5.78
8	3c	High	Serous	29.20	29.55± 0.03	0.35
9	3c	High	Serous	27.38	27.15± 0.10	-0.23
10	3c	Null	Adenocarcinoma	27.54	25.44± 0.10	-2.10
11	3c	Null	Adenocarcinoma	37.16	26.55± 0.02	-10.61
12	3c	High	Serous	24.41	31.21± 0.17	6.8
13	3c	High	Serous	35.03	28.27± 0.18	-6.76
14	3c	High	Carcinoma	23.82	31.58± 0.12	7.76

Figure 6-13 *Expression of GPR55 in stage 3 ovarian carcinoma histotypes.* The expression levels of GPR55 compared to GUSB in different histological types of stage 3 ovarian cancer. Scatter plot shows the CT values of GPR55 and GUSB in each sample (top), detailed information of patients mentioned in the table (below).

As shown **Figure 6-13**, GPR55 gene was expressed in all stage 3 ovarian cancer patient samples analysed. CT values ranged from 25.44 cycles to 31.58 indicating substantial heterogeneity in levels of GPR55 expression. For the stage 1 ovarian cancer samples, CT values varied less, however, levels of GUSB expression as the housekeeper gene chosen were also more variable for the stage 3 samples. Most of the stage 3 ovarian cancer samples tested showed a lower

CT for GpR55 than for GUSB whereas this was not the case for the stage 1 samples suggesting higher expression of the receptor in the advanced stages. However, heterogeneity in GUSB expression also indicates the necessity of another housekeeping gene. Among the patient samples tested, the adenocarcinomas showed amongst the highest levels of GpR55 with Δ CTs of -10.61 and -2.1 (patient samples 11 & 10). A single low-grade serous ovarian cancer sample analysed showed a Δ CT value of -5.78 whereas the samples acquired from 3 different patients with high grade serous cancer showed much more variable levels of the receptor gene expression with Δ CT values of -6.76, 0.35 and 6.8. Along with the ovarian tumour samples, a non-cancerous ovarian benign sample was also tested however; the tissue sample (50 ng input cDNA) did not express detectable GUSB mRNA up to 40 amplification cycles. Therefore, the sample was further analysed with another housekeeping gene, GAPDH. The ovarian benign tumour sample expressed GpR55 (CT 31.07 ± 0.04) and GAPDH (CT 35.86) with Δ CT -4.79. However, it was not possible to normalise GPR55 mRNA expression in ovarian tumour samples against the non-tumour sample as unexpectedly none of the carcinoma samples expressed GAPDH on analysis (50 ng input cDNA, 40 cycles).

The preliminary analysis has shown the high-level expression of GPR55 in the ovarian tumour samples. Hence, for future studies, it would be ideal to continue further investigation to determine the role of GpR55 in CBD and CBG induced cytotoxicity in ovarian cancer.

Preliminary experiments were also carried out using receptor antagonists to investigate the involvement of CB1, and CB2 receptors in CBD and CBG cytotoxicity in ovarian cancer cells.

6.2.9 Investigation of the involvement of CB1 receptor in CBD/CBG induced cytotoxicity.

The selectivity of CB1 receptor in CBD or CBG induced cytotoxicity was investigated using AM251. AM251 is a selective antagonist, pre-treatment of the ovarian cancer cells with AM251 potentially block the CB1 receptors. The cytotoxicity of CBD or CBG on A2780 and A2780/CP70 in the presence of AM251 was tested to determine the involvement of CB1 receptors.

The cytotoxicity of AM251 alone on the ovarian cancer cells were tested by MTT assay (as described in **section 2.4**), and the results were summarised below

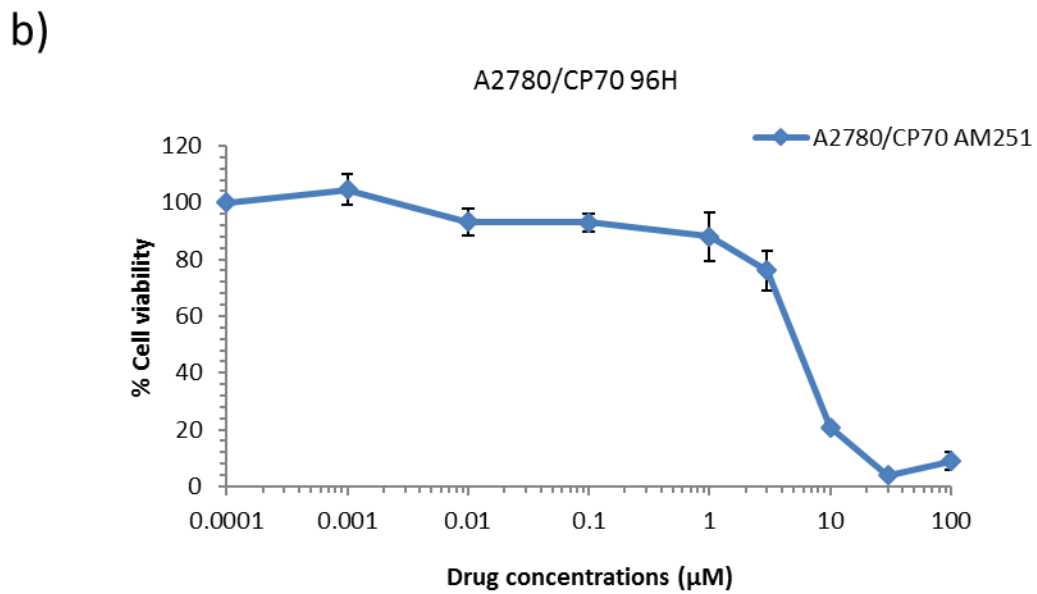
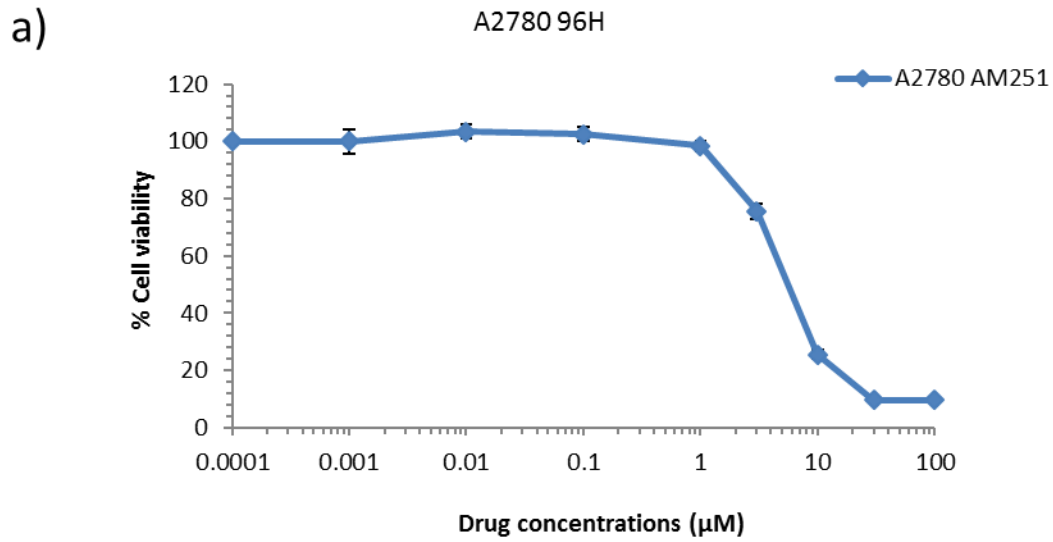
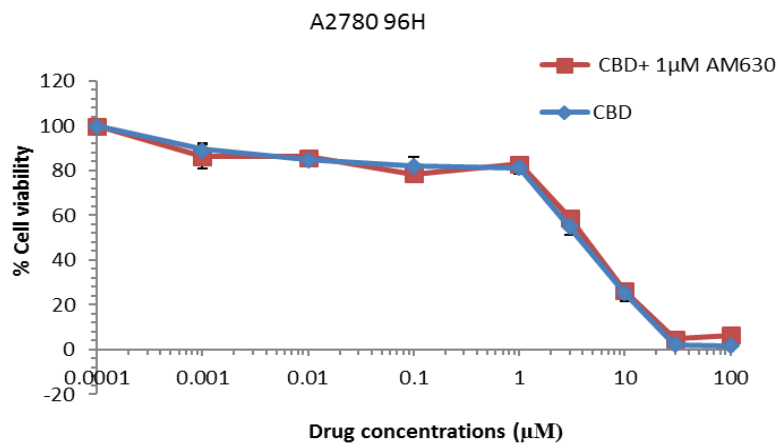


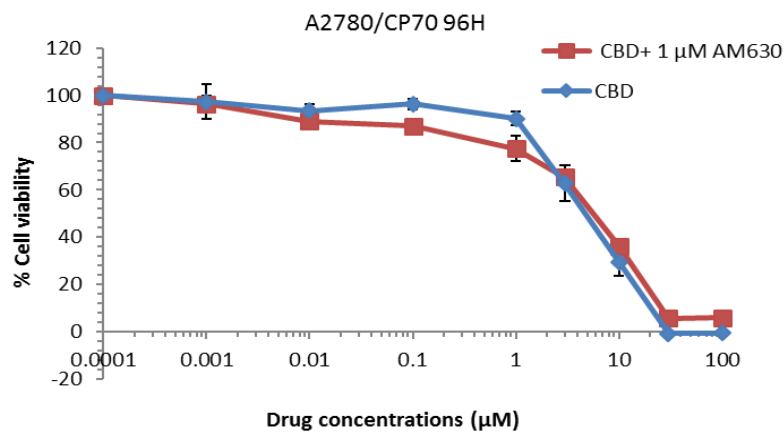
Figure 6-14. **Cytotoxicity of AM251 on A2780 and A2780/CP70 cells.** The dose-response effects of AM251 on A2780 (a) and A2780/CP70 (b) after 96 h exposure. It represents the mean \pm standard error of mean of $n=3$, n represents the number of biological experiments

As shown in **Figure 6-14**, 1 μM of AM251 indicated sub-lethal effects on both A2780 and A2780/CP70 with viability $98 \pm 1.5\%$ and $97 \pm 7\%$ respectively. 1 μM of AM251 was used as working antagonist concentration for further experiments (Jiang et al., 2007)

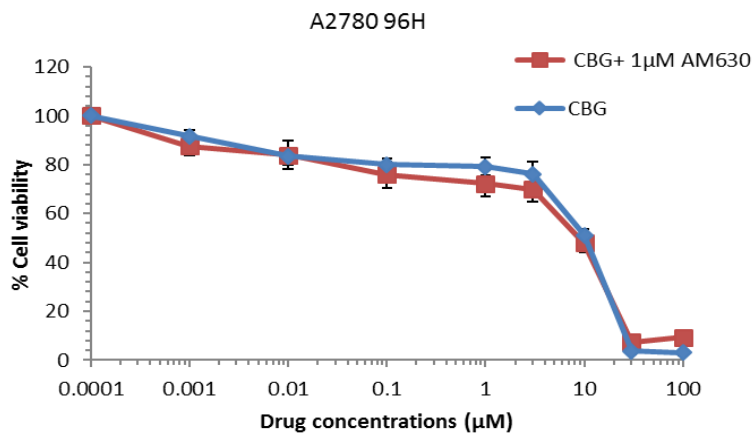
a)



b)



c)



d)

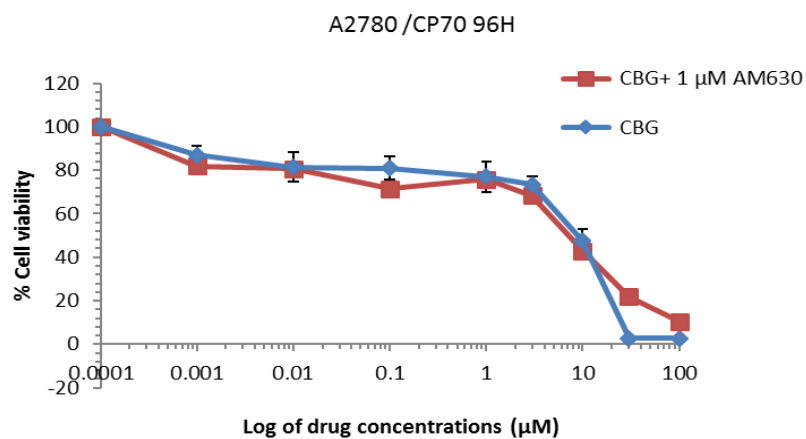


Figure 6-15. Cytotoxicity of CBD or CBG in the presence of CB1 antagonist. The comparison of the dose-response effects CBD or CBG alone, and CBD/ CBG in combination with 1 μ M of AM251 on A2780 (a&c) and A2780/CP70 (b&d) after 96 h exposure. 1% ethanol was used as a solvent control for CBD alone whereas 1 μ M of AM251 was used as a control for the combination. It represents the mean \pm standard error of mean of N=3, N represents the number of experiments.

As shown in **Figure 6-15**, No significance difference was observed in the A2780 cells in the dose- response to CBD, and CBG in the presence or absence of CB1 antagonist AM251. The IC₅₀ values achieved for CBD or CBG in combination with AM251 were similar to the IC₅₀ values achieved of CBD or CBG alone on A2780 cells. However, a significant difference (P< 0.01) was observed in the IC₅₀ value of CBG when combined with AM251 ($13.35 \pm 0.77 \mu\text{M}$) compared to CBG alone ($7.12 \pm 1.17 \mu\text{M}$) in A2780/CP70 cells suggest the possibility of CB1 involvement in CBG cytotoxicity on A2780/ CP70 cells. .

6.2.10 Investigation of the involvement of CB2 receptor in CBD or CBG induced cytotoxicity.

The selectivity of the CB2 receptor in CBD or CBG induced cytotoxicity was investigated using AM630. AM630 is a selective antagonist for the CB2 receptor, pre-treatment of the ovarian cancer cells with AM630 can potentially block the receptor for CBD or CBG. The cytotoxicity

of CBD or CBG on A2780 and A2780/CP70 in the presence of AM630 was tested to determine the involvement of CB2 receptors.

Similar experiments were carried out to cytotoxicity of AM630 alone on the ovarian cancer cells were tested by MTT assay (as described in section 2.4), and the results were summarised below.

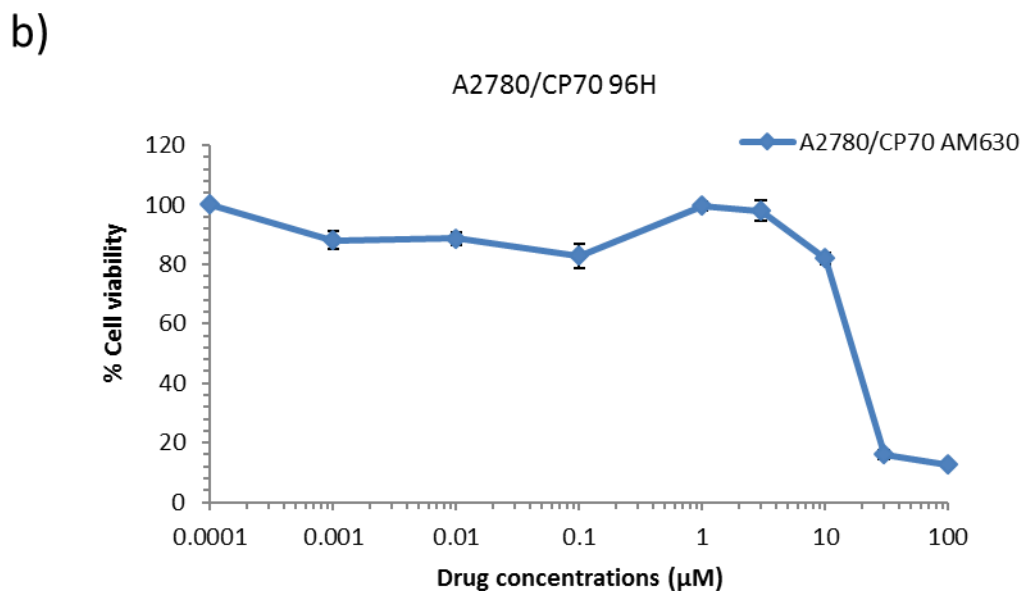
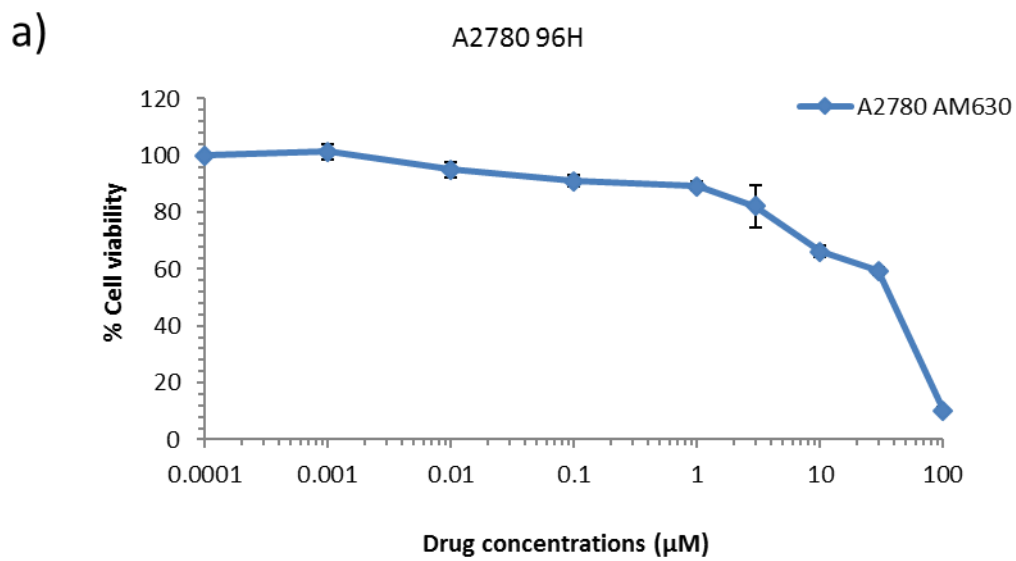
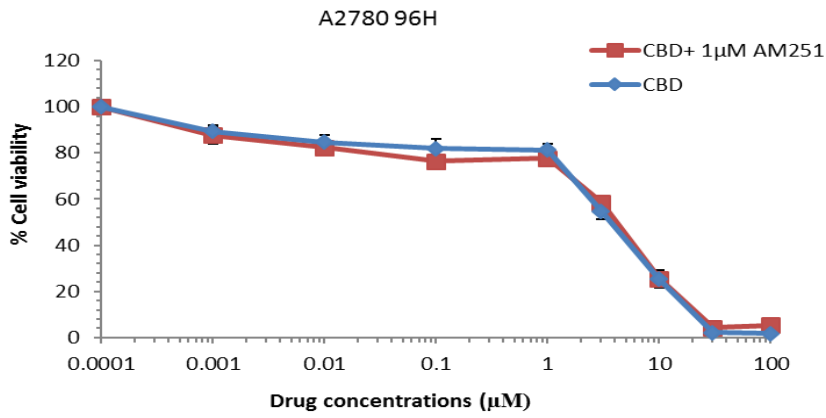


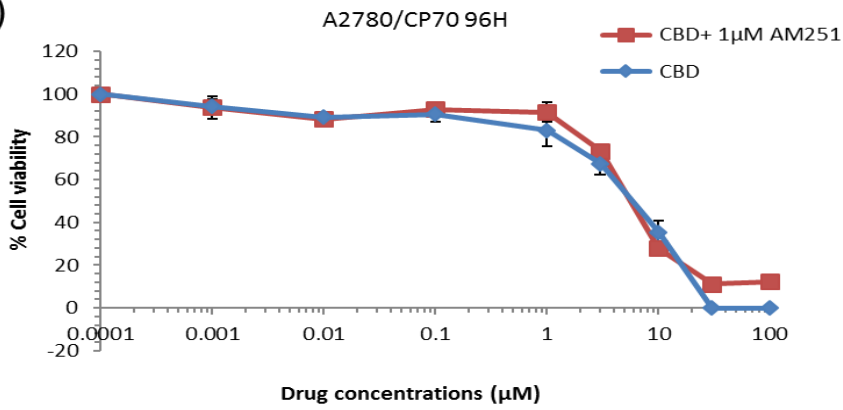
Figure 6-16. Cytotoxicity of AM630 on A2780 and A2780/CP70 cells. The dose-response effects of AM630 on A2780 (a) and A2780/CP70 (b) after 96 h exposure. It represents the mean \pm standard error of mean of $n=3$, n represents the number of experiments

As described in section 6.2.8, the cytotoxicity of CBD or CBG on A2780 and A2780/CP70 in the presence of 1 μ M of CB2 antagonist AM630 (Jiang et al., 2007). The results were summarised as below **Figure 6-16**.

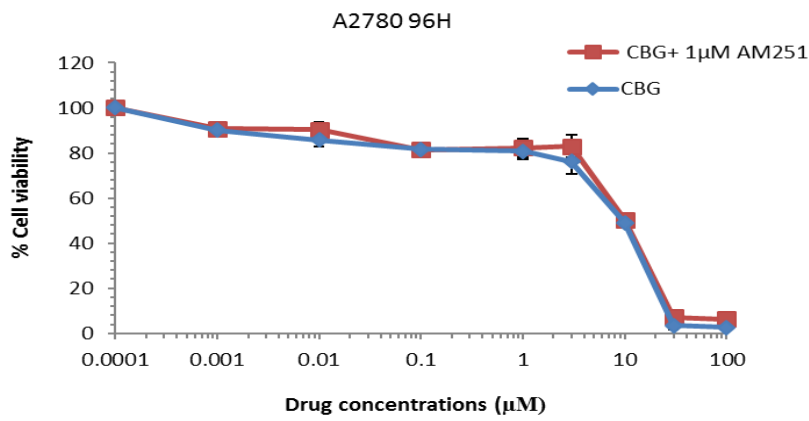
a)



b)



c)



d)

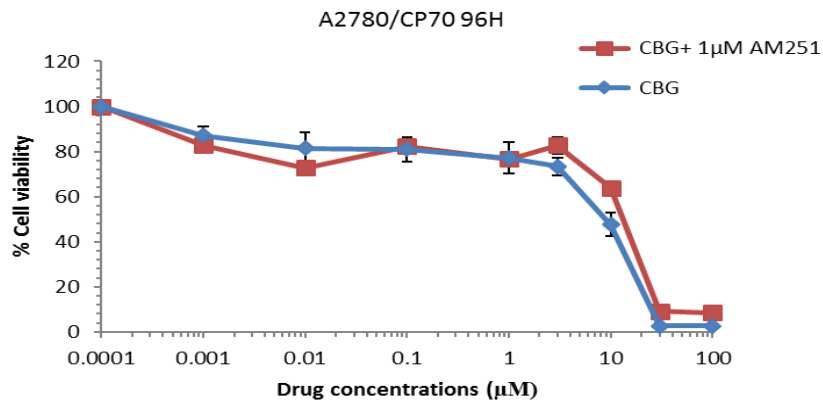


Figure 6-17. Cytotoxicity of CBD or CBG in the presence of CB2 antagonist. The comparison of the dose-response effects CBD or CBG alone, and CBD/ CBG in combination with 1 μ M of AM630 on A2780 and A2780/CP70 after 96 h exposure. 1% ethanol was used as a solvent control for CBD alone whereas 1 μ M of AM630 was used as a control for the combination. It represents the mean \pm standard error of mean of n=3, n represents the number of biological experiments.

As shown in **Figure 6-17**, no significant difference in the dose-responses of the cannabinoids in the presence of CB2 antagonist was observed. The IC50 values achieved by CBD or CBG in combination with AM251 were similar to the IC50 values achieved CBD or CBG alone on both the A2780 and A2780/CP70 cells. This suggests that in contrast to the preliminary data for GpR55 (both the cell lines) and CB1 (A2780/CP70 cells), cytotoxicity of CBD or CBG may not be affected by CB2 receptor status.

6.3 Discussion

The purpose of this chapter was to carry out initial investigations as to whether the cannabinoid receptors CB1, CB2 or GPR55 might be involved in mediating any of the observed cytotoxic effects of CBD or CBG. Several complementary approaches were taken including use of selective antagonists and RNAi-mediated receptor knockdown.

CID16020046 is a reported selective antagonist for GPR55, shown to have antagonist properties towards GPR55 at concentrations from 40 nM to 20 μ M (AlSuleimani and Hiley, 2015, Hofmann et al., 2015b). Chemo sensitivity data showed that pre-treatment of the human ovarian cancer cells with 1 μ M CID16020046 increased the IC₅₀ values of CBD and CBG in the A2780 and A2780/CP70 ovarian cancer cells although effects were small and in the case of CBD were not significant. Using a higher concentrations of antagonist in a different experiment assaying levels of apoptosis, the GPR55 antagonist at 10 μ M completely rescued apoptosis in the A2780 cells (61%) induced by 10 μ M CBD to (17%) apoptotic cells. Overall, this data suggests that the GPR55 receptor promotes or at least partially mediates some of the observed cytotoxicity of CBD and CBG. However, as selective antagonism of the GPR55 receptor at the doses used has not been demonstrated here and similarly a reduction in GpR55 protein through RNAi mediated silencing had not been shown these results must be considered with caution and unconfirmed.

The results (6.2.5) indicated modest GPR55 mRNA knockdown by approximately 50% in A2780 cells, which is consistent with published results where Kargl et al studies were able to achieve similar knockdown results in HCT116 cells (Kargl et al., 2016). However, this modest knockdown was not enough to see the difference in protein expression levels but due to time constraints, the cytotoxic effects of CBD and CBG analysed with the modest GPR55

knockdown cells. The results were shown both CBD and CBG cytotoxicity was inhibited in the GPR55 knockdown A2780 cells suggesting possibility of GPR55 involvement.

The results (6.2.8) was shown that GPR55 upregulated in stage 1 and Stage 3 ovarian cancer patients. In stage 3 cancer patients, Gpr55 CT values ranged from 25.44 cycles to 31.58 indicating substantial heterogeneity in levels of GPR55 expression. For the stage, 1 ovarian cancer samples were less varied compared to stage 3 cancer patients. Despite that fact that GUSB was reported as the stable reference gene, and consistent in both normal and malignant ovarian samples with CT values 26.7 ± 0.7 (Lv et al., 2017), GUSB was highly varied among stage 3 cancer patients. These results (6.2.8) indicate that GPR55 is clinically relevant as a potential target for ovarian cancer.

At 1 μM concentration, AM251 and AM630 have been previously reported to have selective antagonistic effects on CB1 and CB2 receptors respectively (Jiang et al., 2007). The chemosensitivity results generated here show that in the presence of 1 μM AM251, the IC_{50} values of CBG in A2780/CP70 Cells increases. This suggests that CBG cytotoxicity on A2780/CP70 cells is partly mediated via CB1. However, knockdown experiments to support this data have not yet been performed. In contrast, there was no difference in cytotoxic effects of CBD and CBG in the presence of AM630 suggesting that their cytotoxic effects are not mediated via CB2 receptors in these ovarian cancer cells. This correlates with reports that anti-cancer properties of CBD are reported to be independent of CB2 receptors (Dariš et al., 2018)

Expression of the cannabinoid receptors in the ovarian cancer cells was also assessed under conditions of hypoxia, as there is a critical need for new therapeutic approaches to target the hypoxic fraction of tumours.

Hypoxia generated in the context of tumour microenvironment associated with induction of angiogenesis, alterations in metabolism and increased tumour metastasis. Over 60% of advanced tumours exhibit a hypoxia environment. The hypoxic environment reduces cell growth rate and can cause cells to enter a quiescent state, which increases tumours resistance to chemotherapy. The high rate resistance to chemotherapy by hypoxic tumours indicate the importance of understanding the alteration of molecular targets in hypoxic environment for new therapy strategies (Muz et al., 2015, Favaro et al., 2011). Cannabinoid receptors are known for heterogeneity, and their expression levels are highly dependent on cancer histology and hormonal response (Dariš et al., 2018). Cannabinoid receptors CB1 and CB2 are reported to over express in ovarian cancer cells and *in vitro* studies showed that the activity of CB1 and CB2 were involved in proliferation of OVCAR-3 and SKOV- 3 ovarian cancer cells (Afaq et al., 2006b). GPR55 receptor was also shown to mediate proliferative effects in ovarian cancer cells (Pineiro et al., 2011). Preliminary results showed (6.2.1) that cannabinoid receptors CB1, CB2 and GPR55 were over expressed in A2780 cells and A2780/CP70 cells under hypoxic conditions at the mRNA level in A2780 cells and A2780/CP70 cells under hypoxic conditions compared to normoxia. Whilst this suggests potential increased dependency on the cannabinoid receptors under these conditions, it remains to be demonstrated that these reporters are upregulated at the protein level and the functional significance of any upregulation. In glioblastoma cells, down regulation of CB1 receptor was reported under hypoxic conditions suggesting the differences in expression of cannabinoid receptors under hypoxia versus normoxia between different cancers (Sugimoto et al., 2017, Dariš et al., 2018).

CHAPTER 7 General Discussion & Future Work

The significant side effects of established chemotherapeutic drugs and the high rate of cancer reoccurrence within short period of treatment indicate the importance of new approaches for the treatment of ovarian cancer (Mangal et al., 2013, Gubbels et al., 2010). The cannabinoids CBD and CBG have been to have no psychoactive side effects in comparison to psychotropic cannabinoids, whilst also showing promising potential activity against many diseases including cancer (Izzo et al, 2009).

7.1 Potency and selectivity of CBD versus CBG towards human ovarian cancer cells

Both CBD and CBG had demonstrated the dose-dependent and time dependant micromolar cytotoxic effects on ovarian cancer cells. CBD and CBG induced cytotoxicity on the ovarian cancer cells at a similar pharmacological concentration compared to the cytotoxicity exerted by them in breast and prostate cancer cells (Izzo et al., 2009, Ligresti et al., 2006). After 96 h, the IC₅₀ values of CBG in the ovarian cancer cells A2780, A2780/CP70 and OVACAR-3 cells were 1.64, 1.22, 1.33 folds higher than the IC₅₀ values of CBD. This result suggests that CBD is slightly more potent than CBG towards the ovarian cancer cells tested. The further investigation in mechanistic studies of CBD and CBG also supported the statement. The mitochondrial membrane potential assay and Annexin V assay were showed that CBD induce apoptosis at lower concentration than CBG. Besides mechanistic studies, the combination of CBG with CBD did not induce a synergistic effect. However, it showed a dose-response cytotoxicity in proportion to the increased concentration of CBD in the mixture. The IC₅₀ values of the CBD and CBG combinations were lower than IC₅₀ values of CBD alone suggest that CBD is a more potent cannabinoid than CBG in ovarian cancer cells. These results correlate with Shrivastava et al., findings where they demonstrated that CBD has higher potency than CBG in breast cancer cells (Shrivastava et al., 2011).

CBD and CBG showed cancer selective toxicity towards ovarian cancer cells A2780/CP70, and A2780/CP70 compared to non- cancer cells PNT2 and ARPE19. The cancer selective cytotoxicity of CBD and CBG was supported by the mechanistic studies of CBD and CBG on the ovarian cancer cells, and non-cancer ARPE19 cells. The Annexin V staining for apoptotic cells demonstrated that both CBD and CBG induced significantly lower percentage of apoptosis in ARPE19 cells compared to the ovarian cancer cells. The increase in ROS levels also suggested the selective induction of ROS by CBD and CBG in the ovarian cancer cells but not in non-cancer PNT2 cells suggesting CBD and CBG induced selective cytotoxicity towards ovarian cancer cells. This could be due to the selective induction of oxidative stress by the cannabinoids. In support of casual role of ROS production in the selective cytotoxicity, the anti-oxidant, α -tocopherol was able to rescue CBD induced cytotoxicity in the ovarian cancer cells.

Both CBD and CBG were reported to inhibit oxidative stress in as a part of neuroprotective mechanism, whilst simultaneously inducing apoptosis by ROS production in various cancers. The multiple mechanism of actions of the cannabinoid among different cells could be another reason for the selective cytotoxicity of CBD and CBG (Humphrey et al., 2011, Marsicano et al., 2002, Gugliandolo et al., 2018, Dariš et al., 2018).

One of the limitations of this work is that CBD and CBG have been screened against limited number of ovarian cancer cells. Whilst CBD and CBG encouragingly showed similar activity towards the A2780/CP70 cisplatin resistant line compared to the parental A2780 cell line indicating cross-resistance is not a problem however, the cannabinoids were less active towards OVCAR-3. This may relate to the genetic alterations in OVCAR3 compared to A2780 and A2780/CP70. For example OVCAR-3 express mutant p53 whilst A2780 cells does not have

p53 mutations. However, the effects of CBD and CBG cytotoxicity in relation to the genetic variations in ovarian cancer has not been addressed (Hernandez et al., 2016). Another limitation is that the non-cancer cells are not tissue- matched, nevertheless the results provided some indication of selectivity prior to any possible progression towards *in vivo* studies.

7.2 The combination of CBD or CBG with chemotherapeutic drugs

The ovarian cancer associated with a diversity of mutations and histological types, it is difficult to get the desired therapeutic effect with a single drug (Natarajan et al., 2018, Kashif et al., 2015, Humphrey et al., 2011). The preclinical studies have shown that cannabinoids increased cytotoxic effect of existing chemotherapeutic drugs when used in combination (Velasco et al., 2012). Cannabinoids combination effects are widely tested in glioma cells. CBD in combination with THC induced shown anti- cancer activity glioma cells (Nabissi et al., 2016). CBD was also shown synergistic with bortezomib, a protease inhibitor on multiple myeloma cells (Morelli et al., 2014). Torres et al were shown that submaximal dose of THC (15mg/kg/d) in combination with temozolamide (5mg/kg/d) induce synergic effect on glioma xenografts (Torres et al., 2011).

Carboplatin and paclitaxel (Taxol) are both currently used as clinical agents in ovarian cancer therapy. CBD was shown additive to synergistic effects in combination with Taxol in LN 231 and 4T1 breast cancer cells (Ward et al., 2014). However, the combination of CBD with carboplatin and CBG with carboplatin or Taxol has not been tested on any cancer cells.

CBD and CBG was shown to increase the efficacy of both carboplatin and Taxol on the ovarian cancer cells. CBD demonstrated better synergistic effects with both carboplatin and Taxol on A2780 cells compared to cisplatin resistant A2780/CP70 cells whereas CBG was shown to have

better combination effects on the cisplatin resistant cells compared to the cisplatin sensitive cells (chapter 4). It is currently unclear as to the reasons of these differences in synergy but it indicates that CBD and CBG are acting differently, and the response will be different for different ovarian cancer cells.

The increase in efficacy of the chemotherapeutic drugs on the ovarian cancer cells could be due to the inhibition effects of the cannabinoids on ABCC1 receptor. Holland et al., demonstrated that plant cannabinoids inhibits ABCC1 in ovarian cancer cells, amongst the compounds tested CBD has shown the highest inhibition effects. ABCC1 is a multi-drug resistance transportation receptor (MRP1), which involves in efflux of anti-cancer drugs in phase II metabolism (Holland et al., 2008). By inhibiting ABCC1 receptor, cannabinoids could have possibly blocked the efflux of carboplatin or paclitaxel, which contributes their efficacy on the ovarian cancer cells. However, this could be determined by directly measuring intracellular levels of carboplatin and paclitaxel when combined with CBD or CBG by mass spectrometry. Evaluating the combination effects of CBD or CBD with the clinical agents by inhibiting ABCC1 receptors in ovarian cancer cells would be another approach.

Both CBD and CBG indicated synergistic effects when combined with carboplatin. This could be due to multiple mechanisms of action. As it was shown that the combination of drugs that exert different or non-overlapping mechanism of actions could improve the therapeutic effect (Kashif et al., 2015). The drug washout experiments (chapter 3) were shown that the cannabinoids and carboplatin showed the difference in cytotoxicity effects when compared to the conventional MTT assay also indicates the possibility of multiple mechanisms involved.

7.3 CBD and CBG mechanisms of action in ovarian cancer cells

Pre-clinical studies (*in vitro* and *in vivo*) were shown that the anti- cancer mechanism of cannabinoids are largely varied among the cancer types, and the effect was highly dependent on dose and the cancer type (Dariš et al., 2018). Having observed activity of CBD and CBG against the human ovarian cancer cells tested, some mode of action studies were conducted. Differential effects on cell cycle, cell death by apoptosis, and cellular proteins involved in stress apoptotic signalling were found.

The cell cycle analysis of the ovarian cancer treated with CBD was shown the possibility of G1 growth arrest at 48 h. The increase in levels of phosphorylated chk 2 (thr68) and p53 (ser15) with CBD treatment also indicates that CBD might induce G1 cell cycle arrest in the ovarian cancer cells by activating chk1 which further phosphorylates p53 at ser15 (Zhao et al., 2008). The activation of phosphorylated p53 at ser15 could be also related to the apoptotic mechanism of CBD on the ovarian cancer cells, as many studies shown that anti- cancer drugs such as irinotecan (Topoisomerase 1 inhibitor) induced apoptosis in hepatocellular carcinoma by activating p53 (ser15) (Takeba et al., 2007). The above results correlates with the G1 growth arrest induced by CBD in breast cancer cells (Ligresti et al., 2006)

The cell cycle analysis of the ovarian cancer cells treated with CBG shown different results to CBD. CBG was shown to induce cell cycle arrest in S phase in A2780 cells and partial growth arrest at S phase and G2/M phase in cisplatin resistant A2780/CP70 cells. The increased in the expression levels of phosphorylated Chk1 (Ser 345) indicates that CBG could induce chk1 mediated G2/M phase cell cycle arrest in ovarian cancer cells (Leung-Pineda et al., 2006). It must be noted, however, that the protein expression changes indicated by protein array analysis here not yet been independently confirmed. For example, Immunoblot analysis of

the individual proteins would help to understand the expression of above proteins in CBD or CBG treated ovarian cancer cells. As mentioned earlier (**section 5.3**), other assays like FACS with BrdU labelling also required to confirm the apparent suggested cell cycle effects.

The anti- cancer activity of CBD and CBG mediated by apoptosis was reported in various cancers. *In vitro* studies reported the induction apoptosis by CBD in breast, prostate, glioma and colon cancers whereas CBG induced apoptosis was observed in prostate and colon cancers (Dariš et al., 2018, Borrelli et al., 2014, Caffarel et al., 2012)

Mitochondria can play an important role in the apoptosis of a cell. Depolarisation of mitochondrial membrane potential will lead to mitochondrial dysfunction and release of apoptotic molecules cytochrome c and smac/DIA- BLO into the cytoplasm, which leads to caspase- dependent apoptosis. Shrivastava et al were able to shown that CBD induced mitochondrial membrane permeability based apoptosis in breast cancer cells. (Shrivastava et al., 2011). The mitochondrial membrane potential assay demonstrated that both CBD and CBG showed the depolarisation of mitochondrial membrane potential in both the A2780, A2780/CP70 ovarian cancer cells after 24 h exposure. The Annexin V assay also demonstrated similar results to mitochondrial membrane assay confirms the involvement of apoptosis in CBD and CBG induced cytotoxicity in the ovarian cancer cells.

The quantification of caspase 3/7 enzyme activity in the ovarian cancer cells with increased concentrations of CBD and CBG demonstrated the involvement of caspases in apoptosis. The increase in the levels of cleaved caspases 3& 7, using ELISA technique demonstrated the similar results; the increase in the levels of cleaved PARP (Ser214) is also an indication of caspase activity (Nicholson et al., 1995, Lazebnik et al., 1994). These results are correlated with caspase-dependent cytotoxicity mechanism of CBD and CBG on prostate cancer cells.

Besides prostate cancer cells, CBD was also shown caspase-dependant apoptosis mechanism in breast and leukaemia cells (Izzo et al., 2009, Dariš et al., 2018, Shrivastava et al., 2011).

Mitochondrial dysfunction is one of the main reasons in production reactive oxygen species. Massi et al were the first group who suggested CBD induces production of ROS in glioma cells in 2006 (Massi et al., 2006). McAllister et al were able to show same results in MDA-MB- 231 breast cancer cells. (McAllister et al., 2011). Borelli et al estimated the ROS production by CBG using 2',7'-dichlorodihydrofluorescein diacetate reagent in colon cancer cells. In my study, 2',7'-dichlorodihydrofluorescein diacetate assay showed that both CBD and CBG induced the ROS production in the ovarian cancer cells. HSP27 is a small heat shock protein, known to promote neuronal survival. *In vitro* studies were shown that HSP27 regulates apoptosis induced by oxidative stress through Akt activation (Liu et al., 2007, Dokas et al., 2011). TAK 1 is an intermediate of TNF α signalling cascade, regulates mitochondrial ROS mediated apoptosis (Wang et al., 2015, Omori et al., 2008). The increased expression levels of stress related proteins HSP27 (ser 82), and TAK1 (ser 482) expression in the ovarian cancer cells treated with CBD and CBG indicate the ROS mediated apoptosis. The rescue of CBD cytotoxicity by antioxidant α - tocopherol indicate that intracellular ROS production contributes the cytotoxicity of CBD in ovarian cancer cells. These results consist with earlier studies where CBD cytotoxicity was compromised in glioma cells in the presence of α - tocopherol (Massi et al., 2013, Massi et al., 2006)

DNA damage induced by anticancer drugs also promote the phosphorylation of p53 (Ser 15). The increased levels of p53 (Ser 15) in CBD treated A2780 cells, and A2780/CP70 cells could be related to DNA damage induced by CBD. Further investigation using DNA damage conformational assays such as comet assay and H2AX assay would help to understand the

involvement of DNA damage mediated cytotoxicity of CBD (Ivashkevich et al., 2012, Collins., 2004). However, there was not enough evidence to support that CBD induces DNA damage mediated cytotoxicity in cancer cells.

7.3.1 Cannabinoid receptors in relation to CBD or CBG cytotoxicity in human ovarian cancer cells

Cannabinoid receptors are reported to be involved in the regulation of tumour progression in many cancers, and preclinical studies in various cancer types have shown that cannabinoids exerted the anti-cancer effects through cannabinoid receptors (Soderstrom et al., 2017). Afaq et al., and Pineiro et al., showed that involvement of cannabinoid receptors CB1, CB2 and GPR55 in promoting proliferation of ovarian cancer cells (Afaq et al., 2006b, Pineiro et al., 2011).

Both CBD and CBG were shown to have low affinity for CB1 and CB2 receptors. The studies have shown CBD acts as an antagonist towards the CB1, and inverse agonist towards CB2. *In vitro* studies were shown the antagonistic effects of CBD on GPR55 receptors (Dariš et al., 2018, Kosgodage et al., 2018b).

In the presence of GPR55 antagonist CID16020046, the cytotoxicity of CBD was rescued in the ovarian cancer cells. A similar profile of action was observed where the cytotoxicity of CBD was reduced in GPR55 knockdown A2780 cells. The reduction in cytotoxicity of CBG was also seen in GPR55 knockdown ovarian cancer cells. These preliminary results indicate that GPR55 might involve in the cytotoxicity of CBD and CBG in the ovarian cancer cells. *In vivo* studies showed the involvement of GPR55 in CBD cytotoxicity in pancreatic cancer cells supports the earlier statement (Ferro et al., 2018). However, due to time constraints, it has not been possible to determine the antagonistic concentration for the GPR55 receptor to validate the

effects of the cannabinoids on the ovarian cancer cells in the presence of antagonist, and the reduction in GPR55 protein expression needs to be validated.

The preliminary results suggested that the possibility of CB1 receptor involvement in CBG cytotoxicity on cisplatin-resistant A2780/CP70 cells. However, this is based solely on the use of single CB1 antagonist. Future investigation with receptor knockdown is required. The preliminary antagonistic studies showed that CBD or CBG cytotoxicity might not be affected by CB2 receptor status in the ovarian cancer cells.

The preliminary studies showed the CB1, CB2 and GPR55 in ovarian cancer cells A2780, A2780/CP70 were upregulated under hypoxia conditions whilst no changes were observed in non-cancer APE19 cells. The results showed CBD and CBG may mediate cytotoxicity via GPR55 receptors, and CB1 receptors in ovarian cancer cells. Importantly, GPR55 mRNA found to be over expressed in ovarian cancer tissue indicating a clinically relevant target for ovarian cancer therapy. However the expression of CB1, CB2 and GPR55 at protein level, and the variation in expression among different stages and grades of ovarian cancers remain to be studied.

Furthermore, cisplatin sensitive and cisplatin resistant A2780 cells showed similar expression levels of CB1 and GPR55 at mRNA level. This could be another possible reason for CBD and CBG similar activity towards cisplatin sensitive and cisplatin resistant cells besides distinctive mechanisms of action to platinum drugs. CB2 receptors were expressed more in cisplatin sensitive cells however, the preliminary results suggested the effects of CBD and CBG on human ovarian cancer cells to be independent of CB2.

The effects of CBD and CBG on the expression levels of cannabinoid receptors (CB1/CB2/GPR55) in ovarian cancer cells yet to be investigated. Future experiments should be

carried to investigate CB receptors expression levels in response to CBD or CBG treatment on OC cells. The effects CBD and CBG on serum starved OC cells to normal OC cells would help in understanding the relation between CB receptors expression levels to the anticancer effects of CBD and CBG.

7.4 Future work- Development of CBD and CBG towards clinic

CBD and CBG have shown preferential anticancer effects towards human ovarian cancer cells *in vitro*. However, one of the limitations of this work is that CBD and CBG have been screened against limited number of ovarian cancer cell lines. Future experiments should include a panel of ovarian cancer cells representing different histotypes to address the effects of CBD and CBG cytotoxicity in relation to the genetic variations and differences expression of CB receptors in ovarian cancer. Development of *In vitro* 3D cell culture models of ovarian cancer cells such as organoids would provide a more physiologically relevant model to test the effects of cannabinoids in addition to in parallel testing in *in vivo* models.

The chemo resistance nature of metastasised ovarian carcinoma is one of the main causes for its high mortality. In order to develop CBD/CBG as potential anticancer drugs it is important to determine the effects of CBD and CBG on tumour invasion and metastasis. Future experiments involving such as wound/healing assay or Transwell/ modified boyden chamber assay will determine the effects of CBD/CBG on ovarian cancer cell metastasis (Pouliot et al., 2013)

This study was mainly focused on the effects of the cannabinoids on ovarian cancer, *in vitro*. However in order to develop CBD/CBG towards clinical trials, *In vivo* studies are essential. *In vivo* models enable researchers to understand the effect of drugs on tumour growth, invasion and metastasis in living model organisms (Bobbs. et al., 2015). The pharmacokinetic

properties of CBD and CBG via different administration routes and exposure times are well studied in rat and mice *in vivo* models (Deiana. et al., 2012). Ovarian cancer xenografts are developed by administering OC cells by intraperitoneal (IP) or intrabursal (IB) into immunocompromised Nude (Foxnl), SCID (severe combined immune deficient) or Non-obese diabetic (NOD)/SCID mice models. A2780 cells have shown to be metastases in mice models, and widely used for chemo resistance studies in xenograft models (Bobbs. et al., 2015). Future experiments are required understanding the effects of administration of CBD and CBG alone or in combination with current chemotherapeutic drugs such as carboplatin and paclitaxel in xenograft models. This involves in optimising *in vitro* doses and exposure times to xenograft models.

The cannabinoid receptor levels were examined only at molecular level. Future experiments involving the determination of CB receptors at protein levels in various ovarian cancer cell types and the effects of CBD and CBG on those cell lines can possibly address the dependency of CBD and CBG effects on the expression of CB receptors in ovarian cancer. Further experiments involving in determination of expression of CBD/ CBG dependant CB receptors in different ovarian cancer histotypes by immunohistochemistry analysis helps to understand whether the target receptors are expressed in clinical settings.

Future experiments involving in understanding the complete mechanism of action of CBD and CBG on ovarian cancer enables to identify a robust biomarker (eg: expression levels of GPR55 in different ovarian cancer histotypes if the cannabinoids mediate their anticancer effects through GPR55), which can increase the sensitivity, and helps the compounds to develop towards clinical trials.

CHAPTER 8 Conclusion

The project was carried out to evaluate the effects of CBD and CBG on ovarian cancer cells. The results indicated that both CBD and CBG induce dose-dependent and time dependent cytotoxic effects on the ovarian cancer cells. The effects of cannabinoids were cancer selective, and CBD was shown to have higher potency compared to CBG. Amongst all the combinations tested, CBD in combination with carboplatin showed the strongest synergistic effect, and the synergism was ovarian cancer selective. The evaluation of CBD and CBG induced cytotoxicity on human ovarian cancer cells *in vitro* has provided evidence to justify conduction of *in vivo* studies in future and has flagged these compounds as potential anticancer drugs or at least as an adjuvant therapy for ovarian cancer treatment.

IX) References

- Afaq, F., Sarfaraz, S., Syed, D. N., Khan, N., Malik, A., Bailey, H. H. & Mukhtar, H. 2006a. Cannabinoid receptors as a target for therapy of ovarian cancer. *Cancer Research*, 66, 1084-1084..
- Alexander, A., Smith, P. F. & Rosengren, R. J. 2009. Cannabinoids in the treatment of cancer. *Cancer Letters*, 285, 6-12.
- Allison, S. J., Cooke, D., Davidson, F. S., Elliott, P. I. P., Faulkner, R. A., Griffiths, H. B. S., Harper, O. J., Hussain, O., Owen-Lynch, P. J., Phillips, R. M., Rice, C. R., Shepherd, S. L. & Wheelhouse, R. T. 2018. Ruthenium-Containing Linear Helicates and Mesocates with Tuneable p53-Selective Cytotoxicity in Colorectal Cancer Cells. *Angewandte Chemie International Edition*, 57, 9799-9804.
- Allison, S. J., Sadiq, M., Baronou, E., Cooper, P. A., Dunnill, C., Georgopoulos, N. T., Latif, A., Shepherd, S., Shnyder, S. D., Stratford, I. J., Wheelhouse, R. T., Willans, C. E. & Phillips, R. M. 2017. Preclinical anti-cancer activity and multiple mechanisms of action of a cationic silver complex bearing N-heterocyclic carbene ligands. *Cancer Letters*, 403, 98-107.
- Alsuleimani, Y. M. & Hiley, C. R. 2015. The GPR55 agonist lysophosphatidylinositol relaxes rat mesenteric resistance artery and induces Ca²⁺ release in rat mesenteric artery endothelial cells. *British Journal of Pharmacology*, 172, 3043-3057.
- Alvarez, F. J., Lafuente, H., Carmen Rey-Santano, M., Mielgo, V. E., Gastiasoro, E., Rueda, M., Pertwee, R. G., Castillo, A. I., Romero, J. & Martínez-Orgado, J. 2008. Neuroprotective Effects of the Nonpsychoactive Cannabinoid Cannabidiol in Hypoxic-Ischemic Newborn Piglets. *Pediatric Research*, 64, 653.
- Ashton, C. H. 1999. Biomedical benefits of cannabinoids? *Addiction Biology*, 4, 111-126.
- Banerjee, S. & Kaye, S. B. 2013. New Strategies in the Treatment of Ovarian Cancer: Current Clinical Perspectives and Future Potential. *Clinical Cancer Research*, 19, 961-968.
- Barlette, J. M. S. 2000. *Ovarian Cancer Methods and Protocols*, Totowa: Human Press.
- Bartek, J. & Lukas, J. 2003. Chk1 and Chk2 kinases in checkpoint control and cancer. *Cancer Cell*, 3, 421-429.
- Bast, R. C., Hennessy, B. & Mills, G. B. 2009. The biology of ovarian cancer: new opportunities for translation. *Nature Reviews Cancer*, 9, 415-428.

- Bifulco, M., Laezza, C., Pisanti, S. & Gazerro, P. 2006. Cannabinoids and cancer: pros and cons of an antitumour strategy. *British Journal of Pharmacology*, 148, 123-135.
- Bijnsdorp, I. V., Giovannetti, E. & Peters, G. J. 2011. Analysis of Drug Interactions. In: CREE, I. A. (ed.) *Cancer Cell Culture: Methods and Protocols*. Totowa, NJ: Humana Press.
- Blázquez, C., Salazar, M., Carracedo, A., Lorente, M., Egia, A., González-Feria, L., Haro, A., Velasco, G. & Guzmán, M. 2008. Cannabinoids Inhibit Glioma Cell Invasion by Down-regulating Matrix Metalloproteinase-2 Expression. *Cancer Research*, 68, 1945-1952.
- Bobbs., A. S., Cole, J. M. & Cowden Dahl, K. D. 2015. Emerging and Evolving Ovarian Cancer Animal Models. *Cancer growth and metastasis*, 8, 29-36.
- Borrelli, F., Fasolino, I., Romano, B., Capasso, R., Maiello, F., Coppola, D., Orlando, P., Battista, G., Pagano, E., Di Marzo, V. & Izzo, A. A. 2013. Beneficial effect of the non-psychoactive plant cannabinoid cannabigerol on experimental inflammatory bowel disease. *Biochemical Pharmacology*, 85, 1306-1316.
- Borrelli, F., Pagano, E., Romano, B., Panzera, S., Maiello, F., Coppola, D., De Petrocellis, L., Buono, L., Orlando, P. & Izzo, A. A. 2014. Colon carcinogenesis is inhibited by the TRPM8 antagonist cannabigerol, a Cannabis-derived non-psychoactive cannabinoid. *Carcinogenesis*, 35, 2787-2797.
- Boyd, L. & Muggia., F. 2018. Carboplatin/Paclitaxel Induction in Ovarian Cancer: The Finer Points. *Oncology (Williston Park)*, 32, 418-424.
- Brown, M. R., Blanchette, J. O. & Kohn, E. C. 2000. Angiogenesis in ovarian cancer. *Best Practice & Research Clinical Obstetrics & Gynaecology*, 14, 901-918.
- Buckanovich, R. J., Brown, J., Shank, J., Griffith, K. A., Reynolds, R. K., Johnston, C., Mclean, K., Uppal, S., Liu, J. R., Cabrera, L. & Mehta, G. 2017. A phase II clinical trial of metformin as a cancer stem cell targeting agent in stage IIc/III/IV ovarian, fallopian tube, and primary peritoneal cancer. *Journal of Clinical Oncology*, 35, 5556-5556.
- Bukowska, B., Rogalska, A. & Marczak, A. 2016. New potential chemotherapy for ovarian cancer — Combined therapy with WP 631 and epothilone B. *Life Sciences*, 151, 86-92.
- Caffarel, M. M., Andradas, C., Pérez-Gómez, E., Guzmán, M. & Sánchez, C. 2012. Cannabinoids: A new hope for breast cancer therapy? *Cancer Treatment Reviews*, 38, 911-918.
- Calaf, G. M., Urzua, U., Termini, L. & Aguayo, F. 2018. Oxidative stress in female cancers. *Oncotarget*, 9, 23824-23842.

- Cell Signaling Technology, I. 2015. PathScan® Stress and Apoptosis Signaling Antibody Array Kit (Chemiluminescent Readout).
- Chakravarti, B., Ravi, J. & Ganju, R. K. 2014. Cannabinoids as therapeutic agents in cancer: current status and future implications. *Oncotarget*, 5, 5852-5872.
- Circu, M. & Aw., T. 2010. REACTIVE OXYGEN SPECIES, CELLULAR REDOX SYSTEMS AND APOPTOSIS. *Free radical biology & medicine*, 48, 749-762.
- Collins., A. 2004. The comet assay for DNA damage and repair: principles, applications, and limitations. *Mol Biotechnol*, 26, 249-61.
- Colombo, N., Van Gorp, T., Parma, G., Amant, F., Gatta, G., Sessa, C. & Vergote, I. 2006. Ovarian cancer. *Critical Reviews in Oncology/Hematology*, 60, 159-179.
- Console-Bram, L., Marcu, J. & Abood, M. E. 2012. Cannabinoid Receptors: Nomenclature and Pharmacological Principles. *Progress in neuro-psychopharmacology & biological psychiatry*, 38, 4-15.
- Cridge, B. J. & Rosengren, R. J. 2013. Critical appraisal of the potential use of cannabinoids in cancer management. *Cancer Management and Research*, 5, 301-313.
- Cunat, S., Hoffmann, P. & Pujol, P. 2004. Estrogens and epithelial ovarian cancer. *Gynecologic Oncology*, 94, 25-32.
- Dariš, B., Tancer Verboten, M., Knez, Ž. & Ferk, P. 2018. Cannabinoids in cancer treatment: Therapeutic potential and legislation. 2018.
- De Petrocellis, L., Ligresti, A., Schiano Moriello, A., Iappelli, M., Verde, R., Stott, C. G., Cristino, L., Orlando, P. & Di Marzo, V. 2013. Non-THC cannabinoids inhibit prostate carcinoma growth in vitro and in vivo: pro-apoptotic effects and underlying mechanisms. *British Journal of Pharmacology*, 168, 79-102.
- Deiana., S., Watanabe, A., Yamasaki, Y., Amada, N., Arthur, M., Fleming, S., Woodcock, H., Dorward, P., Pigliacampo, B., Close, S., Platt, B. & Riedel, G. 2012. Plasma and brain pharmacokinetic profile of cannabidiol (CBD), cannabidivarin (CBDV), Δ^9 -tetrahydrocannabivarin (THCV) and cannabigerol (CBG) in rats and mice following oral and intraperitoneal administration and CBD action on obsessive-compulsive behaviour. *Psychopharmacology*, 219, 859-873.
- Denardo, D. G., Andreu, P. & Coussens, L. M. 2010. Interactions between lymphocytes and myeloid cells regulate pro- versus anti-tumor immunity. *Cancer Metastasis Rev*, 29, 309-16.

- Dokas, L. A., Malone, A. M., Williams, F. E., Nauli, S. M. & Messer, W. S. 2011. Multiple Protein Kinases Determine the Phosphorylated State of the Small Heat Shock Protein, HSP27, in SH-SY5Y Neuroblastoma Cells. *Neuropharmacology*, 61, 12-24.
- Donate, L. E. & Blasco, M. A. 2011. Telomeres in cancer and ageing. *Philos Trans R Soc Lond B Biol Sci*, 366, 76-84.
- Dunn, K. C., Aotaki-Keen, A. E., Putkey, F. R. & Hjelmeland, L. M. 1996. ARPE-19, A Human Retinal Pigment Epithelial Cell Line with Differentiated Properties. *Experimental Eye Research*, 62, 155-170.
- Elmore., S. 2007. Apoptosis: a review of programmed cell death. *Toxicol Pathol*, 35, 495-516.
- Erba, E., Bergamaschi, D., Bassano, L., Ronzoni, S., Di Liberti, G., Muradore, I., Vignati, S., Faircloth, G., Jimeno, J. & D'incalci, M. 2000. Isolation and characterization of an IGROV-1 human ovarian cancer cell line made resistant to Ecteinascidin-743 (ET-743). *British Journal Of Cancer*, 82, 1732.
- Favaro, E., Lord, S., Harris, A. L. & Buffa, F. M. 2011. Gene expression and hypoxia in breast cancer. *Genome Medicine*, 3, 55.
- Fda 2017. FDA approves olaparib tablets for maintenance treatment in ovarian cancer. <https://www.fda.gov/Drugs/InformationOnDrugs/ApprovedDrugs/ucm572143.htm>, accessed September, 2018.
- Fda 2018. FDA approves bevacizumab in combination with chemotherapy for ovarian cancer. <https://www.fda.gov/drugs/informationondrugs/approveddrugs/ucm610664.htm>, accessed September, 2018.
- Ferro, R., Adamska, A., Lattanzio, R., Mavrommati, I., Edling, C. E., Arifin, S. A., Fyffe, C. A., Sala, G., Sacchetto, L., Chiorino, G., De Laurenzi, V., Piantelli, M., Sansom, O. J., Maffucci, T. & Falasca, M. 2018. GPR55 signalling promotes proliferation of pancreatic cancer cells and tumour growth in mice, and its inhibition increases effects of gemcitabine. *Oncogene*.
- Fleury, C., Mignotte, B. & Vayssiere, J. L. 2002. Mitochondrial reactive oxygen species in cell death signaling. *Biochimie*, 84, 131-41.
- Forsheo, T., Murtaza, M., Parkinson, C., Gale, D., Tsui, D. W. Y., Kaper, F., Dawson, S.-J., Piskorz, A. M., Jimenez-Linan, M., Bentley, D., Hadfield, J., May, A. P., Caldas, C., Brenton, J. D. & Rosenfeld, N. 2012. Noninvasive Identification and Monitoring of

- Cancer Mutations by Targeted Deep Sequencing of Plasma DNA. *Science Translational Medicine*, 4, 136ra68-136ra68.
- Fotopoulou, C. 2014. Limitations to the use of carboplatin-based therapy in advanced ovarian cancer. *European Journal of Cancer Supplements*, 12, 13-16.
- Galluzzi, L., Zamzami, N., De La Motte Rouge, T., Lemaire, C., Brenner, C. & Kroemer, G. 2007. Methods for the assessment of mitochondrial membrane permeabilization in apoptosis. *Apoptosis*, 12, 803-813.
- Gilbert, L., Basso, O., Sampalis, J., Karp, I., Martins, C., Feng, J., Piedimonte, S., Quintal, L., Ramanakumar, A. V., Takefman, J., Grigorie, M. S., Artho, G. & Krishnamurthy, S. 2012. Assessment of symptomatic women for early diagnosis of ovarian cancer: results from the prospective DOVe pilot project. *The Lancet Oncology*, 13, 285-291.
- Gomes, A., Fernandes, E. & Lima, J. L. F. C. 2005. Fluorescence probes used for detection of reactive oxygen species. *Journal of Biochemical and Biophysical Methods*, 65, 45-80.
- Gore, M. E., Fryatt, I., Wiltshaw, E., Dawson, T., Robinson, B. A. & Calvert, A. H. 1989. Cisplatin/carboplatin cross-resistance in ovarian cancer. *British Journal of Cancer*, 60, 767-769.
- Gubbels, J. A., Claussen, N., Kapur, A. K., Connor, J. P. & Patankar, M. S. 2010. The detection, treatment, and biology of epithelial ovarian cancer. *Journal of Ovarian Research*, 3, 1-11.
- Gugliandolo, A., Pollastro, F., Grassi, G., Bramanti, P. & Mazzon, E. 2018. In Vitro Model of Neuroinflammation: Efficacy of Cannabigerol, a Non-Psychoactive Cannabinoid. *International Journal of Molecular Sciences*, 19.
- Guzmán, M., Sánchez, C. & Galve-Roperh, I. 2001. Control of the cell survival/death decision by cannabinoids. *Journal of Molecular Medicine*, 78, 613-625.
- Hamilton, T. C., Young, R. C., Mckoy, W. M., Grotzinger, K. R., Green, J. A., Chu, E. W., Whang-Peng, J., Rogan, A. M., Green, W. R. & Ozols, R. F. 1983. Characterization of a Human Ovarian Carcinoma Cell Line (NIH:OVCA-3) with Androgen and Estrogen Receptors. *Cancer Research*, 43, 5379-5389.
- Hanahan, D. & Weinberg, R. A. 2000. The Hallmarks of Cancer. *Cell*, 100, 57-70.
- Hanahan, D. & Weinberg, Robert a. 2011. Hallmarks of Cancer: The Next Generation. *Cell*, 144, 646-674.

- Hanuš, L. O., Meyer, S. M., Muñoz, E., Tagliatela-Scafati, O. & Appendino, G. 2016. Phytocannabinoids: a unified critical inventory. *Natural Product Reports*, 33, 1357-1392.
- Hengartner., M. O. 2000. The biochemistry of apoptosis. *Nature*, 407, 770-776.
- Hernandez, L., Kim, M. K., Lyle, L. T., Bunch, K. P., House, C. D., Ning, F., Noonan, A. M. & Annunziata, C. M. 2016. Characterization of ovarian cancer cell lines as in vivo models for preclinical studies. *Gynecologic oncology*, 142, 332-340.
- Hientz., K., André Mohr, Bhakta-Guha, D. & Efferth, T. 2017. The role of p53 in cancer drug resistance and targeted chemotherapy. *Oncotarget*, 8, 8921–8946.
- Ho., S.-M. 2003. Estrogen, progesterone and epithelial ovarian cancer. *Reproductive biology and endocrinology : RB&E*, 1, 73-73.
- Hofmann, N. A., Yang, J., Trauger, S. A., Nakayama, H., Huang, L., Strunk, D., Moses, M. A., Klagsbrun, M., Bischoff, J. & Graier, W. F. 2015a. The GPR 55 agonist, L-alpha-lysophosphatidylinositol, mediates ovarian carcinoma cell-induced angiogenesis. *Br J Pharmacol*, 172, 4107-18.
- Hofmann, N. A., Yang, J., Trauger, S. A., Nakayama, H., Huang, L., Strunk, D., Moses, M. A., Klagsbrun, M., Bischoff, J. & Graier, W. F. 2015b. The GPR 55 agonist, L- α -lysophosphatidylinositol, mediates ovarian carcinoma cell-induced angiogenesis. *British Journal of Pharmacology*, 172, 4107-4118.
- Holland, M. L., Allen, J. D. & Arnold, J. C. 2008. Interaction of plant cannabinoids with the multidrug transporter ABCC1 (MRP1). *Eur J Pharmacol*, 591, 128-31.
- Humphrey, R., Brockway-Lunardi, L. M., Bonk, D. T., Dohoney, K. M., Doroshov, J. H., Meech, S. J., Ratain, M. J., Topalian, S. L. & Pardoll, D. M. 2011. Opportunities and challenges in the development of experimental drug combinations for cancer. *J Natl Cancer Inst*, 103, 1222-6.
- Irie, H., Banno, K., Yanokura, M., Iida, M., Adachi, M., Nakamura, K., Umene, K., Nogami, Y., Masuda, K., Kobayashi, Y., Tominaga, E. & Aoki, D. 2016. Metformin: A candidate for the treatment of gynecological tumors based on drug repositioning. *Oncology Letters*, 11, 1287-1293.
- Ivashkevich, A., Redon, C. E., Nakamura, A. J., Martin, R. F. & Martin, O. A. 2012. USE OF THE γ -H2AX ASSAY TO MONITOR DNA DAMAGE AND REPAIR IN TRANSLATIONAL CANCER RESEARCH. *Cancer letters*, 327, 123-133.

- Izzo, A., Borrelli, F., Capasso, R., Di Marzo, V. & Mechoulam, R. 2009. Non-psychotropic plant cannabinoids: new therapeutic opportunities from an ancient herb. *Trends in Pharmacological Sciences*, 30, 515-527.
- Jaszczyszyn, A. & Gasiorowski, K. 2008. *Limitations of the MTT Assay in Cell Viability Testing*.
- Javid, F. A., Phillips, R. M., Afshinjavid, S., Verde, R. & Ligresti, A. 2016. Cannabinoid pharmacology in cancer research: A new hope for cancer patients? *European Journal of Pharmacology*, 775, 1-14.
- Jeong, J.-H., Jo, A., Park, P., Lee, H. & Lee, H.-O. 2015. Brca2 deficiency leads to T cell loss and immune dysfunction. *Molecules and cells*, 38, 251-258.
- Jiang, S., Fu, Y., Williams, J., Wood, J., Pandarinathan, L., Avraham, S., Makriyannis, A., Avraham, S. & Avraham, H. K. 2007. Expression and Function of Cannabinoid Receptors CB1 and CB2 and Their Cognate Cannabinoid Ligands in Murine Embryonic Stem Cells. *PLoS ONE*, 2, e641.
- Jones, R. G. & Thompson, C. B. 2009. Tumor suppressors and cell metabolism: a recipe for cancer growth. *Genes Dev*, 23, 537-48.
- Kargl, J., Andersen, L., Hasenohrl, C., Feuersinger, D., Stancic, A., Fauland, A., Magnes, C., El-Heliebi, A., Lax, S., Uranitsch, S., Haybaeck, J., Heinemann, A. & Schicho, R. 2016. GPR55 promotes migration and adhesion of colon cancer cells indicating a role in metastasis. *Br J Pharmacol*, 173, 142-54.
- Kashif, M., Andersson, C., Hassan, S., Karlsson, H., Senkowski, W., Fryknäs, M., Nygren, P., Larsson, R. & Gustafsson, M. G. 2015. In vitro discovery of promising anti-cancer drug combinations using iterative maximisation of a therapeutic index. *Scientific Reports*, 5, 14118.
- Kim, B., Jung, J. W., Jung, J., Han, Y., Suh, D. H., Kim, H. S., Dhanasekaran, D. N. & Song, Y. S. 2017. PGC1 α induced by reactive oxygen species contributes to chemoresistance of ovarian cancer cells. *Oncotarget*, 8, 60299-60311.
- Kosgodage, U. S., Mould, R., Henley, A. B., Nunn, A. V., Guy, G. W., Thomas, E. L., Inal, J. M., Bell, J. D. & Lange, S. 2018a. Cannabidiol (CBD) Is a Novel Inhibitor for Exosome and Microvesicle (EMV) Release in Cancer. *Frontiers in Pharmacology*, 9, 889.
- Kosgodage, U. S., Mould, R., Henley, A. B., Nunn, A. V., Guy, G. W., Thomas, E. L., Inal, J. M., Bell, J. D. & Lange, S. 2018b. Cannabidiol (CBD) Is a Novel Inhibitor for Exosome and Microvesicle (EMV) Release in Cancer. *Frontiers in Pharmacology*, 9.

- Koshiyama, M., Matsumura, N. & Konishi, I. 2014. Recent Concepts of Ovarian Carcinogenesis: Type I and Type II. *BioMed Research International*, 2014, 11.
- Latha., T. S., Panati, K., Gowd, D. S. K., Reddy, M. C. & Lomada, D. 2014. Ovarian Cancer Biology and Immunotherapy. *International Reviews of Immunology*, 33, 428-440.
- Lauckner, J. E., Jensen, J. B., Chen, H.-Y., Lu, H.-C., Hille, B. & Mackie, K. 2008. GPR55 is a cannabinoid receptor that increases intracellular calcium and inhibits M current. *Proceedings of the National Academy of Sciences of the United States of America*, 105, 2699-2704.
- Lazebnik, Y. A., Kaufmann, S. H., Desnoyers, S., Poirier, G. G. & Earnshaw, W. C. 1994. Cleavage of poly(ADP-ribose) polymerase by a proteinase with properties like ICE. *Nature*, 371, 346.
- Ledermann, J., Harter, P., Gourley, C., Friedlander, M., Vergote, I., Rustin, G., Scott, C., Meier, W., Shapira-Frommer, R., Safra, T., Matei, D., Macpherson, E., Watkins, C., Carmichael, J. & Matulonis, U. 2012. Olaparib Maintenance Therapy in Platinum-Sensitive Relapsed Ovarian Cancer. *New England Journal of Medicine*, 366, 1382-1392.
- Lengyel., E. 2010. Ovarian cancer development and metastasis. *The American journal of pathology*, 177, 1053-1064.
- Leung-Pineda, V., Ryan, C. E. & Piwnica-Worms, H. 2006. Phosphorylation of Chk1 by ATR Is Antagonized by a Chk1-Regulated Protein Phosphatase 2A Circuit. *Molecular and Cellular Biology*, 26, 7529-7538.
- Leyva-Illades, D. & Demorrow, S. 2013. Orphan G protein receptor GPR55 as an emerging target in cancer therapy and management. *Cancer Management and Research*, 5, 147-155.
- Liang Zhao, M. G. W. a. J. L.-S. A. 2004. Evaluation of Combination Chemotherapy. *Clinical Cancer Research*, 10, 7994- 8004.
- Liberti, M. V. & Locasale, J. W. 2016. The Warburg Effect: How Does it Benefit Cancer Cells? *Trends Biochem Sci*, 41, 211-218.
- Ligresti , A., Moriello, A. S., Starowicz, K., Matias, I., Pisanti, S., De Petrocellis, L., Laezza, C., Portella, G., Bifulco, M. & Di Marzo, V. 2006. Antitumor Activity of Plant Cannabinoids with Emphasis on the Effect of Cannabidiol on Human Breast Carcinoma. *Journal of Pharmacology and Experimental Therapeutics*, 318, 1375-1387.

- Liou, G. & Storz., P. 2010. Reactive oxygen species in cancer. *Free radical research*, 44, 10.3109/10715761003667554.
- Liu, L., Zhang, X. J., Jiang, S. R., Ding, Z. N., Ding, G. X., Huang, J. & Cheng, Y. L. 2007. Heat shock protein 27 regulates oxidative stress-induced apoptosis in cardiomyocytes: mechanisms via reactive oxygen species generation and Akt activation. *Chin Med J (Engl)*, 120, 2271-7.
- Llauradó, M., Majem, B., Altadill, T., Lanau, L., Castellví, J., Sánchez-Iglesias, J. L., Cabrera, S., De La Torre, J., Díaz-Feijoo, B., Pérez-Benavente, A., Colás, E., Olivan, M., Doll, A., Alameda, F., Matias-Guiu, X., Moreno-Bueno, G., Carey, M. S., Del Campo, J. M., Gil-Moreno, A., Reventós, J. & Rigau, M. 2014. MicroRNAs as prognostic markers in ovarian cancer. *Molecular and Cellular Endocrinology*, 390, 73-84.
- Locksley, R. M., Killeen, N. & Lenardo, M. J. 2001. The TNF and TNF Receptor Superfamilies: Integrating Mammalian Biology. *Cell*, 104, 487-501.
- Luft, F. C. 2015. Approaching the Hayflick limit. *Trends Cardiovasc Med*, 25, 240-2.
- Luqmani, Y. A. 2005. Mechanisms of Drug Resistance in Cancer Chemotherapy. *Medical Principles and Practice*, 14(suppl 1), 35-48.
- Lv, Y., Zhao, S. G., Lu, G., Leung, C. K., Xiong, Z. Q., Su, X. W., Ma, J. L., Chan, W. Y. & Liu, H. B. 2017. Identification of reference genes for qRT-PCR in granulosa cells of healthy women and polycystic ovarian syndrome patients. *Scientific Reports*, 7, 6961.
- Ly, J. D., Grubb, D. R. & Lawen, A. 2003. The mitochondrial membrane potential ($\Delta\psi_m$) in apoptosis; an update. *Apoptosis*, 8, 115-128.
- Macciò, A. & Madeddu., C. 2012. Inflammation and ovarian cancer. *Cytokine*, 58, 133-147.
- Mackenzie, R., Talhouk, A., Eshragh, S., Lau, S., Cheung, D., Chow, C., Le, N., Cook, L. S., Wilkinson, N., Mcdermott, J., Singh, N., Kommos, F., Pfisterer, J., Huntsman, D. G., Köbel, M., Kommos, S., Gilks, C. B. & Anglesio, M. S. 2015. Morphological and Molecular Characteristics of Mixed Epithelial Ovarian Cancers. *The American journal of surgical pathology*, 39, 1548-1557.
- Mangal, M., Sagar, P., Singh, H., Raghava, G. P. S. & Agarwal, S. M. 2013. NPACT: Naturally Occurring Plant-based Anti-cancer Compound-Activity-Target database. *Nucleic Acids Research*, 41, D1124-D1129.

- Marsicano, G., Moosmann, B., Hermann, H., Lutz, B. & Behl, C. 2002. Neuroprotective properties of cannabinoids against oxidative stress: role of the cannabinoid receptor CB1. *Journal of Neurochemistry*, 80, 448-456.
- Massi, P., Solinas, M., Cincina, V. & Parolaro, D. 2013. Cannabidiol as potential anticancer drug. *British Journal of Clinical Pharmacology*, 75, 303-312.
- Massi, P., Vaccani, A., Bianchessi, S., Costa, B., Macchi, P. & Parolaro, D. 2006. The non-psychoactive cannabidiol triggers caspase activation and oxidative stress in human glioma cells. *Cellular and Molecular Life Sciences CMLS*, 63, 2057-2066.
- Mcdermott, M., Eustace, A. J., Busschots, S., Breen, L., Crown, J., Clynes, M., O'donovan, N. & Stordal, B. 2014. In vitro Development of Chemotherapy and Targeted Therapy Drug-Resistant Cancer Cell Lines: A Practical Guide with Case Studies. *Frontiers in Oncology*, 4, 40.
- Monk, B. J. & Anastasia, P. J. 2016. Ovarian Cancer: Current Treatment and Patient Management. *Journal of the advanced practitioner in oncology*, 7, 271-273.
- Morelli, M. B., Offidani, M., Alesiani, F., Discepoli, G., Liberati, S., Olivieri, A., Santoni, M., Santoni, G., Leoni, P. & Nabissi, M. 2014. The effects of cannabidiol and its synergism with bortezomib in multiple myeloma cell lines. A role for transient receptor potential vanilloid type-2. *International Journal of Cancer*, 134, 2534-2546.
- Moss, E. L., Moran, A., Reynolds, T. M. & Stokes-Lampard, H. 2013. Views of general practitioners on the role of CA125 in primary care to diagnose ovarian cancer. *BMC Women's Health*, 13, 8-8.
- Mougiakakos, D., Choudhury, A., Lladser, A., Kiessling, R. & Johansson, C. C. 2010. Regulatory T cells in cancer. *Adv Cancer Res*, 107, 57-117.
- Muz, B., De La Puente, P., Azab, F. & Azab, A. K. 2015. The role of hypoxia in cancer progression, angiogenesis, metastasis, and resistance to therapy. *Hypoxia*, 3, 83-92.
- Nabissi, M., Morelli, M. B., Offidani, M., Amantini, C., Gentili, S., Soriani, A., Cardinali, C., Leoni, P. & Santoni, G. 2016. Cannabinoids synergize with carfilzomib, reducing multiple myeloma cells viability and migration. *Oncotarget*, 7, 77543-77557.
- Natarajan, P., Taylor, S. E. & Kirwan, J. M. 2018. Ovarian cancer: current management and future directions. *Obstetrics, Gynaecology & Reproductive Medicine*, 28, 171-176.
- Navarro, G., Varani, K., Reyes-Resina, I., Sánchez De Medina, V., Rivas-Santisteban, R., Sánchez-Carnerero Callado, C., Vincenzi, F., Casano, S., Ferreiro-Vera, C., Canela, E. I.,

- Borea, P. A., Nadal, X. & Franco, R. 2018. Cannabigerol Action at Cannabinoid CB1 and CB2 Receptors and at CB1–CB2 Heteroreceptor Complexes. *Frontiers in Pharmacology*, 9.
- Neff., R. T., Leigha Senter & Salani, R. 2017. BRCA mutation in ovarian cancer: testing, implications and treatment considerations. *Ther Adv Med Oncol*, 9, 519- 531.
- Nicholson, D. W., Ali, A., Thornberry, N. A., Vaillancourt, J. P., Ding, C. K., Gallant, M., Gareau, Y., Griffin, P. R., Labelle, M., Lazebnik, Y. A., Munday, N. A., Raju, S. M., Smulson, M. E., Yamin, T.-T., Yu, V. L. & Miller, D. K. 1995. Identification and inhibition of the ICE/CED-3 protease necessary for mammalian apoptosis. *Nature*, 376, 37.
- Nishitoh, H. 2012. CHOP is a multifunctional transcription factor in the ER stress response. *The Journal of Biochemistry*, 151, 217-219.
- Omori, E., Morioka, S., Matsumoto, K. & Ninomiya-Tsuji, J. 2008. TAK1 Regulates Reactive Oxygen Species and Cell Death in Keratinocytes, Which Is Essential for Skin Integrity. *The Journal of Biological Chemistry*, 283, 26161-26168.
- Ostadhadi, S., Rahmatollahi, M., Dehpour, A.-R. & Rahimian, R. 2015. Therapeutic Potential of Cannabinoids in Counteracting Chemotherapy-induced Adverse Effects: An Exploratory Review. *Phytotherapy Research*, 29, 332-338.
- Ozaki, T. & Nakagawara, A. 2011. Role of p53 in Cell Death and Human Cancers. *Cancers*, 3, 994-1013.
- Ozols, R. F. 2006. Challenges for chemotherapy in ovarian cancer. *Annals of Oncology*, 17, v181-v187.
- Pertwee, R. G. 2006. Cannabinoid pharmacology: the first 66 years. *British Journal of Pharmacology*, 147, S163-S171.
- Pertwee, R. G., Howlett, A. C., Abood, M. E., Alexander, S. P. H., Di Marzo, V., Elphick, M. R., Greasley, P. J., Hansen, H. S., Kunos, G., Mackie, K., Mechoulam, R. & Ross, R. A. 2010. International Union of Basic and Clinical Pharmacology. LXXIX. Cannabinoid Receptors and Their Ligands: Beyond CB₁ and CB₂. *Pharmacological Reviews*, 62, 588-631.
- Petrillo, M., Nero, C., Amadio, G., Gallo, D., Fagotti, A. & Scambia., G. 2016. Targeting the hallmarks of ovarian cancer: The big picture. *Gynecologic Oncology*, 142, 176-183.
- Pineiro, R., Maffucci, T. & Falasca, M. 2011. The putative cannabinoid receptor GPR55 defines a novel autocrine loop in cancer cell proliferation. *Oncogene*, 30, 142-152.

- Portenoy, R. K., Ganae-Motan, E. D., Allende, S., Yanagihara, R., Shaiova, L., Weinstein, S., Mcquade, R., Wright, S. & Fallon, M. T. 2012. Nabiximols for Opioid-Treated Cancer Patients With Poorly-Controlled Chronic Pain: A Randomized, Placebo-Controlled, Graded-Dose Trial. *The Journal of Pain*, 13, 438-449.
- Pouliot, N., Pearson Hb & A, B. 2013. *Investigating Metastasis Using In Vitro Platforms*, Austin (TX), Madame Curie Bioscience Database [Internet].
- Pucci, B., Kasten, M. & Giordano, A. 2000. Cell Cycle and Apoptosis. *Neoplasia (New York, N.Y.)*, 2, 291-299.
- Rauh-Hain, J. A., Krivak, T. C., Del Carmen, M. G. & Olawaiye, A. B. 2011. Ovarian Cancer Screening and Early Detection in the General Population. *Reviews in Obstetrics and Gynecology*, 4, 15-21.
- Reekie, T. A., Scott, M. P. & Kassiou, M. 2017. The evolving science of phytocannabinoids. *Nature Reviews Chemistry*, 2, 0101.
- Rescigno, P., Cerillo, I., Ruocco, R., Condello, C., De Placido, S. & Pensabene, M. 2013. New Hypothesis on Pathogenesis of Ovarian Cancer Lead to Future Tailored Approaches. *BioMed Research International*, 2013, 13.
- Robinson., G. 2016. *A comparison of the cytotoxic effects of fatty acids on in vitro breast and prostate cell lines*. PhD, University of Huddersfield.
- Rock, E. M., Goodwin, J. M., Limebeer, C. L., Breuer, A., Pertwee, R. G., Mechoulam, R. & Parker, L. A. 2011. Interaction between non-psychotropic cannabinoids in marijuana: effect of cannabigerol (CBG) on the anti-nausea or anti-emetic effects of cannabidiol (CBD) in rats and shrews. *Psychopharmacology*, 215, 505-512.
- Romero, I. & Bast., R. C. 2012. Minireview: Human Ovarian Cancer: Biology, Current Management, and Paths to Personalizing Therapy. *Endocrinology*, 153, 1593–1602.
- Saad., A. F., Hu, W. & Sood, A. K. 2010. Microenvironment and Pathogenesis of Epithelial Ovarian Cancer. *Hormones and Cancer*, 1, 277-290.
- Saelens, X., Festjens, N., Walle, L. V., Gorp, M. V., Loo, G. V. & Vandenabeele, P. 2004. Toxic proteins released from mitochondria in cell death. *Oncogene*, 23, 2861-2874.
- Sarfaraz, S., Adhami, V. M., Syed, D. N., Afaq, F. & Mukhtar, H. 2008. Cannabinoids for Cancer Treatment: Progress and Promise. *Cancer Research*, 68, 339-342.
- Schmid, B. C. & Oehler, M. K. 2014. New perspectives in ovarian cancer treatment. *Maturitas*, 77, 128-136.

- Schneider, E., Montenarh, M. & Wagner, P. 1998. Regulation of CAK kinase activity by p53. *Oncogene*, 17.
- Schutte, B., Nuydens, R., Geerts, H. & Ramaekers, F. 1998. Annexin V binding assay as a tool to measure apoptosis in differentiated neuronal cells. *Journal of Neuroscience Methods*, 86, 63-69.
- Sharma, M., Hudson, J. B., Adomat, H., Guns, E. & Cox, M. E. 2014. <i>In Vitro&/i>; Anticancer Activity of Plant-Derived Cannabidiol on Prostate Cancer Cell Lines. *Pharmacology & Pharmacy*, Vol.05No.08, 15.
- Shevyrin., V. A. & Morzherin., Y. Y. 2015. Cannabinoids: structures, effects, and classification. *Russian Chemical Bulletin*, 64, 1249-1266.
- Shi, Q.-X., Yang, L.-K., Shi, W.-L., Wang, L., Zhou, S.-M., Guan, S.-Y., Zhao, M.-G. & Yang, Q. 2017. The novel cannabinoid receptor GPR55 mediates anxiolytic-like effects in the medial orbital cortex of mice with acute stress. *Molecular Brain*, 10, 38.
- Shields, J. D., Kourtis, I. C., Tomei, A. A., Roberts, J. M. & Swartz, M. A. 2010. Induction of lymphoidlike stroma and immune escape by tumors that express the chemokine CCL21. *Science*, 328, 749-52.
- Shrivastava, A., Kuzontkoski, P. M., Groopman, J. E. & Prasad, A. 2011. Cannabidiol Induces Programmed Cell Death in Breast Cancer Cells by Coordinating the Cross-talk between Apoptosis and Autophagy. *American Association for Cancer Research*, 10, 1161-1172.
- Singer, E., Judkins, J., Salomonis, N., Matlaf, L., Soteropoulos, P., Mcallister, S. & Soroceanu, L. 2015. Reactive oxygen species-mediated therapeutic response and resistance in glioblastoma. *Cell Death & Disease*, 6, e1601.
- Slee, E. A., Adrain, C. & Martin, S. J. 2000. Executioner Caspase-3, -6, and -7 Perform Distinct, Non-redundant Roles during the Demolition Phase of Apoptosis. *Journal of Biological Chemistry*, 276, 7320-7326.
- Soderstrom, K., Soliman, E. & Van Dross, R. 2017. Cannabinoids Modulate Neuronal Activity and Cancer by CB1 and CB2 Receptor-Independent Mechanisms. *Frontiers in Pharmacology*, 8, 720.
- Sousa, G. F. D., Wlodarczyk, S. R. & Monteiro, G. 2014. Carboplatin: molecular mechanisms of action associated with chemoresistance. *Brazilian Journal of Pharmaceutical Sciences*, 50, 693-701.

- Steino, A., Bacha, J. A., Garner, W. J., Kanekal, S., Siddik, Z. H. & Brown, D. M. 2013. Abstract B252: The unique mechanism of action of VAL-083 may provide a new treatment option for some chemo-resistant cancers. *Molecular Cancer Therapeutics*, 12, B252-B252.
- Storz., P. 2005. Reactive oxygen species in tumor progression. *Front Biosci*, 10, 1881-1896.
- Sugimoto, N., Ishibashi, H., Nakamura, H., Yachie, A. & Ohno-Shosaku, T. 2017. Hypoxia-induced inhibition of the endocannabinoid system in glioblastoma cells. *Oncology Reports*, 38, 3702-3708.
- Sundar, S., Neal, R. D. & Kehoe, S. 2015. Diagnosis of ovarian cancer. *BMJ : British Medical Journal*, 351.
- Surin., A. M., Sharipov, R. R., Krasil'nikova, I. A., Boyarkin, D. P., Lisina, O. Y., Gorbacheva, L. R., Avetisyan, A. V. & Pinelis, V. G. 2017. Disruption of functional activity of mitochondria during MTT assay of viability of cultured neurons. *Biochemistry (Moscow)*, 82, 737-749.
- Susin, S. A., Daugas, E., Ravagnan, L., Samejima, K., Zamzami, N., Loeffler, M., Costantini, P., Ferri, K. F., Irinopoulou, T., Prévost, M.-C., Brothers, G., Mak, T. W., Penninger, J., Earnshaw, W. C. & Kroemer, G. 2000. Two Distinct Pathways Leading to Nuclear Apoptosis. *The Journal of Experimental Medicine*, 192, 571-580.
- Tai, S. & Fantegrossi, W. E. 2014. Synthetic Cannabinoids: Pharmacology, Behavioral Effects, and Abuse Potential. *Current Addiction Reports*, 1, 129-136.
- Takeba, Y., Kumai, T., Matsumoto, N., Nakaya, S., Tsuzuki, Y., Yanagida, Y. & Kobayashi, S. 2007. Irinotecan activates p53 with its active metabolite, resulting in human hepatocellular carcinoma apoptosis. *J Pharmacol Sci*, 104, 232-42.
- Torres, S., Lorente, M., Rodríguez-Fornés, F., Hernández-Tiedra, S., Salazar, M., García-Taboada, E., Barcia, J., Guzmán, M. & Velasco, G. 2011. A Combined Preclinical Therapy of Cannabinoids and Temozolomide against Glioma. *American Association for Cancer Research*, 10, 90-103.
- Valdeolivas, S., Navarrete, C., Cantarero, I., Bellido, M. L., Muñoz, E. & Sagredo, O. 2015. Neuroprotective properties of cannabigerol in Huntington's disease: studies in R6/2 mice and 3-nitropropionate-lesioned mice. *Neurotherapeutics*, 12, 185-99.
- Velasco, G., Sánchez, C. & Guzmán, M. 2012. Towards the use of cannabinoids as antitumour agents. *Nat Rev Cancer*, 12, 436-444.

- Wang, J. S., Wu, D., Huang, D. Y. & Lin, W. W. 2015. TAK1 inhibition-induced RIP1-dependent apoptosis in murine macrophages relies on constitutive TNF-alpha signaling and ROS production. *J Biomed Sci*, 22, 76.
- Ward, S. J., Mcallister, S. D., Kawamura, R., Murase, R., Neelakantan, H. & Walker, E. A. 2014. Cannabidiol inhibits paclitaxel-induced neuropathic pain through 5-HT(1A) receptors without diminishing nervous system function or chemotherapy efficacy. *British Journal of Pharmacology*, 171, 636-645.
- Weinberg, R. 2013. *The Biology of Cancer*, New York Garland Science.
- Wen, S., Zhu, D. & Huang, P. 2013. Targeting cancer cell mitochondria as a therapeutic approach. *Future medicinal chemistry*, 5, 53-67.
- Xu, D., Wang, J., Zhou, Z., He, Z. & Zhao, Q. 2015. Cannabinoid WIN55, 212-2 induces cell cycle arrest and inhibits the proliferation and migration of human BEL7402 hepatocellular carcinoma cells. *Molecular Medicine Reports*, 12, 7963-7970.
- Yang, L., Pang, Y. & Moses, H. L. 2010. TGF-beta and immune cells: an important regulatory axis in the tumor microenvironment and progression. *Trends Immunol*, 31, 220-7.
- Zhang., Y., Cao, L., Nguyen, D. & Lu, H. 2016. TP53 mutations in epithelial ovarian cancer. *Translational Cancer Research*, 5, 650-663.
- Zhao, H., Traganos, F. & Darzynkiewicz, Z. 2008. Phosphorylation of p53 on Ser15 during cell cycle caused by Topo I and Topo II inhibitors in relation to ATM and Chk2 activation. *Cell cycle (Georgetown, Tex.)*, 7, 3048-3055.
- Zuardi, A. W. 2008. Cannabidiol: from an inactive cannabinoid to a drug with wide spectrum of action. *Revista Brasileira de Psiquiatria*, 30, 271-280.

CHAPTER 9 Appendix

Table 9-1 selective index values of CBD on ovarian cancer cells compared to non- cancer cells ARPE19 and PNT2

ARPE19 CBD	24h	48h	72h	96h	PNT2 CBD	24h	48h	72h	96h
A2780	2.05	2.10	2.91	3.38	A2780	3.30	2.59	3.84	4.15
CP70	1.57	1.28	1.78	2.21	CP70	2.49	1.52	2.35	2.48
OVCAR3	0.67	0.83	0.73	1.33	OVCAR3	1.09	0.83	0.97	1.60

Table 9-2 selective index values of CBG on ovarian cancer cells compared to non- cancer cells ARPE19 and PNT2

ARPE19 CBG	24h	48h	72h	96h	PNT2 CBG	24h	48h	72h	96h
A2780	2.10	1.52	2.04	3.04	A2780	2.43	1.65	2.12	3.20
CP70	1.87	1.37	1.56	2.43	CP70	2.41	1.48	1.59	2.56
OVCAR3	0.74	0.67	0.74	1	OVCAR3	0.86	0.76	0.77	0.93

Table 9-3 IC₅₀ values of carboplatin alone, and in combination with CBD or CBG on A2780 cells

A2780	24h	48h	72h	96h
carboplatin	7.9±0.51µM	4.79±0.24µM	2.64±0.5µM	2.5±0.3µM
100nM CBD+ carboplatin	2.91±1.62µM	0.82±0.62µM	0.80±0.13µM	0.23±0.13µM
100nM CBG+ carboplatin	8.01±1.62µM	4.92±1.36µM	2.56±0.63µM	1.46±0.1µM

Table 9-4 IC₅₀ values of carboplatin alone, and in combination with CBD or CBG on A2780/CP70 cells

A2780/CP70	24h	48h	72h	96h
carboplatin	66.5±3.35	48.7±0.4μM	45.5±2.6μM	44.9±3.2μM
100nM CBD+ Carbo	56.7±2.6μM	37.5±1.2μM	36.1±1.5μM	23.6±0.7μM
100nM CBG+ Carbo	65.2±1.6μM	36.5±3.2μM	32.1±2.75μM	29.5±0.5μM

Table 9-5 IC₅₀ values of Taxol alone, and in combination with CBD or CBG on A2780 cells

A2780	24H	48H	72H	96H
Taxol	23.05±1.2nM	18.87± 0.83M	14.33± 0.7nM	13.23± 0.5nM
Taxol+ 100nM CBD	19.12±2.3nM	18.75± 0.8nM	8.94± 0.5nM	8.32± 1.3nM
Taxol+ 100nM CBG	19.25±1.6nM	18.80± 0.3nM	16.86± 0.8nM	14.01± 2.3nM

Table 9-6 IC₅₀ values of Taxol alone, and in combination with CBD or CBG on A2780/CP70 cells

A2780/CP70	24H	48H	72H	96H
Taxol	51.27±2.4nM	41.26±2.3nM	25.74±1.3nM	22.89±0.6nM
Taxol+ 100nM CBD	50.88±1.2nM	27.35±0.9nM	22.75±0.9nM	19.69±1.6nM
Taxol+ 100nM CBG	45.16±1.2nM	39.88±0.9nM	23.75±1.0nM	18.73±0.67nM

Table 9-7 Fold change in apoptosis and stress related proteins in A2780 and A2780/CP70 cells treated with CBD for 24 h

A2780 CBD 24 H	0 μ M	10 μ M	30 μ M
p44/42	1.00	1.49	1.76
Akt	1.00	0.87	1.54
Bad	1.00	1.08	1.68
HSP27	1.00	1.12	1.68
smad2	1.00	1.00	1.48
p53	1.00	2.63	5.00
p38 MAPK	1.00	1.08	1.99
SAPK/JNK	1.00	0.94	1.51
PARP	1.00	1.74	7.19
caspase-3	1.00	1.13	2.66
caspase-7	1.00	0.99	1.50
I κ B α	1.00	1.18	1.42
chk1	1.00	0.99	1.29
chk2	1.00	1.07	2.33
ikb α	1.00	1.13	1.67
elf2 α	1.00	0.94	1.52
TAK 1	1.00	0.95	1.40
Survivin	1.00	0.98	1.16
α - Tubulin	1.00	0.96	0.83

CP70 CBD 24 H	0 μ M	10 μ M	30 μ M
p44/42	1.00	1.13	0.75
Akt	1.00	0.93	0.74
Bad	1.00	1.41	1.52
HSP27	1.00	1.48	1.58
smad2	1.00	1.05	1.29
p53	1.00	2.76	3.26
p38 MAPK	1.00	0.96	1.21
SAPK/JNK	1.00	1.29	1.49
PARP	1.00	1.33	1.53
caspase-3	1.00	1.44	1.89
caspase-7	1.00	1.19	1.33
I κ B α	1.00	1.18	1.51
chk1	1.00	1.29	1.53
chk2	1.00	1.42	1.70
ikb α	1.00	1.65	1.98
elf2 α	1.00	1.27	1.55
TAK 1	1.00	0.98	1.79
Survivin	1.00	1.20	1.42
α - Tubulin	1.00	1.30	1.33

Table 9-8 Fold change in apoptosis and stress related proteins in A2780 and A2780/CP70 cells treated with CBG for 24 h

A2780 CBG 24H	0μM	10μM	30μM	CP70 CBG 24H	0μM	10μM	30μM
p44/42	1.00	0.42	0.52	p44/42	1.00	2.33	0.90
Akt	1.00	0.70	1.93	Akt	1.00	2.29	0.78
Bad	1.00	1.14	1.43	Bad	1.00	1.49	2.22
HSP27	1.00	1.28	1.07	HSP27	1.00	2.48	3.68
smad2	1.00	2.03	1.53	smad2	1.00	1.68	2.28
p53	1.00	0.96	0.94	p53	1.00	1.02	1.21
p38 MAPK	1.00	1.25	1.70	p38 MAPK	1.00	1.56	3.43
SAPK/JNK	1.00	0.74	1.03	SAPK/JNK	1.00	1.10	3.28
PARP	1.00	1.00	1.01	PARP	1.00	1.24	2.52
caspase-3	1.00	1.18	1.39	caspase-3	1.00	1.42	2.31
caspase-7	1.00	1.16	1.34	caspase-7	1.00	1.43	2.31
IkBalph	1.00	0.92	1.58	IkBalph	1.00	2.29	7.30
chk1	1.00	1.19	1.41	chk1	1.00	1.32	4.61
chk2	1.00	0.98	1.04	chk2	1.00	1.15	2.11
ikbα	1.00	1.42	1.90	ikbα	1.00	5.25	0.93
elf2α	1.00	1.89	2.08	elf2α	1.00	1.52	3.68
TAK 1	1.00	1.09	1.68	TAK 1	1.00	2.93	3.36
Survivin	1.00	1.12	2.23	Survivin (total)	1.00	3.54	3.86
α- Tubulin	1.00	0.98	0.68	α- Tubulin	1.00	1.19	1.66

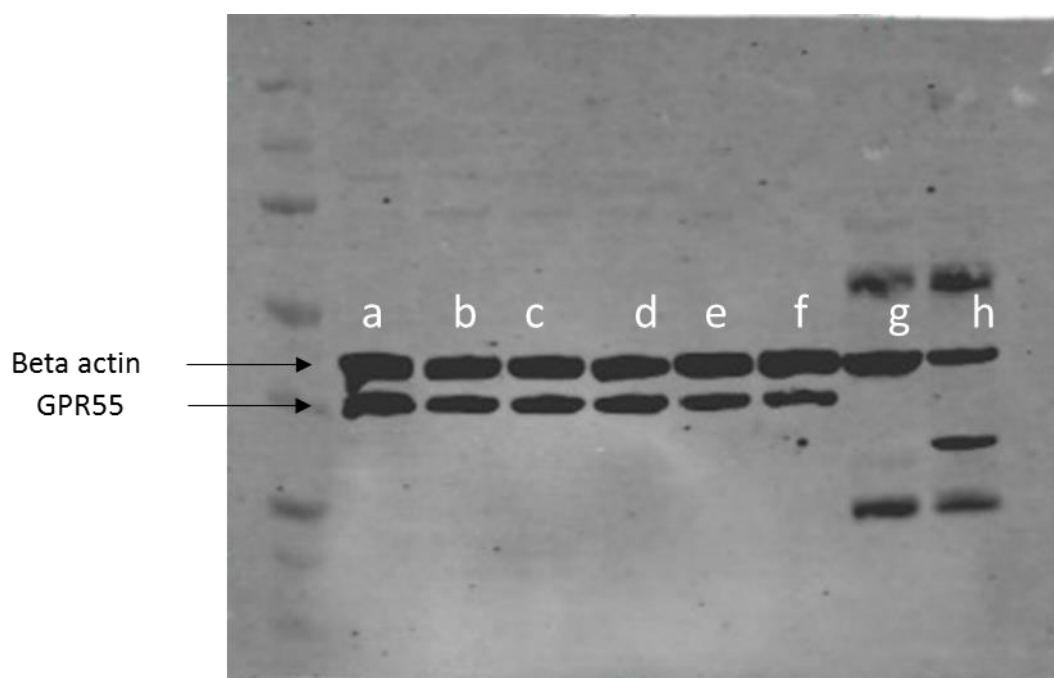


Figure 9-1. Validation of GPR55 antibody for western blot analysis. GPR55 antibody was validated using mice healthy colon tissue samples expressing WT GPR55 receptor and knockout GPR55 samples. Samples a and b represent A2780 cells control and siRNA knockdown GpR55 cells after 48 h, samples c and d represent A2780 cells control and siRNA knockdown GpR55 cells after 72 h, samples e and f represent A2780/CP70 cells control and siRNA knockdown GpR55 cells after 72 h, samples g and h represent WT and KO GPR55 mice healthy colon samples